Adaptive OFDM and CDMA Algorithms for SISO and MIMO Channels

Adaptive OFDM and CDMA Algorithms for SISO and MIMO Channels

Proefschrift

ter verkrijging van de graad van doctor
aan de Technische Universiteit Delft,
op gezag van de Rector Magnificus prof. dr. ir. J. T. Fokkema
voorzitter van het College van Promoties,
in het openbaar te verdedigen op maandag 23 mei 2005 om 13:00 uur

door

Haiyan CHE

Master of Science in Telecommunications and Electronics Technique,
Beijing Institute of Technology (P. R. China),
Geboren te Fuxin, P. R. China

Dit proefschrift is goedgekeurd door de promotoren:
Prof. dr. ir. L. P. Ligthart
Prof. dr. R. Prasad

Samenstelling promotiecommissie:

Rector Magnificus	voorzitter
Prof. dr. ir. L. P. Ligthart	Technische Universiteit Delft, promotor
Prof. dr. R. Prasad	Aalborg University, Denmark, promotor
Prof. dr. ir. I. G. M. M. Niemegeers	Technische Universiteit Delft
Prof. dr. ir. J. C. Haartsen	Universiteit Twente
Prof. dr. H. Rohling	Technische Universität Hamburg-Harburg, Duitsland
Dr. H. Nikookar	Technische Universiteit Delft
Prof. ir. P. van Genderen	Reservelid

ISBN 90-76928-08-8

Copyright 2005 @ Haiyan CHE

To my parents,
my sister,
and my boyfriend.

Summary

The objective of this thesis is to study adaptive modulation algorithms for Single Input Single Output (SISO) and Multiple Input Multiple Output (MIMO) channels. The adaptive modulation technique has the advantages of flexibility, providing high transmission quality and throughput; and it can lead to a smaller volume of radio and more applications.

The major contribution of the author is discussed in the following paragraphs.

To the best of the author's knowledge, the strategy and working procedures of the adaptive modulation technique have not yet been described in the literature. We propose strategies and work procedures for adaptive modulation in this dissertation. In addition, for the first time, it is proposed that the development of adaptive modulation consists of three stages, in which the adaptivity is taken to a higher level.

We assert in this thesis that adaptive modulation algorithms involve two themes, i.e., channel and modulation. We analyze two types of channels: SISO and MIMO channels. We investigate the SISO channel in time, frequency, and space domains, which is efficient for designing adaptive modulation algorithms. Further, initially we propose three approaches as solutions to problems in each of the domains, i.e., adaptive techniques (time domain), OFDM (frequency domain), and MIMO technique (space domain). These three approaches are investigated in this thesis. We study the concept, structure, and characteristics of MIMO channels. The gains of three MIMO schemes and parameters influencing these gains are generalized. What is more, we introduce a new factor, the Rician K gain, to describe the MIMO gain with respect to that of SISO channels. In addition, we work out the SNR gains of these three MIMO schemes compared with SISO channels for a large SNR range, which have not been found in literature. This is indispensable for the design of adaptive modulation algorithms for MIMO channels.

With regard to modulation, we list the parameters of OFDM and CDMA modulations for adaptive OFDM and adaptive CDMA algorithms to be designed. In order to obtain direct relationships between modulation parameters and throughput, we derive two throughput formulas, an OFDM formula and a CDMA formula. We show that the traditional commonly held belief that the subcarrier bandwidth influences transmission quality is true only if the channel RDS is constant. To explain this, we define a new parameter, P_{FR}, as the product of subcarrier bandwidth Δf and RDS. How this parameter works and by what factors it is limited are studied in this thesis.

Subsequently, we propose three successful adaptive modulation algorithms, i.e., an adaptive OFDM algorithm for SISO channels, an adaptive OFDM algorithm for MIMO channels, and an adaptive CDMA algorithm for MIMO channels. Perfect channel estimation is assumed in our work. For the adaptive OFDM algorithms, we propose three subband settings. Remarkable throughput gains are obtained from all these adaptive modulation algorithms in simulations. We put forward the new idea of employing more than one MIMO scheme in a system and adapting these schemes using our adaptive modulation algorithms. Simulation results show that extra gains can be obtained by this method. The performance gains of our algorithms are dependent on the channel situation. The influence of channel parameters on these relative gains is investigated in this work as well. We introduce an SNR boundary matrix to set processing gains and modulation levels in our adaptive CDMA algorithm for MIMO channels.

Abbreviations

ACI	Adjacent Cell Interference
AM	Adaptive Modulation
AWGN	Additive White Gaussian Noise
BER	Bit Error Rate
BPSK	Binary Phase Shift Keying Modulation
CDF	Cumulative Distribution Function
CDMA	Code Division Multiple Access
DPS	Delay Power Spectrum
FFT	Fast Fourier Transform
FSR	FFT time to Symbol period Ratio in an OFDM symbol
ICI	Inter Carrier Interference
IFFT	Inverse Fast Fourier Transform
ISI	Inter Symbol Interference
LAS-CDMA	Large Area Synchronous CDMA
LOS	Line of Sight
MA	Multiple Access
MAI	Multiple Access Interference
MIMO	Multiple Input Multiple Output
MISO	Multiple Input Single Output
MMSE	Minimum Mean-Squared Error
NRP	Normalized Received Power
OFDM	Orthogonal Frequency Division Multiplexing
OSIC-MMSE	Ordered Successive Interference Cancellation MMSE
PDF	Probability Density Function
PDP	Power Delay Profile
QAM	Quadrature Amplitude Modulation
QPSK	Quadrature Phase Shift Keying Modulation
QoS	Quality of Service
RDS	Root mean square Delay Spread
rms	Root mean square
SE	Spectrum Efficiency
SER	Symbol Error Rate
SIMO	Single Input Multiple Output
SISO	Single Input Single Output
SIR	Signal to Interference Ratio

SINR	Signal to Interference plus Noise Ratio
SM	Spatial Multiplexing
SNR	Signal to Noise Ratio
SNR_i	SISO input SNR
SSNR	Start SNR
STBC	Space Time Block Coding
STC	Space Time Coding
MIMO-tx-sel-rx-MRC	MIMO transmit selection receive Maximum Ratio Combining
ZF	Zero Forcing

Symbols

a	Path Loss Exponent
A	Peak amplitude of Line of Sight signal
B	Total bandwidth
B_C	Coherence bandwidth
B_d	Frequency bandwidth of data or information signal
B_D	Doppler spread
B_S	Information bearing signal bandwidth
Bt	Transmission bandwidth for CDMA systems
C	Capacity
E_S	Received symbol energy
f_c	Carrier frequency
G_P	Processing Gain or Spreading Factor
G_{SNR}	Gain in Signal to Noise Ratio
K	Rician K factor
K_G	Rician K gain of MIMO over SISO
L	Length of shift register for PN code in CDMA systems
M	Modulation level
m	Number of receive antennas
N_{cd}	Length of chip code in CDMA systems
N_d	Number of information signal subcarriers
N_p	Number of multipath rays
N_S	Number of subcarriers in OFDM system
N_{SB}	Number of subbands in OFDM systems
N_{sbg}	Number of subcarriers in the gth subband for OFDM systems
N_0	Spectral density of AWGN noise power (W/Hz)
N_J	Received interference power spectrum density (W/Hz)
N_u	user number per sector in CDMA systems
n	Number of transmit antennas
P	Power
P_e	Error probability
P_R	Received Power
P_T	Total transmit power
$r(t)$	Received signal in time domain
R_b	Bit rate
R_c	Coding rate

R_{tb}	Total bit rate of a system
R_{cd}	Rate of chip code in CDMA systems
R_S	Symbol rate
S	Data symbol in frequency domain
s	Data symbol in time domain
SE	Spectrum Efficiency
SE_{am}	SE of adaptive OFDM algorithm in MIMO channels
SE_{as}	SE of adaptive OFDM algorithm in SISO channels
SE_{MIMO}	SE of OFDM system in MIMO channels without adaptivity
$SINR_BD$	SINR boundary matrix
T_{cd}	Period of chip code in CDMA systems
T_b	Bit duration
T_C	Coherence time
T_{FFT}	Effective transmission time in an OFDM symbol, i.e., FFT time
T_g	Guard time in an OFDM symbol
T_S	Symbol period
T_w	Windowing time in an OFDM symbol
Z	Slope of the linear decrease of power delay profile of time domain channel model
β	Roll-off factor of raised cosine filter
ρ	Amplitude of multipath rays
σ	rms value of the received voltage signal for Gaussian noise
σ_{int}^2	Interference power in CDMA systems
σ_τ	rms delay spread
$\sigma_{\max}$	Maximum delay spread
Δf	Subcarrier bandwidth of OFDM system
η	Power spectrum density

Table of Contents

Summary ……...VII

Abbreviations ……... IX

Symbols …….. XI

Table of Contents …….. XIII

Chapter 1 – Introduction ……..…. 1

1.1 Research Background ……. 1

1.2 Research Motivation …….. 3

1.3 Scope and Novelties of this Dissertation …… 3

1.4 Outline of the Thesis ……..….. 5

References ……...…….. 7

Chapter 2 – Channel Characteristics …….. 13

2.1 Introduction ……..….. 13

2.2 Space Domain ……...…… 16

2.3 Frequency Domain ……...……. 17

2.4 Time Domain ……...……. 18

2.5 Relation between the Parameters in Different Domains ……... 20

2.6 Categories of Small-Scale Fading ……. 21

2.7 Rayleigh and Rician Distributions …… 22

2.8 Channel Models in Time and Frequency Domain ……..…….. 24

2.8.1 Channel Model in Time Domain ……..…… 24

2.8.2 Channel Model in Frequency Domain ……..……... 25

2.9 Influence of Rician *K* Factor and Delay Spread on Channel Properties in Frequency Domain ……..…… 27

2.10 Evaluation of Channel Properties in Different Domains ……..…….. 31
2.11 Conclusions …….…… 32
References ……...…… 34
Chapter 3 – Adaptive Modulation Analysis ……... 37
3.1 Introduction …….…….. 37
3.2 Introduction of Adaptive Modulation ……... 39
3.2.1 Development of Adaptive Modulation …… 39
3.2.2 Definition of Adaptive Modulation …….……. 41
3.2.3 Architecture of Adaptive Modulation Systems..…….. 43
3.2.4 Objective of Adaptive Modulation …….……. 44
3.2.5 Adaptive Modulation Categories ……. 44
3.2.6 Advantages of Adaptive Modulation ……... 45
3.2.7 Disadvantages and Limits of Adaptive Modulation Systems …….. 45
3.3 Parameters Influencing Throughput ……. 46
3.3.1 Introduction …….……. 46
3.3.2 Throughput Formulas for OFDM Systems …….…… 47
3.3.3 Throughput Formula for CDMA Systems …….…….. 51
3.4 Parameters Influencing QoS ……. 51
3.4.1 Performance of Parameters in the OFDM Throughput Formula ……. 51
3.4.2 New Factor for OFDM System Performance in a Time-Varying Channel ……. 54
3.4.2.1 Effect of Subcarrier Bandwidth ……..…… 55
3.4.2.2 Relationship between Subcarrier bandwidth and RDS ……..……. 56
3.4.2.3 Influence of P_{FR} on BER ……. 60
3.4.2.4 Prerequisites for P_{FR} ……... 61
3.4.3 Performance of Parameters in the CDMA Throughput Formula …..……..…. 67
3.5 Strategies for Adaptive Modulation Algorithms ……...…….....… 67
3.5.1 Work Procedures for Setting-up Adaptive Modulation Algorithms …....……... 67
3.5.2 Work Procedures for Adaptive OFDM Algorithms ……...…….……. 68
3.5.3 Work Procedures for Adaptive CDMA Algorithms ……..…….……. 74
3.6 Conclusions …….…….. 80
References ……...…… 84

Chapter 4 – Multiple Input Multiple Output (MIMO) Systems …….. 89
4.1 Introduction ……..…….. 89
4.2 Definition of MIMO Systems ……... 90
4.2.1 MIMO Systems with One Modulator/Demodulator …… 91
4.2.2 MIMO Systems with Multiple Modulators/Demodulators …….. 92
4.2.3 MIMO Channel Functions ……... 93
4.3 Advantages and Disadvantages of MIMO …… 94
4.4 Analysis of MIMO Systems Compared with Non – MIMO Systems ……..…… 95
4.4.1 Single Input Single Output (SISO) Systems …… 96
4.4.2 Single Input Multiple Output (SIMO) Systems ……...…… 96
4.4.3 Multiple Input Single Output (MISO) Systems ……...…… 97
4.4.4 MIMO Systems …… 99
4.5 MIMO Schemes ……..…… 100
4.6 Influence of Line of Sight (LOS) on MIMO ……..…….. 103
4.7 Simulation Results of SNR and Spectral Efficiency Gain of MIMO ……. 105
4.7.1 SNR Gain for Different 2 x 2 MIMO Schemes ……. 105
4.7.2 Spectral Efficiency (SE) Gain for Different 2 x 2 MIMO Schemes …….. 107
4.8 Generalization of SNR and Capacity of MIMO …….……...…. 109
4.8.1 Diversity Scheme ……..……. 109
4.8.2 SM Scheme …… 109
4.9 Rician *K* Factor Gain of MIMO over SISO ……...……. 110
4.9.1 BER Performance of the Considered SISO Model …… 111
4.9.2 Rician *K* Gain …….…… 113
4.10 Conclusions ……... 120
References ……. 124
Chapter 5 – Adaptive Modulation Algorithms for SISO and MIMO Channels ……... 127
5.1 Introduction ……. 127
5.2 Adaptive OFDM Algorithms for SISO Channels ……... 128
5.2.1 A Global Flow Chart of Adaptive OFDM Algorithms for SISO Channels ….. 128
5.2.2 Guard Time Setting …… 131
5.2.3 Setting of the Subcarrier Bandwidth …….. 132

5.3 Subband Setting of Adaptive OFDM Algorithms ……..…. 133
5.3.1 Analysis of Subband Settings ……...……. 133
5.3.2 Proposals for Consecutive Subband Setting …….. 138
5.4 Adaptive OFDM Algorithms for MIMO Channels …… 143
5.4.1 Global Flow Chart of Adaptive OFDM Algorithms for MIMO Channels …….143
5.4.2 Setting MIMO Parameters ……. 144
5.5 Adaptive CDMA Algorithms for MIMO Channels …… 145
5.6 Simulators and Assumptions of the Algorithms …….……...……. 149
5.6.1 Simulators of Algorithms for SISO/MIMO Channels ……..……. 149
5.6.2 Assumptions Used in the Simulations ……...…… 151
5.7 Simulation Results of Adaptive OFDM Algorithms for SISO Channels ……... 152
5.8 Simulation Results of Adaptive OFDM Algorithms for MIMO Channels ……..... 157
5.9 Simulation Results of Adaptive CDMA Algorithms for MIMO Channels……. 166
5.10 Conclusions ……..…..... 171
References ……..……...… 174
Chapter 6 – Conclusions and Recommendations ……. 175
6.1 Conclusions ……. 175
6.2 Novelties ……. 179
6.3 Recommendations for Future Work …… 180
Appendix A – OFDM Modulation ……. 181
A.1 Schematic of OFDM Transmission Systems ……. 181
A.2 Structure of OFDM Symbols ……. 184
A.3 OFDM Parameters ……. 185
A.4 Error Probability Analysis ……. 187
References ……. 189
Appendix B – CDMA Modulation ……. 191
B.1 Schematic of CDMA Systems …… 191
B.2 CDMA Parameters ……. 195
B.3 Signal to Interference plus Noise Ratio (SINR) Analysis for CDMA Systems ……. 197
B.4 Error Probability Analysis …….……. 198
References ……..……... 200

Appendix C – Results of Capacity and Output SNR of Different MIMO Systems ….. 201
C.1 Formulas of Output SNR and Capacity of Different MIMO Systems ……...…… 201
C.2 Simulation Results of CDF of Capacity and Output SNR ……. 202
References ……..…... 208
Publications by the Author ……. 209
Journal Papers ……... 209
Conference Papers …… 209
Reports …….. 210
Publication Cross-Reference Table ……... 211
Samenvatting ……... 213
Acknowledgements …….. 215
Curriculum Vitae …… 217

Chapter 1

Introduction

1.1 Research Background

Adaptive modulation is an important component of software radio [1]. The adaptive technique is indispensable to make software radio flexible and re-configurable. In 1991, adaptive modulation was first proposed by Steele and Webb to combat the time-selective fading of wireless channels [2, 3]. Its purpose is to change the wide sense modulation parameters, i.e., the modulation levels, coding rate, and the parameters of multiple access and multiplexing in accordance with the instantaneous channel situation to get a higher throughput and/or better transmission quality [4]. When the channel is favorable, higher modulation parameters are assigned to get a higher throughput; when the channel quality is poor, lower modulation parameters are assigned to guarantee the transmission quality of the system.

Adaptive modulation is developed in three stages [4]. The first stage is narrow sense adaptive modulation in a certain multiple access (MA) system. The adaptive parameters are the narrow sense modulation parameters, i.e., the modulation level and coding rate. Adaptive modulation in the "wide sense" (i.e., where the adaptive parameters include parameters of multiple access/multiplexing modulation, e.g., TDMA, CDMA, OFDM) originates from adaptive modulation in the "narrow sense" in TDMA systems. In TDMA systems, adaptive modulation is used to change the modulation level, symbol rate, coding rate and power dynamically according to the instantaneous channel situation to meet the system transmission requirements and to get a maximum throughput. Related work has been reported in the literature, e.g., [5-7]. Adaptive modulation in CDMA systems becomes less important due to the change of system strategy in CDMA systems. The basic strategy in CDMA systems uses adaptive DS/SS (Direct Sequence/Spread Spectrum) parameter control [8]. Thus, adaptive modulation in

CDMA systems is mainly related to coding. Adaptive modulation in OFDM systems has been studied at, for example, the University of Southampton [9]. Based on the predicted channel conditions, they used appropriate modulation for each group of subcarriers; severely faded subcarriers were excluded; the coding rate of error correction was considered; and preequalization was applied [8-19]. Narrow sense adaptive modulation in MC-CDMA systems has not got much attention. This is because MC-CDMA modulation includes OFDM and CDMA parameters, each of which attracts the attention for adaptation.

The second stage in the development of an adaptive modulation technique is adaptive multiple access/multiplexing schemes, in which multiple access (MA) or multiplexing parameters are adaptive. Adaptability is taken to a higher level by a change in system strategy. Adaptive CDMA has been studied by changing DS/SS parameters, e.g., the processing gain in SISO systems [8]. Adaptive OFDM is used to adapt OFDM parameters according to the channel situation [20]. Adaptation in cyclic extension/guard time, for example, is applied to use a longer guard time in case of longer delay spread and a shorter one in the opposite case. As for adaptive MC-CDMA, not much work on this problem has been reported in literature [10].

An adaptive modulation technique with an even higher level of adaptation has been proposed by Osaka University in Japan, i.e., adaptive selection of MA schemes, [21]. This is the third stage in the development of an adaptive modulation technique. The idea is to change MA schemes (e.g, TDMA, CDMA) by a certain criterion according to user's QoS like the requested transmission rate, tolerable BER, delay, and various factors to maximize system capacity under current channel conditions and frequency bandwidth available. The research begins with the choice between TDMA and CDMA. It is expected to give solutions to many practical difficulties, e.g., how to support more applications/services in one system.

The Multiple Input Multiple Output (MIMO) technology was proposed to alleviate the fading from multi-paths and turn it into an advantage by employing multiple transmit and receive antennas [22]. MIMO has two kinds of schemes, i.e., diversity schemes and Spatial Multiplexing (SM) schemes [23]. Diversity schemes can improve the transmission quality by exploiting the diversity gain offered by multiple transmit antenna set-up. Spatial multiplexing schemes can improve the throughput by sending independent signals from each transmit antenna via parallel multiple channels.

Space time coding is a diversity scheme. Alamouti, Jafarkhani and Calderbank have proposed space-time block coding [24-26]. The performance of space-time block codes has been investigated in literature [27-28]. What is more, space-time trellis coding has been proposed by Tarokh, Seshadri, Calderbank and Naguib [29-34]. Space-time trellis coding combines designed channel coding, modulation, diversity at transmit and optional diversity at receive. The performance criteria for designing space-time trellis codes are outlined in [29] for slow and flat fading channels. Space-time coding for fast and frequency-selective fading channels has been described in literature as well [35-38]. In order to eliminate Inter Symbol Interference (ISI), OFDM was combined with space-time coding by numerous researchers [39-46].

SM schemes have been proposed by Paulraj and Kailath [47], and were later practically demonstrated by Foschini [48] in Bell Labs. SM is a technology that exploits the ability of

MIMO systems to practically achieve the theoretical capacity limit. SM schemes use spatial multiplexing at the transmitter. A high rate bit stream is demultiplexed among the multiple transmit antennas, each of which transmits an independently modulated/coded signal, simultaneously and in the same frequency band [48-50]. Various techniques have been investigated to recover the signals at receive, for example, Zero-Forcing (ZF) [51-53], Minimum Mean-Squared Error (MMSE) [51-52], Successive Interference Cancellation MMSE (SIC-MMSE) [54], and Ordered Successive Interference Cancellation MMSE (OSIC-MMSE) [46, 55-56].

Comparison of diversity schemes and SM schemes has been studied in literature [57-62]. The results show that MIMO techniques can improve the throughput or the transmission quality of radio systems [60]. However, methods from one category (e.g., SM) often have to sacrifice their gain (e.g., data rate) to get the other benefit (e.g., diversity) [23, 60-61]. A mathematical interpretation of the trade-off between the two approaches is presented in [61]. Just because of this, the results in the literature indicate that adaptive OFDM for MIMO channels can hardly outperform adaptive OFDM for SISO channels in terms of throughput (or transmission quality) without sacrificing transmission quality (or throughput) [63]. Our proposals in this thesis, however, will provide a breakthrough in this matter. The correlation effect among the antennas has been investigated in the literature as well, for different MIMO technologies [64].

1.2 Research Motivation

One of the important properties of a wireless channel is its non-deterministic character. This results in an unstable performance and throughput if the configuration of a transmission system is constant. Adaptive modulation can solve this problem. By changing the values of the modulation parameters dynamically, we can significantly improve the system performance and throughput. Moreover, a system can serve various applications by means of using adaptive modulation techniques. For these reasons, we investigated adaptive modulation techniques.

1.3 Scope and Novelties of this Dissertation

In this thesis we concentrate on adaptive OFDM algorithms for SISO (Single Input Single Output) and MIMO systems and adaptive CDMA algorithms for MIMO systems. We divide the work into three parts: channel, modulation, and adaptive modulation algorithm, as shown in Figure 1.3-1. Instant and perfect channel estimation is assumed to be available for systems in this thesis.

- Channel

We investigate SISO and MIMO channels in this thesis (see Figure 1.3-1). We do not build new SISO channel models, nor do we design new MIMO schemes.

The novelty related to SISO channel is that we analyze the channel in terms of different domains: time domain, frequency domain, and space domain, which is convenient for the design of adaptive modulations. Further, we indicate solutions/techniques to the problems in each of the different domains. The contribution of this thesis related to MIMO channel is that we provide MIMO gain in terms of the Rician *K* and SNR over a large range. This has not been found in literature.

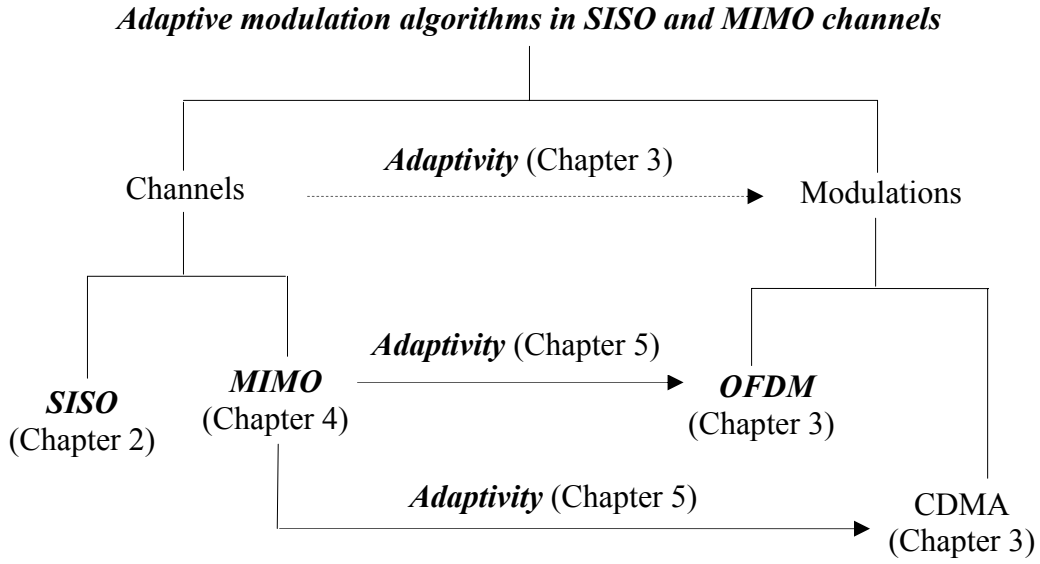


Figure 1.3-1. The scope and novelties of the thesis
(The novelties of the work are in the parts in bold and italics)

- Modulation

In this work we investigate OFDM and CDMA modulation (see Figure 1.3-1).

The novelties related to modulation in this dissertation are that we derive new throughput formulas for OFDM and CDMA modulation; additionally we define a new parameter influencing the transmission quality of OFDM systems, and describe how it works.

- Adaptive modulation algorithm

The contribution of this thesis related to adaptive modulation algorithms is that we find strategies and work procedures for adaptive modulation; we propose new adaptive OFDM algorithms with different subband settings for SISO systems. Further, we combine adapting MIMO parameters into our adaptive OFDM algorithms. In our adaptive CDMA algorithms for MIMO systems, we combine adapting MIMO parameters into an adaptive CDMA algorithm to get a higher throughput at the required transmission quality, which is also novel.

1.4 Outline of the Thesis

Figure 1.4-1 presents the organization of the thesis. We will investigate channel characteristics in terms of time, frequency, and space domain in Chapter 2. Techniques to solve channel fading will be provided for each domain.

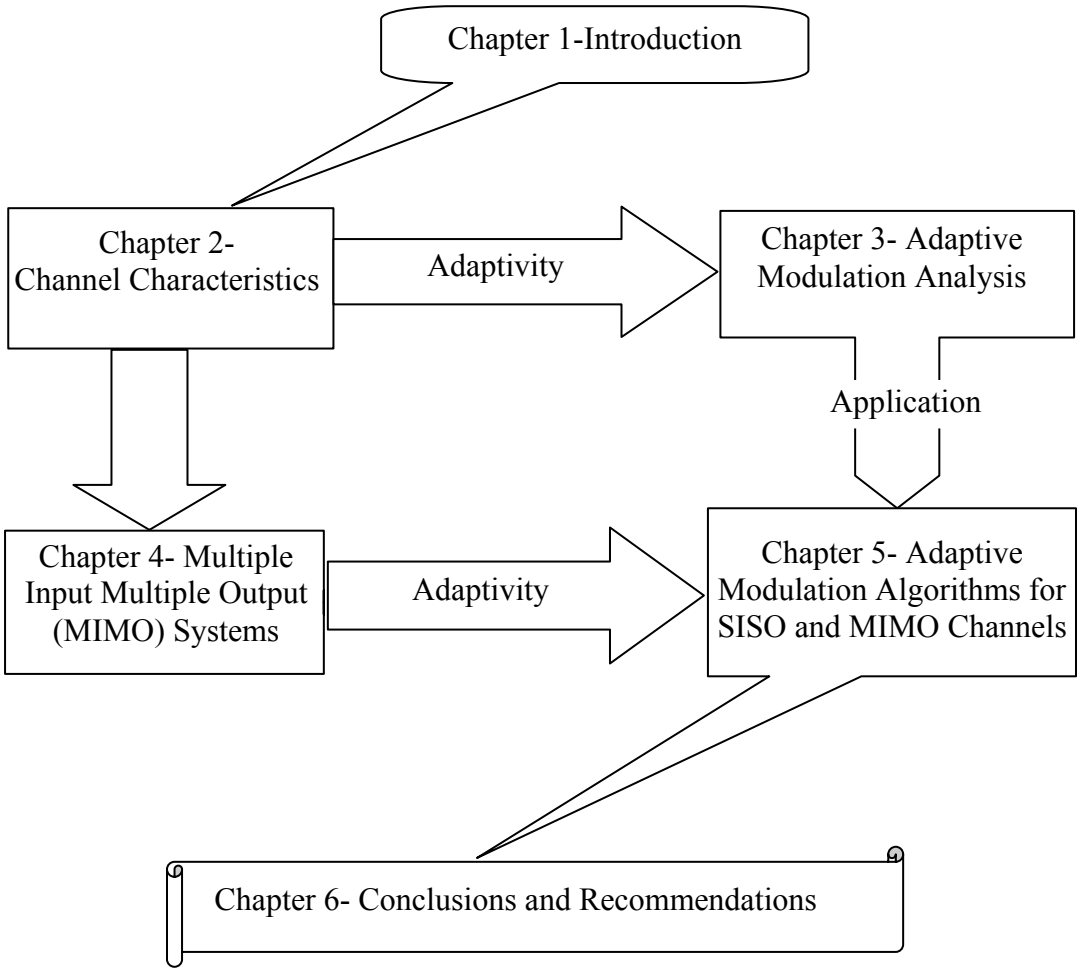


Figure 1.4-1. Outline of the thesis

In Chapter 3 the concept, developing process, strategy and work procedure of adaptive modulation will be investigated by means of examples of adaptive OFDM modulation and adaptive CDMA modulation. We will mainly focus on adaptive OFDM. The adaptivity is based on the current channel, described in Chapter 2.

MIMO channels will be analyzed in Chapter 4. Different MIMO schemes will be elucidated. In addition, MIMO gains of different schemes will be studied for adaptive modulation algorithms.

In Chapter 5 we propose three adaptive modulation algorithms, i.e., adaptive OFDM algorithms for SISO channels with three subband-settings; one for MIMO channels; and an adaptive CDMA algorithm for MIMO channels. Simulation results will be presented to evaluate the algorithms.

Conclusions and recommendations will be summarized in Chapter 6.

References

[1] Che, H.; Hajian, M.; Ligthart, L.P.; Prasad, R.; "Software radio is walking into implementation stage", 12th Tyrrhenian International Workshop on Digital Communications "Software Radio Technologies and Services", Portoferraio, Italy; September 2000, invited paper;

[2] Steele, R., and Webb, W., "Variable rate QAM for data transmission over Rayleigh fading channels," *Proceedings of Wireless 1991*, Calgary, Alberta, p1-14;

[3] Webb, W.; Steele, R.; "Variable rate QAM for mobile radio," *IEEE Transactions on Communications,* vol. 43, July 1995;

[4] Che, H.; Ligthart, L.P.; Prasad, R.; "A Throughput Formula for Adaptive OFDM System", 5th IEEE Malaysia International Conference on Communications - MICC Conference, P299-303; Kuala Lumpur, Malaysia; October 2001;

[5] Goldsmith, A. J., "Adaptive Coded Modulation for Fading Channels" IEEE Transactions on Communications. Vol.46, No.5, May 1998;

[6] Mizuno, M., "High Speed Multimedia-Multimode TDMA Radio Transmission System for IMT-2000" IEICE Transaction on Communications, vol. E81-B, No.7 July 1998;

[7] Ue, T., "Symbol Rate and Modulation Level-controlled Adaptive Modulation/TDMA/TDD System for High-Bit-Rate Wireless Data Transmission" IEEE Transactions on Vehicular Technology. Vol.47, No.4 November 1998;

[8] Ganesh, R., Pahlavan, K., Zvonar, Z., *Wireless Multimedia Network Technologies*, Boston: Kluwer, 2000;

[9] Hanzo, L., Webb, W., and Keller, T., eds., *Single- and Multi-carrier Quadrature Amplitude Modulation.* Wessex, England: John Wiley &Sons, Ltd, 3rd ed., 2000. ISBN 0471492396;

[10] Hanzo, L., Munster, M., Choi, B-J, and Keller, T., *OFDM and MC-CDMA for broadband multi-user communications, WLANs and broadcasting.* John Wiley and IEEE Press, 2003, http://www-mobile.ecs.soton.ac.uk;

[11] Hanzo, L., Wong, C., and Yee, M., *Adaptive Wireless Trasceivers.* John Wiley, IEEE Press, 2002, http://www-mobile.ecs.soton.ac.uk;

[12] Torrance, J. and Hanzo, L., "Latency and networking aspects of adaptive modems over slow indoors Rayleigh fading channels", *IEEE Transactions on Vehicular Technology,* vol. 48, no.4, pp.1237-1251, 1998;

[13] Torrance, J. and Hanzo, L., "Performance upper bound of adaptive QAM in slow Rayleigh fading environments", in *ISPACS '96,* Singapore, pp. 1653-1657, Nov. 1996;

[14] Torrance, J., and Hanzo, L., "Interference aspects of adaptive modems over slow Rayleigh fading channels", *IEEE Transactions on Vehicular Technology,* vol. 48, pp. 1527-1545, Sep. 1999;

[15] Keller, T., and Hanzo., L., "Adaptive orthogonal frequency division multiplexing schemes", *Proceedings of ACTS Mobile Communications Summit '98,* Rhodos, Greece, pp.794-799, Jun. 1998;

[16] Keller, T., and Hanzo, L., "Blind-detection assisted sub-band adaptive turbo-coded OFDM schemes", *Proceedings of VTC '99,* Houston, USA, pp. 127-130, Mar. 1999;

[17] Matsuako, H., Sampei, S., Morinaga, N., and Kamio, Y., "Adaptive modulation systems with variable coding rate concatenated code for high quality multi-media communication systems", *Proceedings of IEEE Vehicular Technology Conference,* Atlanta, USA, pp. 487-491, Apr. 1996;

[18] Chua, S. G., and Goldsmith, A., "Variable-rate variable-power mQAM for fading channels" *Proceedings of IEEE VTC '96,* Atlanta, GA, USA, pp. 815-819, 1996;

[19] Lau, V., and Macleod, M., "Variable rate trellis coded QAM for high bandwidth efficiency applications in Rayleigh fading channels" *Proceedings of IEEE VTC '98,* Ottawa, Canada, pp. 348-352, May 1998;

[20] Kalet, I., "The multitone channel", *IEEE Transactions on Communications*, vol. 37, pp. 119-124, Feb. 1989;

[21] Hara, S., Kitazawa, D., Yomo, H., "Adaptive Access Scheme Selection in Software-Based Wireless Multimedia Communications" 12th Tyrrhenian International Workshop on Digital Communications-Software Radio Technologies and Services, 2000, Italy;

[22] Song, B.G., Ritcey, J. A., "Overlaying Multiple Users in Acoustic Communications Using MIMO Spatial Diversity Equalization", 29th Asilomar Conference on Signals, Systems and Computers, Pacific Grove, CA, USA, Oct. 30 – Nov.2, 1995

[23] Catreus, S.; Greenstein, L. J.; Erceg, V.; "Some Results and Insights on the Performance Gains of MIMO Systems" IEEE Journal on Selected Areas in Communications, vol. 21, No. 5 June 2003;

[24] Alamouti, S., "A simple transmit diversity technique for wireless communications", *IEEE Journal on Selected Area in Communications,* vol. 16, pp. 1451-1458, Oct. 1998;

[25] Tarokh, V., Jafarkhani, H., and Calderbank, A., "Space time block codes from orthogonal designs", *IEEE Transactions on Information Theory,* vol. 45, pp. 1456-1467, Jul. 1999;

[26] Tarokh, V., Jafarkhani, Calderbank, A., "Space-time block coding for wireless communications: Performance results", *IEEE Journal on Selected Area in Communications,* vol. 17, pp. 451-460, Mar. 1999;

[27] Liew, T., and Hanzo, L., "Space-time block codes and concatenated channel codes for wireless communications", *Proceedings of the IEEE,* vol. 90, pp.183-219, Feb. 2002;

[28] Hanzo, L., Liew, T, and Yeap, B., *Turbo Coding, Turbo Equalisation and Space-Time Coding.* John Wiley, IEEE Press, 2002; http://www-mobile.ecs.soton.ac.uk;

[29] Seshadri, N., Tarokh, V., and Calderband, A., "Space-time codes for high data rate wireless communication: Code construction" *Proceedings of IEEE Vehicular Technology Conference '97,* Phoenix, Arizona, pp. 637-641, 1997;

[30] Tarokh, V., Seshadri, N., and Calderbank, A., "Space-time codes for high data rate wireless communication: Performance criterion and code construction", *Proceedings of IEEE International Conference on Communications '97,* Montreal, Canada, pp. 299-303, 1997;

[31] Tarokh, V., Naguib, A., Seshadri, N., and Calderbank, A., "Space-time codes for high data rate wireless communication: Mismatch analysis", *Proceedings of IEEE International Conference on Communications '97,* Montreal, Canada, pp. 309-313, 1997;

[32] Tarokh, V., Seshadri, N., and Calderbank, A., "Space-time codes for high data rate wireless communication: Performance criterion and code construction" *IEEE Transactions on Information Theory,* vol. 44, pp. 744-765, Mar. 1998;

[33] Naguib, A., Tarokh, V., Seshadri, N., and Calderbank, A., "A Space-time coding modem for high-data-rate wireless communication", *IEEE Journal on Selected Areas in Communications,* vol. 16, pp. 1459-1478, Oct. 1998;

[34] Tarokh, V., Naguib, A., Seshadri, N., and Calderbank, A., "Space-time codes for high data rate wireless communication: Performance criteria in the presence of channel estimation errors, mobility, and multiple paths", *IEEE Transactions on Communications,* vol. 47, pp. 199-207, Feb. 1999;

[35] Naguib, A., Seshadri, N., and Calderbank, A., "Increasing data rate over wireless channels", *IEEE Signal Processing Magazine,* vol. 17, pp. 76-92, May 2000;

[36] Bauch, G., Naguib, A., and Seshadri, N., "MAP equalization of space-time coded signals over frequency selective channels", *Proceedings of Wireless Communications and Networking Conference,* New Orleans, USA, Sep. 1999;

[37] Bauch, G., and Al-Dhahir, N., "Reduced-complexity turbo equalization with multiple transmit and receive antennas over multipath fading channels", *Proceedings of Information Sciences and Systems,* Princeton, USA, pp. WP3 13-18, Mar. 2000;

[38] Choi, W. J., and Cioffi, J., "Space-time block codes over frequency selective fading channels", *Proceedings of VTC 1999 Fall,* Amsterdam, The Netherlands, pp. 2541-2545, Sep. 1999;

[39] Agrawal, D., Tarokh, V., Naguib, A., and Seshadri, N., "Space-time coded OFDM for high data-rate wireless communication over wideband channels", *Proceedings of IEEE Vehicular Technology Conference, Ottawa, Canada,* pp. 2232-2236, May 1998;

[40] Li, Y., Seshadri, N., and Ariyavisitakul, S., "Channel estimation for OFDM systems with transmitter diversity in mobile wireless channels", *IEEE Journal on Selected Areas in Communications,* vol. 17, pp. 461-471, Mar. 1999;

[41] Li, Y., Chuang, J., and Sollenberger, N., "Transmitter diversity for OFDM systems and its impact on high-rate data wireless networks", *IEEE Journal on Selected Areas in Communications,* vol. 17, pp. 1233-1243, Jul. 1999;

[42] Liu, Z., Giannakis, G., Scaglione, A., and Barbarossa, S., "Block precoding and transmit-antenna diversity for decoding and equalization of unknown multipath channels", *Proc 33rd Asilomar Conference Signals, Systems and Computers, Pacific Grove, Canada,* pp. 1557-1561, Nov. 1999;

[43] Liu, Z., and Giannakis, G., "Space-time coding with transmit antennas for multiple access regardless of frequency-selective multipath", *Proc 1st Sensor Array and Multichannel SP Workshop,* Boston, USA, Mar. 2000;

[44] Lu, B. and Wang, X., "Space-time code design in OFDM systems," Global Telecommunication Conference, 2000. GLOBECOM`00. IEEE, Vol. 2, pp. 1000-1004, 2000;

[45] Piechocki, R., Fletcher, P., Nix, A., Canagarajah, N., and McGeehan, J., "Performance of spacetime coding with HIPERLAN/2 and IEEE 802.11a WLAN standards on real channels," Vehicular Technology Conference, 2001, VTC 2001 Fall. IEEE VTS 54th, Vol. 2, pp. 848-852, 2001;

[46] So, D. K. C, and Cheng, R. S., "Performance evaluation of space-time coding over frequency selective fading channel," Vehicular Technology Conference, 2002, VTC 2002 Spring. IEEE VTS 55th, Vol. 2, pp. 635-639, 2002;

[47] Paulraj, A. and Kailath, T., "Increasing capacity in wireless broadcast systems using distributed transmission/directional reception," U. S. Patent, no. 5,345,599, 1994;

[48] Foschini, G. J., and Gans, M. J., "On limits of wireless communications in a fading environment when using multiple antennas," *Wireless Pers.Commun.*, vol. 6, pp. 311–335, Mar. 1998;

[49] Telatar, I. E., "Capacity of multi-antenna Gaussian channels," *Eur. Trans. Telecomm.*, vol. 10, pp. 585–595, Nov./Dec. 1999;

[50] Foschini, G. J., Golden, G. D., Valenzuela, R. A., and Wolniansky, P. W., "Simplified processing for wireless communication at high spectral efficiency," *IEEE J. Select. Areas Commun.—Wireless Commun. Series*, vol. 17, pp. 1841–1852, Nov. 1999;

[51] Gore, D. A., Heath, R. W. Jr., and Paulraj, A. J., "Performance Analysis of Spatial Multiplexing in Correlated Channels," submitted to Communications, IEEE Transactions Mar. 2002;

[52] Bolcskei, H. and Paulraj, A., "Multiple -Input Multiple-output (MIMO) wireless systems," In J. Gibson, editor, *The communications Hadbook.* CRC Press, 2001

[53] Zelst, A. van, "Space Division Multiplexing Algorithm," Proc. of IEEE MEleCon 2000.3, pp. 1218-1221, May 2000;

[54] Debbah, M., Muquet, B., de Courville, M, Muck, M., Simoens, S., and Loubaton, P., "MMSE Successive Interference Cancellation Scheme for new Spread OFDM Systems," Vehicular Technology Conference, Tokyo, Japan, May 2000;

[55] Catreux, S., Driessen, P. F., and Greenstein, L. J., "Data throughputs using multiple-input multiple-output (MIMO) techniques in a noise-limited cellular environment," *IEEE Trans. Wireless Commun.*, vol. 1, pp. 226–235, Apr. 2002;

[56] Ariyavisitakul, S. L., "Turbo space-time processing to improve wireless channel capacity," in *Proc. IEEE Int. Conf. Communications ICC 2000*, vol. 3, New Orleans, LA, June 2000, pp. 1238–1242;

[57] Heath, R.W., "Space-Time Signaling in Multi-Antennas Systems," Ph.D. dissertation, Dept. Elec. Eng., Stanford Univ., Stanford, CA, Nov. 2001;

[58] Nabar, R. U., Bölcskei, H., Erceg, V., Gesbert, D., and Paulraj, A. J., "Performance of multi-antenna signaling strategies in the presence of polarization diversity," *IEEE Trans. Signal Processing*, vol. 50, pp. 2553–2562, Oct. 2002;

[59] Hassibi, B., and Hochwald, B. M., "High-Rate codes that are linear in space and time," *IEEE Trans. Inform. Theory*, vol. 48, pp. 1804–1824, July 2002;

[60] Gesbert, D., and Akhtar, J., "Breaking the barriers of Shannon's capacity: An overview of MIMO wireless systems," Telektronikk Telenor Journal. Jan. 2002;

[61] Zheng, L., and Tse, D. N. C., "Diversity and multiplexing: A fundamental tradeoff in multiple antennas channels," *IEEE Trans. Inform. Theory*, vol. 49, pp. 1073–1096, May 2003;

[62] Lee, Hoo-Jin; Patil, Shailesh; Raj, Raghu G.; "Fundamental overview and simulation of MIMO systems for Space-Time coding and Spatial Multiplexing", http://www.ece.utexas.edu/~wireless/EE381K11_Spring03/project.htm;

[63] Liew, T. H., Hanzo, L., "Space-time Trellis and space-time block coding versus adaptive modulation and coding aided OFDM for wideband channels", submitted to IEEE Transaction on Vehicular Technology, Dec. 2003;

[64] Shiu, D. S., et al., "Fading Correlation and its effect on the capacity of multielement antenna systems," IEEE Trans. Commun., Vol. 48, pp. 502-513, Mar. 2000.

Chapter 2

Channel Characteristics

2.1 Introduction

In wireless communications the channel characteristics are of fundamental importance because they limit the transmission quality and throughput directly. In traditional radio systems (i.e., non-adaptive radio systems), the long-term statistical properties of the channel are measured and evaluated before system design. But in adaptive modulation systems, the situation is more complicated. To guarantee that the adaptive function works properly, information about the short-time statistical or even instantaneous properties of the channel is required continuously.

The main limiting factors of a mobile communication system originate from the radio medium. These are mainly:

- Attenuation. The signal strength weakens with distance. Typical attenuation is between 50 and 150 dB depending on distance. [1]
- Shadowing. Obstacles between the base station and the mobile station weaken the signal further.
- Noise. Thermal noise (and possibly other noise) is present in the signal and reduces the quality of signal detection.
- Multipath fading and time dispersion. Reflections and diffractions distort the received signal by spreading it in time. Depending on the bandwidth of the system, this may result in fast variations in signal strength and/or inter symbol interference (ISI).

- Interference. Other transmitters using the same frequency or nearby frequencies may interfere with the desired signal. This may often be seen as extra noise.

Wireless channels can be categorized into two groups: “Large Scale Fading” and “Small Scale Fading”. Traditional propagation models estimate the mean power received at given distances from the transmitter. For large distances (in the order of kilometers), large scale propagation models are used. Small-scale fading describes rapid fluctuations in amplitude, phase, or multipath delay of a radio signal over a short period of time or a short travel distance. It is caused by interference between the multipath waves [2].

Mobile radio channels are extremely random and can vary from simple Line-of-Sight (LOS) paths to severely obstructed multiple paths for different locations, frequency bands and/or moments. Figure 2.1-1 shows that in space domain, a channel has different characteristics (e.g., amplitude) at different locations. We call this space diversity or space-selective fading. Figure 2.1-2 refers to frequency domain characteristics, meaning that the channel has different characteristics at different frequencies. We call this frequency diversity or frequency-selective fading. Figure 2.1-3 shows that in the time domain, a channel has different characteristics at different times. We call this time diversity or time-selective fading. Based on this we can classify channel fading into Space Selective fading (i.e., Space diversity), Frequency Selective fading (i.e., Frequency Diversity), and Time Selective fading (i.e., Time Diversity). This chapter discusses the channel properties in space, frequency, and time domain.

Traditionally channel characteristics are categorized into large-scale fading and small- scale fading. In this chapter the channel characteristics which will be used in our adaptive modulation algorithm will be investigated in terms of their properties in space, frequency, and time domain. Correspondingly, we propose solutions to the fading for each of the three domains. MIMO (Multiple Input Multiple Output) is a solution to space diversity; OFDM (Orthogonal Frequency Division Multiplexing) is a solution to frequency diversity; and adaptivity is a solution to time diversity. At every moment (in the time domain), our adaptive modulation algorithm adapts MIMO parameters and OFDM parameters to combat space-selective fading and frequency-selective fading, respectively.

The structure of this chapter is as follows. In Section 2.2 the channel properties in the space domain will be described. The channel properties in the frequency domain and the time domain will be discussed in Section 2.3 and Section 2.4, respectively. As a requirement of adaptive modulation, the relations among the parameters in different domains will be investigated in Section 2.5. We continue our investigations with small scale fading channel, in order to derive the criteria for adaptive modulation algorithms. We can then change the channel into beneficial type of fading by adapting parameters. In Section 2.7, Rayleigh and Rician distributions are introduced since they will be exploited in our channel model. The channel models in time and frequency domain which will be used in the thesis will then be provided in Section 2.8. The analysis of the channel models will be given in Section 2.9. There we analyze the influence of the Rician K factor and the delay spread on the channel properties in the frequency domain, which will be the basis for the adaptation of the OFDM

parameters in Chapter 5. In Section 2.10 we evaluate our proposal based on the channel properties by offering a solution to channel fading in each domain. Finally we conclude the discussion in Section 2.11.

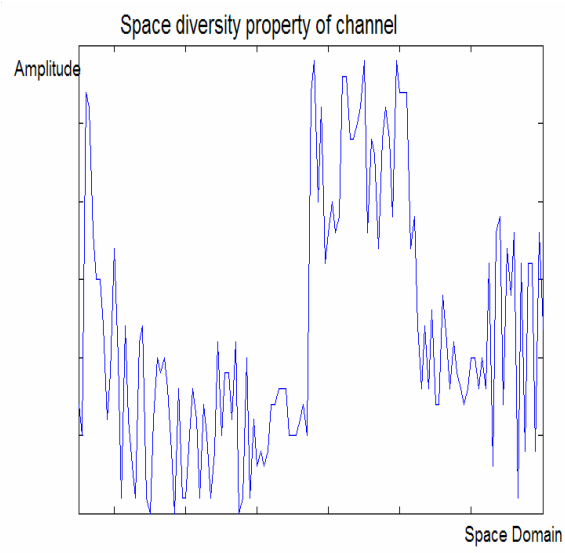


Figure 2.1-1. Channel property in space domain

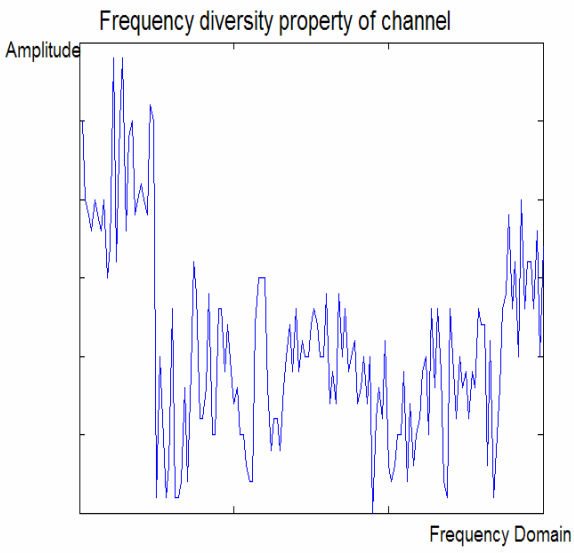


Figure 2.1-2. Channel property in frequency domain

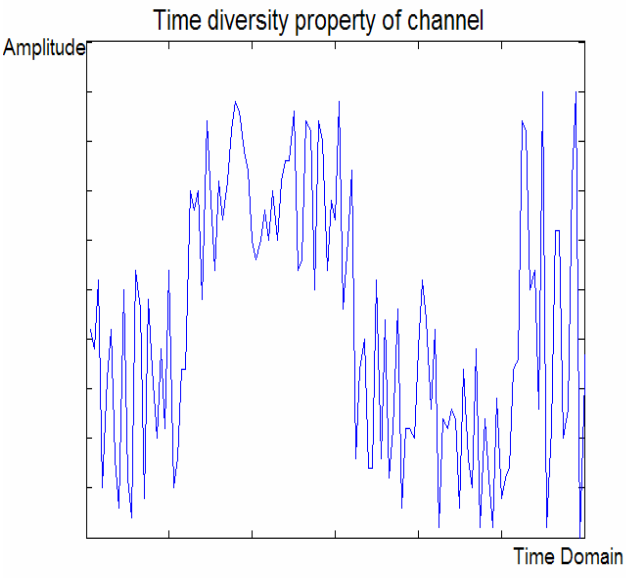


Figure 2.1-3. Channel property in time domain

2.2 Space Domain

The channel properties in space domain include path loss and space diversity. Path loss is connected with large-scale fading while space diversity belongs to small-scale fading. Traditional propagation models estimate the mean received power at a given distance from the transmitter, which is called path loss estimation. When the distance variation is in the order of a wavelength, the channel can show significantly different random characteristics. This is called space diversity.

- Path Loss

Path loss models describe the signal attenuation between a transmit and a receive antenna as function of propagation distance and other parameters. Some models include many details of the terrain profile to estimate the signal attenuation, whereas others just consider carrier frequency and distance [3]-[8]. Antenna height is another critical parameter. The well-know path loss power law yields [2]

$$P :: d^{-a},$$

where a is the path loss exponent ($a = 2$ for free space; $a < 2$ for indoor environments; $a > 2$ for outdoor urban areas).

From theory and measurement we know that the average received signal power decreases logarithmically with distance for both indoor and outdoor environments. What is more, at any distance *d*, the path loss *PL(d)* at a particular location is random and has a log-normal distribution around a mean (distance-dependent) value [9]. If we include the location variability, a large-scale model of path loss *PL*(*d*) at a particular distance *d* can be written as [10]

$$PL(d)[dB] = \overline{PL}(d) + X_\sigma = \overline{PL}(d_0) + 10a\log(\frac{d}{d_0}) + X_\sigma, \tag{2.1}$$

where $\overline{PL}(d)$ is the average large-scale path loss for a transmitter-receiver separation *d*; X_σ is a zero-mean Gaussian distributed random variable (in dB) with standard deviation σ (also in dB); d_0 is the reference distance between the transmitter and the receiver; $\overline{PL}(d_0)$ is the average large-scale path loss for the transmitter-receiver separation d_0; and *a* is the path-loss exponent.

When objects in the radio channel are static for a given time period, and the channel is characterized by flat fading for a given frequency bandwidth, then the channel properties differ only at different locations. In other words, fading is purely a phenomenon in space domain.

- Space Diversity

From equation 2.1 we know that the channel path loss is caused by large-scale statistical estimation together with a random effect. The effect is caused by small-scale fading in the space domain and explains the space diversity. The hindrance of space diversity can be combated by using multiple antennas. Multiple Input Multiple Output (MIMO) is a technique that takes advantage of space diversity to improve system performance and capacity. We will discuss the MIMO technique in chapter 4.

2.3 Frequency Domain

In the frequency domain, the channel suffers from two aspects: frequency modulation and frequency diversity.

- Frequency Modulation

The relative motion between the base station and the mobile station results in random frequency modulation. Due to the relative motion between the mobile station and the base station, each multipath wave undergoes an apparent shift in frequency. The shift in the received signal frequency due to motion is called the Doppler shift, and it is directly proportional to the velocity and direction of motion of the mobile station with respect to the direction of the arrival of the received multipath wave.

The Doppler shift B_D can be expressed as [11]

$$B_D = \frac{v}{\lambda}\cos\theta = \frac{v}{c} f_c \cos\theta , \tag{2.2}$$

where ν is the velocity of the mobile station, λ is the wavelength, θ is the spatial angle between the direction of the incoming wave and the moving direction of the mobile station, c is the velocity of the light, and f_c is the carrier frequency. We can see from this equation that if the mobile station moves towards the direction of the incoming wave, the Doppler shift is positive and the received frequency increases; if the mobile station moves away from the direction of the incoming wave, the Doppler shift is negative and the received frequency is lowered. Therefore, multipath signals arriving from different directions increase the signal bandwidth. When ν and/or θ changes, the Doppler shift changes correspondingly, which causes Doppler spread.

- Frequency Diversity

Frequency diversity is discussed together with another parameter in the frequency domain, i.e., the coherence bandwidth.

The coherence bandwidth is a statistical measure of frequency range over which the channel can be considered “flat” (i.e., in such channel all spectral components pass with approximately equal gain and linear phase). The coherence bandwidth gives the range of

frequencies over which frequency components are amplitude correlated. The coherence bandwidth determines what type of fading occurs in the channel (this will be discussed in Section 2.6), and therefore it will play a basic role in adapting the modulation parameters. The relation between the coherence bandwidth and its time domain equivalent, the delay spread, will be discussed in Section 2.5.

Frequency-selective fading is in strong contrast to flat fading. Flat fading means that all frequency components transmitted through the channel bandwidth are affected by the same magnitude of fading. Conversely, frequency-selective fading, also known as differential fading, means that some parts within the channel bandwidth are affected more by fading than other parts. If the coherence bandwidth of the channel is smaller than the bandwidth of the transmitted signal, the signal suffers from frequency-selective fading (or frequency diversity). This fading will distort the received signal.

2.4 Time Domain

One of the most important differences between wired and wireless radio channels is that the latter varies with time, i.e., it suffers from time-selective fading.

A mobile radio channel may be modeled as a linear filter with a time-varying impulse response. The traditional channel model, i.e., the impulse response model, is a model in the time domain. The small-scale variations of a mobile radio signal can be related directly to the impulse response of the mobile radio channel. If $x(t)$ represents the transmitted signal, $y(t)$ represents the received signal, and $h(t,\tau)$ represents the impulse response of the time-varying multipath radio channel; the received signal can be expressed as a convolution of the transmitted signal with the channel impulse response.

$$y(t) = \int_{-\infty}^{\infty} x(\tau)h(t,\tau)d\tau = x(t) \otimes h(t,\tau), \tag{2.3}$$

where variable t is the time variation, and τ is the channel multipath delay for a fixed value of t.

Multipath reflections of the RF carrier are better known in terms of time dispersion or delay spreading. Time dispersion or delay spreading occurs when a single signal travels from its source to the receive antenna via two or more paths of different lengths. One part of the signal travels directly; while the others are reflected during their travel and take longer time to reach the receive antenna. The signal at receive affected by time dispersion is deteriorated. Reflections must be considered when one plans or optimises digital radio systems that use high data rates.

Time dispersion can be characterized by excess delay, mean excess delay and rms delay spread.

- Root Mean Square Delay Spread (σ_τ)

An important time parameter is the Root mean square Delay Spread (RDS), the square root of the second centralized moment of the power delay profile. The RDS is a good measure of the multipath spread of the channel. It can be used to estimate the potential effect of inter-symbol interference.

$$\sigma_\tau = \sqrt{\overline{\tau^2} - \overline{\tau}^2} \tag{2.4}$$

$$\overline{\tau} = \frac{\sum_k P(\tau_k)\tau_k}{\sum_k P(\tau_k)} \tag{2.5}$$

$$\overline{\tau^2} = \frac{\sum_k P(\tau_k)\tau_k^2}{\sum_k P(\tau_k)} \tag{2.6}$$

In the equations above $P(\tau_k)$ means the power of the multipath at the moment of τ_k.

- Maximum Excess Delay (X dB)

The maximum excess delay (X dB) of the power delay profile is defined as the time delay during which multipath energy falls to XdB below the maximum.

- Coherence Time

Another parameter in time domain is the coherence time, which defines the "staticness" of the channel. The coherence time is the time during which the channel is strongly correlated to the amplitude of the received signal. The coherence time can be denoted by T_C. Different symbols that are transmitted over channel within the coherence time are affected by the same amount of magnitude fading. Hence, we have a channel with relatively slow fading. Different symbols that are transmitted over the channel out of the coherence time, on the other hand, may be affected by different amount of magnitude fading. Therefore, we get a channel with relatively fast fading (this will be discussed in Section 2.6). This means that due to this fast fading some parts of the symbol are affected more than other parts. This property will be considered in our adaptive modulation algorithm. By assigning the value of a certain parameter, we can produce a slow fading channel instead of a fast fading channel, which will offer better performance.

2.5 Relation between the Parameters in Different Domains

We have discussed channel characteristics and its parameters in space, frequency, and time domain. These characteristics do not exist in isolation, that is to say, they are related to each other. Some parameters in one domain may influence the characteristics in another domain.

- Coherence Bandwidth and rms Delay Spread

We know that the power delay profile and the magnitude frequency response of a mobile radio channel are related through the Fourier transform. It is therefore possible to obtain an equivalent description of the channel in the frequency domain using its frequency response characteristics. In analogy to the delay spread parameters in time domain, the coherence bandwidth is used to characterize the channel in the frequency domain. The rms delay spread and the coherence bandwidth are inversely proportional to one another, although their exact relationship is a function of the exact multipath structure [2].

The coherence bandwidth is denoted by *Bc* and it is inversely proportional to the rms delay spread, σ_τ . When the envelope correlation function is more than 90%, the coherence bandwidth has the following relationship with the rms delay spread [12]:

$$B_C \approx \frac{1}{50\sigma_\tau}, \tag{2.7}$$

and when the envelope correlation function is more than 50%, the coherence bandwidth is

$$B_C \approx \frac{1}{5\sigma_\tau}. \tag{2.8}$$

Since the two parameters depend on each other, we can consider them as one parameter set in a system design.

- Coherence Time and Doppler Spread

The coherence time is directly affected by the Doppler shift; it is the time domain dual of the Doppler spread. The Doppler spread and coherence time are inversely proportional to one another. That is,

$$T_C \approx \frac{1}{B_D}. \tag{2.9}$$

Similarly, we can consider these two parameters as one parameter set in the system design.

2.6 Categories of Small-Scale Fading

Depending on the relation between signal parameters (i.e., the bandwidth, symbol period, etc.) and channel parameters (i.e., the rms delay spread, the Doppler spread, etc.), small-scale fading can be categorized based on two aspects: multipath delay spread and Doppler spread. Multipath delay spread leads to time dispersion and frequency-selective fading; so based on this, small-scale fading can be categorized into flat fading and frequency-selective fading. The multipath delay spread is a channel parameter in time domain, while the phenomenon that the channel is flat or frequency selective corresponds to the frequency domain. Thus, the time domain parameter, multipath delay spread, influences the channel characteristic in frequency domain.

Doppler spread leads to frequency dispersion and time-selective fading, so in terms of this, small-scale fading can be categorized into fast fading and slow fading. The Doppler spread is a channel parameter in frequency domain, while the phenomenon that the channel changes fast or slow belongs to time domain. Similarly, the frequency domain parameter, the Doppler spread, influences the channel characteristic in time domain. Knowing these relationships will help us in designing the system.

Table 2.6-1 gives the categories of small-scale fading. If the coherence bandwidth of the channel is much larger than the bandwidth of the transmitted signal, the received signal undergoes flat fading. Then, the symbol period is much longer than the multipath delay spread of the channel. In contrast, if the coherence bandwidth of the channel is smaller than the bandwidth of the transmitted signal, the received signal suffers from frequency-selective fading. In this case, the symbol period is smaller than the multipath delay spread of the channel. When this happens, the received signal is distorted and Inter Symbol Interference (ISI) is induced. What is more, it is much more complex to model frequency-selective fading channels than flat fading channels since each multipath has to be modeled and the channel needs to be modeled as a linear filter. Therefore, it is preferable to deal with a flat fading channel for signal transmission. However, since we can not change the multipath delay spread and coherence bandwidth of the channel, we can only try to design the symbol period and signal bandwidth such that flat fading of the channel results for the transmitted signal. Hence, given the delay spread, to improve the performance of the transmission, we choose such a value for the symbol period in the adaptive modulation algorithm that we get a flat fading channel instead of a frequency-selective one.

Table 2.6-1 Categories of Small Scale Fading

Categorization basis	Fading types	condition
Multipath delay spread	Flat fading	$B_S \ll B_C$; $T_S \geq 10\sigma_\tau$
	Frequency-selective fading	$B_S > B_C$; $T_S < 10\sigma_\tau$
Doppler spread	Fast fading	$T_S > T_C$; $B_S < B_D$
	Slow fading	$T_S \ll T_C$; $B_S \gg B_D$
B_C: coherence bandwidth of channel; B_S: signal bandwidth; T_C: coherence time of channel; T_S: symbol period; σ_τ : rms delay spread of channel; B_D: Doppler spread;		

Based on the Doppler spread, the channel can be classified as fast fading or slow fading. If the channel impulse response (in time domain) changes quickly within the symbol period, i.e., if the coherence time of the channel is smaller than the symbol period of the transmitted signal, the channel creates fast fading on the received signal. This will result in signal distortion. If the channel impulse response changes at a much slower rate than the transmitted baseband signal, the channel creates slow fading on the received signal. Under this condition, the channel behaves static all over certain symbol periods. It is easy to see that a slow fading channel is preferable as it results in a more stable transmission quality. But the Doppler spread is not determined by the system's design. However, we can try to design the symbol period and signal bandwidth to give slow fading on the transmitted signal. Therefore, given the Doppler spread, we choose such a value for the signal bandwidth/subcarrier bandwidth in the adaptive modulation algorithm that we get a slow fading channel instead of a fast fading one, as it results in better performance.

2.7 Rayleigh and Rician Distributions

In mobile radio channels, often Rayleigh and Rician distributions are used to describe the statistical time-varying nature of the received envelope of a flat fading signal. We exploit them in our work, too, so here we give the main characteristics based on reference [2].

- Rayleigh Fading Distribution

The Rayleigh distribution can be seen as a distribution of the envelope of the sum of two quadrature Gaussian noise signals. The Probability Density Function (PDF) of Rayleigh distribution equals

$$p(r) = \begin{cases} \frac{r}{\sigma^2} e^{-\frac{r^2}{2\sigma^2}} & (\infty \geq r \geq 0) \\ 0 & (r < 0) \end{cases} \quad (2.10)$$

,

where r is the received signal envelope voltage, σ is the rms value of the received voltage signal of each of the Gaussian components, and σ^2 is the time-average power of the received signal of each of the Gaussian components.

The mean value, r_{mean}, of the Rayleigh distribution becomes

$$r_{mean} = E[r] = \int_0^\infty rp(r)dr = \sigma\sqrt{\frac{\pi}{2}} = 1.2533\sigma, \tag{2.11}$$

and for the variance of the Rayleigh distribution σ_r^2 (representing the ac power in the signal envelope) we find

$$\sigma_r^2 = E[r^2] - E^2[r] = \int_0^\infty r^2 p(r)dr - \frac{\sigma^2\pi}{2} = \sigma^2(2 - \frac{\pi}{2}) = 0.4292\sigma^2. \tag{2.12}$$

- Rician Fading Distribution

When the received signal has a dominant stationary (non-fading) component, i.e., a line-of-sight (LOS) propagation path, the small scale fading envelope distribution is Rician. In a Rician distribution, the random multipath components arriving at different angles are superimposed on a stationary dominant signal.

The Rician distribution is

$$p(r) = \begin{cases} \frac{r}{\sigma^2} e^{-\frac{(r^2+A^2)}{2\sigma^2}} I_0(\frac{Ar}{\sigma^2}) & (A \geq 0, r \geq 0), \\ 0 \qquad (r < 0) \end{cases} \tag{2.13}$$

where A is the peak amplitude of the dominant signal and $I_0(\bullet)$ is the modified Bessel function of the first kind and zero-order, which equals

$$I_0(y) = \frac{1}{2\pi}\int_{-\pi}^{\pi} e^{y\cos t} dt.$$

The Ricean distribution is often described in terms of a parameter K which is defined as

$$K = \frac{power\ in\ the\ dominant\ path}{power\ in\ the\ scattered\ paths} = \frac{A^2}{2\sigma^2}. \tag{2.14}$$

When K decreases to zero, the channel degenerates to Rayleigh fading, whereas if K is infinite, the channel has a deterministic line of sight.

2.8 Channel Models in Time and Frequency Domain

2.8.1 Channel Model in Time Domain

A channel model is indispensable for the study of wireless communications. The multipath fading radio channel may be characterized mathematically as a linear time-variant filter. In the time domain, the channel output signal can be derived by convoluting the bandpass input signal with the time variant channel impulse response function $h(\tau,t)$. The channel impulse response function can be given by

$$h(\tau;t)=\sum_i \rho_i(t)e^{j\theta_i(t)}\delta(\tau-\tau_i(t)), \tag{2.15}$$

where $\rho_i(t),\theta_i(t),$ and $\tau_i(t)$ denote the amplitude, phase, and excess delay for the *i*th received pulse, respectively; τ represents the excess delay whereas the *t* dependence gives the changes with time of the very structure of the impulse response; and $\delta(\bullet)$ is the Dirac Delta function.

Obviously, the amplitudes, phases and excess delays for all received pulses constitute the time domain channel model here. From literature [13], we take the following distribution rules for the amplitude and phases and the model of the power delay profile for an indoor radio channel:

- The ray phases are mutually independent (i.e., uncorrelated) random variables and are uniformly distributed over $[-\pi, \pi]$, which was validated by checking all measurement subsets.

- If we assume that all the rays can be generated in terms of the same statistical process and that this ray generation process is a wide sense stationary process with respect to variable *t*, the amplitudes of the scattered rays follow the Rayleigh distribution (given by equation 2.10) and the PDF of the amplitudes of all the rays (including LOS) follows the Rician distribution (given by equation 2.13).

- Figure 2.8-1 presents the model of the average Power Delay Profile (PDP) for a multipath radio channel. The first ray is the LOS with the highest power. Then there are rays with a constant level until excess delay $\tau=\tau_1$, after which rays follow with a linearly decreasing power level in dB. This average PDP in dB can be expressed as

$$10\log\left(\overline{\rho^2(\tau)}\right) = \begin{cases} 10\log\left(\overline{\rho^2(0)}\right) & \tau = 0 \quad \text{(LOS)} \\ 10\log\left(\overline{\rho^2(0)}\right) - \Delta_{LOS} & 0 < \tau < \tau_1 \quad \text{(constant level part)} \\ 10\log\left(\overline{\rho^2(\tau_1)}\right) - Z(\tau - \tau_1) & \tau \geq \tau_1 \quad \text{(linearly decreasing part)} \end{cases}, \quad (2.16)$$

where $\rho(0)$ denotes the LOS amplitude; $\rho(\tau)$ the amplitude of the ray reaching the receiver at delay τ ; Δ_{LOS} the difference between the LOS power and the power of the constant level part; and Z the slope of the linearly decreasing part in the PDP. If we relate this to the Rician distribution, the power/amplitude of the LOS can be obtained from the Rician K factor based on equation (2.14), and the amplitude of the other multipath rays can be obtained correspondingly using the equation above.

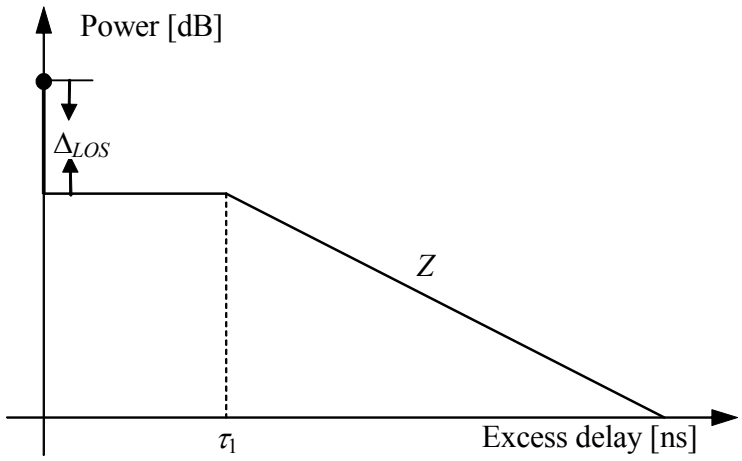


Figure 2.8-1. A model of average power delay profile

2.8.2 Channel Model in Frequency Domain

In the Ph.D. thesis of [14], a channel model of the Delay Power Spectrum (DPS) in frequency domain is given, see Figure 2.8-2. This model (i.e., the channel transfer function) is obtained by applying the Fourier transform to the impulse response of the channel (see equation (2.17)). This process proves also that time dispersion of the channel makes the channel frequency selective, which was shown in Section 2.5 and 2.6.

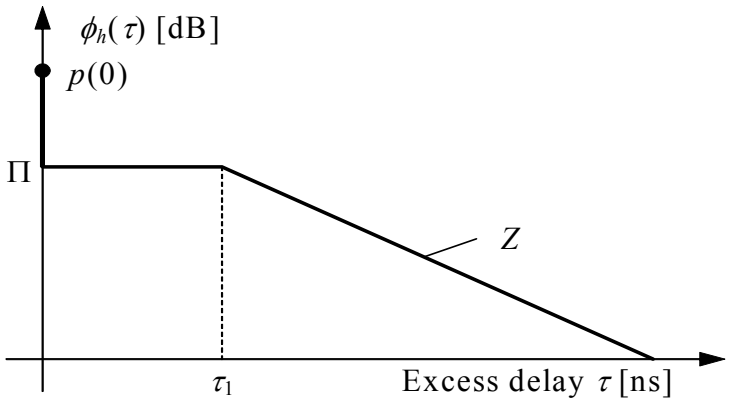


Figure 2.8-2. Model of delay power spectrum

We get

$$H(f,t)=\int_{-\infty}^{\infty} h(\tau,t)e^{-j2\pi f\tau}d\tau=\sum_i \rho_i(t)e^{-j[2\pi f\tau_i(t)+\theta_i(t)]}, \tag{2.17}$$

where $h(\tau,t)=\sum_i \rho_i(t)e^{-j\theta_i(t)}\delta(\tau-\tau_i(t))$, describes the impulse response of the channel in the time domain. $\phi_h(\tau)$ denotes the power at a delay τ, and the relation with the channel impulse response is

$$\phi_h(\tau)=E\{|h(\tau)|^2\}.$$

The shape of the DPS is assumed to be identical to that of the average PDP; only an expression is required to obtain equivalent power from both models. We define

$$\phi_h(\tau)=\begin{cases}0 & \tau<0\\ p(0)\delta(\tau) & \tau=0\\ \Pi & 0<\tau\le\tau_1\\ \Pi e^{-\gamma(\tau-\tau_1)} & \tau>\tau_1\end{cases}, \tag{2.18}$$

where $p(0)=|h(0)|^2$ stands for the power of the LOS component, Π is the power density of the constant-level part, and γ is the decay exponent defined as $\gamma=\frac{Z}{10}\ln 10$. Z in [dB/ns] denotes the slope of the linearly decreasing part of the average PDP.

We define the Normalized Received Power (NRP) as the ratio of the received power and the transmitted power, that is,

$$NRP = \frac{P_R}{P_T}, \tag{2.19}$$

where P_R stands for the received power and P_T denotes the transmitted power. NRP is assumed to be one in our work in this thesis.

From the continuous DPS $\phi_h(\tau)$ defined in equation (2.18), expressions for the values of NRP, the K factor, and the rms delay spread (σ_τ) can be derived. Equations (2.20) - (2.24) show the results of this derivation [14].

$$E\{\text{NRP}\} = \int_0^{\tau_{\max}} \phi_h(\tau) d\tau = p(0) + \Pi \cdot \left[\tau_1 + \frac{1}{\gamma}\right] \tag{2.20}$$

$$E\{\text{K}\} = \frac{p(0)}{E\{\text{NRP}\} - p(0)} = \frac{p(0)}{\Pi \cdot (\tau_1 + 1/\gamma)} \tag{2.21}$$

$$E\{\text{NRP}\} \cdot E\{\overline{\tau}\} = \int_0^{\tau_{\max}} \tau \phi_h(\tau) d\tau = \Pi \cdot \left[\frac{\tau_1^2}{2} + \frac{\tau_1}{\gamma} + \frac{1}{\gamma^2}\right] \tag{2.22}$$

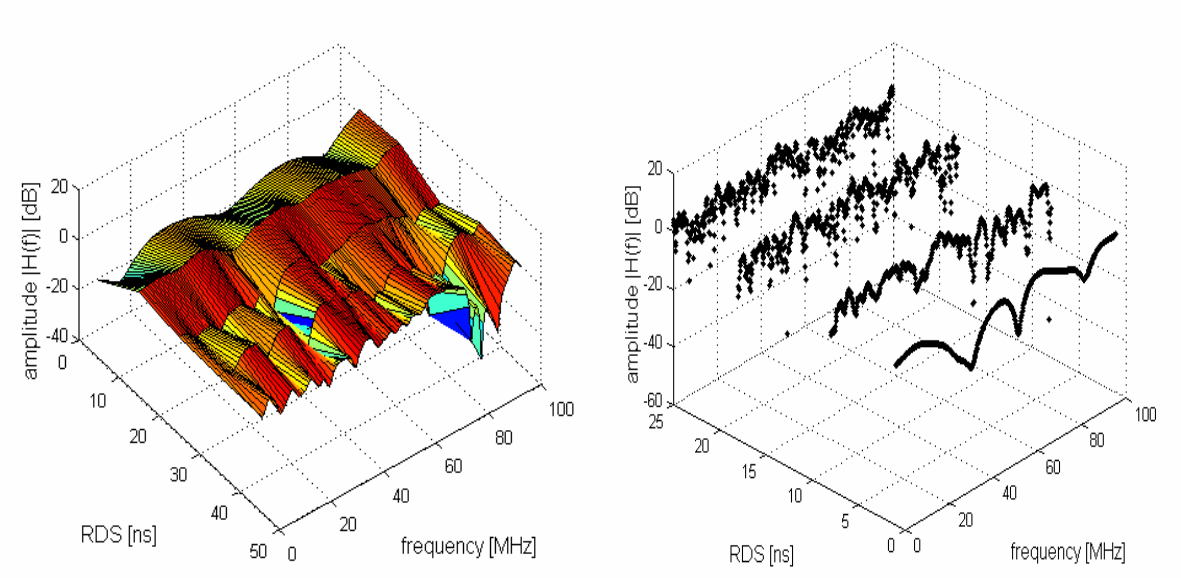
$$E\{\text{NRP}\} \cdot E\{\overline{\tau^2}\} = \int_0^{\tau_{\max}} \tau^2 \phi_h(\tau) d\tau = \Pi \cdot \left[\frac{\tau_1^3}{3} + \frac{\tau_1^2}{\gamma} + \frac{2\tau_1}{\gamma^2} + \frac{2}{\gamma^3}\right] \tag{2.23}$$

$$E\{\sigma_\tau\} = \sqrt{E\{\overline{\tau^2}\} - (E\{\overline{\tau}\})^2} \tag{2.24}$$

2.9 Influence of Rician *K* Factor and Delay Spread on Channel Properties in Frequency Domain

In the Frequency Domain (FD) model of the channel, three channel parameters {*NRP*, *K*, σ_τ} (the normalized received power, Rician *K*-factor, and rms delay spread) sufficiently describe the wide-band behavior of practical, Ricean fading channels. In order to adapt modulation parameters based on the channel parameters, we need to know what influence the channel parameters have on channel performance.

Figure 2.9-1 and 2.9-2 show channel properties in frequency domain in terms of rms Delay Spread (RDS in the figures), and Rician *K* factor, based on simulations. Both the frequency domain model and the time domain model were simulated and they have similar simulation results, as shown in Figure 2.9-1 and 2.9-2. In Figure 2.9-1 we assume a *K* of 0dB and in Figure 2.9-2 an RDS of 42.1ns.



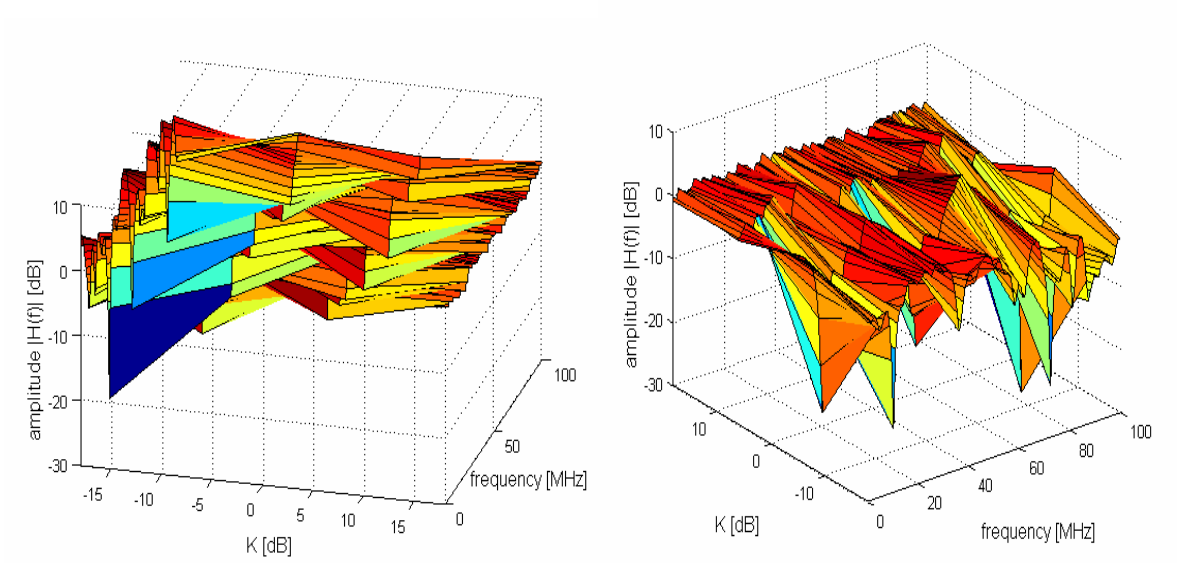
(a) Top view (b) Side view

Figure 2.9-1. Amplitude of frequency domain channel transfer function versus RDS and frequency (*K* = 0dB)

Figure 2.9-1 shows that a larger delay spread results in faster variations in the amplitude of channel transfer function in frequency domain. This tells us that a larger number of subcarriers should be assigned in an OFDM system when the delay spread is larger. From Figure 2.9-2 we learn that when the *K*-factor decreases, the amplitude of channel transfer function in frequency domain fades faster. For large *K* factors, the amplitude of the channel transfer function in the frequency domain does not fade much. In conclusion, when the *K* factor is large, we do not need to assign a small subcarrier bandwidth even if the delay spread is large. However, with what *K* factor does the effect of delay spread become negligible for the subcarrier bandwidth design? To determine this, we carried out the simulation shown in Figure 2.9-3.

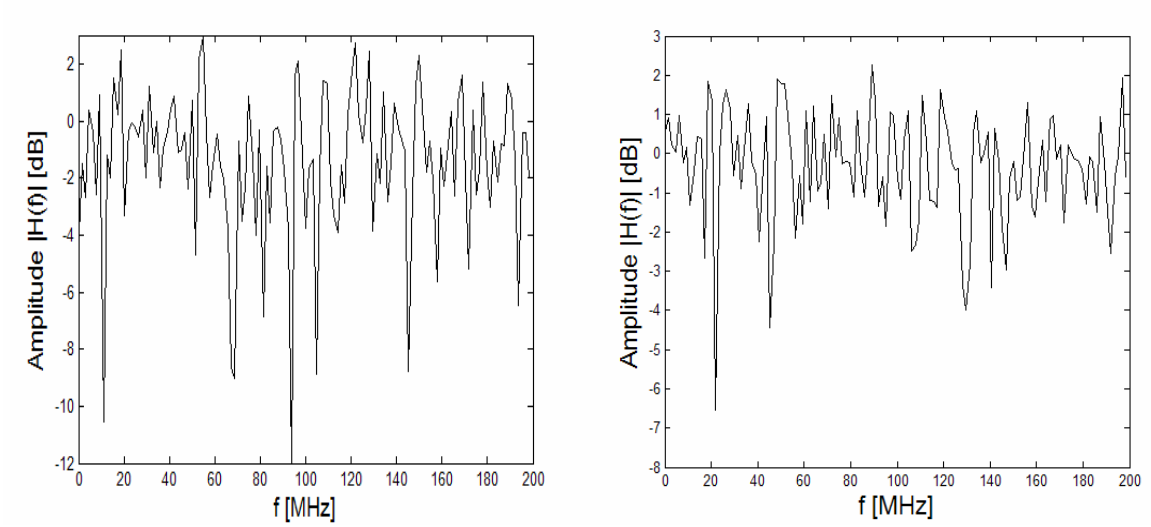
Figure 2.9-3 presents the channel amplitude transfer function over frequency for an RDS of 30ns and a Rician *K* factor of 0dB, 6dB, 10dB, and 15dB, respectively. This figure confirms that a larger *K* factor causes the channel amplitude to fade faster in the frequency domain. For

K=0dB, the amplitude fading may reach 12dB at some frequency point; for *K*=6dB, the amplitude fading reaches 6dB; for *K*=10dB, the amplitude fading is less than 2.2dB over the entire frequency band; and for *K*=15dB, the amplitude fading is limited to 1dB over the entire frequency band. So we can conclude that for a Rician *K* factor larger than 10dB, the amplitude of the channel transfer function in the frequency domain does not fade much, and therefore, we do not need to set the subcarrier bandwidth in terms of the delay spread, although the amplitude fluctuates fast when the delay spread is large.

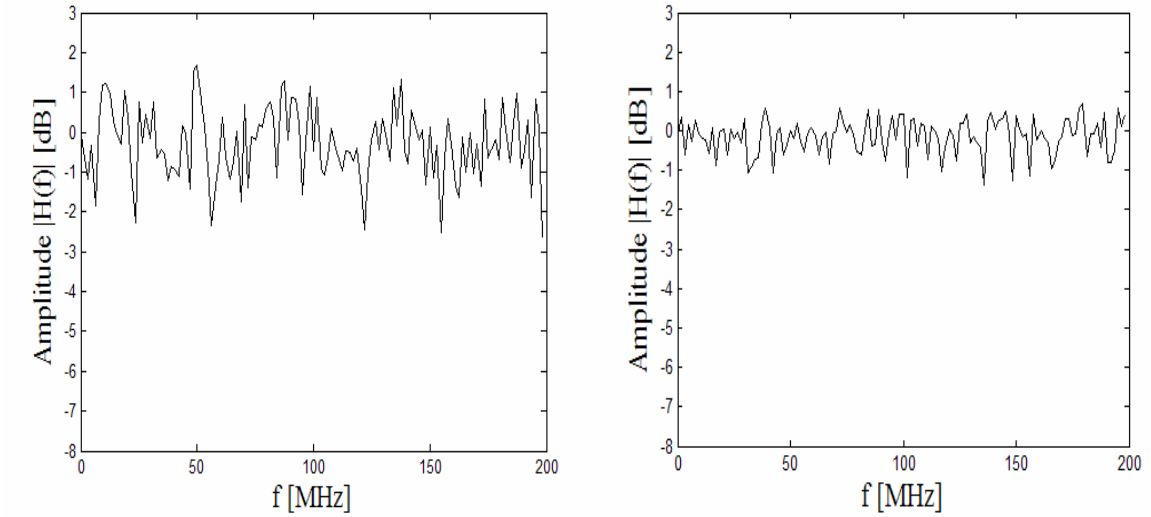


(a) Bottom view (b) Side view

Figure 2.9-2. Amplitude of channel transfer function against frequency and *K*-factor (RDS=42.1ns)



(a) K = 0dB (b) K = 6dB



(c) K = 10dB (d) K = 15dB

Figure 2.9-3. Channel transfer function with RDS =30ns and different Rician *K* values

Therefore, we can generalize the influence of the Rician *K* factor and the delay spread on the channel properties in frequency domain as follows:

- The delay spread is related to the rate of the amplitude variations in the FD channel transfer function. The higher the delay spread, the higher the rate of variation in the amplitude of the channel.

- The Rician *K* factor determines the size of the variation in the FD channel transfer function. The larger K, the smaller the variation.
- When the Rician *K* factor is smaller than 10dB, and we want to combat the frequency-selective fading of the channel, a smaller subcarrier bandwidth should be assigned when there is a larger delay spread in the OFDM system.

2.10 Evaluation of Channel Properties in Different Domains

We have investigated the channel property in three domains: in space, frequency, and time domain. Correspondingly the channel has space-selective fading, frequency-selective fading, and time-selective fading. These types of fading may deteriorate the system's performance. Solutions are required to combat these types of fading, or even better, to turn them into advantages.

In the thesis, we exploit MIMO technology (this will be discussed in Chapter 4) to take advantage of the multipaths in the space domain and to further improve the channel quality, as shown in Table 2.10-1. OFDM modulation can be exploited to divide the whole bandwidth into many subcarriers with smaller bandwidth. By assigning the subcarrier bandwidth properly, we turn a frequency-selective fading channel into a flat fading channel, and an improvement of its performance can be expected. This can be the solution to the problem of frequency diversity in frequency domain (see Table 2.10-1). As for the time diversity property of the channel, we use an adaptive algorithm to assign different parameters at different moments on the basis of the current channel situation (also indicated in Table 2.10-1). These parameters include MIMO and OFDM parameters. In other words, moment by moment, in agreement with the channel properties in the space and frequency domain, those MIMO and OFDM parameters are assigned that takes the most advantage of the space diversity and turn the frequency-selective fading channel into a flat fading one. Thus, the moment the space diversity and/or the frequency diversity of the channel change, the adaptive modulation algorithm will change the MIMO and/or OFDM parameters using certain criteria to get optimal performance. By doing this, channel fading in space, frequency and time domain will all be improved. Details of this algorithm will be discussed in Chapter 3 and Chapter 5.

Table 2.10-1 Channel Characteristics in three domains

	Space domain	Frequency domain	Time domain
Disadvantage	Space selective fading	Frequency selective fading	Time selective fading
Solution	MIMO	OFDM	Adaptivity
Objective	Exploit multipath	Flat fading	Slow fading

2.11 Conclusions

In this chapter we discussed channel characteristics. Traditionally channels can be categorized into large-scale and small-scale fading channels. Large-scale fading is mainly represented by path loss, which is caused by long-distance propagation (in the order of kilometers). Small-scale fading presents the effect of multipath transmission.

Considering the nature of adaptive modulation, we discussed the channel characteristics in three domains: space, frequency, and time domain, as shown in Table 2.11-1. The channel characteristics in space domain are related to large-scale path loss and small-scale random fluctuations due to multipath propagation. The random fluctuation over a small change in distance (in the order of a wavelength) leads to space diversity (or space-selective fading). The fact that space diversity is random and difficult to model introduces a lot of uncertainty in the system design and makes it difficult to enhance the system's performance. However, a new technology, multiple antennas transmission, e.g., MIMO, creates a solution to this problem. MIMO can change the disadvantage of multipath propagation into an advantage (this will be discussed in chapter 4).

Table 2.11-1 Channel Characteristics in three domains

	Space domain	Frequency domain	Time domain
Parameters	*d;* random fluctuation	B_D; $B_C \approx \frac{1}{50\sigma_\tau}$	$T_C \approx \frac{1}{B_D}$; σ_τ
Disadvantage	Space diversity	Frequency diversity	Time diversity
Solution	MIMO	OFDM	Adaptivity
Objective	Exploit multipath	Flat fading ($T_S \geq 10\sigma_\tau$)	Slow fading ($B_S \gg B_D$)
Note	*d*: transmitter-receiver distance; MIMO: Multiple Input Multiple Output; B_D: Doppler spread; B_C: coherence bandwidth of the channel, considered for correlation larger than 90%; OFDM: Orthogonal Frequency Division Multiplexing; T_S: symbol period; σ_τ : rms delay spread; T_C: coherence time of the channel; B_S: bandwidth of transmitted signal.		

The channel parameters in frequency domain are Doppler spread and coherence bandwidth (see Table 2.11-1). The channel parameters in time domain are the coherence time and the rms delay spread. Doppler spread results from the relative motion between the base station and the mobile station. It can lead to time-selective fading (or time diversity) in time domain because the Doppler spread is inversely proportional to the coherence time of the channel.

Rms delay spread results from multipath delay. The coherence bandwidth of the channel is inversely proportional to the rms delay spread. Therefore, rms delay spread can lead to frequency-selective fading (or frequency diversity) in frequency domain. OFDM (Orthogonal Frequency Division Multiplexing) offers a solution to frequency diversity since it can turn frequency-selective fading to flat fading by using a symbol period that is longer than the rms delay spread (this will be discussed in chapter 3). In addition, adaptivity offers a solution to time-selective fading in time domain since it can almost always make the signal bandwidth much larger than the Doppler spread by changing the parameters of transmission system in terms of the channel parameters (this will be discussed in chapter 3).

We briefly described the Rayleigh and Rician distribution since they will be used in this work. Channel models in time and frequency domain from the literature were discussed.

Adaptive modulation is used to change the modulation parameters instantaneously based on the instantaneous channel parameters. In addition, for every moment, we focus on the channel property in frequency domain. In this chapter we analyzed the influence of some parameters (the Rician *K* factor; the rms delay spread) on the frequency transfer function of the channel. The delay spread is related to the rate of amplitude variations in the FD channel transfer function. The higher the delay spread, the higher the rate. Therefore, we can link the delay spread with the subcarrier bandwidth in OFDM systems. When the delay spread is large, the channel will fluctuate more in frequency domain, and a smaller subcarrier bandwidth should be assigned, and vice versa. The Rician *K* factor determines the size of the variation in the FD channel transfer function. The larger *K* is, the smaller the variation. We found by simulations that when the Rician *K* factor was larger than 10dB, the amplitude of the channel transfer function in frequency domain faded less than 2.2dB. Under these conditions it is not necessary to assign a smaller subcarrier bandwidth to combat frequency-selective fading, not even if the channel transfer function fluctuates a lot due to a large delay spread. Therefore, only for a Rician *K* factor smaller than 10dB, a subcarrier bandwidth should be assigned based on the delay spread of the channel: the larger the delay spread, the smaller the subcarrier bandwidth should be set.

In agreement with the channel properties in the three domains, we proposed three technologies to combat, or even better, to take advantage of the fading in the three domains. In our adaptive modulation algorithm, MIMO and OFDM modulation parameters will be assigned based on the channel situation of that specific moment in space and frequency domain. When the channel situation changes, new values of these parameters will be assigned based on the instantaneous channel properties. This algorithm will be further investigated in Chapter 3 and 5.

References

[1] Ojanperä, T., Prasad, R., "An Overview of Air Interface Multiple Access for IMT-2000/UMTS" IEEE Communications Magazine, September 1998;

[2] Rappaport, T. S., *Wireless Communications: Principles and Practice*, ISBN 0-13-042232-0, Prentice Hall PTR, 2002;

[3] Molisch, A.F., Foerster, J.R., Pendergrass, M., "Channel models for ultrawideband personal area networks", IEEE Wireless Communications, v10, Issue: 6, Dec. 2003 p14 – 21;

[4] Rummler, W., Coutts, R., Liniger, M., "Multipath fading channel models for microwave digital radio", IEEE Communications Magazine, v24, Issue: 11, Nov 1986, p30 – 42;

[5] Greenstein, L., "A Multipath Fading Channel Model for Terrestrial Digital Radio Systems", IEEE Transactions on Communications, v26, Issue: 8, Aug 1978, p1247 – 1250;

[6] Watterson, C., Juroshek, J., Bensema, W., "Experimental Confirmation of an HF Channel Model", IEEE Transactions on Communications, v18, Issue: 6, Dec 1970, p792 – 803;

[7] Lavergnat, J., Sylvain, M., "Selective Fading Radio Channels: Modeling and Prediction", IEEE Journal on Selected Areas in Communications, v5, Issue: 3, April 1987, p378 – 388;

[8] Heddergott, R., Leuthold, P.E., "An extension of stochastic radio channel modeling considering propagation environments with clustered multipath components", IEEE Transactions on Antennas and Propagation, v51, Issue: 8, Aug. 2003, p1729 – 1739;

[9] Cox, D. C., Murray, R., and Norris, A., "800 MHz Attenuation Measured in and around Suburban Houses", AT &T Bell Laboratory Technical Journal, vol. 673, No. 6, July-August 1984;

[10] Bernhardt, R. C., "Macroscopic Diversity in Frequency Reuse Systems", IEEE Journal on Selected Areas in Communications, vol-SAC 5, pp862-878, June 1987;

[11] Steele, R, *Mobile Radio Communications*, John Wiley & Sons, 1992;

[12] Lee, W. C. Y., *Mobile Cellular Telecommunications Systems*, McGraw Hill Publications, New York, 1989;

[13] Smulders, P. F. M., *Broadband Wireless LANs: A Feasibility Study*, Ph.D thesis in Eindhoven University of Technology, The Netherlands, 1995

[14] Witrisal, K, *OFDM Air-Interface Design for Multimedia Communications*, Ph.D thesis in Delft University of Technology, The Netherlands, 2002

Chapter 3

Adaptive Modulation Analysis

3.1 Introduction

Wireless channels vary randomly with time, which limits the transmission performance and throughput of wireless communication systems. Adaptive Modulation (AM) is used to adapt the "wide-sense" modulation parameters dynamically according to the instantaneous channel parameters in order to guarantee the transmission quality and to get high throughput. Obviously, adaptive modulation is a solution to the disadvantage of wireless channels (i.e., that they vary). In this thesis we use the term "narrow-sense" modulation parameters to describe the traditional modulation parameters, i.e., the modulation level and coding rate, and "wide-sense" modulation parameters" to describe parameters including both "narrow-sense" modulation parameters and multiple access modulation parameters, i.e., OFDM, CDMA, MC-CDMA, TDMA, and FDMA.

Investigating adaptive modulation is different from investigating traditional modulation. In research on traditional modulation, basic modulation technology is studied and combined with new technology or modified to improve it. We found that in adaptive modulation it is prerequisite to study the inner-relationships within the modulation parameters and the channel parameters themselves as well as the inter-relationships between them. Therefore, to build an efficient adaptive modulation algorithm, one first has to carry out a study on these relationships. Then the criteria should be set up that the adaptive modulation algorithm should use to decide whether and how to change the modulation parameters.

A lot of work has been done on adaptive modulations [1]-[10]. However, our literature search did not reveal any investigation on the strategy and work procedures of adaptive modulation. In this chapter, the concept, developing process, strategy and work procedures of adaptive modulation will be investigated by means of examples of adaptive OFDM modulation and adaptive CDMA modulation. We will mainly focus on adaptive OFDM, and some attention will be given to adaptive CDMA. First we describe a three-stage developing process, the strategies and work procedures for adaptive modulation algorithms. Following the requirements for adaptive modulation algorithms, we derive the throughput formulas for OFDM systems and CDMA systems. The influence of modulation parameters on transmission quality will be analyzed for both OFDM and CDMA systems. Because the channel situation and the modulation settings in adaptive modulation systems can vary, we will introduce a new parameter, P_{FR} for OFDM systems, which is the product of the subcarrier bandwidth and rms delay spread. Analysis and simulation results will be given to prove that in adaptive OFDM systems P_{FR} is the parameter influencing the transmission quality, instead of the subcarrier bandwidth. Working conditions of P_{FR} will be described.

In Section 3.2, a description of adaptive modulation is given. We define adaptive modulation systems, describe their architecture, their objectives as well as different categories of such systems, including advantages and disadvantages. What is more, we propose a development scheme for adaptive modulation in a three-stage process, in which the level of adaptation is raised step by step.

The objective of adaptive modulation is to improve the throughput and transmission quality of wireless communication systems. In Section 3.3, we investigate the parameters influencing throughput in OFDM and CDMA systems. We derive bit rate formulas in terms of "wide-sense" modulation parameters for OFDM systems and CDMA systems, which are novel. With these formulas, the bit rate can be obtained at a certain moment given the values of the modulation parameters.

In Section 3.4, we investigate the parameters influencing the transmission QoS. All parameters in the throughput formula of OFDM systems are analyzed. Further, we introduce a new parameter that influences the transmission quality in OFDM systems, i.e., P_{FR}, the product of the subcarrier bandwidth and rms delay spread. This parameter makes sense for OFDM systems in varying channels. Analysis and simulation results show that smaller P_{FR} produces better BER performance. However, P_{FR} has only its effect under certain conditions. P_{FR} influences BER only when SNR is larger than a certain value; we call this value "Start SNR". The Rician K factor also limits the function of P_{FR}. The Start SNR increases with K. When K is larger than a certain value (we call this K value "*Top K*"), P_{FR} does not influence BER any more. For CDMA systems, we briefly describe the influence of CDMA parameters on the transmission QoS.

In Section 3.5, the strategies and work procedures of adaptive OFDM and adaptive CDMA algorithms are proposed. We put forward that the working method for adaptive modulation is different from that for traditional modulation. The emphasis of adaptive modulation lies in

finding all relationships (inner-relationships and inter- relationships) among the modulation parameters and channel parameters. Based on these strategies, we propose work procedures for adaptive modulation algorithms in nine steps. The adaptive OFDM algorithm is analyzed following this nine-step procedure, as well as the adaptive CDMA algorithm.

Conclusions are summarized in Section 3.6.

3.2 Introduction of Adaptive Modulation

3.2.1 Development of Adaptive Modulation

With the advancement of wireless communications, adaptive algorithms are becoming more and more attractive due to their advantages of flexibility, efficient use of the frequency spectrum, high throughput, and good transmission quality. Adaptive algorithms change the values of modulation parameters dynamically according to the current channel situation. When the channel is good, those values can be assigned for the modulation parameters so that high throughput can be obtained; when the channel is bad, the values can be assigned for the modulation parameters so that good transmission quality at lower transmission rate can be guaranteed. This makes the system flexible and able to use the frequency spectrum efficiently; meanwhile, high throughput and good transmission quality can be obtained. For some applications, e.g., software radios, they are indispensable. The adaptive modulation technique is a promising adaptive technique in wireless communications. The content of this section is based on an existing article by the author [11].

Non-adaptive modulation systems use fixed modulation parameters to get a certain throughput and to guarantee transmission quality at the same time. In other words, there is a compromise between the quality of service (QoS) and transmission throughput when deciding these parameters. Obviously this strategy is not optimal since the channel varies most of the time. When the channel is very good, spectrum and power will be wasted as parameters for a worse situation are used; and when it is very bad, maybe the compromised parameters could not guarantee the transmission quality. The adaptive modulation technique provides a solution to this problem. The adaptive modulation technique is meant to change the “wide-sense” modulation parameters (including multiple access scheme parameters) dynamically according to the instantaneous channel situation in order to satisfy the system transmission requirements and to get maximum throughput.

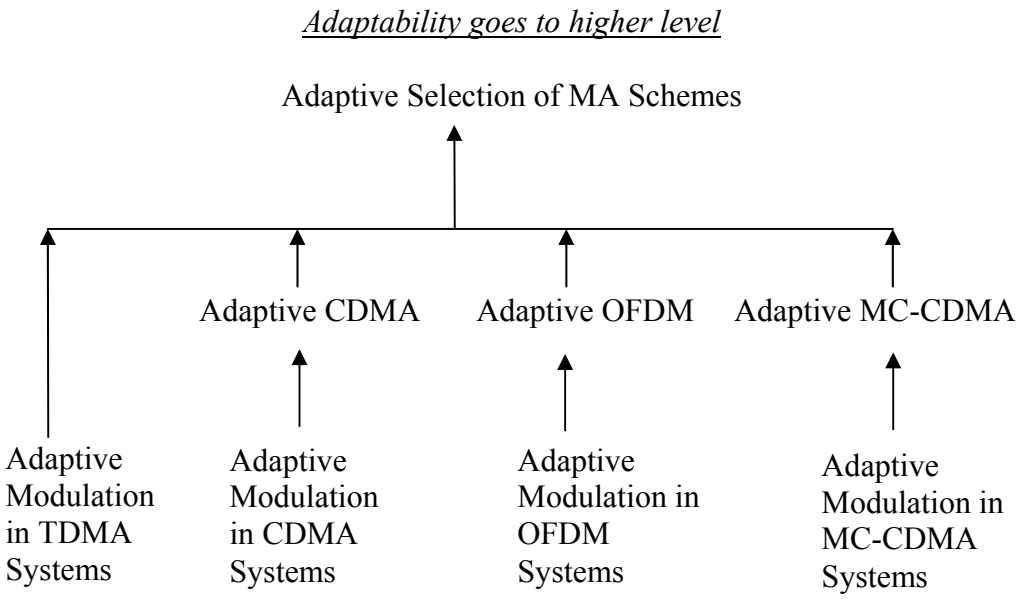


Figure 3.2-1. Developing process for adaptive modulation techniques

The "wide-sense" adaptive modulation technique (including Multiple Access schemes) experiences three stages, as depicted in Figure 3.2-1. During this process, the level of adaptation is raised step by step.

The first stage is "narrow-sense" adaptive modulation in a certain multiple access (MA) system. The adaptive parameters are the "narrow-sense" modulation parameters, i.e., the modulation level, and coding rate. The "wide-sense" adaptive modulation techniques (including multiple access modulation, e.g., TDMA, CDMA, OFDM) originate from adaptive modulation in a "narrow-sense" (only modulation level, coding rate) for a TDMA system. In a TDMA system, adaptive modulation is used to change the modulation level, symbol rate, coding rate, and power dynamically according to the instantaneous channel situation to meet the system transmission requirements and to get maximum throughput. Related work has been reported in literature, e.g., [12], [13], [14]. Adaptive modulation in CDMA systems is less important due to the different system strategy in CDMA systems. The basic strategy in CDMA systems is Adaptive DS/SS (Direct Sequence/Spread Spectrum) parameter control [15], so adaptive modulation in CDMA system is mainly related to coding. Adaptive modulation in OFDM systems has been studied at, for example, the University of Southampton. Based on the predicted channel conditions, appropriate modulation for each group of subcarriers was employed; severely faded subcarriers were excluded; the coding rate of error correction was considered; and preequalization was combined [15]. "Narrow-sense" adaptive modulation in the MC-CDMA system has not received much attention. This is because MC-CDMA modulation has OFDM and CDMA parameters, which attracts the attention for adaptation separately.

The second stage in the adaptive modulation technique is adaptive multiple access/multiplexing schemes, in which the multiple access (MA) or multiplexing parameters are adaptive. As mentioned before, adaptability goes to a higher level with the change of system strategy. Adaptive CDMA has been studied by changing DS/SS parameters, e.g., the processing gain in SISO systems [15]. Adaptive OFDM adapts OFDM parameters according to the channel situation. Adaptation in cyclic extension/guard time, for example, is to use a longer guard time in case of a longer delay spread and a shorter guard time in case of a shorter delay spread. As for adaptive MC-CDMA, it seems that not much interest has yet been shown in it.

An adaptive modulation technique with an even higher level of adaptation has been proposed, namely, adaptive selection of MA schemes, by Osaka University in Japan [16]. This is the third stage in the development of adaptive modulation technique. The idea is to change MA schemes (e.g, TDMA, CDMA) by a certain criterion according to user's QoS, such as the requested transmission rate, tolerable BER, delay and various factors to maximize system capacity under the channel condition and available frequency bandwidth. The research begins with the selection between TDMA and CDMA. It will give solutions to many practical difficulties, e.g., to support more applications/services in one system.

In this thesis we concentrate on adaptive OFDM in SISO and MIMO systems and adaptive CDMA in MIMO systems. These are in the second stage of Figure 3.2-1. We propose new adaptive OFDM algorithms with different subband settings in SISO systems. Further, we combine adapting MIMO parameters into our adaptive OFDM algorithms for MIMO systems. In our adaptive CDMA algorithms for MIMO systems, we combine adapting MIMO parameters into an adaptive CDMA algorithm to get higher throughput at the required transmission quality, which is also novel.

3.2.2 Definition of Adaptive Modulation

The development process of adaptive modulation has been discussed; this section will describe adaptive modulation.

Definition:

> An adaptive Modulation algorithm is used to change "wide-sense" modulation parameters (including multiple access scheme parameters) dynamically according to the instantaneous channel situation in order to satisfy the system transmission requirements and to get the maximum throughput [17].
>
> For example, adaptive OFDM is one of the adaptive modulation techniques. Adaptive OFDM is used to adapt OFDM parameters according to the instantaneous channel situation to get the required transmission quality and high throughput. Likewise, adaptive CDMA is used to adapt CDMA parameters according to the instantaneous channel situation to get the required transmission quality and high throughput as well.

Now we know that adaptive modulation is used to switch modulation formats dynamically to achieve optimal throughput when the received SNR level varies over a wide range with time. It can increase system capacity [18]. The basic concept of adaptive transmission is real-time balancing of the link budget through adaptive variation of the transmitted power level, symbol transmission rate, constellation size, coding rate/scheme, or any combination of these parameters [19].

According to the definition, there are two aspects in this activity (as indicated in Figure 3.2-2): modulation and channel. The modulation parameters are determined by the channel properties in the adaptive modulation algorithm. In other words, modulation parameters should be a function of the channel parameters in the adaptive modulation algorithm, i.e.,

Modulation parameters = f(channel parameters),

where $f(Q)$ means a function of Q.

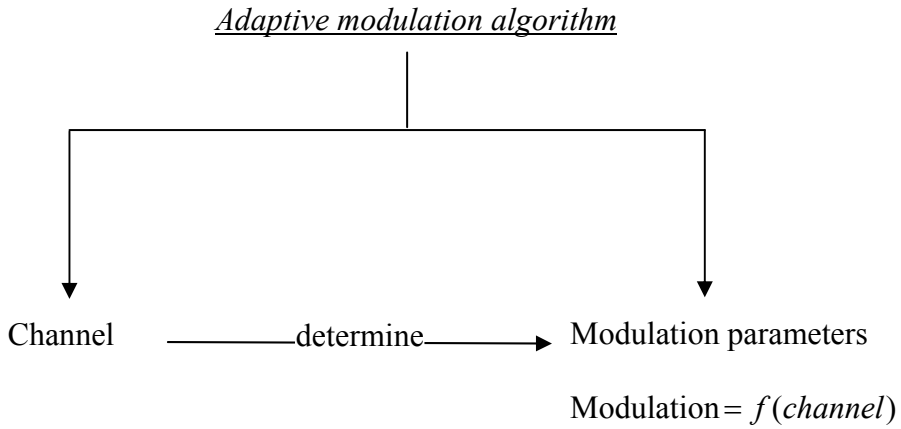


Figure 3.2-2. Schematic description of the adaptive modulation algorithm

In practice, the channel varies, so the modulation parameters need to vary correspondingly. Therefore, we have to "adapt" the modulation parameters, and that is why we need the "adaptive modulation algorithm", which indicates how to perform this activity, or how to adapt the parameters.

Adaptive modulation offers the opportunity to use more than one set of modulation parameters (i.e., the modulation level, power, coding rate, processing gain for CDMA, guard time for OFDM, etc.) in one system at different times.

3.2.3 Architecture of Adaptive Modulation Systems

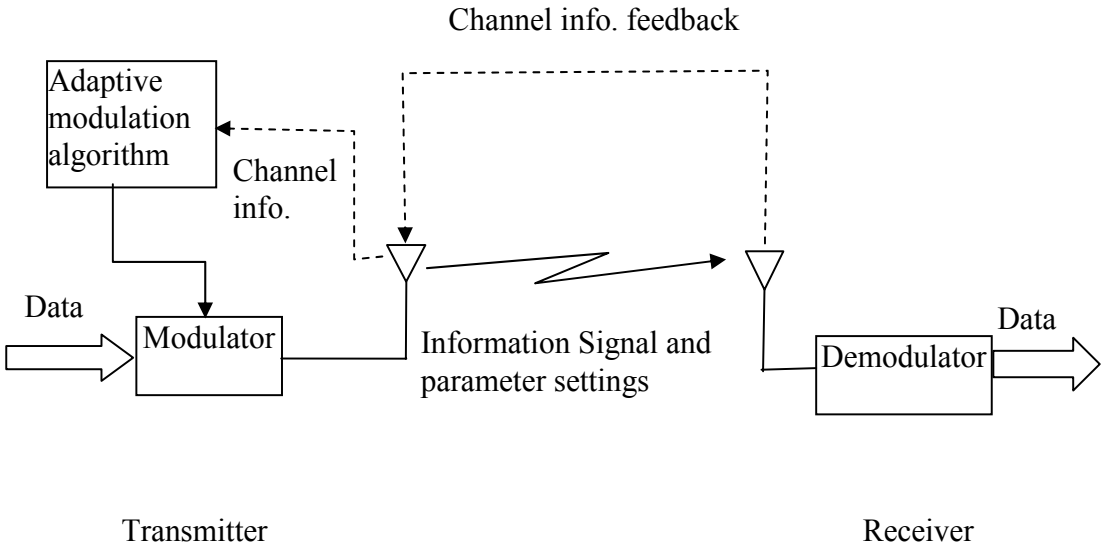


Figure 3.2-3. Architecture of adaptive modulation systems for SISO channels

Figure 3.2-3 presents the architecture of adaptive modulation systems. It shows that adaptive modulation is used to change the modulation parameters with the channel situation. In order to do this, the channel situation should be known by the transmitter before transmission, for which reason the acquisition of the channel information is indispensable. This is called channel estimation. There are two different methods for channel estimation. One is that the transmitter gets the feedback of the channel information from the receiver; the other that the transmitter itself estimates the channel.

Channel estimation is an essential prerequisite for an adaptive modulation system. By itself it is a complicated research topic, so we do not discuss it in this thesis. To perform the function of adaptive modulation, an efficient algorithm has to be built, by means of which modulation parameters can be configured based on the instantaneous channel condition. The channel information is the input for the adaptive modulation algorithm.

At the receiver, the settings of the modulation parameters should be known, so that the signals can be demodulated correctly.

The resulting flow chart of adaptive modulation systems looks as follows:

1) Measure and predict the channel conditions accurately, in other words, estimate the channel;
2) Build up an algorithm to adapt the modulation parameters in terms of the channel conditions;
3) Obtain the settings of the modulation parameters at the receiver.

In this thesis, we concentrate on the second step, that is, on building the adaptive modulation algorithms. In our simulations, we assume that we have perfect channel estimation and that the receiver knows the exact settings of the modulation parameters.

3.2.4 Objective of Adaptive Modulation

The task in wireless communications consists mainly of two aspects: the transmission Quality of Service (QoS) and the throughput. Adaptive modulation is created for the same purpose. The main goal of adaptive modulation is to find a software solution for a flexible, compatible and multiple application system with small volume, for example, via software radio. The advantage of adaptive modulation is that it can realize higher transmission QoS and higher throughput by efficient usage of the channel situation. Therefore, in our work on adaptive modulation we will concentrate on the following:

- To get higher transmission QoS;
- To get higher throughput (bit rate and frequency spectrum efficiency).

In our work, we use BER to represent QoS.

3.2.5 Adaptive Modulation Categories

There are two categories of adaptive modulation: slow adaptive modulation and fast adaptive modulation, which are defined by how often the transmission settings are updated. In slow adaptive modulation, transmission parameters are assigned when the user connects to the system and they remain constant throughout the transmission. In this case the parameter settings are based on the channel situation at the moment the user starts communications every time. If the channel does not vary fast, this can improve the transmission quality and throughput. In fast adaptive modulation, the parameters are controlled slot by slot based on the instantaneous channel conditions, and thus the transmitter can adjust to fading channel conditions for each slot or for a few slots [20]. Although fast adaptive modulation is effective in improving transmission quality, the average bit rate is subject to the channel conditions. Therefore, the scheme is more suitable to support data transmission rather than for constant bit rate services, such as voice transmission [21]. We study the fast adaptive modulation algorithm in our work.

3.2.6 Advantages of Adaptive Modulation

Intelligent radio communications that include not only adaptive reception techniques, such as the adaptive equalizer, but also adaptive transmission control techniques, is a new and attractive concept for future wireless personal multimedia communication systems. This is because it has high potential to achieve high quality and a high transmission bit rate with high flexibility under traffic and propagation path conditions that vary in time and space. The adaptive modulation technique is one of the effective intelligent radio communication techniques, [21]. Mobile radio links are subject to severe multipath fading, which may severely degrade the link Carrier to Noise Ratio (CNR) and consequently increase the BER. Fading compensation such as an increased link budget margin or interleaving with channel coding is typically required to improve link performance. However, these techniques are designed relative to worst-case channel conditions, resulting in poor utilization of the full channel capacity for a good percentage of the time (i.e., under shallow fading conditions). Adapting certain parameters of the transmitted signal with the fading channel leads to better utilization of the channel spectrum, [19].

In the conventional system, a large power margin and interference margin is set in the stage of link design so that a certain level of quality is guaranteed even in a worst propagation environment. Therefore, the service area as well as system capacity are restricted, resulting in a less efficient system, [22].

Without wasting power or sacrificing BER, adaptive modulation provides a higher average link spectral efficiency by taking advantage of the time varying nature of wireless channels: they transmit at high speeds under favourable channel conditions and respond to channel degradation through a smooth reduction of their data throughput.

Adaptive modulation realizes higher throughput and higher quality transmission in land mobile communications than fixed modulation level systems by making some modulation parameters variable according to the instantaneous situation of the channel.

3.2.7 Disadvantages and Limits of Adaptive Modulation Systems

Adaptive modulation looks like an ideal technique that can solve a lot of problems in transmission systems and make these systems more efficient. But is it easy to realize? From the analysis given before, it can be seen that the answer is no. Adaptive modulation is a non-trivial task in practice, because to realize it, one needs to solve the following problems:

- Accurate SNR measurements at the receiver are required;
- The interference may change more quickly than the feedback round trip;
- The fading channel may vary between channel estimation and data transmission;
- The optimal switching points in the algorithm are a function of the mobile speed;

- There is the risk that the optimal switch point moves after deployment due to changes in interference statistics, channel characteristics (e.g. Rayleigh, Rician, Gaussian), and delay spread [18];
- Adaptive systems are best suited to applications without stringent delay constraints because the probability of outage can be quite high, especially for channels with a low average SNR. Therefore, buffering of the input data may be required, [19];
- Because data is sensitive to errors, a data protocol in a duplex wireless network usually includes a feedback mechanism for acknowledgments, [20]. One problem of adaptive modulation is how to continuously adapt the transmit power and data rate to the estimated channel, particularly for high-speed mobile applications, where the channel changes quickly, [23];
- Two major factors may contribute to unreliable data transmissions: channel quality estimation error and user mobility, [20].

Therefore, the support of other techniques is needed to make adaptive modulation systems function satisfactorily.

3.3 Parameters Influencing Throughput

3.3.1 Introduction

For completeness of the thesis, we summarize the basic concepts of OFDM and CDMA in Appendix. It will help readers to understand the work clearly. In Appendix A, OFDM modulation is described. We list the OFDM modulation parameters and their relations for adaptive OFDM algorithms. In Appendix B, CDMA modulation is described. The CDMA modulation parameters and their relations are listed for adaptive CDMA algorithms.

One of the objectives of adaptive modulation is to improve throughput. In order to do that, one first needs to know the parameters influencing throughput. In this section, we will investigate these and then give a formula for throughput. This has also been published in [11].

In terms of the signal to noise ratio (SNR) of the channel, there is a well-known formula for channel capacity [24],

$$C = B\log_2(1+SNR) \qquad [bps], \tag{3.1}$$

where C is channel capacity, and B is the channel bandwidth.

We mentioned before that adaptive modulation is used to change modulation parameters to channel situations in order to guarantee the required transmission quality and to reach a certain throughput. This means that the systems need to know the throughput as a feedback, meanwhile the required transmission quality can be guaranteed. This raises a main question: “when the channel situation permits only certain values of a set of modulation parameters,

how can we calculate the throughput with these modulation parameters?" A formula for this did not yet exist. Such a formula is convenient for system design and necessary for adaptive modulation systems.

3.3.2 Throughput Formulas for OFDM Systems

It is well known that the modulation level and coding rate influence the throughput. In OFDM systems, due to parallel transmission and cyclic extension, there are more parameters that determine the throughput.

Starting from the simple case with identical subcarrier configuration, this means that all subcarriers have the same configurations (modulation, coding, bandwidth, power, etc). In this case, the total bit rate of the OFDM system is

$$R_{tb} = \frac{(bits/subcarrier/symbol) \times number\ of\ data\quad subcarriers}{symbol\ duration}\ \text{[bps]}. \tag{3.2}$$

when R_c denotes coding rate, M modulation level, N_d number of data subcarriers, T_s symbol duration, B_d frequency bandwidth of the information signal or data, T_{FFT} FFT time, $\Delta f = 1/T_{FFT}$ subcarrier bandwidth, and FSR = T_{FFT}/T_s the FFT time to symbol duration ratio, the total information bit rate equals

$$\begin{aligned} R_{tb} &= (R_c \log_2 M) N_d / T_s = (R_c \log_2 M)(B_d / \Delta f) / T_s \\ &= (R_c \log_2 M) B_d (T_{FFT} / T_s) = (R_c \log_2 M) B_d FSR \end{aligned}. \tag{3.3}$$

Hence, it is easy to conclude that in order to increase the bit rate, we can either increase the modulation level (M), coding rate (R_c), or N_d / T_s ratio. Figure 3.3-1 explains equation (3.3), where "↑" means increasing the value and "↓" means decreasing the value. In order to make it explicit, we here repeat the symbol implications. T_g stands for the guard time of the OFDM symbol, and T_w for the window time of the OFDM symbol. It is straightforward that to increase N_d / T_s, we can increase N_d and keep T_s constant or keep N_d constant and decrease T_s. Three methods can thus be used to increase the bit rate: the first is to increase the modulation level or coding rate; the second is to increase the bandwidth used for information transmission; and the third is to increase FSR, that is, to decrease the guard time and/or window time. These methods can only be used when the channel situation permits a change in the values of these parameters.

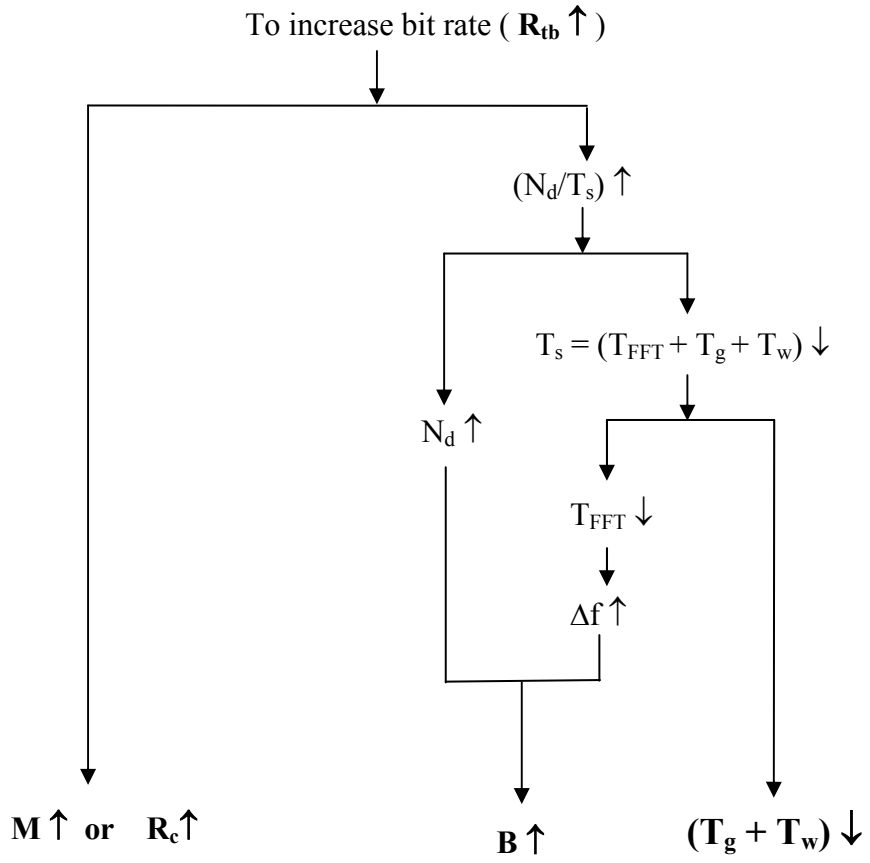


Figure 3.3-1 Throughput (bit rate) parameters
("↑" means increasing the value and "↓" means decreasing the value)

With the available bandwidth B, we can make an approximation for equation (3.3). The maximum bit rate can be expressed as

$$\mathrm{Max}(R_{tb}) = (R_C \cdot \log_2 M) B \cdot \mathrm{FSR}\,. \tag{3.4}$$

The premise for this approximation is that the whole bandwidth and all subcarriers can be used for information transmission.

For the general situation, i.e., where we are not restricted to an identical subcarrier configuration, every subcarrier may have different values for the modulation parameter. In this case, the total bit rate should be a summation of the bit rate of all the subcarriers. Thus, we can write the bit rate as

$$R_{tb} = \sum_{i=1}^{N_d} (R_{Ci} \cdot \log_2 M_i \cdot FSR_i \cdot \Delta f_i), \tag{3.5}$$

where the subscript 'i' means the i-th data (information) subcarrier. Of course, to obtain a different subcarrier bandwidth, we need a different technique, e.g., the wavelet technique, for OFDM systems. When $N_d = 1$, equation (3.5) accounts for the bit rate for a certain subcarrier. For the case of $R_{ci} = R_c$; $M_i = M$; $FSR_i = FSR$; $\Delta f_i = \Delta f$, equation (3.5) becomes

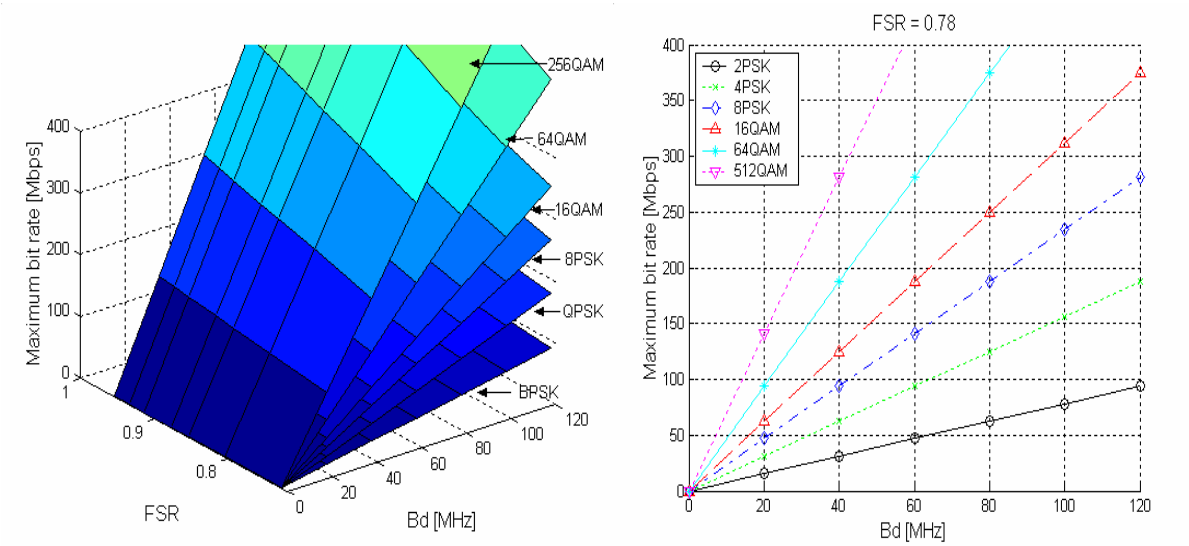
$$\begin{aligned} R_{tb} &= R_c \cdot \log_2 M \cdot FSR \cdot \Delta f \cdot N_d \\ &= (R_c \cdot \log_2 M) \cdot FSR \cdot B_d \end{aligned},$$

which is the same as equation (3.3).

If the limit of Δf tends to zero, i.e., $\Delta f \to 0$, the maximum bit rate yields

$$R_{tb} = \int_{B_d} [R_c(f) \cdot \log_2 M(f) \cdot FSR(f)] df . \tag{3.6}$$

Equation (3.6) is just a mathematical derivation. In practice the subcarrier bandwidth can hardly be infinitely small. So equation (3.5) is most useful. Equations (3.3) - (3.6) are applicable under the condition that the channel situation permits these parameter values, that is, that the values of these parameters on the right-hand side of equations (3.3) - (3.6) are determined by the channel condition (e.g., the SNR, frequency selectivity, etc).



(a) Maximum bit rate vs. information bandwidth and FSR

(b) Maximum bit rate vs. data bandwidth

Figure 3.3-2. Plots of the maximum bit rate formula

Figure 3.3-2 (a) gives a visual explanation of equation (3.3). This Figure reveals that at a given information bandwidth and modulation level, the maximum bit rate increases linearly with FSR; at a given modulation level and FSR, the maximum bit rate increases linearly with the information bandwidth; and at a given FSR and information bandwidth, the maximum bit rate increases logarithmically with modulation level. Figure 3.3-2 (b) gives a projected side view of Figure 3.3-2 (a), that is, a maximum bit rate versus data bandwidth for a given FSR of 0.78. The maximum bit rate in these two figures includes information and coding. In other words, when coding is used, the information bit rate will be much lower.

From these figures we learn that the maximum bit rate is proportional to the data bandwidth and FSR for an identical subcarrier configuration. For the general situation (equation (3.5)), the bit rate of each subcarrier is proportional to the subcarrier bandwidth and FSR of this subcarrier.

In conclusion, for a certain subcarrier or a group of subcarriers, four parameters determine the bit rate: the coding rate, modulation level, bandwidth, and FSR. Equation (3.3) to (3.5) give the mathematical description of the bit rate in terms of these parameters. In an adaptive OFDM system we can vary these parameters according to the channel situation to achieve good QoS and to reach a certain bit rate.

3.3.3 Throughput Formula for CDMA Systems

We have given the throughput formula for OFDM systems. If we compare CDMA with OFDM symbols, we can say that CDMA systems have one subcarrier, no guard time, and therefore no FSR. If we neglect window time, and take $N_S = 1$, $T_g = 0$, $T_w = 0$, and FSR = 1, equation (3.3) becomes

$$R_{tb} = (R_c \cdot \log_2 M) \cdot B_d = (R_c \cdot \log_2 M) \cdot Bt / Gp . \quad (3.7)$$

This is the throughput formula for CDMA systems in terms of bit rate, where B_d is total data frequency bandwidth, R_C coding rate, M modulation level, and Gp processing gain. Again, all values of parameters on the right side of the formula are determined by the channel situation.

From equation (3.7) we can conclude that the bit rate of CDMA systems is linearly proportional to coding rate and transmission bandwidth, logarithmically proportional to modulation level, and inversely proportional to processing gain.

3.4 Parameters Influencing QoS

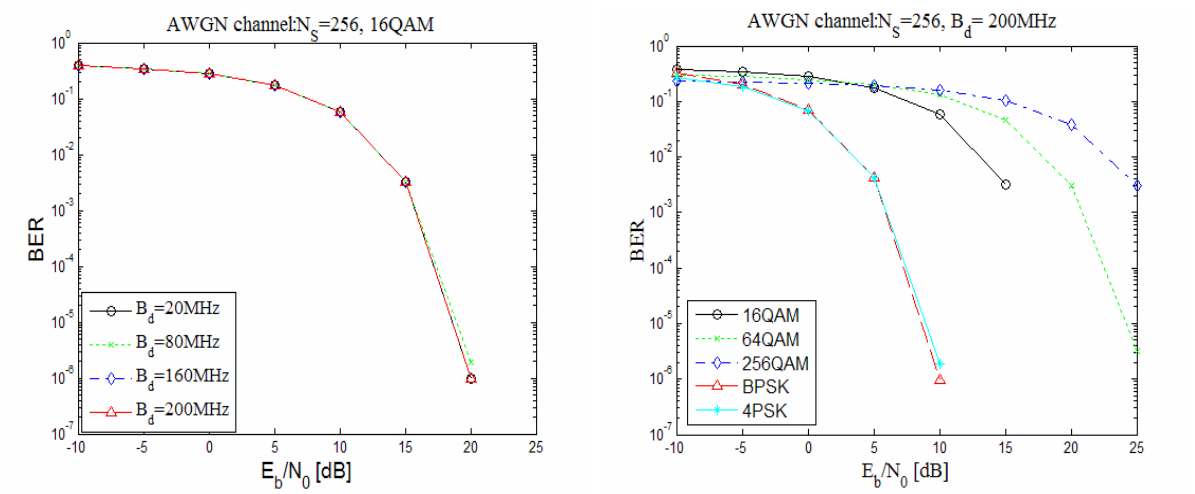
3.4.1 Performance of Parameters in the OFDM Throughput Formula

We have mentioned that some parameters (i.e., the coding rate, modulation level, bandwidth, and FSR) determine the throughput in an OFDM system. Now we investigate how these parameters affect the transmission QoS. The coding rate is not considered here because in this case it is similar to the modulation level. The BER versus SNR (here the ratio between energy per bit and noise power, i.e., E_b/N_0) is used to evaluate the transmission QoS. A simple case (an AWGN channel) is considered here. We assume that the entire bandwidth and all the subcarriers can be used for information transmission. NRP is assumed to be one in our simulations, which means receive power P_R equal to transmit power P_T. The content of Section 3.4.1 has been published by the author in [11].

Table 3.4-1. Simulation parameters for Figure 3.4-1 (a)

B_d (MHz)	R_{tb} (Mbps)	Δf (KHz)	N_S	T_s (μs)	T_{FFT} (μs)	T_g (μs)	P_T	FSR
20	$15.6\log_2 M$	78.125	256	16.4	12.8	2.4	-30 dBW	0.78
80	$62.4\log_2 M$	312.5	256	4.1	3.2	0.6		
160	$124.8\log_2 M$	625	256	2.05	1.6	0.3		
200	$156\log_2 M$	781.25	256	1.64	1.28	0.24		
M=16; Rc=1								

Table 3.4-1 presents the simulation parameters for Figure 3.4-1 (a). B denotes total available bandwidth; R_{tb} total bit rate of OFDM system; Δf subcarrier bandwidth; N_S subcarrier number; T_s symbol period; T_{FFT} FFT time in one symbol duration; T_g guard time in one symbol; P_T total transmission power; and FSR ratio of FFT time to symbol duration. We have mentioned that N_d is the number of data subcarriers. Practically N_S is larger than N_d since we need to use some subcarriers for the transmission of pilot symbols. However, here we assume that they are equal. P_T is transmit power. These symbol implications hold for the Tables 3.4-2, 3.4-3, and 3.4-4.



(a) Different bandwidth (b) Different modulation level

Figure 3.4-1. BER vs. SNR performance

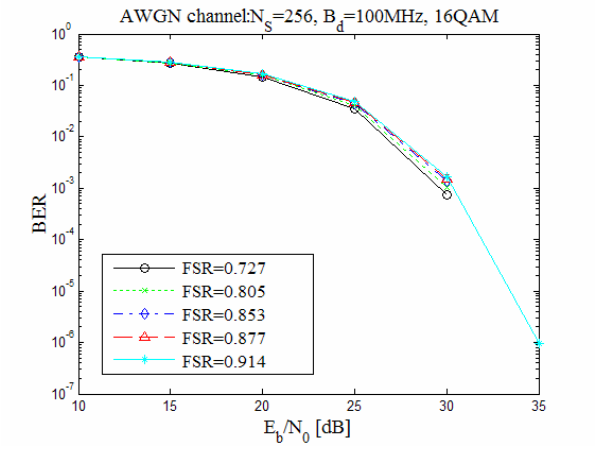


Figure 3.4-2. BER vs. SNR for different FSR (F/G in the figure means T_{FFT}/T_g)

Table 3.4-2. Simulation parameters for Figure 3.4-1 (b)

B (MHz)	R_{tb} (Mbps)	Δf (KHz)	N_S	T_s (μs)	T_{FFT} (μs)	T_g (μs)	P_T (dBW)	FSR
200	$1.5 \log_2 M$	781.25	256	1.64	1.28	0.24	-30	0.78
M = 4, 8, 16, 64, 256; Rc=1								

Table 3.4-3. Constant simulation parameters for Figure 3.4-2

N_S	B (MHz)	T_{FFT} (μs)	T_w (μs)	M	Rc	Δf (KHz)	P_T (dBW)
256	100	2.56	0.12	16QAM	1	390.625	-30

Table 3.4-4. Varying simulation parameters for Figure 3.4-2

FSR	T_{FFT}/T_g (F/G)	T_S (μs)	T_g (μs)
0.955	$+\infty$	2.56	0
0.934	42.7	2.74	0.06
0.914	21.3	2.8	0.12
0.877	10.7	2.92	0.24
0.853	8	3	0.32
0.805	5.1	3.18	0.5
0.727	3.0	3.52	0.84

Table 3.4-2 to 3.4-4 give the simulation parameters for Figures 3.4-1 (b) and 3.4-2. No coding is considered, e.g., *Rc* = 1. In Figure 3.4-1 (a), *FSR,* modulation level, and subcarrier number are constant; a change in total bandwidth is obtained by changing the subcarrier bandwidth. In Figure 3.4-1 (b), only modulation level varies. For Figure 3.4-2, total bandwidth, modulation level, subcarrier number, and FFT time are constant; a change in FSR is obtained by changing the guard time (the symbol duration varies correspondingly).

We discussed earlier that given a certain FSR, we can only get a higher bit rate by increasing the bandwidth or the modulation level. From Figure 3.4-1 (a), we can see that the "BER versus SNR per bit (E_b/N_0)" performance is almost the same for different bandwidths. From Figure 3.4-1 (b) we learn that the BER performance of higher modulation levels visibly degrade when E_b/N_0 is larger than around 3dB. By comparing Figure 3.4-1 (a) and (b) we note on the one hand, that when the bit rate is increased with the modulation level, the BER degrades much more than when the bandwidth is increased. On the other hand, the method of increasing modulation level will give a higher bandwidth efficiency, as the method of increasing bandwidth does not change the bandwidth efficiency. Since it is not practical to

increase the total bandwidth, this method can be used for one subcarrier or for a group of subcarriers.

An increase in guard interval results in more energy loss. A decrease in guard interval results in more sensitivity to frequency selective fading. FSR is a function of the guard time. From Figure 3.4-2 we can see that a varying FSR hardly affects the BER performance in an AWGN channel. For a frequency-selective fading channel, however, we expect a large difference in performance when FSR is changed. FSR can be derived from delay spread; then we use equations (3.3) and (3.5) to adapt coding rate, modulation level, and bandwidth according to the channel condition and throughput requirement to get a better QoS. This shows how the formulas can be applied. This approach may be especially useful for constant bit rate transmissions.

In conclusion, to make use of the throughput formula derived in section 3.3.2, we studied what influence varying parameters has on BER performance. Increasing modulation level (or coding rate) results in much worse BER performance; increasing FSR hardly changes BER performance in AWGN channels; increasing bandwidth does not degrade BER, but of course, it requires larger bandwidth, which is not so practical. So the goal is to find a compromise in adaptive OFDM in order to reach or keep a desired bit rate.

3.4.2 New Factor for OFDM System Performance in a Time-Varying Channel

In literature, the influence of channel situations on BER performance has been studied in [25], [26], e.g., BER versus SNR, BER versus K factor in a Rician channel. The influence of modulation parameters, e.g., the modulation level, coding rate, etc. on BER has been documented too in [26]. For varying channel situations, however, these may still be insufficient to improve the transmission quality. In order to improve the transmission quality, we still need to know the combined effect of the channel situation and modulation parameters. In this section we introduce a factor based on both OFDM modulation and a Rician channel, which influences the BER performance. Both theory and simulation results will be analyzed. The content of Section 3.4.2 has been published by the author in [27] and [28].

For an OFDM transmission system, we can roughly divide the related parameters into two categories: OFDM modulation parameters and channel parameters. Table 3.4-5 shows the characteristic OFDM and Rician channel parameters. From our analysis of the channel in chapter 2 we know that a larger Rician K factor and/or a larger SNR means a better channel situation, and therefore better BER performance can be expected. The previous section shows that for lower modulation levels the performance improves as well. Moreover, a smaller Root mean square Delay Spread (RDS) and/or smaller subcarrier bandwidth should give a better BER performance.

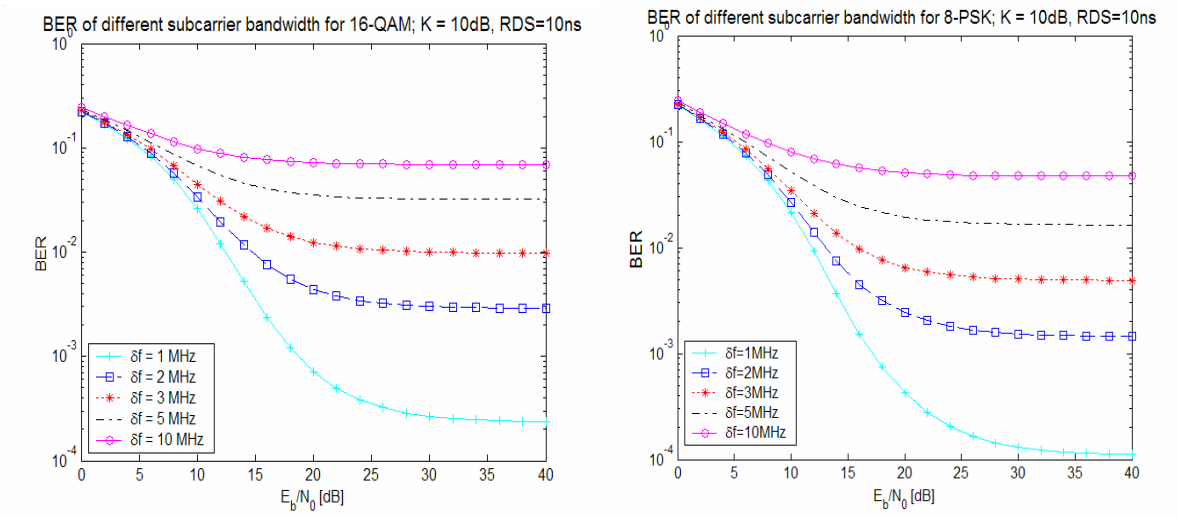
Now we raise the following questions: how do these parameters affect BER? Do the parameters work independently? The following section will give the answer for the parameters subcarrier bandwidth and RDS.

Table 3.4-5. Parameters of OFDM modulation and Rician channels

OFDM parameters	Rician Channel parameters
Guard time	RDS
Subcarrier bandwidth Δf	K
Modulation level M	SNR

3.4.2.1 Effect of Subcarrier Bandwidth

We discussed in Chapter 2 that delay spread leads to frequency selectivity in a fading channel. In addition, the narrower subcarrier bandwidth in frequency domain in OFDM results in a larger symbol duration in time domain. A larger symbol duration in time domain is more robust to delay spread. This explains why, in a frequency selective fading channel, when the subcarrier bandwidth is within a certain range (this will be described in Equation (3.8)), reduced subcarrier bandwidths may lead to an improved transmission performance, as can be seen in Figure 3.4-3. Figure 3.4-3 gives the simulation results for 16QAM and 8PSK modulations in a Rician channel with a *K* factor of 10dB and an RDS of 10ns. Subcarrier bandwidths of 1MHz, 2MHz, 3MHz, 5MHz, and 10MHz have been simulated. The subcarrier bandwidth of 1 MHz gave the best BER performance and the subcarrier bandwidth of 10MHz the worst. From the simulation results it seems that the narrower the subcarrier bandwidth, the better the BER performance we get. However, could we legitimately conclude from this result that a narrower subcarrier gives better BER performance? To discover this, we investigate the relation between this bandwidth and RDS.



(a) 16QAM (b) 8PSK

Figure 3.4-3. BER of different subcarrier bandwidths for 16QAM and 8PSK

3.4.2.2 Relationship between Subcarrier Bandwidth and RDS

In an OFDM system, we need to set the subcarrier bandwidth. A large subcarrier bandwidth may lead to more distortion, due to the frequency selective fading (see Appendix A). A small subcarrier bandwidth may also lead to more distortion, due to time-selective fading (or fast-fading, from random frequency modulation noise). Moreover, the smaller the subcarrier bandwidth, the larger the ICI. We cannot set any value for the subcarrier bandwidth. The subcarrier bandwidth should not be smaller than the coherence bandwidth in order to combat ICI, and it should not be larger than the reciprocal of RDS to combat frequency-selective fading caused by delay spread (or RDS). Therefore, the subcarrier bandwidth should be between the reciprocal of RDS and the coherence bandwidth B_C, i.e.,

$$\mathrm{B_C} \le \Delta f \le \frac{1}{\mathrm{RDS}}. \tag{3.8}$$

For a frequency correlation above 0.9, we assume that [28]

$$B_C \approx \frac{1}{50RDS}. \tag{3.9}$$

If we replace B_C with equation (3.9), equation (3.8) becomes

$$\frac{1}{50RDS} \le \Delta f \le \frac{1}{\mathrm{RDS}}. \tag{3.10}$$

Table 3.4-6 gives the minimum and maximum subcarrier bandwidth for an OFDM system with a total bandwidth of 400MHz, given the rms delay spread. Correspondingly, the minimum and maximum number of subcarriers can be obtained.

Table 3.4-6. Subcarrier bandwidth and number of subcarriers versus RDS

RDS (ns)	Min(Δf)	Max(Δf)	B	Min(Nsbc)	Max(Nsbc)
1	20MHz	1 GHz	400 MHz	1	20
10	2 MHz	100MHz		4	200
50	400 KHz	20 MHz		20	1000
100	200 KHz	10 MHz		40	2000
200	100 KHz	5 MHz		80	4000
300	67 KHz	3.33 MHz		121	5970

We now introduce a new parameter, P_{FR}, as the product of the subcarrier bandwidth Δf and the RDS, i.e.,

$$P_{FR} = \Delta f \cdot RDS \,. \tag{3.11}$$

According to equation (3.10), P_{FR} will be in the range $0.02 \leq P_{FR} \leq 1$.

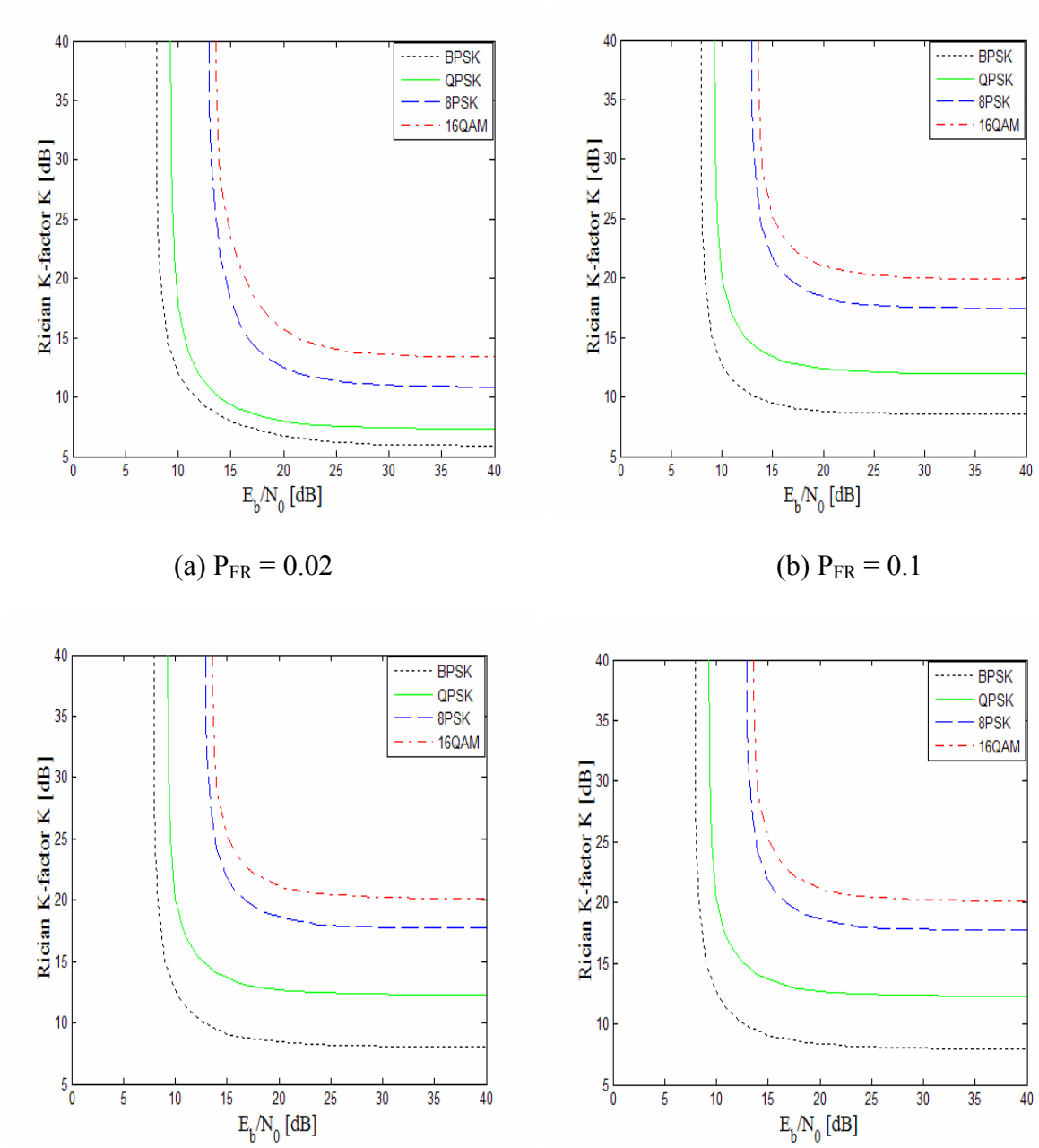
In the simulations we selected P_{FR} = 0.02, 0.1, 0.5, 1, and simulated modulation levels versus K-factor and SNR for a certain BER. For each value of $P_{FR,}$ different values of RDS and Δf were taken, as can be seen in Table 3.4-7.

Table 3.4-7. Simulation parameters for Figure 3.4-4

RDS(ns)		1	10	50	100	200
Δf (GHz)	P_{FR} =0.02	0.02	0.002	0.0004	0.0002	0.0001
	P_{FR} =0.1	0.1	0.01	0.002	0.001	0.0005
	P_{FR} =0.5	0.5	0.05	0.01	0.005	0.0025
	P_{FR} =1	1	0.1	0.02	0.01	0.005

We have simulated the *K* versus SNR relation over the SNR range of 0 to 40dB, and for a BER of 10^{-3}. By doing this, we can obtain the SNR required for a BER of 10^{-3}, given the Rician *K* factor, and/or the Rician *K* value required for a BER of 10^{-3}, given a certain SNR value. Four modulation levels are simulated and plotted in Figure 3.4-4 and Figure 3.4-5, i.e., BPSK, QPSK, 16QAM, and 64QAM. The channel model exploited in the simulations is the frequency selective fading channel with Rician distribution, described in Chapter 2.

From the simulation results in Figure 3.4-4, we note that, when the product of Δf and RDS, (i.e., P_{FR}) is fixed, for all different values of RDS and Δf, the lines of Rician *K* factor versus SNR for a certain BER overlap. This leads to the simple relationship: BER is a function of P_{FR} (this will be explained in Section 3.4.2.3).



(a) P_{FR} = 0.02

(b) P_{FR} = 0.1

(c) P_{FR} = 0.5

(d) P_{FR} = 1

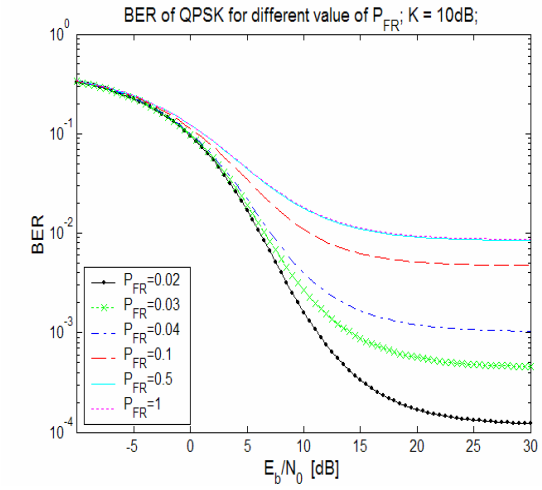
Figure 3.4-4. Rician *K* versus SNR for different modulations with selected values of P_{FR} (P_{FR} = RDS x Δf; BER = 10^{-3})

3.4.2.3 Influence of P_{FR} on BER

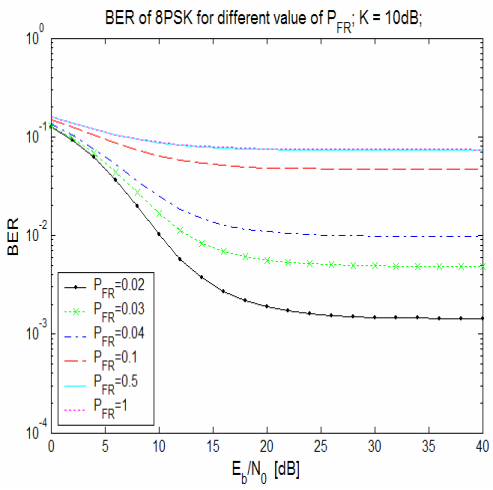
We have analyzed in Section 3.4.2.2 that RDS and Δf do not affect individually the BER performance, but their product P_{FR} does. This can be explained in the following way: given that the other channel parameters and OFDM modulation parameters are constant, by increasing RDS one will increase the frequency selectivity of the channel (as discussed in Chapter 2), and further increase the BER; if the given channel parameters and other OFDM modulation parameters are constant, by decreasing the subcarrier bandwidth in a frequency selective fading channel one can make the system more robust to frequency selective fading and therefore decrease the BER; the subcarrier bandwidth is assigned in terms of the channel frequency selectivity. Hence, a smaller subcarrier bandwidth is used to combat the frequency selectivity of the channel resulting from delay spread (or RDS). The subcarrier bandwidth and RDS can compensate for each other's influence on the BER. When the RDS increases, we can decrease the subcarrier bandwidth to keep the BER constant, and vice versa. In Figures 3.4-5 we present the influence of P_{FR} on BER from simulations. Still, we exploit the channel model discussed in Chapter 2, i.e., the frequency selective fading channel with Rician distribution of the amplitude of the channel function. Since P_{FR} can have an impact on BER instead of the individual RDS and subcarrier bandwidth, we just give the values of P_{FR} here.

In the simulation of Figure 3.4-5, we assume a K factor of 10dB, and simulate BER versus SNR for different values of $P_{FR.}$ QPSK, 8PSK, 16QAM have been simulated. From the simulation results we learn that for all these modulations, when SNR is quite small (e.g., smaller than 0dB), a different P_{FR} gives almost no difference in BER performance and all have high error rate; but when SNR is larger, smaller P_{FR} can give better BER performance. This is because the influence of subcarrier bandwidth and RDS is not unlimited. When SNR is small, we can not get a desirable BER no matter what value the subcarrier bandwidth is set.

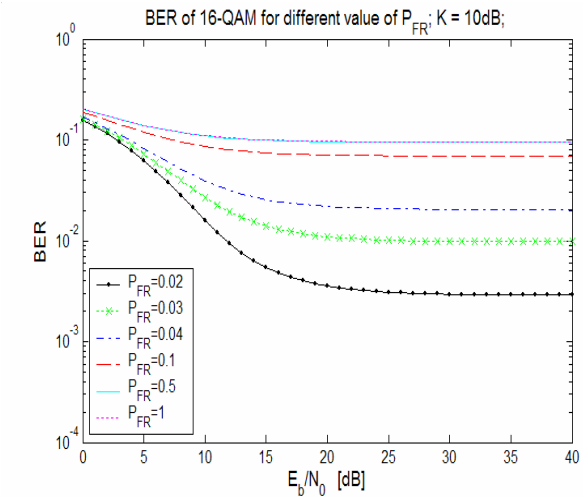
In conclusion, the traditional belief that a smaller subcarrier bandwidth gives better BER performance is true only for a constant channel situation, or in other words, for a constant delay spread. When the product of subcarrier bandwidth and RDS is fixed, changing the values of the subcarrier bandwidth and/or the RDS does not influence the BER performance. The product of the subcarrier bandwidth and RDS is therefore an important factor to influence BER performance. From simulations we have learned that when the SNR is above 0 dB, the relationship yields: the smaller the product, the better the BER performance. However, for a constant channel situation, the RDS is a constant value, so a smaller P_{FR} means a smaller subcarrier bandwidth. In this case, a smaller subcarrier bandwidth can give a better BER performance. The result is useful to improve the OFDM system performance for a varying channel situation and is important for adaptive OFDM.



(a) QPSK



(b) 8PSK



(c) 16QAM

Figure 3.4-5. BER vs. SNR for different values of P_{FR} and for different modulations

3.4.2.4 Prerequisites for P_{FR}

We have investigated how P_{FR} influences BER performance of OFDM systems within a certain SNR range: the smaller P_{FR} is, the better the BER performance. In this context, questions can be raised as: "what is this SNR range? and by which parameter is it

influenced?" To find this out, we have simulated BER versus SNR for different P_{FR} and different K factors. Several modulation schemes have also been considered.

We simulated BER versus ratio of energy per bit to noise power spectral density (E_b/N_o) for different P_{FR} for BPSK, QPSK and 16QAM modulations. The simulation conditions are: for each modulation and each K value, P_{FR} values of 0.02, 0.03, 0.04, 0.1, 0.5 and 1 have been simulated, separately. K factors of –10, 0, 6, 10, 20dB were chosen for BPSK; K factors of 0, 5, 10, 14, 20dB for QPSK; K factors of 5, 10, 15, 20, 25, 28dB for 16QAM. Figure 3.4-6 to 3.4-8 show the simulation results.

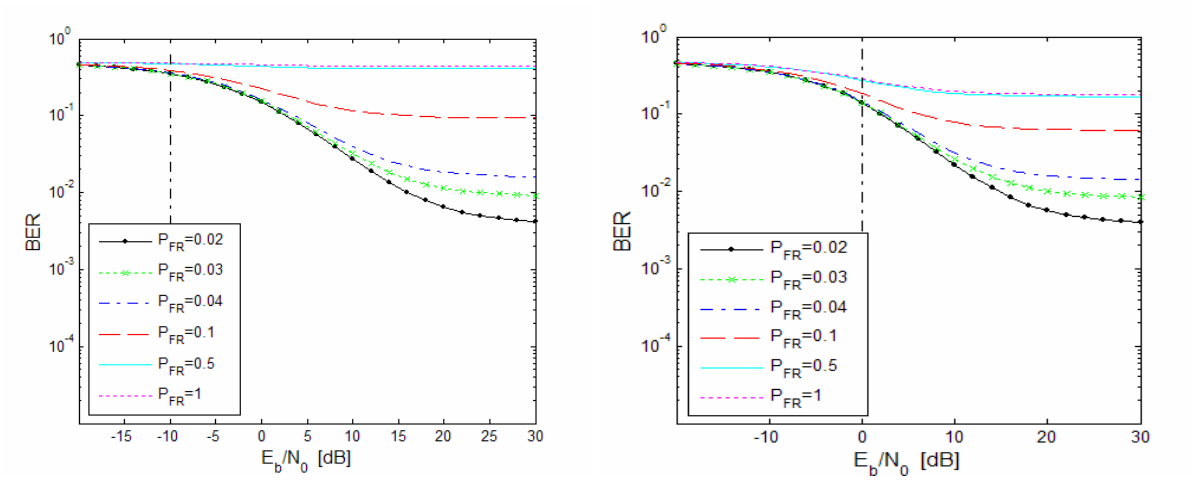
From the simulation results in these figures, we gained the insight that:

- The smaller P_{FR}, the larger BER difference for a change in $P_{FR;}$ changing P_{FR} between 0.5 and 1 hardly affect BER; this is because when P_{FR} =0.5, BER is already worst, i.e., around 0.6, so that it is difficult to see the influence for an even larger P_{FR};
- Only when SNR is larger than a certain value (we call this value: "start SNR"), by changing P_{FR} one can influence BER; in order to improve BER effectively, we can take this start SNR slightly larger than the starting point where BER lines for different P_{FR} begin to differentiate;
- For larger Rician K values, this starting point becomes larger;
- When Rician K factor is very large, the influence of P_{FR} on BER becomes irregular, i.e., a reasonable and regular influence cannot be seen any more; we define the largest K value where P_{FR} influences BER performance as *top K*. When K is larger than a certain value (20dB for BPSK, QPSK, which can be derived from Figure 3.4-6 and 3.4-7), P_{FR} has no influence on BER. This is because the LOS becomes dominant for a large K and because delay spread from multipath does not have a large impact on BER performance. Therefore, the influence of the product of the subcarrier bandwidth and RDS diminishes.

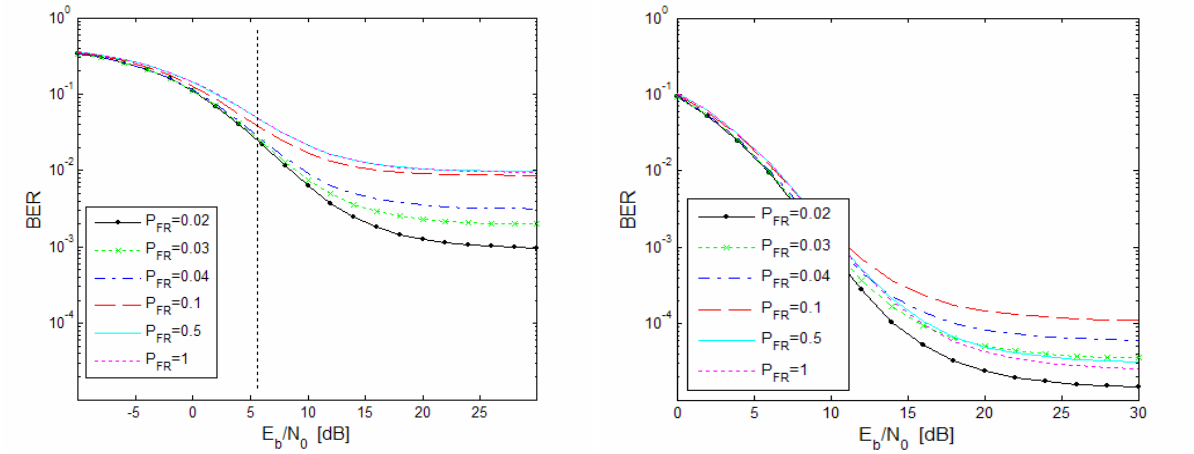
In order to describe our findings clearly, the following definitions are given:

Start SNR (SSNR): it is indicated above that when the SNR is above a certain value, different P_{FR} can have different BER performance. We define the SNR such that BER performances for different P_{FR} begin to differentiate from the Start SNR, written as SSNR. By checking this point in the simulations, we obtain SSNR values for different K factors and different modulations. In practice, the SSNR value will be taken a little bit larger than the exact starting point.

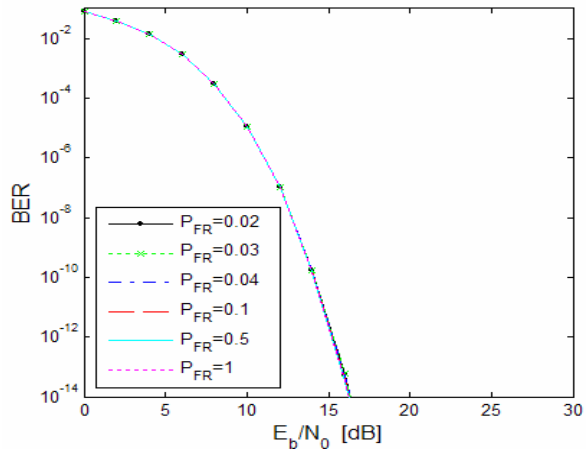
Top K: When the Rician K is very large, influence of P_{FR} on BER becomes irregular; we will call the largest K value where P_{FR} still influences the BER performance as "*top K*".



(a) K = -10dB (b) K = 0dB

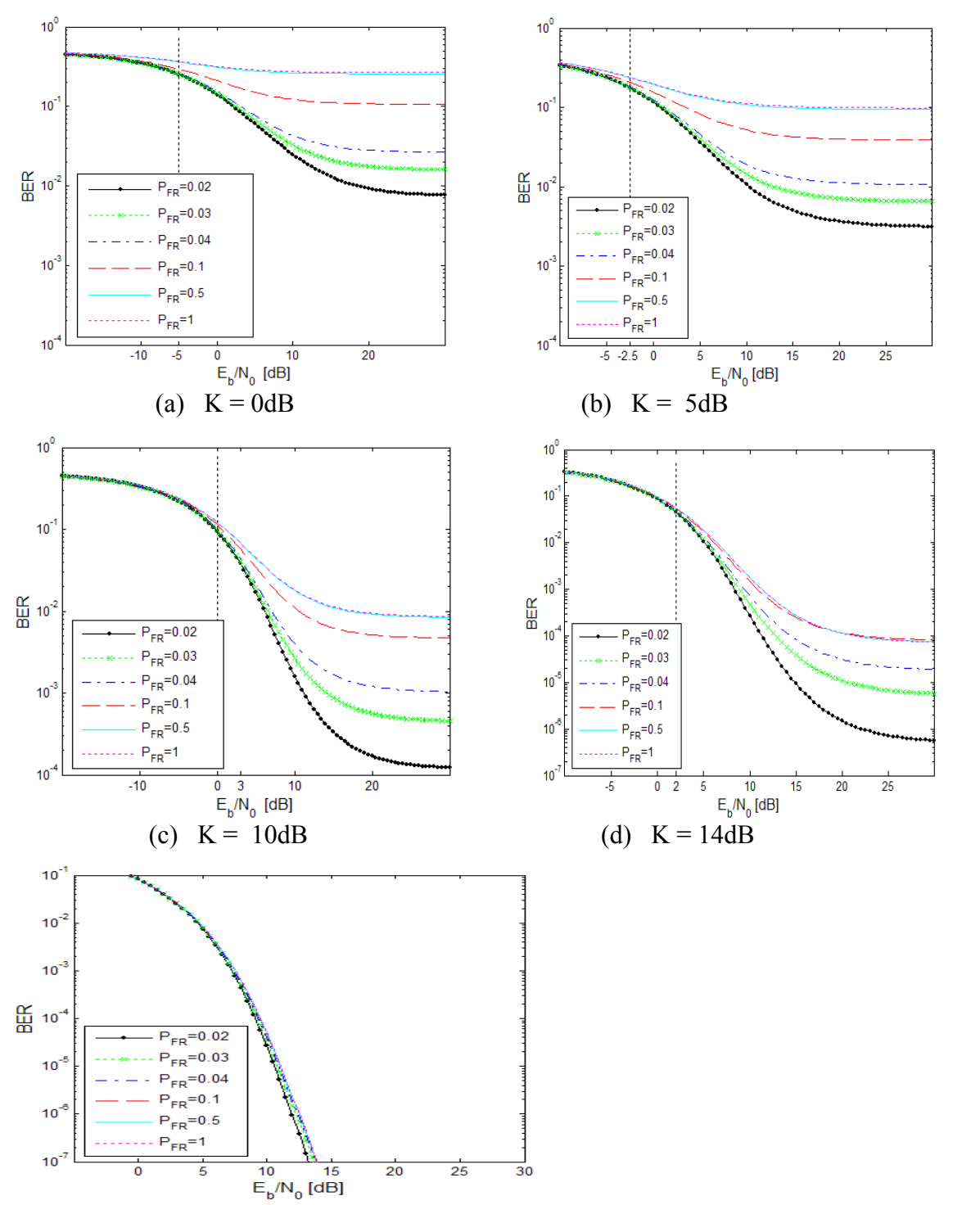


(c) K = 6dB (d) K = 10dB



(e) K = 20dB

Figure 3.4-6. Influence of P_{FR} on BER for different K values for BPSK

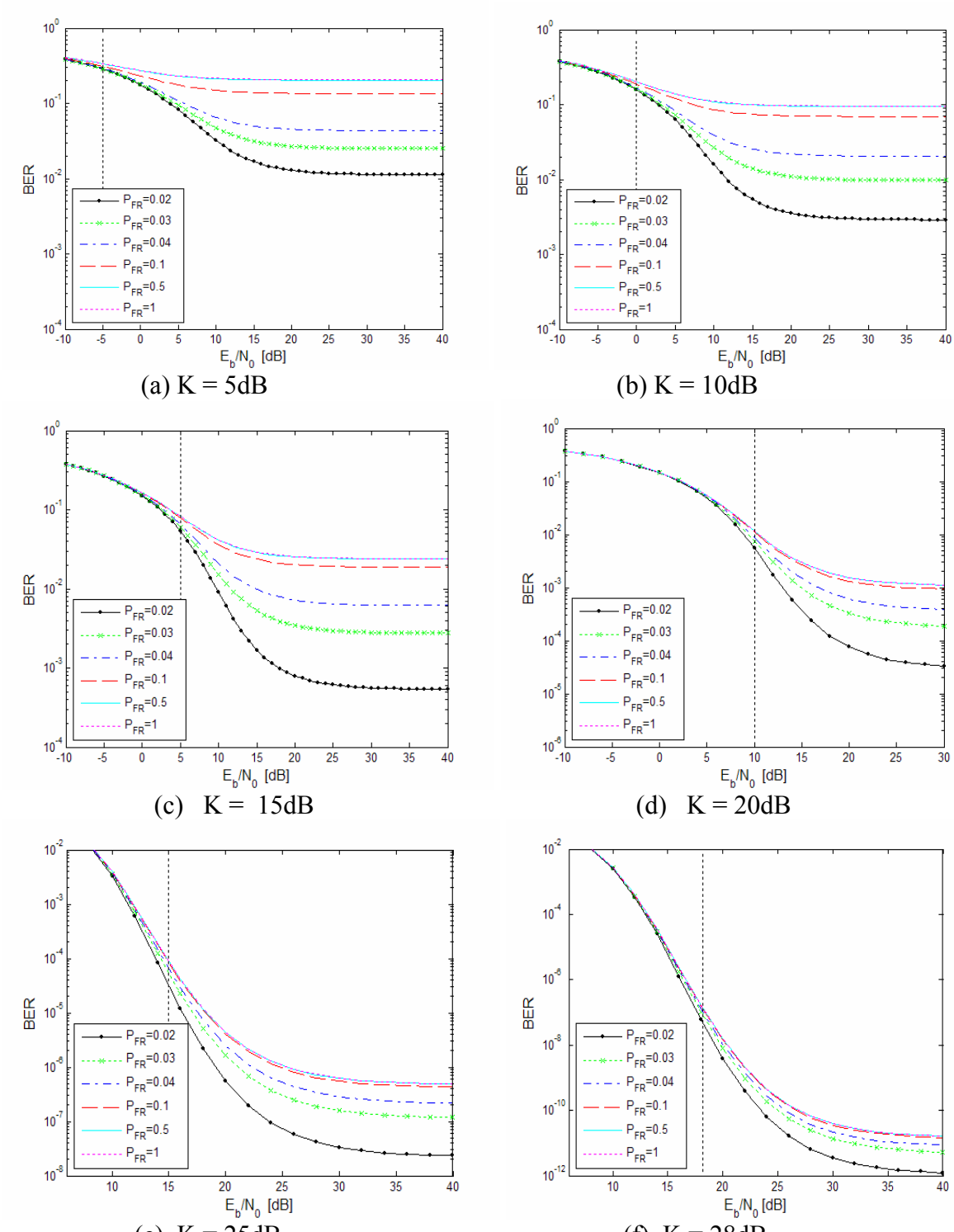


(a) K = 0dB (b) K = 5dB

(c) K = 10dB (d) K = 14dB

(e) K = 20dB

Figure 3.4-7. Influence of P_{FR} on BER for different K values for QPSK



(a) K = 5dB (b) K = 10dB

(c) K = 15dB (d) K = 20dB

(e) K = 25dB (f) K = 28dB

Figure 3.4-8. Influence of P_{FR} on BER for different K values for 16QAM

From the simulation results, we notice that for each modulation, the start SNR (SSNR) where P_{FR} affects BER depends on K. It is possible to find a rough relationship between Start SNR and K. We list all SSNR and K for different modulations and derive a relation between SSNR and K. This relationship has been obtained from Figures 3.4-6 to 3.4-8, and is modulation dependent (see Table 3.4-8).

Table 3.4-8. Start SNR versus K for different modulations

modulation	BPSK			QPSK				16QAM					
K value in dB	-10	0	6	0	5	10	14	5	10	15	20	25	28
Start SNR[dB]	-10	0	6	-5	-2.5	0	2	-5	0	5	10	15	18
function	SSNR= K			SSNR=K/2-5				SSNR=K-10					
Top K [dB]	6			14				28					

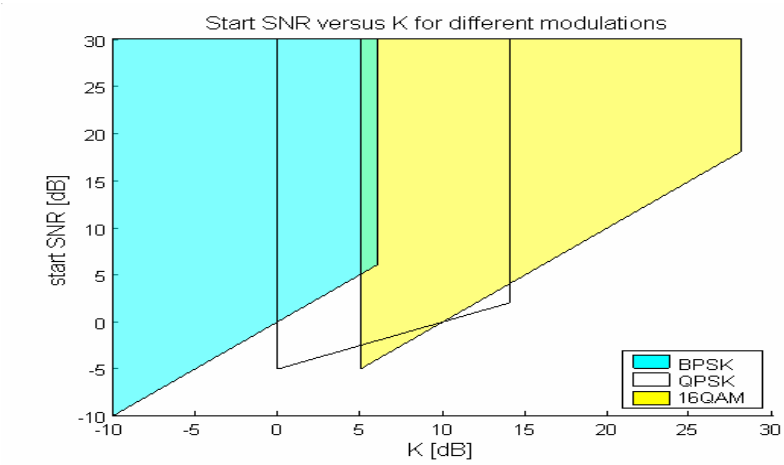


Figure 3.4-9. Start SNR versus K for BPSK, QPSK, 16QAM

For BPSK (Figure 3.4-6), a smaller P_{FR} results in a lower BER only when the Rician K factor is between -10dB and 6dB and the start SNR between -10dB and 6dB. Based on this, we have plotted the start SNR versus K for BPSK in Figure 3.4-9. In the same way, we have obtained the start SNR versus K for QPSK and 16QAM (Figures 3.4-7 and 3.4-8). Figure 3.4-9 shows Start SNR as a function of Rican K factor. Adjusting P_{FR} can change BER only inside the region for each modulation. For BPSK modulation, for example, adjusting P_{FR} can only change BER in the marked region for BPSK; for QPSK modulation, adjusting P_{FR} only works in the marked region for QPSK; and for 16QAM, adjusting P_{FR} can only change a BER in the

marked region for 16QAM. They overlap in some areas, which means that in these areas it works for both/all modulations. Of course 30dB is not the maximum SNR at which the adjusted P_{FR} will work, that is to say, the upper limit of this figure can be extended upwardly.

From the simulations we now know that *top K* and SSNR are functions of modulation level *M*. If we use *top K(M)* to represent the *top K* value for the assigned modulation level *M*, and the Start SNR(*M*) represents the Start SNR value for the assigned modulation level *M*, the work conditions for adjusting P_{FR} can be generalized as:

- $K <$ *top K(M)*;
- SNR > start SNR(*M*);
- P_{FR} is in the range [0.02 1];
- P_{FR} value between [0.5 1] is one state; so we take the P_{FR} state from 0.02 to 0.5 with step of 0.01 (0.02:0.01:0.5) and state 0.5 means P_{FR} from 0.5 to 1.

3.4.3 Performance of Parameters in the CDMA Throughput Formula

Similarly, for CDMA systems, BER will increase with coding rate and modulation levels; it will not change with the transmission bandwidth, however, given that the other parameters remain constant. From the objective of processing gain, we expect that the BER will decrease with increase of processing gain. All of this has been proved in literature [30], [31], [32], [33], [34], [35].

3.5 Strategies for Adaptive Modulation Algorithms

3.5.1 Work Procedures for Setting-up Adaptive Modulation Algorithms

The difference between non-adaptive and adaptive modulation systems is that non-adaptive systems are designed based on a statistical channel condition over a long time interval; once the modulation parameters of the system have been assigned, they remain constant and invariable; adaptive modulation systems are designed based on the random, instantaneous channel situation. What is more, the modulation parameters are adaptive during transmission under different channel conditions. To benefit from the adaptive function, an adaptive modulation algorithm is required with some rules to change the modulation parameters. An adaptive modulation algorithm cannot choose and change any parameter. The action of adaptive modulation algorithms is to build up criteria in order to make an optimum combination of the values of selected modulation parameters. They should be used efficiently to lead to a better transmission quality and/or throughput.

The work of adaptive modulation is different from the traditional work of modulation. The traditional approach is to study basic modulation technology and combine and/or modify some aspects in the technology to get improvement. In adaptive modulation it is prerequisite

to study inner-relationships within modulation parameters and channel parameters themselves as well as inter-relationships between them. In order to build up an efficient adaptive modulation algorithm, therefore, relationship study should be executed firstly; and then criteria should be set up, based on which the adaptive modulation algorithm can decide whether to change and how to change modulation parameters.

We mentioned before that the process of adaptive modulation involves two interrelated sets of parameters: modulation and channel parameters. In order to determine the criteria for the algorithm, one should capture the information from these two parameter sets. The work steps of adaptive modulation algorithms can be generalized as [17],

1. List all related parameters with respect to channel characteristics;

2. List all related parameters with respect to relevant modulation characteristics;

3. Find out the relationships among parameters with respect to the channel characteristics;

4. Find out the relationships among parameters with respect to the relevant modulation characteristics;

5. Find out the relationships between parameters with respect to the channel characteristics and parameters with respect to the modulation characteristics;

6. After building up a database described above for adaptive modulation algorithms, one should try to denote the transmission QoS and throughput in terms of modulation parameters and channel parameters. Since the objective of the algorithm is to improve the QoS and throughput, we have to relate the two aspects (i.e., channel and modulation) to both QoS and throughput;

7. Investigate the feasibility and benefit of changing each of the modulation parameters. This feasibility study includes two aspects: whether it is feasible to change this parameter in theory, and whether it is beneficial to change this parameter;

8. Build up the complete algorithm to adjust modulation parameters dynamically according to the channel parameters;

9. Evaluate the adaptive modulation algorithm in terms of throughput and QoS via simulations.

3.5.2 Work Procedures for Adaptive OFDM Algorithms

Having described the work procedures in Section 3.5.1, we show here how to build adaptive OFDM algorithms [36].

a) Find out the parameters that can represent the characteristics of the two aspects: channel and modulation. This covers Steps 1 and 2 of the procedure of adaptive modulation algorithms.

   The channel parameters have been investigated in Chapter 2, and the OFDM parameters are investigated in Appendix A. The parameters are listed in Table 3.5-1, including the "narrow-sense" modulation parameters, i.e., modulation level, coding rate, and power.

Table 3.5-1. Parameters representing OFDM modulation and channel character

OFDM parameters			Channel parameters
TD	FSR, T_g,T_S, T_{FFT}		RDS
FD	B, Δf, N_s		K
Other parameters	M, R_c power		SNR
			B_D
			NRP

TD – *Time Domain parameters;*
FD – *Frequency Domain parameters;*
FSR – *FFT to Symbol duration Ratio;*
T_g – *Guard time;*
T_S – *Symbol duration;*
T_{FFT} – *FFT time;*
B – *Total bandwidth;*
Δf – *Subcarrier bandwidth;*
N_s – *Number of subcarriers;*
M – *Modulation level for MPSK or M-QAM;*
R_c – *Coding rate;*
RDS – *Root mean square Delay Spread;*
K – *Rician K-factor;*
SNR – *Signal to Noise Ratio;*
B_D – *Doppler spread;*
NRP – *Normalized Received Power.*

b) Discover the relationships among the parameters with respect to channel characteristics, and the relationships among the parameters with respect to OFDM

modulation. This covers Steps 3 and 4 of the procedure of adaptive modulation algorithms.

The relationships among parameters with respect to the channel have been investigated in Chapter 2. The relationships among the parameters with respect to the OFDM modulation are given Appendix A. They are summarized here:

$B = N_S \bullet \Delta f$;
$T_S = T_{FFT} + T_g$;
FSR=T_{FFT}/T_S;
$T_{FFT} = \frac{1}{\Delta f}$.

Since some parameters depend on each other, it is not necessary to design all parameters in the adaptive OFDM algorithm. Meanwhile, we assume that the normalized received power is equal to one and is not considered in the algorithm. Thus, Table 3.5-1 can be simplified into Table 3.5-2.

Table 3.5-2. Parameters related to the design of adaptive OFDM algorithms

OFDM parameters			Channel parameters
TD	T_g		RDS
FD	Δf *or* N_s		*K*
Other parameters	*M*, R_c		*SNR*
			B_D

c) After listing the parameters related to the design of adaptive OFDM algorithms, one should build relationships between the parameters with respect to channel characteristics and parameters with respect to the modulation characteristics. In other words, it should be found out based on which channel parameter which OFDM modulation parameters should be set. This is Step 5 of the procedure of adaptive modulation algorithms.

From our investigation on OFDM modulation we know that the guard time should be set around four times the RDS delay spread to combat ISI, so the RDS determines guard time. In Chapter 2, it was investigated that the fluctuation of the channel transfer function in frequency domain is determined by RDS and Rician *K* factor. We know that when the channel fluctuates more in frequency domain, we should assign a higher number of subcarriers, that is, a smaller subcarrier bandwidth. What is more, the subcarrier bandwidth should be much larger than

Doppler spread in order to combat ICI. Hence, the RDS, Rician K and Doppler spread determine the setting of the subcarrier bandwidth and the number of subcarriers. Furthermore, it is well known that the SNR of the channel determines the modulation levels and coding rate. Table 3.5-3 describes the relationships between the OFDM modulation and the channel.

Table 3.5-3. Mapping OFDM parameters to channel parameters

OFDM parameters			Channel parameters
TD	T_g	←	RDS
FD	Δf *or* N_s	←	K
Other parameters	M, R_c		B_D
		←	SNR

d) The next step is to denote the transmission QoS and throughput in terms of modulation parameters and channel parameters. Since the objective of the algorithm is to improve the QoS and throughput, both are related to the two aspects: channel and modulation. This is Step 6 of the procedure of adaptive modulation algorithms.

In OFDM, if the bit rate is exploited to represent throughput, the total information bit rate, as derived in Section 3.3, can be written as

$$R_{tb} = \sum_{i=1}^{N_d} (R_{ci} \bullet \log_2 M_i \bullet FSR_i \bullet \Delta f_i) \ .$$

This equation represents a general situation and i means the ith information subcarrier. For identical subcarrier configurations, the bit rate can be written as

$$R_{tb} = (R_c \cdot log_2 M) \cdot B_d \cdot FSR,$$

where FSR = T_{FFT}/T_s, i.e., FFT time to symbol duration ratio, $\Delta f = 1/T_{FFT}$, B_d total data frequency bandwidth, and N_d number of information subcarriers. Again, all parameters on the right side of the formula are determined by the channel situation.

If BER is exploited to represent the QoS in OFDM, from the analysis we described before we know that BER increases with modulation levels, coding rate, and P_{FR}, and decreases with an increase of the SNR and Rician K factor. This relation can be expressed as

$$BER \propto \quad \{M, R_C, P_{FR}, \frac{1}{K}, \frac{1}{SNR}\}, \tag{3.12}$$

where $\propto$ denotes that the variable on the left side of equation (3.12) will go to the same direction (increase or decrease) with each of the variables on the right side when other variables are constant. In other words, BER increases with M, R_C, P_{FR}, and decreases with increasing K, and SNR.

e) Investigate the feasibility and benefit of changing each of the modulation parameters. This is Step 7 of the procedure of adaptive modulation algorithms.

From our investigation sofar we have obtained the OFDM modulation parameters, FSR, T_g, T_S, T_{FFT}, B, Δf, N_s, M, and R_c. The OFDM modulation parameters that should be considered for adaptation are T_g, Δf (or N_s), M, and R_c. Now let us study the feasibility of adapting these parameters. Actually, we have mentioned before that the total available bandwidth B is given before the system design and it is not practical to change this parameter. The set of modulation parameters to be designed is the set of independent parameters representing OFDM modulation parameters. Therefore, it is only necessary to study the feasibility of changing these independent OFDM modulation parameters. Nevertheless, the related parameters should be considered to evaluate the feasibility of adapting each of these independent OFDM modulation parameters.

It is known from literature that modulation level and coding rate can be adapted [37], [38], [39], [40]. It does not seem to be a problem to change the subcarrier bandwidth itself. However, if we look at its related parameters, i.e., the number of subcarriers, which can only be equal to the power of two, as discussed before, we should take care when setting the subcarrier bandwidth. The other parameter related to the subcarrier bandwidth is FFT time. From the relation of parameters $B = N_S \times \Delta f$, and $T_{FFT} = \frac{1}{\Delta f}$, we obtain

$$T_{FFT} = N_S \cdot \frac{1}{B} \quad . \tag{3.13}$$

From this equation it follows straightforwardly that the FFT time is N_S times the sampling time of the whole bandwidth. It is possible to change this parameter in the adaptive modulation algorithm. As for the guard time, theory permits and implementation is feasible to adapt the guard time in OFDM systems.

Hence, in potential we can adapt all these independent OFDM modulation parameters, i.e., T_g, Δf (or N_s), M, and R_c, in adaptive OFDM systems. There is no problem in theory and implementation is feasible. In addition, from the study of the influence of these parameters on BER and throughput, we conclude that it can be beneficial to adapt these parameters in an adaptive OFDM system.

f) Build up the complete algorithm to adjust the modulation parameters dynamically according to the channel parameters. This is Step 8 of the procedure of adaptive modulation algorithms.

Figure 3.5-1 describes the process of adaptive OFDM algorithms in a simple way. Given the channel situation by channel parameters, and the system requirements, the OFDM modulation parameters are adapted at every moment by a certain rule. The system detects the channel situation continuously and inputs it in the adaptive algorithm. The algorithm assigns values for the modulation parameters correspondingly. Details will be given in Chapter 5.

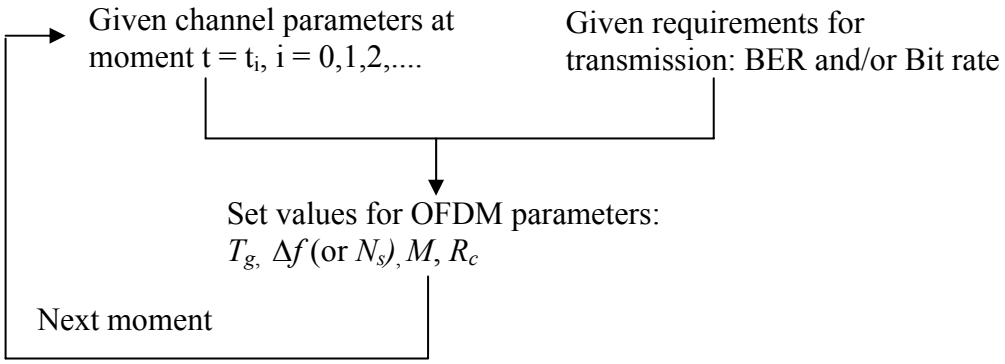


Figure 3.5-1. Simple flow chart of adaptive OFDM algorithms

g) Evaluate the adaptive modulation algorithm by the actual throughput and QoS. This is Step 9 of the procedure of adaptive modulation algorithms.

The objective of adaptive modulation is to improve the transmission quality of service (QoS) and throughput, as discussed before. According to this, the efficiency of adaptive modulation algorithms should be evaluated based on the QoS and throughput.

The QoS can be represented by the BER. The parameters influencing the BER have been investigated already. Throughput can be represented by the bit rate or spectrum efficiency. The spectrum efficiency is defined as the number of transmitted bits per second per Hertz of system bandwidth. Therefore, it can be measured by the bit rate to bandwidth ratio [39]. Hence, the bandwidth efficiency is determined based on the modulation type, coding rate, etc.

To make a clear link between the "nine-step" work procedure discussed in Section 3.5.1 and the work procedure of stages "a) to g)" in this section, we give Table 3.5-4. The work procedures in Section 3.5.3 obey this link too.

Table 3.5-4. Link between the "nine-step" procedure and the "a) to g)" stages of the process of the adaptive modulation algorithm

Nine-step procedures		a) ~g) stages of algorithm
1	→	a)
2		
3	→	b)
4		
5	→	c)
6	→	d)
7	→	e)
8	→	f)
9	→	g)

3.5.3 Work Procedures for Adaptive CDMA Algorithms

Following the work procedures described in Section 3.5.1, we now discuss the work procedure of adaptive CDMA algorithms.

a) Determine which parameters can represent the characteristics of two themes: channel and modulation. This covers Step 1 and 2 of the procedure of adaptive modulation algorithms.

   The channel parameters and the CDMA parameters have been investigated in Chapter 2 and in Appendix B, respectively. Interference limits the performance of CDMA systems, thus, SINR is used here to represent the channel characteristics instead of SNR. Table 3.5-5 lists all parameters, including the "narrow-sense" modulation parameters, i.e., modulation level, coding rate, and power.

Table 3.5-5. Parameters representing CDMA modulation and channel

CDMA parameters			Channel parameters
TD	B_S, Bt, R_S, R_{cd}, Gp,R_b		RDS
FD	T_S, T_{cd}, T_b		K
Other parameters	M, R_c		$SINR$
	N_u		B_D
	power		NRP

TD – *Time Domain parameters;*
FD – *Frequency Domain parameters;*
B_S – *Bandwidth of signal;*
Bt – *Total bandwidth;*
R_S – *Symbol rate;*
R_{cd} – *Chip rate;*
Gp – *Processing gain;*
R_b – *Bit rate;*
T_S – *Symbol period;*
T_{cd} – *Period of chip code;*
T_b – *Bit period;*
M – *Modulation level for MPSK or M-QAM;*
R_c – *Coding rate.*
N_u – *Number of users in one cell;*
RDS – *Root mean square Delay Spread;*
K – *Rician K-factor;*
SINR – *Signal to Interference plus Noise Ratio;*
B_D – *Doppler spread;*
NRP – *Normalized Received Power.*

b) Discover the relationships among the parameters with respect to channel characteristics (in principle, the algorithm can be used for both uplink and downlink if the channel estimation can be obtained at both the base station and mobile station) and the relationships among the parameters with respect to CDMA modulation. This covers Steps 3 and 4 of the procedure of adaptive modulation algorithms.

The relationships among parameters with respect to the channel have been investigated in Chapter 2. The relationships among the parameters with respect to CDMA modulation are given in Appendix B. They are summarized here,

$$Bt = Gp \times B_S$$
$$Bt = R_{cd}$$
$$B_S = R_S$$
$$T_S = T_{cd} Gp$$
$$T_{cd} = \frac{1}{R_{cd}}$$
$$T_S = \frac{1}{R_S} = T_b \log_2 M$$

Since some parameters are dependent on each other, it is not necessary to design all parameters in the adaptive CDMA algorithm. Like in adaptive OFDM, we assume that the normalized received power is equal to one for every user and is not taken into account in the algorithm. The total bandwidth is fixed in practical systems. CDMA utilizes wideband transmission, and therefore, the bandwidth will be much larger than Doppler spread. Doppler spread, hence, will not lead to fast fading and does not need to be considered. Some solutions, e.g., a Rake receiver, are exploited in CDMA systems to combat the multipath effects. Hence, delay spread can be solved in CDMA systems. In a DS-CDMA system, the interference from multiple users in the same cell and from multipaths, as described in Appendix B, can be written as [42]

$$\sigma_{\text{int}}^2 = \frac{T_S^2}{3Gp}\left[1 + \frac{N_u(N_p + K)}{1 + K}\right], \tag{3.14}$$

if the NRP equals one. σ_{int}^2 denotes interference power (see Appendix B). In the equation, T_S denotes symbol duration, Gp processing gain, N_u number of users in the same cell, N_p the number of multipaths, and K the Rician K factor. It is straightforward that the effect of MAI, interference of LOS of the other users in the same cell, and multipath are all included in the interference. In other words, SINR can be exploited to represent the effect of MAI and delay spread. Therefore, SINR can be used as a channel parameter in CDMA systems.

Thus, Table 3.5-5 can now be simplified into Table 3.5-6.

Table 3.5-6. Parameters used to design adaptive CDMA algorithms

CDMA parameters			Channel parameters
FD	*Gp*, R_{cd}		*SINR*
Other parameters	N_u		
	M, R_c		

c) After listing the parameters related to the design of adaptive CDMA algorithms, the relationships should be built up between parameters with respect to channel characteristics and parameters with respect to modulation characteristics. In other words, we should find out based on which channel parameter each of the CDMA modulation parameters should be set. This is Step 5 of the procedure of adaptive modulation algorithms.

Since only one parameter is exploited to represent the channel property, it is straightforward that all CDMA parameters should be assigned by this parameter. However, if we look at equation (3.14) again, we find that some CDMA parameters, i.e., the number of users in the same cell, symbol period, and processing gain, also contribute to the interference. In other words, CDMA modulation parameters are not only determined by channel parameters, but also can determine channel parameters in CDMA systems. This is different from OFDM systems. In addition, it is well known that the SNR of the channel determines the modulation levels and coding rate. Table 3.5-7 describes the relationships between CDMA modulation and the channel.

Table 3.5-7. Mapping CDMA parameters and channel parameters

CDMA parameters			Channel parameters
FD	*Gp*, R_{cd}		*SINR*
Other parameters	N_u		
	M, R_c		

d) The next step is to denote transmission QoS and throughput in terms of modulation parameters and channel parameters. Since the objective of the algorithm is improving QoS and throughput, we have to relate the two themes

(channel and modulation) to these. This is Step 6 of the procedure of adaptive modulation algorithms.

If the bit rate represents the throughput, the total information bit rate, as derived in Appendix B, can be written in CDMA systems as

$$R_{tb} = (R_c \cdot \log_2 M) \cdot B_d = (R_c \cdot \log_2 M) \cdot B_t / Gp ,$$

where B_d is the total data frequency bandwidth, R_C the coding rate, M the modulation level, and G_P the processing gain. Again, all parameters on the right side of the formula are determined by the channel situation.

If BER represents QoS in CDMA systems, from the analysis in Section 3.4 and Appendix B we know that BER increases with modulation levels, coding rate, and with the decrease of processing gain *Gp*, and decreases with an increase of SINR. This relation can be expressed as

$$BER \propto \{M, R_C, N_u, \frac{1}{Gp}, \frac{1}{SINR}\}, \tag{3.15}$$

where $\propto$ denotes just that the variable on the left side will go into the same direction (increases or decreases) with each of the variables on the right side if the other variables are constant; it does not mean that we have a linear proportional relation with a constant coefficient. In other words, BER will increase with M, R_C, or N_u, and decrease with increasing *Gp* and/or SINR.

e) Investigate the feasibility and benefit of changing each of the modulation parameters. This is Step 7 of the procedure of adaptive modulation algorithms.

From our investigation we have obtained the CDMA modulation parameters, T_S, T_b, Bt, B_S, R_S, R_b, R_{cd}, T_{cd}, Gp, N_u, M, and R_c. The CDMA modulation parameters to design are R_{cd}, N_u, Gp, M, and R_c. Now let us study the feasibility of adapting these parameters. Actually, we have mentioned before that the total available bandwidth B is given in the system concept and it is not practical to change this parameter. The set of modulation parameters to design is the set of independent parameters representing CDMA modulation parameters. Therefore, it is only necessary to study the feasibility of changing these independent CDMA modulation parameters. Nevertheless, the related parameters should be considered to evaluate the feasibility of adapting each of the independent CDMA modulation parameters.

We know that the chip rate equals the transmit bandwidth. Chip codes are signatures of individual users in CDMA systems. The signal of each user is

recognized at the receiver by its chip code; therefore, the chip code cannot be changed in CDMA systems.

The modulation level and coding rate are known to be adaptable like they are in OFDM systems. The throughput can be changed by changing the modulation levels and coding rate. The number of active users in a cell is flexible since it is not possible that the number of users using the mobile remains the same all the time. When the channel is bad, the QoS can be guaranteed by decreasing the number of active users. As for processing gain, in theory and practice, it is possible to change processing gain in CDMA systems. What is more, by assigning a large processing gain in a bad channel situation, we can improve transmission quality; by assigning a small processing gain in a good channel situation, more information can be transmitted. Hence, it is beneficial to adapt the processing gain.

To conclude, it is feasible to adapt some of the independent CDMA modulation parameters, i.e., N_u, Gp, M, and R_c, in adaptive CDMA systems. There is no problem in theory or in practice. Moreover, from our study of the influence of these parameters on BER and throughput, we can conclude that it can be beneficial to adapt these parameters. For adaptive CDMA algorithms, Table 3.5-6 is replaced by Table 3.5-8.

Table 3.5-8. CDMA parameters and channel parameters for adaptive CDMA algorithms

CDMA parameters			Channel parameters
FD	*Gp*	⟷	*SINR*
Other parameters	N_u	⟷	
	M, R_c	⟷	

f) Build up the complete algorithm to adjust modulation parameters dynamically according to channel parameters. This is Step 8 of the procedure of adaptive modulation algorithms.

Figure 3.5-2 describes the process of adaptive CDMA algorithms in a simple way. Given a channel situation described by channel parameters and system requirements, the CDMA modulation parameters are adapted at every moment by a certain rule. Unlike OFDM systems, when the channel is very bad, CDMA systems can change the channel SINR by changing certain CDMA parameters. The system detects the channel situation continuously and inputs it in the adaptive

algorithm. The algorithm assigns values for the modulation parameters correspondingly. Details of the algorithm will be given in Chapter 5.

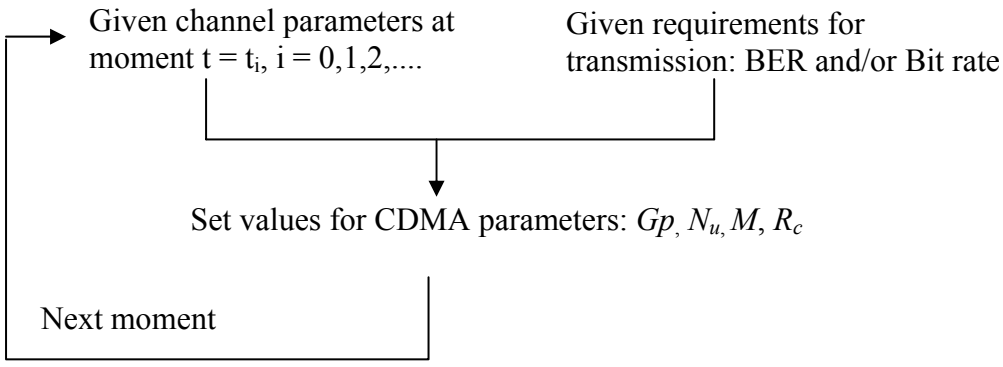


Figure 3.5-2. Simple flow chart of adaptive CDMA algorithms

g) Evaluate the adaptive modulation algorithm by throughput and QoS. This is Step 9 of the procedure of adaptive modulation algorithms.

Like in adaptive OFDM algorithms, QoS can be represented by BER. The throughput can be represented by the bit rate or spectrum efficiency. The bandwidth efficiency is determined by the processing gain, modulation type, coding rate, and total bandwidth.

3.6 Conclusions

In this chapter we investigated the concept of adaptive OFDM and CDMA modulation, their strategies, and work procedures. In order to describe adaptive OFDM and CDMA modulation clearly, we summarized the theory, properties and parameters of OFDM and CDMA modulation in Appendix A and B. The relationships among the OFDM modulation parameters as well as those among CDMA modulation parameters have been analyzed as prerequisites of adaptive modulation algorithms.

We have given an introduction to adaptive modulation. We put forward that the “wide-sense” adaptive modulation technique (including Multiple Access schemes) experiences three stages. During this process, the adaptability for the next stage is taken to a higher level. The first stage is “narrow-sense” adaptive modulation in a certain multiple access system. The adaptive parameters are “narrow-sense” modulation parameters, e.g., the modulation level, coding rate,

etc. The second stage in adaptive modulation is adaptive multiple access/multiplexing schemes, in which multiple access or multiplexing parameters become adaptive. The third stage, with an even higher level of adaptivity, is to change MA schemes (e.g., TDMA, CDMA) by means of a certain criterion according to user's QoS such as requested transmission rate, tolerable BER, delay and various factors to maximize system capacity under actual channel conditions and available frequency bandwidth. The research began with the selection between TDMA and CDMA.

In the section of introduction of adaptive modulation, we generalized that adaptive modulation is used to adapt "wide-sense" modulation parameters dynamically with instantaneous channel parameters with a certain criterion in order to guarantee the transmission quality and to get better throughput. The adaptive modulation technique is a solution to the variability of the channel. The schematic of adaptive modulations was presented. We indicated that there are two aspects in the activity of adaptive modulation: the modulation and channel. The architecture of adaptive modulation systems was discussed. To make an adaptive modulation system function properly, accurate measurement and prediction of the channel conditions are required; an algorithm to adapt the modulation parameters in terms of the channel conditions is essential; and knowledge of the modulation parameter at the receiver is indispensable. In this thesis, we concentrated on the second step, that is, building the adaptive modulation algorithm. In our simulations, we assumed that we have perfect channel estimation and the receiver knows the exact settings of the modulation parameters. The objective of adaptive modulation is the same as that of other technologies for wireless communications, that is, to improve the transmission QoS and throughput. Based on the frequency with which the modulation parameters are adapted, adaptive modulation can be categorized as "fast adaptive modulation" or "slow adaptive modulation". We focus on fast adaptive modulation in the thesis. The advantage of adaptive modulation is obvious, that is, it can make more efficient use of the channel resources. However, it is not so easy to implement it in a real system. The channel estimation, for example, can not be guaranteed to be known always in time; and hardware implementation is also a challenge at the moment.

After introducing adaptive modulation, we analyzed "wide-sense" modulation parameters influencing transmission throughput. We derived the throughput formula for OFDM systems. For the general situation, i.e., one that is not restricted to an identical subcarrier configuration, every subcarrier may have a different value for the modulation parameter. In this case, the total bit rate should be the summation of the bit rate of all subcarriers. The equations of bit rate have been given in equation (3.5) and (3.6).

The throughput formula for CDMA systems was derived afterwards. The formula in terms of bit rate was given in equation (3.7). From this equation we can conclude that the bit rate of CDMA systems is linearly proportional to coding rate and transmission bandwidth, logarithmically proportional to modulation level, and inversely proportional to processing gain.

We showed that adaptive modulation is used to improve transmission throughput and QoS. After discussing which parameters influence throughput, we investigated the parameters influencing QoS. In order to make use of the throughput formula we derived, we studied the influence of varying these parameters on BER performance. Increasing modulation level (or coding rate) results in worse BER performance; increasing FSR leads to a decrease in guard time and may degrade BER performance in multipath fading channels; increasing bandwidth does not degrade BER, but of course, it requires larger bandwidth, which is not so practical. Considering the property of adaptive modulation, we introduced a new parameter, P_{FR} as the product of subcarrier bandwidth Δf and RDS. We analyzed the range of values of P_{FR}. From simulations we found that the traditional belief, i.e., smaller subcarrier bandwidth gives better BER performance, is true only for a constant channel situation. When the product of subcarrier bandwidth and RDS is fixed, changing the values of subcarrier bandwidth and/or RDS does not influence BER performance. The product of subcarrier bandwidth and RDS is therefore an important factor for influencing BER performance. From simulations we learned that when SNR is above 0 dB, the relationship yields: the smaller the product, the better BER performance. Nevertheless, for a fixed channel situation, RDS is known as a constant value, so smaller P_{FR} means smaller subcarrier bandwidth. In this case, smaller subcarrier bandwidth can give a lower BER. The result is useful to improve OFDM system performance for a varying channel situation and is thus important for adaptive OFDM systems. Further, we analyzed how P_{FR} influenced BER performance via simulations. We found that only when SNR is larger than a certain value (which we defined as "start SNR"), changing P_{FR} can influence BER. When the Rician K factor is large, the influence of P_{FR} on BER becomes irregular; we defined the largest K value that gives legitimate BER performance for different P_{FR} as "*top K*". When K is larger than a certain value (20dB for BPSK, QPSK), P_{FR} has no effect on BER. From simulations we know that "*top K*" and SSNR are functions of modulation level, M. If we use "*top K(M)*" to represent the "*top K*" value for the assigned modulation level M, Start SNR(M) represents the Start SNR value for the assigned modulation level M. The conditions for adjusting P_{FR} can be generalized as:

- $K <$ *top K(M)*;
- SNR > start SNR(M);
- P_{FR} is in the range [0.02 1];
- P_{FR} states are taken from 0.02 to 0.5 with steps of 0.01 (0.02:0.01:0.5); P_{FR} between [0.5 1] is one state; and state 0.5 means P_{FR} from 0.5 to 1.

The influence of CDMA parameters on BER performance was described briefly since it has been investigated in literature.

We stated that the work of adaptive modulation differs from the traditional investigations on modulation. These traditional investigations focus on studying basic modulation technology and combining some new technology in the modulation or modifying something in hardware or software to get improvement. It is prerequisite to study the inner-relationships within the modulation parameters and the channel parameters themselves as well as the inter-relationships between them. We further raised that in order to build an efficient adaptive

modulation algorithm, therefore, one should first do a relationship study; then criteria should be set up, based on which the adaptive modulation algorithm can decide whether and how to change modulation parameters. The work procedure of adaptive modulation algorithms was initiated in the thesis. The "nine-step" work procedure of adaptive modulation algorithms can be summarized as:

1. List all related parameters with respect to channel characteristics;

2. List all related parameters with respect to relevant modulation characteristics;

3. Find relationships among parameters with respect to channel characteristics;

4. Find relationships among parameters with respect to relevant modulation characteristics;

5. Discover relationships between parameters with respect to channel characteristics and those with respect to modulation characteristics;

6. After building the database for adaptive modulation algorithms, one should try to denote transmission QoS and throughput in terms of modulation parameters and channel parameters. Since the objective of the algorithm is to improve the QoS and throughput, we have to relate the two aspects (i.e., channel and modulation) to QoS and throughput;

7. Investigate the feasibility and benefit of changing each modulation parameter. This feasibility study includes two aspects: whether it is feasible to change this parameter in theory, and whether it is beneficial to change this parameter;

8. Build the complete algorithm to adjust modulation parameters dynamically according to channel parameters;

9. Evaluate the adaptive modulation algorithm based on throughput and QoS.

Adaptive OFDM and CDMA algorithms were analyzed following these procedures, respectively. Details of these algorithms will be given in Chapter 5.

References

[1] Ue, T., Sampei, S., Morinaga, N., Hamaguchi, K., "Symbol rate and modulation level-controlled adaptive modulation/TDMA/TDD system for high-bit-rate wireless data transmission", IEEE Transactions on Vehicular Technology, vol. 47, Issue 4, Nov. 1998, p1134 – 1147;

[2] Ue, T., Sampei, S., Morinaga, N., "Symbol rate and modulation level controlled adaptive modulation system with TDMA/TDD for high bit rate transmission in high delay spread environments", Electronics Letters, vol. 32, Issue 4, 15 Feb. 1996, p304 – 305;

[3] Otsuki, S., Sampei, S., Morinaga, N., "Square-QAM adaptive modulation/TDMA/TDD systems using modulation level estimation with Walsh function", Electronics Letters , vol. 31, Issue 3, 2 Feb. 1995, p169 – 171;

[4] Inoue, T., Sampei, S., Morinaga, N., "DS-CDMA and adaptive modulation based TDMA dual mode scheme for high speed data transmission service in wireless multimedia communication systems", IEEE Vehicular Technology Conference, VTC 2001 Spring, vol.1, 6-9 May 2001, p585 – 589;

[5] Rohling, H., Grunheid, R., "Adaptive coding and modulation in an OFDM-TDMA communication system", 48th IEEE Vehicular Technology Conference, vol. 2, 18-21 May 1998, p773 - 776;

[6] Ue, T., Sampei, S., Morinaga, N., "Symbol rate and modulation level controlled adaptive modulation/TDMA/TDD for personal communication systems", IEEE 45th Vehicular Technology Conference, vol.1, 25-28 July 1995, p306 - 310;

[7] Chatterjee, S., Fernando, W.A.C., Wasantha, M.K., "Adaptive modulation based MC-CDMA systems for 4G wireless consumer applications", IEEE Transactions on Consumer Electronics, vol. 49 , Issue 4 , Nov. 2003, p995 – 1003;

[8] Keller, T., Hanzo, L., "Adaptive modulation techniques for duplex OFDM transmission", IEEE Transactions on Vehicular Technology, vol. 49, Issue 5, Sept. 2000, p1893 – 1906;

[9] Ikeda, T., Sampei, S., Morinaga, N., "TDMA-based adaptive modulation with dynamic channel assignment for high-capacity communication systems", IEEE Transactions on Vehicular Technology, vol. 49, Issue 2, March 2000, p404 – 412;

[10] Lau, V. K. N., Maric, S. V., "Variable rate adaptive modulation for DS-CDMA Communications", IEEE Transactions on Vehicular Technology, vol. 47, Issue 4, April 1999, p577 – 589;

[11] Che, H., Ligthart, L. P., Prasad, R., "A Throughput Formula for Adaptive OFDM System", 5th IEEE Malaysia International Conference on Communications - MICC Conference, p299-303; Kuala Lumpur, Malaysia; October 2001;

[12] Goldsmith, A. J., "Adaptive Coded Modulation for Fading Channels" IEEE Transactions on Communications. Vol.46, No.5, May 1998;

[13] Mizuno, M., "High Speed Multimedia-Multimode TDMA Radio Transmission System for IMT-2000" IEICE Transaction on Communications, vol. E81-B, No.7 July 1998;

[14] Ue, T., "Symbol Rate and Modulation Level-controlled Adaptive Modulation/TDMA/TDD System for High-Bit-Rate Wireless Data Transmission" IEEE Transactions on Vehicular Technology. Vol.47, No.4 November 1998;

[15] Ganesh, R., *Wireless Multimedia Network Technologies*, 2000;

[16] Hara, S., Kitazawa, D., Yomo, H., "Adaptive Access Scheme Selection in Software-Based Wireless Multimedia Communications" 12th Tyrrhenian International Workshop on Digital Communications-Software Radio Technologies and Services, 2000, Italy;

[17] Che, H., Prasad, R., Ligthart, L.P., "A Strategy for Adaptive Modulation Algorithms Using Rician *K* Gain of MIMO", submitted to IEEE Microwave and Wireless Components Letter;

[18] Nobelen, R. van, "Towards Higher Data Rates for IS-136" VTC 1998;

[19] Alouini, M. S., "Adaptive M-QAM Modulation Over Nakagami Fading Channels"1997 Global Communications Conference, November 1997;

[20] Fry, T. A., "Data Capacity of TDMA/FDMA System with Adaptive Modulation"IEEE VTC'98;

[21] Sampei, S., "Experimental Results of a Multi-Mode Adaptive Modulation/TDMA/TDD System for High Quality and High Bit Rate Wireless Multimedia Communication Systems"IEEE VTC'98;

[22] Ikeda, T., "Adaptive Modulation with Dynamic Channel Assignment (AMDCA) for TDMA Microcellular Systems" Electronics and Communications in Japan, Part 1, Vol.82, No.1, 1999. pp55-64;

[23] Chua, S. G., "Adaptive Coded Modulation for Fading Channels" 1997 IEEE International Conference on Communications ICC'97 vol.3 P1488-92;

[24] Hanzo, L., Webb, W., Keller, T., *Single- and Multi-Carrier Quadrature Amplitude Modulation*, John Wiley & Sons, Ltd, 2000;

[25] Okada, M., Hara, S., Morinaga, N., "Bit Error Rate Performances of Orthogonal Multicarrier Modulation Radio Transmission Systems", IEICE TRANS. COMMUN. Vol. E76-B, No. 2 February 1993;

[26] Witrisal, Klaus, *OFDM Air-Interface Design for Multimedia Communications,* Ph.D thesis, Delft University of Technology, The Netherlands, 2002;

[27] Che, H., Ligthart, L. P., Prasad, R., "Influencing Factor for OFDM System Performance in a Varying Channel", 2002 International Conference on Software, Telecommunications and Computer Networks, Split, Croatia; October 2002;

[28] Che, H., Ligthart, L. P., Prasad, R., "Working Conditions for an Influencing Factor on the Performance of Adaptive OFDM System under a Varying Channel", The 14th IEEE International Symposium on Personal, Indoor and Mobile Radio Communications (PIMRC 2003), Beijing, China; September 2003;

[29] Rappaport, T. S., *Wireless Communications: Principles and Practice*, ISBN 0-13-042232-0, Prentice Hall PTR, 2002;

[30] Ni, J., J., Barton, R.J., "Multicoding and adaptive modulation for uncertain CDMA channels", The Thirty-Fourth Asilomar Conference on Signals, Systems and Computers, 29 Oct.-1 Nov. 2000, p786 – 791, vol.1;

[31] Doroslovacki, M., "Constrained adaptive algorithms for code acquisition and interference cancellation in asynchronous DS-CDMA systems", The Thirty-Fourth Asilomar Conference on Signals, Systems and Computers, 29 Oct.-1 Nov. 2000, p792 – 796, vol.1;

[32] Cotae, P., "Transmitter adaptation of DS-CDMA signals in multipath channels", The Thrity-Seventh Asilomar Conference on Signals, Systems & Computers, Nov. 9-12, 2003, p428 – 432, vol. 1;

[33] Saifuddin, A., Kohno, R., "Adaptive multilevel code selection and MUI cancellation for DS/CDMA over fading channel", IEE Communications, Feb. 1999, p35 – 42, vol. 146, Issue 1;

[34] Kim, S. W., "Rate and power adaptation in code division multiple access communications", Electronics Letters, 11 June 1998, p1200 – 1201, vol. 34, Issue 12;

[35] Choi, B.J., Munster, M., Yang, L.-L., Hanzo, L., "Performance of Rake receiver assisted adaptive-modulation based CDMA over frequency selective slow Rayleigh fading channels", Electronics Letters, 15 Feb 2001, p247 – 249, vol. 37, Issue 4;

[36] Che, H., Prasad, R., Ligthart, L.P., "Strategies for Adaptive Modulation Algorithms and Three Subband Settings for Adaptive OFDM Algorithms", submitted to IEEE Communications Magazine;

[37] Keller, T., Liew, T. H., Hanzo, L., "Adaptive Rate RRNS Coded OFDM Transmission for Mobile Communication Channels", IEEE 51st Vehicular Technology Conference (VTC 2000 Spring), May 2000, Tokyo, Japan;

[38] Czylwik, A., "Adaptive OFDM for Wideband Radio Channels", IEEE Global Telecommunications Conference, November, 1996, London, UK;

[39] Baum, K., Classon, B., Cutts, K., Desai, V., "Performance Analysis of an Adaptive OFDM Packet Data System", International Zurich Seminar on Broadband Communications, February, 2000, Zurich, Switzerland;

[40] Zhong, Y., Saulnier, G. J., Lee, D., Medley, M. J., "FEC Coding with a Rate Adaptive Spread Spectrum OFDM System", Conference on Military Communications (MILCOM'99), November, 1999, Atlantic City, NJ, USA;

[41] Proakis, J. G, "Digital Communications", 4rd edition, McGraw Hill, 2000;

[42] Misser, H. S., Prasad, R., "Bit Error Probability Evaluation of a Microcellular Spread-Spectrum Multiple Access System in a Shadowed Rician Fading Channel", IEEE 42nd Vehicular Technology Conference, 10-13 May 1992, p439-442, vol.1, Denver, CO, USA.

Chapter 4

Multiple Input Multiple Output (MIMO) Systems

4.1 Introduction

In this chapter we describe MIMO systems.

In wireless communication systems, sources (frequency and time sources) are important as they determine the limit for transmission quality and throughput. Generally, the concept of parallel transmission is applied to achieve high throughput and a better transmission quality. In CDMA (Code Division Multiple Access) systems, signals from different users operate (work in parallel) in time and frequency domain, but are separated in code domain. Therefore, this is a sort of "parallelism" realized by codes, which we call "software parallelism". In OFDM (Orthogonal Frequency Division Multiplexing) systems, signals work in parallel in time domain and are separated in frequency domain; it is a kind of "parallelism" realized by FFT (Fast Fourier Transform), and we call it "semi- software parallelism".

The MIMO system uses the concept of parallel transmission in a different way. It realizes multiple outputs by multiple transmit antennas and multiple inputs by multiple receive antennas. Signals work in parallel in time and frequency domain, but are separated in space domain. It is hardware parallelism. The unique signatures of input streams are provided by hardware without frequency spreading. Table 4.1 compares the concept of parallelism as applied by CDMA, OFDM, and MIMO. In this chapter we discuss the MIMO system and its application in adaptive modulation.

Table 4.1 Parallelism in CDMA, OFDM, and MIMO

	Signal parallel in	Signal separated in	Type of "parallel"
OFDM	Time domain	Frequency domain	Semi-software parallelism
CDMA	Time and frequency domain	Code domain	Software parallelism
MIMO	Time and frequency domain	Space domain	Hardware parallelism

This chapter is organized as follows:
First we introduce the concept and structure of MIMO systems in Section 4.2. We describe how to derive the MIMO channel function from the SISO (Single Input Single Output) channel function. In Section 4.3 advantages and disadvantages of MIMO are given. In wireless communications, the capacity and SNR (Signal to Noise Ratio) are always used to evaluate a technology. In Section 4.4 we analyse the capacity and SNR of MIMO systems with respect to those of non-MIMO systems (SISO, SIMO - Single Input Multiple Output, MISO - Multiple Input Single Output). There are different MIMO schemes to execute the function of MIMO. In Section 4.5 we categorize them into the Spatial Multiplexing (SM) scheme and the Diversity scheme. The SNR and capacity (or Spectral Efficiency (SE)) of these different schemes are also given. In many cases, a Line Of Sight (LOS) may exist in wireless transmission systems. Therefore, the influence of LOS gets attention in Section 4.6. There is always a difference between theory and simulation. In order to describe MIMO schemes in more detail, we present simulation results of SNR and capacity (or SE) for different MIMO schemes in Section 4.7. After that, we generalize some factors (e.g., number of transmit antennas; number of receive antennas) that influence SNR and capacity of MIMO systems in Section 4.8. In literature, the gain of MIMO systems is always presented in terms of SNR improvement. We found, however, that the SNR is not enough to describe the gain of transmission quality of MIMO systems. In Section 4.9 we introduce a "Rician *K* factor gain" and give results derived from simulations. Conclusions are summarized in Section 4.10.

4.2 Definition of MIMO Systems

To explain MIMO, we begin with the simpler SISO (Single Input Single Output) system. Figure 4.2-1 shows a SISO channel, with one transmit and one receive antenna. Correspondingly, there is only one channel vector: *h(t)*.

MIMO is part of the category of smart antenna systems. Traditional smart antenna systems employ multiple antennas at the receiver, whereas in a general MIMO system, multiple antennas are employed, both at transmit and at the receive sides. The addition of multiple antennas at transmit combined with advanced signal processing algorithms at transmit and receive results in a significant advantage over traditional smart antenna systems - both in terms of capacity and diversity [1].

Figure 4.2-2 gives an example of a 2 by 2 MIMO channel. There are two transmit and two receive antennas. Therefore, the 2 by 2 MIMO channel has four channel vectors: h_{11}, h_{12}, h_{21}, and h_{22}, which form a channel matrix: the difference between the SISO channel and the MIMO channel is that the parameter of the SISO channel is a single transfer function, while that of the MIMO channel is a matrix of transfer functions.

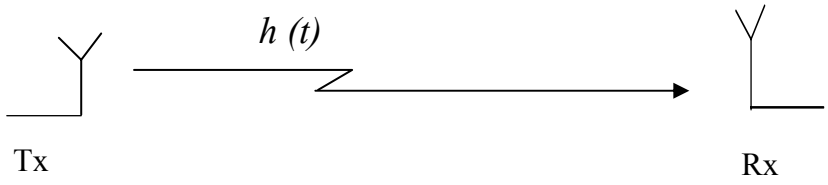


Figure 4.2-1. SISO channel

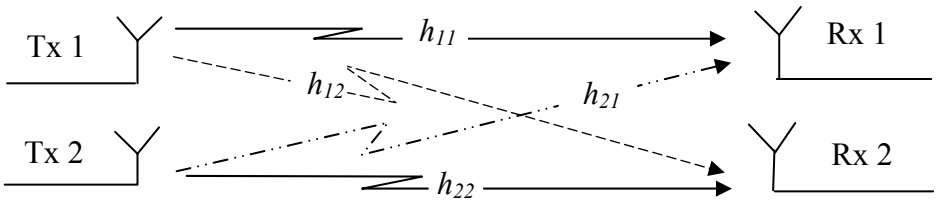


Figure 4.2-2. 2 x 2 MIMO channel

So we can define MIMO system in the following way: "If a wireless communication system has multiple antenna elements at both transmit and receive ends, we call it a MIMO system". By using some proper signal processing schemes, one can improve transmission quality and/or throughput in a MIMO system. Due to modulators append in a MIMO system, we distinguish two different kinds of MIMO systems, which will be described next.

4.2.1 MIMO Systems with One Modulator/Demodulator

A schematic representation of a MIMO system with one modulator is given in Figure 4.2-3. The system has n transmitting antennas and m receiving antennas. The channel impulse response is given by matrix $\boldsymbol{H}$. The signals to (and from) all the antennas are all from (and to) one modulator (demodulator). This case will be studied in our work.

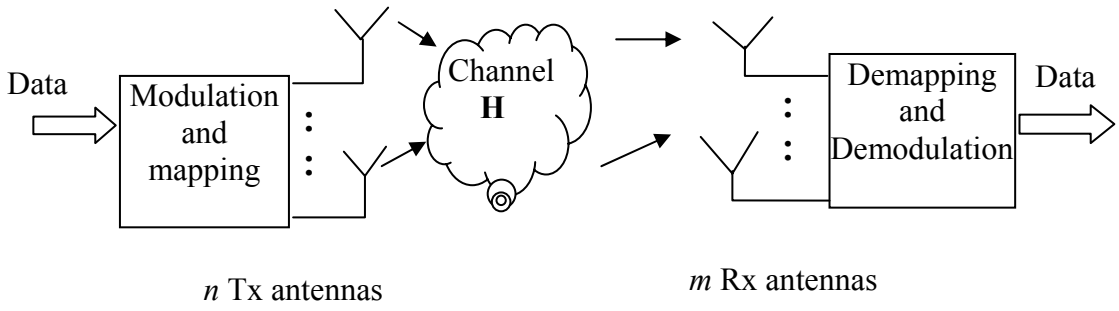


Figure 4.2-3. One-Modulator/Demodulator MIMO system with *n* transmit and *m* receive antennas

4.2.2 MIMO Systems with Multiple Modulators/Demodulators

Figure 4.2-4 gives another type of MIMO system with multiple modulators/demodulators. Each modulator/demodulator is connected with one antenna. At the transmit side, the data stream is converted from serial to parallel and fed to different modulators. After independent modulation, each group of data is transmitted simultaneously via its own antenna. In the receiver, each group of data received from different antennas is fed to a different demodulator. After parallel to serial conversion, the demodulated data becomes one data stream. In this thesis this type of MIMO will not be further considered.

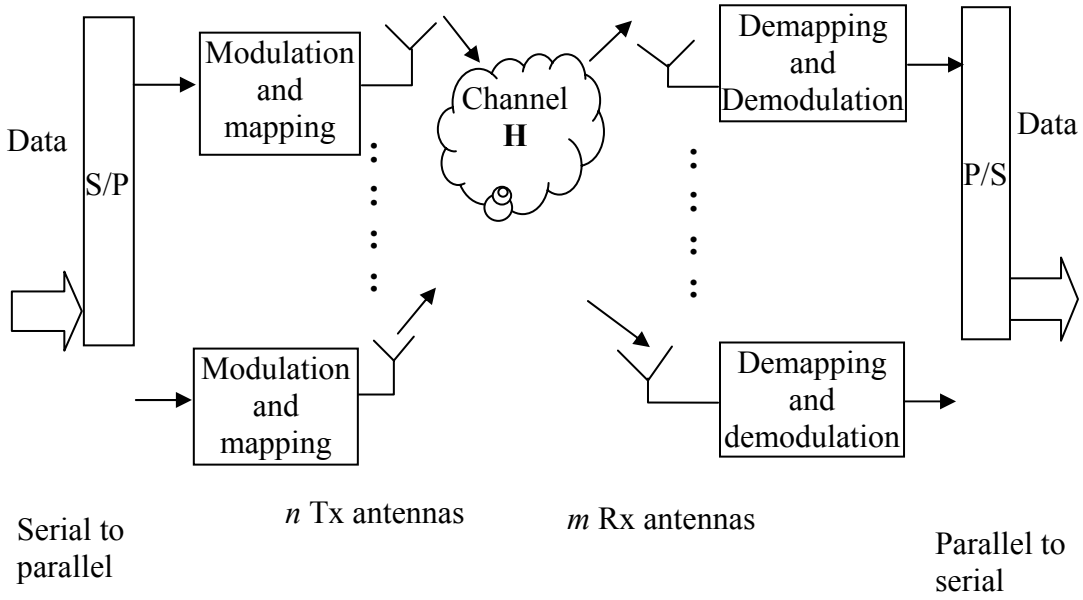


Figure 4.2-4. Multiple-Modulator/Demodulator MIMO system with *n* transmit and *m* receive antennas

4.2.3 MIMO Channel Functions

In a Single Input Single Output (SISO) system, the wireless link between transmit and receive sides can be modelled as a filter with a time-varying impulse response. The base-band impulse response of a channel, with discrete multi-path components, can be written as [2],

$$h_b(t,\tau) = \sum_{i=0}^{L-1} a_i(t,\tau) \exp\left(j\left(2\pi f_c \tau_i(t) + \phi_i(t,\tau)\right)\right) \delta\left(\tau - \tau_i(t)\right), \tag{4.1}$$

where

$h_b(t,\tau)$: Base-band impulse response of the channel as function of time t and the delay τ.

L: the number of multi-paths

$a_i(t,\tau)$: Real amplitude of the channel

$\phi_i(t,\tau)$: Phase shift due to the channel

$2\pi f_c \tau_i(t)$: Phase shift due to free space propagation of the i^{th} multi-path

$\tau_i(t)$: Excess delay of the i^{th} multipath

In a MIMO system, the wireless link between each antenna pair can be expressed using the channel impulse response matrix *H*, whose elements can be expressed as:

$$h_{b_{n',m'}}(t,\tau)=\sum_{i=0}^{L-1}a_{n',m',i}(t,\tau)\exp\left(j\left(2\pi f_c\tau_{n',m',i}(t)+\phi_{n',m',i}(t,\tau)\right)\right)\delta\left(\tau-\tau_{n',m',i}(t)\right), \quad (4.2)$$

where $h_{b_{n',m'}}(t,\tau)$ represents the base-band channel impulse response of the n^{th} transmit antenna and the m^{th} receive antenna, as function of time *t* and delay τ.

The matrix characterizing the MIMO channel can be written as:

$$H=\left[h_{b_{n',m'}}\right]=\begin{bmatrix} h_{b_{1,1}}h_{b_{2,1}}\cdots h_{b_{n,1}} \\ h_{b_{1,2}}h_{b_{2,2}}\cdots h_{b_{n,2}} \\ \vdots \\ h_{b_{1,m}}h_{b_{2,m}}\cdots h_{b_{n,m}} \end{bmatrix}_{m\times n}. \quad (4.3)$$

4.3 Advantages and Disadvantages of MIMO

- *Advantages of MIMO*

In wireless communications, the objectives are to increase throughput and transmission quality. MIMO systems can take advantage of the shortcoming of a wireless channel – the multipath- and turn it into an advantage [1]. In MIMO systems, random fading [3]-[5] and multipath delay spread [6], [7] can be used to increase throughput. MIMO systems offer an increase in capacity without the need to increase bandwidth and/or power. Spatial Multiplexing (SM) is a technology that exploits this feature of MIMO systems in order to achieve the theoretical capacity limit in practice. Spatial Multiplexing uses different transmit antennas which send different signals. The signals are multiplexed in the channel and in the receive antennas, and then demultiplexed in the receiver. A schematic representation of the SM scheme is given in Figure 4.3-1 [8].

Apart from improving throughput, MIMO systems can also improve transmission quality. Diversity [9] is a technology used in MIMO for this purpose. Multiple antennas can be used to minimize the effect of fading caused by multi-path propagation. When the antennas at the receive side are adequately spaced, then several copies of the transmitted signal are received

through different channels and with different fading. The probability, that all received copies of the transmitted signal are in deep fading, can be regarded as small. We can thus deduce that diversity should improve the quality of the wireless link.

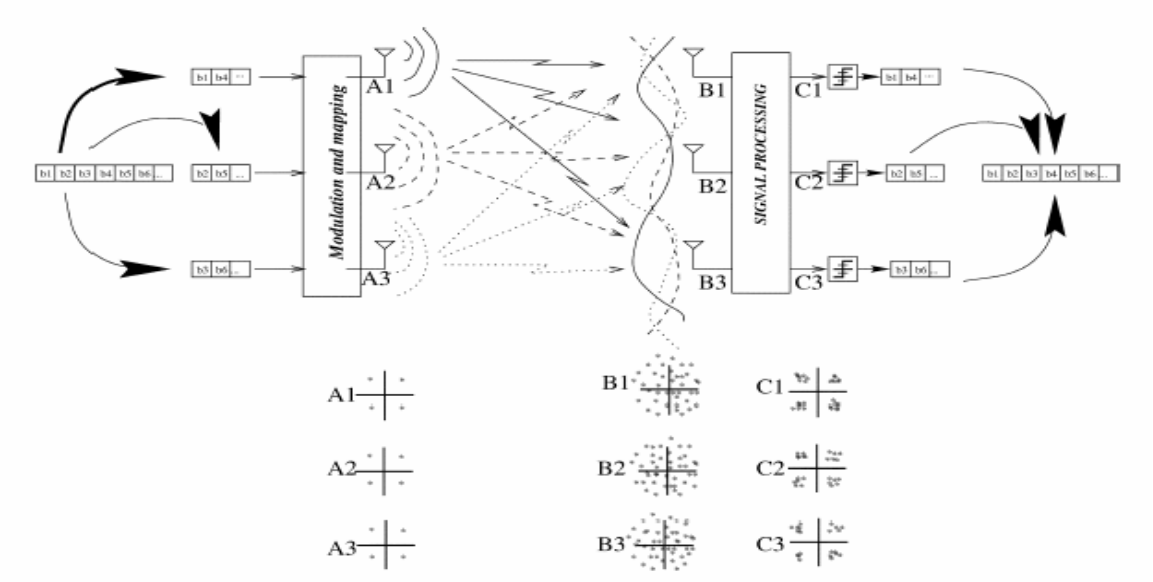


Figure 4.3-1. Schematic representation of a basic spatial multiplexing scheme with 3 transmit and 3 receive antennas [8].

- *Disadvantages and limitations of MIMO*

One obvious disadvantage of MIMO is that they contain more antennas: MIMO increases complexity, volume, and hardware costs of the system compared to SISO.

MIMO systems are not always beneficial knowing that channel conditions depend on the radio environment. When there is Line of Sight (LOS), a higher LOS strength at receive will result in better performance and capacity in SISO system, while in MIMO systems capacity is reduced with higher LOS strength [10], [11]. This is because strong contributions from LOS lead to higher correlation among antennas, which reduces the advantage of using a MIMO system.

4.4 Analysis of MIMO Systems Compared with Non - MIMO Systems

In the following we consider some benefits of utilizing multiple antennas on the transmit side, the receive side, or both. Hence we describe expressions for SNR (Signal-to-Noise Ratio) and for spectrum efficiency. The non-MIMO systems are SISO, SIMO, and MISO systems.

4.4.1 Single Input Single Output (SISO) Systems

We consider a fading channel, in which Additive White Gaussian Noise (AWGN) with zero mean and variance σ^2 affects the receiver of a SISO system (as Figure 4.2-1). The received signal, *Y*, can be expressed as $Y = hX + N_0$, where *h, X* and N_0 represent the normalized complex channel impulse response coefficient, the transmitted signal and the AWGN, respectively.

The SNR at the receiver can then be expressed as follows [12]:

$$SNR = \frac{|h|^2 P_T}{\sigma^2}, \tag{4.4}$$

where SNR is received Signal-to-Noise Ratio; *h* is normalized complex channel impulse response coefficient; P_T is total transmitted power and σ^2 is variance of AWGN.

The spectrum efficiency (SE) equals:

$$SE = \log_2(1 + \frac{P_T}{\sigma^2}|h|^2) \quad b/s/Hz \ . \tag{4.5}$$

4.4.2 Single Input Multiple Output (SIMO) Systems

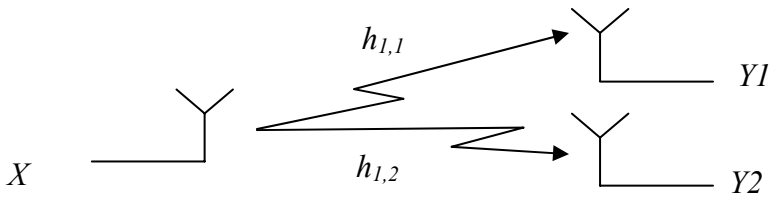


Figure 4.4-1. 1 x 2 SIMO system. *X* is input signal. *Y1* and *Y2* are output signals. $h_{1,1}$ and $h_{1,2}$ are sub-channels between each transmit-receive pair.

Figure 4.4-1 shows a 1 x 2 SIMO system. *X* is input signal. *Y1* and *Y2* are output signals. $h_{1,1}$ and $h_{1,2}$ are sub-channels between each transmit-receive pair. Again we consider a fading

channel, in which the AWGN noise vector $\mathbf{N_0}$ with variance σ^2 is added at receive side. Here, vector $\mathbf{N_0}$ is a two-element vector. The output vector, $\boldsymbol{Y}$, can be expressed as:

$$Y = \begin{bmatrix} Y1 \\ Y2 \end{bmatrix} = \begin{bmatrix} h_{1,1} \\ h_{1,2} \end{bmatrix} X + \mathbf{N}_0 .$$

From this relation we derive the expression for post-processed SNR for the 1 x 2 SIMO case.

$$SNR = \frac{P_T \sum_{j=1}^{2} \left| h_{1,j} \right|^2}{2\sigma^2} \tag{4.6}$$

Here, $h_{1,j}$ is the channel impulse response coefficient of the j^{th} sub-channel. For a 1 x m SIMO system, we obtain post-processed SNR

$$SNR = \frac{P_T \sum_{j=1}^{m} \left| h_{1,j} \right|^2}{m\sigma^2} . \tag{4.7}$$

Like in the SISO case, we can translate SNR gain into spectrum efficiency (SE):

$$SE = \log_2 (1 + \frac{P_T}{m\sigma^2} \sum_{j=1}^{m} \left| h_{1,j} \right|^2) \quad b/s/Hz . \tag{4.8}$$

We can see from this formula, that increasing the number of receive antennas gives a logarithmic increase in spectrum efficiency.

4.4.3 Multiple Input Single Output (MISO) Systems

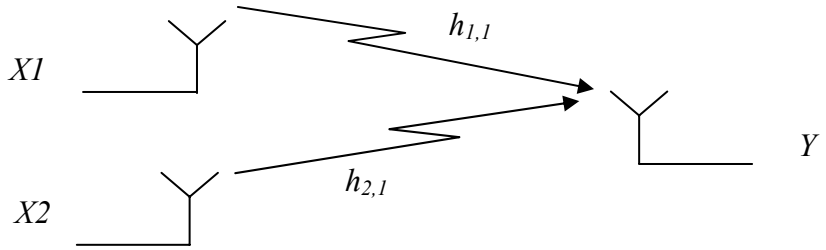


Figure 4.4-2. 2 x 1 MISO system. *X1* and *X2* are input signals. *Y* is output signal. $h_{1,1}$ and $h_{2,1}$ are sub-channels between each transmit-receive pair.

The figure above shows a 2 x 1 MISO system. *X1* and *X2* are input signals at transmit. *Y* is output signal at receive. $h_{1,1}$ and $h_{2,1}$ are sub-channels between each transmit-receive pair. Again we consider a fading channel, in which AWGN noise N_0 with variance σ^2 is added at the output. The total transmit power P_T is constant and is divided equally over the two transmit antennas. Both antenna signals are not mutually correlated.

Output vector, $\boldsymbol{Y}$, becomes:

$$Y = \begin{bmatrix} h_{1,1} & h_{2,1} \end{bmatrix} \begin{bmatrix} X1 \\ X2 \end{bmatrix} + N_0 .$$

From this relation we derive the expression for post-processed SNR for this 2 x 1 MISO case.

$$SNR = \frac{P_T \sum_{i=1}^{2} \left| h_{i,1} \right|^2}{n\sigma^2} = \frac{1}{n} \frac{P_T \sum_{i=1}^{2} \left| h_{i,1} \right|^2}{\sigma^2} \tag{4.9}$$

Here $h_{i,1}$ is the channel impulse response of the i^{th} sub-channel. For n x 1 MISO systems, the post-processed SNR yields:

$$SNR = \frac{P_T \sum_{i=1}^{n} \left| h_{i,1} \right|^2}{n\sigma^2} = \frac{1}{n} \frac{P_T \sum_{i=1}^{n} \left| h_{i,1} \right|^2}{\sigma^2} . \tag{4.10}$$

From this formula we cannot extract directly the effect of the number of transmit antennas on SNR. Increasing the number of transmit antennas may lead to SNR gain or deterioration.

Like in the SISO and SIMO cases, we can translate the post-processed SNR into spectrum efficiency (SE):

$$SE = \log_2(1 + \frac{1}{n}\frac{P_T}{\sigma^2}\sum_{i=1}^{n}\left|h_{i,1}\right|^2) \quad b/s/Hz\,. \tag{4.11}$$

This formula also shows a non-obvious relationship between number of transmit antennas and spectrum efficiency. However, it also shows a logarithmic relationship between them.

4.4.4 MIMO Systems

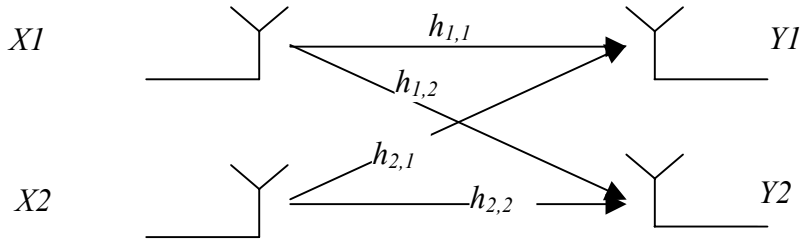


Figure 4.4-3. 2 x 2 MIMO system. *X1* and *X2* are input signals. *Y1* and *Y2* are output signals. $h_{1,1}$, $h_{1,2}$, $h_{2,1}$ and $h_{2,2}$ are sub-channels between each transmit-receive pair.

Figure 4.4-3 describes a 2 x 2 MIMO system. *X1* and *X2* are input signals at transmit. *Y1* and *Y2* are output signals at receive. $h_{1,1}$, $h_{1,2}$, $h_{2,1}$ and $h_{2,2}$ are sub-channels between each transmit-receive pair. The total transmit power P_T is constant and divided equally over the two transmit antennas. Both signals are not correlated. Like in SISO, SIMO and MISO, we assume an AWGN vector $\boldsymbol{N_0}$ with variance σ^2 that is added at the output. The sizes of $\boldsymbol{N_0}$ and $\boldsymbol{Y}$ are the same. The output vector, $\boldsymbol{Y}$, can be expressed as follows:

$$Y = \begin{bmatrix} Y1 \\ Y2 \end{bmatrix} = \begin{bmatrix} h_{1,1} & h_{2,1} \\ h_{1,2} & h_{2,2} \end{bmatrix} \begin{bmatrix} X1 \\ X2 \end{bmatrix} + \mathbf{N_0}\,.$$

From this relation we derive the expression for post-processed SNR for the 2 x 2 MIMO case:

$$SNR = \frac{\frac{P_T}{2}\sum_{i=1}^{2}\sum_{j=1}^{2}\left|h_{i,j}\right|^2}{2\sigma^2} \quad . \tag{4.12}$$

Here $h_{i,j}$ is the channel impulse response coefficient of the $(i,j)^{th}$ sub-channel; the other parameters are the same as those defined before. For an n x m MIMO system, the post-processed SNR formula becomes:

$$SNR = \frac{\frac{P_T}{n}\sum_{i=1}^{n}\sum_{j=1}^{m}\left|h_{i,j}\right|^2}{m\sigma^2} = \frac{1}{nm}\frac{P_T}{\sigma^2}\sum_{i=1}^{n}\sum_{j=1}^{m}\left|h_{i,j}\right|^2 . \tag{4.13}$$

This formula looks complicated. What kind of SNR gain (positive or negative) we may get depends on MIMO schemes (we discuss this aspect later) and the actual channel conditions.

For the spectrum efficiency of MIMO, we know from literature [3], [5], [13] that

$$SE = \log_2\left[\det(I_m + \frac{P_T}{n\sigma^2}HH^*)\right] \quad b/s/Hz\,, \tag{4.14}$$

where I_m is identity matrix with size m, * means transpose conjugate and H is an m x n channel matrix:

$$H = \begin{bmatrix} h_{1,1} & h_{2,1} & \cdots & h_{n,1} \\ \vdots & \ddots & & \\ & & \ddots & \\ h_{1,m} & & & h_{n,m} \end{bmatrix}.$$

The spectrum efficiency of the formula above increases linearly with the minimum of the receive antenna number (m) and transmit antenna number (n) [3], [13].

4.5 MIMO Schemes

In order to fulfill the required tasks in MIMO systems, signal processing at both ends is needed to distribute and deal with symbols. There are two kinds of schemes for this: Spatial Multiplexing (SM) and Diversity.

The SM scheme can improve throughput (i.e., capacity), while the diversity scheme can improve the link quality (i.e., post-processing SNR) by using multiple transmit antennas. Analytical and simulation results in [14] show that the relevant SNR metric is 6-12 dB higher for diversity-based schemes than for SM-based schemes, and SM-based schemes yield capacity metrics which range from 30% higher to double that of diversity-based schemes. If the SM scheme has to improve link quality, capacity has to be sacrificed; and if the diversity scheme has to improve capacity, link quality has to be sacrificed [15]. So there is always such trade-off between these two schemes.

In the following, for each technology of SM and diversity scheme, the post-processed SNR and capacity with ideal coding are taken from [14]. The conditions under which these results were obtained are as follows:

- Complex Gaussian channel (flat Rayleigh fading channel);
- Additive White Gaussian noise with zero mean and variance σ^2;
- All Tx-Rx path gains h_{ij} have the same mean power gain, $E\left(|h|^2\right) = g$; and they are independent on their experienced fading, i.e., there exists zero path gain correlation;
- Total transmit power of all antennas is P_T; the receiver input SNR is defined as: input SNR $= P_T g / \sigma^2$;
- For 2x2 tx-sel-rx-MRC (MIMO transmit selection receive Maximum Ratio Combining), the transmitter knows instantaneously which antenna at transmit achieves the largest post-processed receive SNR;
- Continuous modulation and perfect coding are assumed such that BER = 0;
- Perfect channel estimation is assumed.

Now we discuss the SM scheme and diversity scheme technologies one by one.

- SM scheme

The SM scheme exploits the advantage of parallelism of MIMO at transmit side. Different antennas simultaneously transmit different independent signals in parallel and in the same frequency band, which may improve system capacity [3], [5], [16]. At receive side, first the mixing channel matrix is identified through training symbols, and then the individual bit streams are separated and estimated [8]. There exist several SM technologies that depend on the methods exploited at receive to recover the signals: zero-forcing (ZF) [17]-[19], Minimum Mean Square Error (MMSE) [17], [18], Ordered Successive Interference Cancellation MMSE (OSIC-MMSE) [20], [16], etc. The SM scheme requires that the number of transmit antennas is smaller than or equal to the number of receive antennas in order to realize parallel and multiplexing transmission.

The MIMO-OSIC-MMSE is a very popular SM scheme, which can achieve a better capacity gain than other SM schemes, e.g., MIMO-MMSE, MIMO-ZF (Zero Forcing). Therefore, we

give here attention to OSIC-MMSE. The MMSE technology combines signals linearly to get minimum mean square error between estimated signal and transmitted signal. OSIC-MMSE recursively exploits MMSE for the received signals. The substream with the highest post-processing SNR is detected first and its contribution is subtracted from the total received vector signal. The same process is repeated until all the substreams are detected. So this technology uses MMSE in an optimal order. In this way it can realize some diversity gain without sacrificing data rate gain and it is the only technology that provides both diversity and throughput gain [14]. The post processing $SNR_{mimo_osic_mmse}$ and capacity $C_{mimo_osic_mmse}$ it gives for a 2 x 2 MIMO system are:

$$\begin{aligned} SNR_{1,mimo_osic_mmse} &= \max_{i=1,2}\{SNR_{i,mimo_mmse}\} \\ &= \max_{i=1,2}\{\underline{h}_i^{\,H}(\underline{h}_j\underline{h}_j^{\,H} + \frac{2\sigma^2}{P_T}\begin{bmatrix}1 & 0\\ 0 & 1\end{bmatrix})_i^{-1}\underline{h}_i\} \qquad (j \neq i) \end{aligned} , \tag{4.15}$$

$$SNR_{2,mimo_osic_mmse} = \frac{\underline{h}_j^{H}\underline{h}_j P_T}{2\sigma^2}$$

$$C_{mimo_osic_mmse} = \sum_{i=1}^{2}\log_2(1 + SNR_{i,mimo_osic_mmse}) \ , \tag{4.16}$$

where the 2 x 2 channel matrix is

$$H = \begin{bmatrix} h_{11} & h_{12} \\ h_{21} & h_{22} \end{bmatrix} = \begin{bmatrix} \underline{h}_1 & \underline{h}_2 \end{bmatrix}, \tag{4.17}$$

with $\underline{h}_1 = \begin{bmatrix} h_{11} \\ h_{21} \end{bmatrix}$, $\underline{h}_2 = \begin{bmatrix} h_{12} \\ h_{22} \end{bmatrix}$.

- Diversity scheme

The diversity scheme was designed specially for link quality improvement. Space Time Coding (STC), for example, is such a diversity scheme. It jointly encodes signal streams from different antennas. In general the coding level does not improve system throughput compared with SISO systems [21]-[23]. Therefore, a diversity scheme does not improve throughput and/or capacity.

Here we introduce two diversity schemes: MIMO-Alamouti, and MIMO-tx-sel-rx MRC.

(1) MIMO-Alamouti:

MIMO-Alamouti [22] is a space-time block code diversity technology. For post processed SNR_{2X2A} and capacity C_A it gives for a 2 x 2 MIMO system are:

$$\begin{aligned} SNR_{2X2A} &= (SNR_{11} + SNR_{12} + SNR_{21} + SNR_{22})/2 \\ SNR_{ij} &= \left|h_{ij}\right|^2 P_T/\sigma^2 \end{aligned} \tag{4.18}$$

$$C_A = \log_2(1 + SNR_{2X2A}) \tag{4.19}$$

where $i, j \in [1, 2]$; P_T is total transmit power, h_{ij} is instantaneous path gain from transmit antenna j to receive antenna i.

(2) MIMO-tx-sel-rx MRC:
MIMO-tx-sel-rx MRC technology selects that transmit antenna among all transmit antennas that offers the largest post-processed SNR. Only this antenna is used to transmit the signal. At receive, Maximum Ratio Combining (MRC) is used to get the maximum post-processed SNR. The post-processed SNR_{2X2sel} and capacity C_{sel} it gives for a 2 x 2 MIMO system are:

$$\begin{aligned} SNR_{2X2sel} &= \max\left\{(SNR_{11} + SNR_{21}), (SNR_{12} + SNR_{22})\right\} \\ SNR_{ij} &= \left|h_{ij}\right|^2 P_T/\sigma^2 \end{aligned} \tag{4.20}$$

$$C_{sel} = \log_2(1 + SNR_{2X2sel}) \tag{4.21}$$

where $i, j \in [1, 2]$; P_T is total transmit power, h_{ij} is instantaneous path gain from transmit antenna j to receive antenna i.

4.6 Influence of Line of Sight (LOS) on MIMO

In microcellular mobile radio, a dominant path, line-of-sight (LOS) path, may be present at the receive side, in addition to many scattered paths, [24]. In such situation, random multipath components arriving at different angles are superimposed on a stationary dominant signal. At the output of an envelope detector, this has the effect of adding a DC component to the random multipath. The Probability Density Function (PDF) of the received envelope is assumed to be Rician. The channel is assumed to be a Rician fading channel. The PDF of the Ricean distribution is given by [2]:

$$p(r)=\begin{cases}\dfrac{r}{\sigma^2}e^{-\frac{(r^2+A^2)}{2\sigma^2}}I_0(\dfrac{Ar}{\sigma^2}); & for(A\geq 0, r\geq 0),\\ 0; & for(r<0)\end{cases} \tag{4.22}$$

where r is the amplitude of the received signal; σ^2 is the Gaussian process variance of the real and imaginary parts of the complex received signal envelope; A denotes the peak amplitude of the dominant signal, and $I_0(\bullet)$ is the modified Bessel function of the first kind and zero order.

The Ricean distribution is often described in terms of parameter K, which is defined as

$$K=\frac{power\ in\ the\ dominant\ \ path}{power\ in\ the\ scattered\ \ paths}=\frac{A^2}{2\sigma^2}. \tag{4.23}$$

When K is zero, the channel is Rayleigh, whereas if K is infinite, the channel is deterministic.

Sometimes in literature K is defined as the ratio of the power in the scattered paths to the power in the dominant path [24]. However, we use function (4.23).

The Rayleigh fading channel is a feature corresponding to large cells. Macrocells having a diameter of about 2 km can exhibit both Rayleigh fading and Rician fading, but usually with low values of K. When microcells are used, K can vary widely, but often it is above five, and values of 30 are not uncommon [24].

For Ricean fading situation a higher K value means better path loss and less fading. It is well known that in SISO, a Ricean channel gives better performance and capacity than a Rayleigh channel and generally the higher the K value, the better the performance and capacity under the condition that other channel parameters (e.g., the SNR value) are the same. In MIMO systems, however, the result is different.

In MIMO systems with Rician subchannels ($K\neq 0$):
As the relative LOS strength increases, i.e., with higher K values, the Rician channel shows lower useable spatial degrees of freedom and hence a lower capacity for the same SNR is expected. So MIMO systems do not improve the capacity near base stations compared with SISO, but they do improve capacity or quality of service far away from the base station [8].

In MIMO systems with Rayleigh subchannels ($K=0$):
In this case, improvements in SNR and/or in capacity can be achieved. Therefore the results presented in the rest of this chapter can be used in our MIMO system.

4.7 Simulation Results of SNR and Spectral Efficiency Gain of MIMO Systems

In the previous sections we have analysed SNR and spectral efficiency gain of MIMO systems compared with those of non-MIMO systems. Now we give results from simulations[1]. We exploit schemes described before and use some results from literature. Then we do further derivation and simulation to get results suitable for adaptive modulation. The systems we consider are (maximum) 2 x 2 MIMO systems.

4.7.1 SNR Gain for Different 2 x 2 MIMO Schemes

In [14], analysis and simulations have been done to improve SNR of different MIMO schemes compared with SISO or SIMO. Using this method, we carried out further simulations. In Table 4.7-1, we give the results of SNR gain for different 2x2 MIMO schemes in relation to output SNR of SISO. The gain in output SNR is equal to output SNR for SISO subtracted from the output SNR for a given scheme and value of input SNR. These SNR gains were derived from graphs in Appendix C.

Table 4.7-1. SNR gain of different 2x2 MIMO schemes in relation to output SNR of SISO system, for different values of the input SNR [25]

	input SNR [dB]							
	5	10	15	20	25	30	35	40
Scheme	output SNR gain in dB for different values of input SNR							
SISO	-4.9	0.2	5.1	10.4	15	20.5	25.2	30.2
2x2 MIMO-Alamouti	9.3	9.3	9.3	9.1	9.3	9	9.1	9.1
2x2 MIMO-tx-sel-rx-MRC	10.5	10.5	10.5	10.1	10.4	10.1	10.3	10.3
2x2 MIMO-OSIC-MMSE	5.5	3	2	1.3	1.4	0.7	1	1

From our results in Table 4.7-1 for SISO output SNR, we learn that there is a difference of about 10 dB between the 10^{th} percentile of the Cumulative Distribution Function (CDF) of the output SNR and the input SNR.

To visualize the SNR gain, we plotted in Figure 4.7-1 output SNR as function of SISO input SNR and in Figure 4.7-2 output SNR gain over SISO output SNR versus the input SNR for different 2x2 MIMO schemes.

[1] I wish to appreciate the contribution from my student, A. Nassereddine, to the simulations of MIMO gains, i.e., the SNR gain and Rician *K* gain. Detailed descriptions of the work can be found in [26].

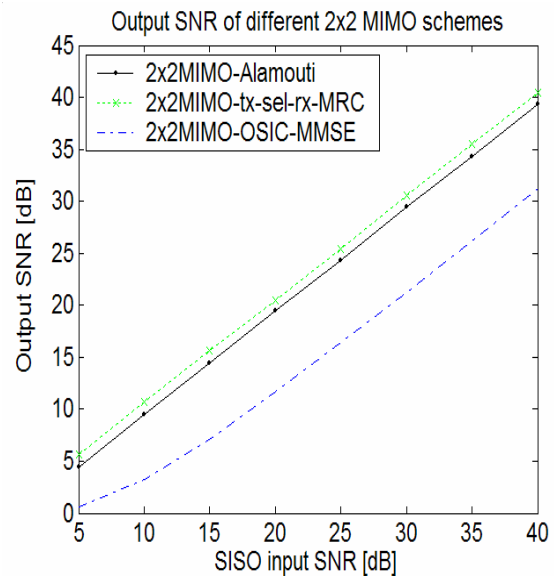


Figure 4.7-1. Output SNR of different 2x2 MIMO Schemes versus SISO input SNR [26]

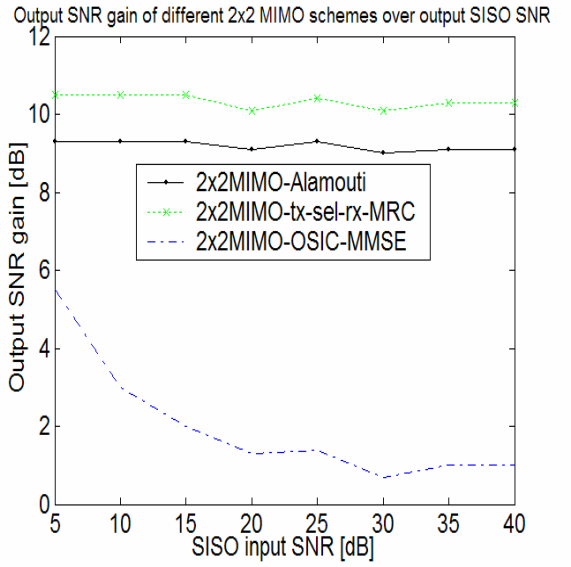


Figure 4.7-2. Output SNR gain of different 2x2 MIMO schemes with respective output SISO SNR versus the input SISO SNR [26]

From Figure 4.7-1 we learn that output SNR's of 2x2 MIMO schemes of MIMO-Alamouti, MIMO-tx-sel-rx-MRC, and MIMO-OSIC-MMSE are linear-like functions with SISO input SNR. This is true as well for MIMO output SNR's versus the SISO output SNR since the SISO output SNR is around 10dB lower than the input SISO SNR. The diversity schemes "MIMO-Alamouti and MIMO-tx-sel-rx-MRC" achieve a higher output SNR gain than the SM scheme "MIMO-OSIC-MMSE". Comparing the two diversity technologies, the MIMO-tx-sel-rx-MRC gives an output SNR that is approximately 1dB better than that of the MIMO-Alamouti technology [25].

Figure 4.7-2 gives output SNR gain of different 2x2 MIMO schemes (compared with the output SISO SNR) versus input SISO SNR. We can draw the same conclusions from Figure 4.7-1. What is more, we find that output SNR gain of both diversity schemes (MIMO-Alamouti and MIMO-tx-sel-rx-MRC) is almost constant over different input SISO SNR's, i.e., it is not a function of input SISO SNR. However, the output SNR gain of the SM scheme (MIMO-OSIC-MMSE) does vary with the input SISO SNR: it decreases with increasing input SISO SNR [25].

4.7.2 Spectral Efficiency (SE) Gain for Different 2x2 MIMO Schemes

Based on the formulas in Appendix C we simulated and generalized the spectral efficiency for some 2x2 MIMO schemes. In table 4.7-2, we give spectral efficiency of different 2x2 MIMO schemes for different input SNR values of SISO.

Table 4.7-2. Spectral efficiency of different 2x2 MIMO schemes for different input SNR values

	input SNR in dB										
	2	4	6	8	10	15	20	25	30	35	40
scheme	Spectral efficiency for different values of input SNR										
SISO	0.2	0.3	0.5	0.7	1	2	3.4	5.2	6.8	8.4	10
2x2 MIMO-Alamouti	1.2	1.6	2	2.7	3.2	4.8	6.4	8.2	9.9	11.5	13
2x2 MIMO-tx-sel-rx-MRC	1.5	1.9	2.4	3.1	3.5	5.1	6.8	8.6	10.2	11.9	13.5
2x2 MIMO-OSIC-MMSE	1.3	1.8	2.4	3.2	3.9	6.1	8.7	11.9	15	18.2	21.6

To visualize the SE gain and to analyse the properties of the different MIMO schemes, we plotted in Figure 4.7-3, the spectral efficiency of SISO system and some 2x2 MIMO schemes as a function of the input SNR. In Figure 4.7-4, we plotted the SE gain of these MIMO schemes compared to that of SISO in relation to SISO input SNR.

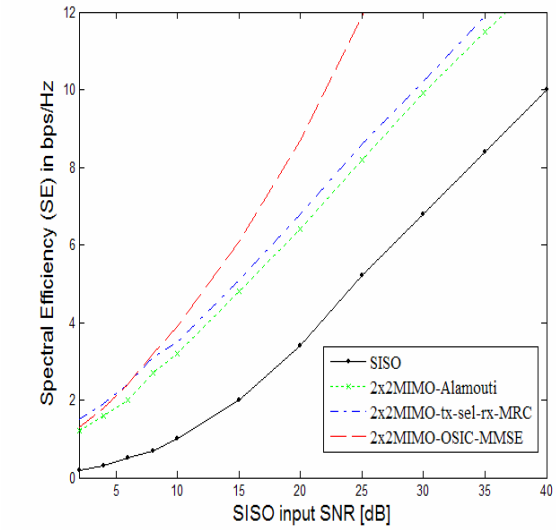


Figure 4.7-3 SE of different MIMO schemes vs. SISO input SNR [26]

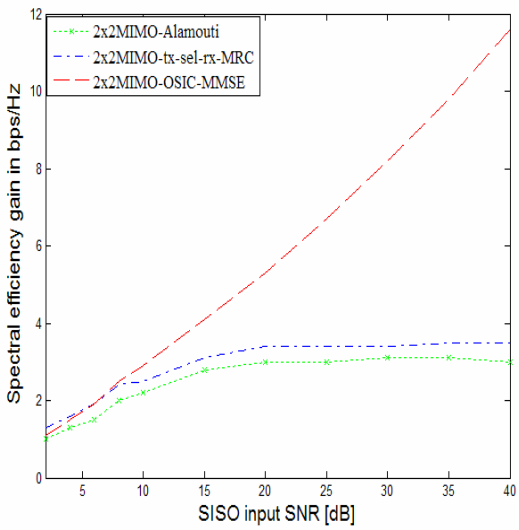


Figure 4.7-4. SE gain of several MIMO schemes (relative to SE of SISO) vs. SISO input SNR[26]

From Figure 4.7-3 we find that SE of all these MIMO schemes is higher than that of SISO. At low input SNR, the SEs of all these MIMO schemes do not differ much. The SE of SM scheme MIMO-OSIC-MMSE grows faster than that of the diversity schemes (MIMO-Alamouti and MIMO-tx-sel-rx-MRC) with increasing input SNR.

From Figure 4.7-4 we can draw the same conclusion as from Figure 4.7-3. What is more, this figure also shows that when the SISO input SNR is larger than 15dB, the SE gain of diversity schemes (MIMO-Alamouti and MIMO-tx-sel-rx-MRC) becomes almost constant; in other words, the SE Gain of both diversity schemes is not a function of SISO input SNR, nor a function of the SISO output SNR. However, the SE gain of the SM scheme (MIMO-OSIC-MMSE) does increase with increasing the SISO input SNR, so it is a function of the SISO SNR [25].

The results for SNR gain shown in Figures 4.7-2 through 4.7-4 indicate that the “SM scheme gain” is a function of SISO SNR both with respect to its SNR gain and SE gain, while the “diversity scheme gain” is constant over SISO SNR both with respect to SNR gain and SE gain. An overview is given in Table 4.7.3.

Table 4.7-3 SNR gain and SE gain of MIMO compared with that of SISO for SM and diversity schemes

	SNR gain	Spectral efficiency gain
SM scheme	Decreases with SISO SNR	Linear increase with SISO SNR
Diversity scheme	Constant over SISO SNR	Constant over SISO SNR

4.8 Generalization of SNR and Capacity of MIMO

In the literature much work on SNR and capacity gain of MIMO is described. We summarize the results of [14] below, and list them in Table 4.10-1 and Table 4.10-2.

4.8.1 Diversity Scheme

(1) SNR gain
Number of transmit/receive antennas:

- In a system with one receive antenna and a larger number of transmit antennas, increasing the number of transmit antennas (till 4) will provide significant SNR gain of MIMO over SIMO; however, the gain will decrease with increasing number of receive antennas. In other words, with a small number of receive antennas (e.g., 1 or 2), we can improve SNR by increasing the number of transmit antennas. This gain is independent of input SNR.

(2) Capacity gain
Number of transmit antennas:

- For a diversity scheme, the capacity gains of MIMO compared to SIMO schemes, increase slowly (and at a decreasing rate) with the number of transmit antennas.

Number of receive antennas:

- For a diversity scheme, the capacity gains of MIMO compared to SIMO schemes, decreases with increasing number of receive antennas.

SISO input SNR:

- For a diversity scheme, the capacity gains of MIMO compared to SIMO schemes, decreases with input SNR.

4.8.2 SM Scheme

(1) SNR gain
Number of transmit antennas:

- With the same number of receive antennas, a MIMO scheme has a worse SNR than a SIMO scheme, because it loses diversity and it divides the transmit power among all transmit antennas. A larger number of transmit antennas results in therefore SNR deterioration.

Number of receive antennas:

- SNR gain of MIMO compared to SIMO schemes, is a function of the receiver input SNR. For high input SNR, the deterioration decreases with increasing number of receive antennas; and for low input SNR, the deterioration is constant with the number of receive antennas. The final SNR loss (for low input SNR and high input SNR with large number of receive antennas) converges to the loss from transmission power division, i.e., the loss is $10\log_{10}n$ = 3.0 dB, 4.8 dB, 6.0 dB for a number of transmit antennas of n = 2, 3, 4, respectively.

(2) Capacity gain

Number of transmit antennas:

- The capacity gain of MIMO compared to SIMO, increases quickly with increasing number of transmit antennas.

Number of receive antennas:

- The capacity gain of MIMO compared to SIMO, increases with increasing number of receive antennas.

Input SISO SNR:

- The capacity gain of MIMO compared to SIMO, increases with increasing the input SNR.

4.9 Rician *K* Factor Gain of MIMO over SISO

We showed above that MIMO systems give SNR gain and/or Spectral Efficiency (SE) gain, compared to SISO and SIMO systems. SNR represents Quality of Service (QoS); and SE represents throughput or capacity. Let us look at QoS.

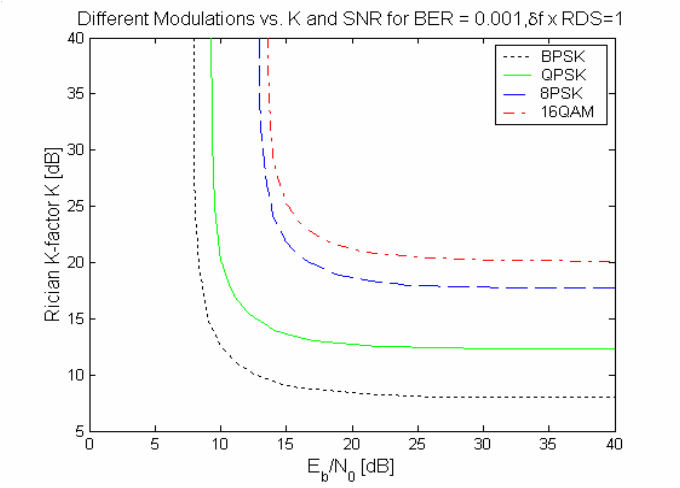


Figure 4.9-1. The required Rician *K* factor value versus SNR for different modulations (BER =10^{-3})

Figure 4.9-1 is a simulation result of the required Rician *K* factor value versus SNR at a BER of 10^{-3} for different modulations in an OFDM system. This simulation was done with the prerequisite that the product of the OFDM subcarrier bandwidth and RDS is equal to 1 [28]. From this figure we can see that when the Rician *K* is lower than a certain value, it is not possible to get the required BER, not even if SNR is large. But we know that MIMO systems can achieve a BER of 10^{-3} easily with Rician *K* factor zero (Rayleigh channel). This means that MIMO schemes can improve more than just SNR. In other words, the SNR gain is not the only QoS gain of MIMO systems compared to SISO/SIMO systems. Based on this we studied the Rician *K* factor gain of MIMO compared to SISO systems.

4.9.1 BER Performance of the Considered SISO Model

The Symbol Error Rate (SER) performance in a Rayleigh fading channel for M-PSK modulation can be expressed by the following equation [25],

$$P=\frac{(-1)^{L-1}(1-\mu^2)^L}{\pi(L-1)!}\left(\frac{\partial^{L-1}}{\partial b^{L-1}}\left\{\frac{1}{b-\mu^2}\left[\frac{\pi}{M}(M-1)-\frac{\mu\sin(\pi/M)}{\sqrt{b-\mu^2\cos^2(\pi/M)}}\cot^{-1}\frac{-\mu\cos(\pi/M)}{\sqrt{b-\mu^2\cos^2(\pi/M)}}\right]\right\}\right)_{b=1}, \quad (4.24)$$

where M is modulation level, L is diversity order, $\mu = \sqrt{\frac{\bar{\gamma}_c}{1+\bar{\gamma}_c}}$, and $\bar{\gamma}_c$ is the average received SNR per channel. The SNR per bit is $\bar{\gamma}_b = \frac{L\bar{\gamma}_c}{k}$, with $k = \log_2 M$. The SER performance given above can be approximated, when $\bar{\gamma}_b >> 1$ and $L = 1$, by

$$P = \frac{M-1}{(M\log_2 M)[\sin^2(\pi/M)]2\bar{\gamma}_b} \quad , \tag{4.25}$$

which gives the BER performance.

This bit error probability is plotted in Figure 4.9-2 for different modulation levels.

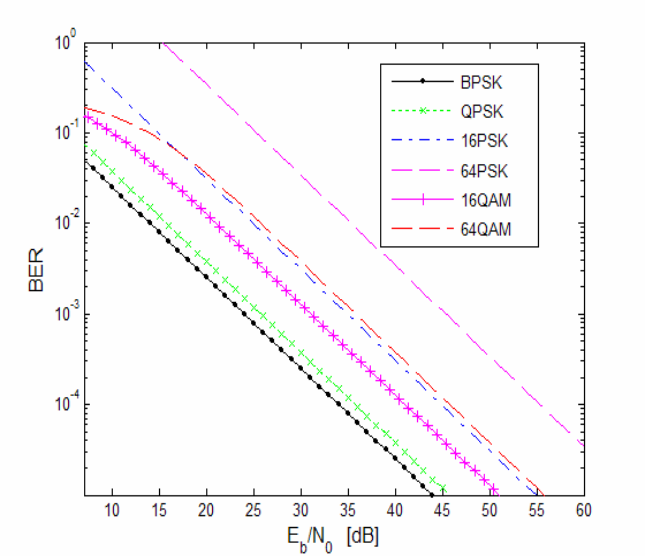


Figure 4.9-2. Bit error probability of BPSK, QPSK, 16PSK, 64PSK, 16QAM and 64QAM modulations in Rayleigh fading channels

We know that there is an advantage to using M-QAM modulation instead of M-PSK for large values of M. This advantage is $\frac{3M^2}{2(M-1)\pi^2}$ [28].

Table 4.9-1 lists this ratio in dB for several values of M.

Table 4.9-1. BER improvement of M-QAM compared to M-PSK [26]

M	$10*\log\left(\frac{3M^2}{2(M-1)\pi^2}\right)$ **[dB]**
8	1.43
16	4.14
32	7.01
64	9.95

In figure 4.9-2 we plotted under Rayleigh channel conditions the bit error probability of SISO when M-PSK and M-QAM is used. This was done for several values of *M*. The bit error probability of BPSK, QPSK, 16QAM, and 64QAM will be compared with the MIMO BER to derive the Rician *K* gain.

4.9.2 Rician K Gain

We mentioned before that the MIMO system does not only achieve an SNR gain compared to the SISO system, but also a gain in the Rician *K* factor. We define this gain as the Rician *K* gain, denoted by K_G. Now we show what Rician *K* gain the different MIMO schemes can achieve.

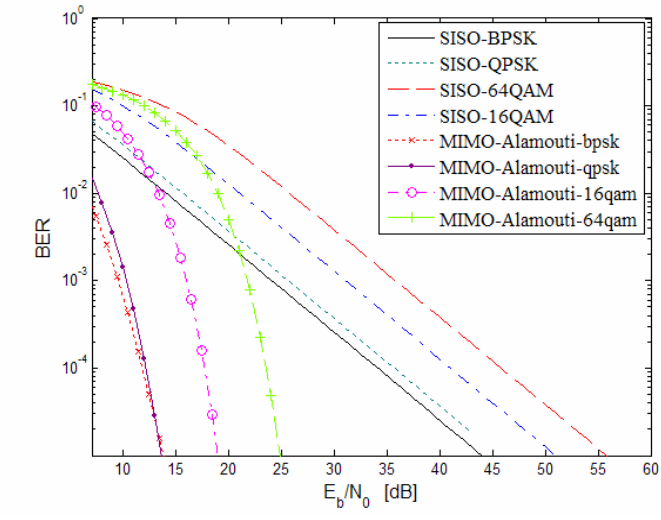


Figure 4.9-3. BER vs. SNR for different modulations in SISO channel and 2 x 2 MIMO-Alamouti scheme in Rayleigh fading channel

Figure 4.9-3 gives BER versus SNR for different modulations in a SISO channel with Rician *K* factor zero and different modulations of 2x2 MIMO-Alamouti schemes with Rician *K* factor zero. For every modulation level, the MIMO system achieves a better BER than the SISO system. Instead of translating this improvement into an SNR gain, we translate it into a Rician K factor gain. For every modulation, we try to find out the Rician *K* factor value that results in the best match between BER of the SISO channel and that of the MIMO channel.

We carried out simulations to find out the Rician *K* values of SISO systems that give a similar BER performance as MIMO systems. This *K* value in dB minus the *K* value in dB of the MIMO systems is the Rician *K* gain in dB. However, for the *K* value of MIMO systems we take here is zero dB, so the *K* value we get in simulations equals the Rician *K* gain. In order to find out the Rician *K* gain, we used the "try and compare" method. We chose two *K* values: K_1, and K_2 first ($K_1 < K_2$), and compared their simulation results with the MIMO curve to see which of the two is closer to the MIMO curve. If the two simulated curves lay on the same side of the MIMO curve and the smaller *K* (K_1) is closer to the MIMO curve, we abandon the larger *K* (K_2) and chose a K_3 which is even smaller than K_1 ($K_3 < K_1$). If the two curves lay on both sides of the MIMO curve, we chose a K_3 ($K_1 < K_3 < K_2$). We compared the two simulation curves for K_3 and K_1 (or K_2) with the MIMO curve and repeated the above procedures until we found a *K* whose curve matched the MIMO curve best.

We will work out the Rician *K* gain of 2x2 MIMO systems here (MIMO-Alamouti, MIMO-tx-sel-rx-MRC, MIMO-OSIC-MMSE), but this method can also be used to study the Rician *K* gain of *n*x*m* MIMO systems (*n* is the number of transmit antennas and *m* is the number of receive antennas). The modulations we simulate here are BPSK, QPSK, 16QAM and 64QAM.

In our simulations, we consider a slow fading Rician channel. We assume perfect knowledge of the channel at the receiver and uncorrelated antennas at transmit- and receive side. We will mainly focus on two target BER values in our BER performance comparison: 10^{-3} and 10^{-5}.

Figure 4.9-4 gives the Rician *K* gain and SNR correction of the MIMO-Alamouti scheme for different modulations in terms of BER versus SNR performance. From the figure we see that the BER versus SNR performance of the MIMO-Alamouti scheme and that of the SISO system with a Rician *K* factor cross at only one point (i.e., one SNR value). This means that it is not possible to find a *K* value that makes the BER versus SNR curve match the SISO curve for all SNR values. In other words, the curves never overlap completely. Therefore, we need SNR correction to describe the Rician *K* gain of MIMO systems [26].

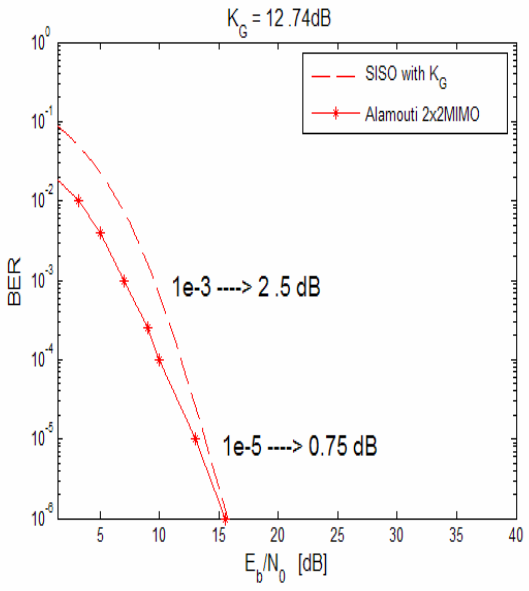
The simulation results reveal that the MIMO-Alamouti scheme gives for BPSK modulation a Rician *K* gain (K_G) of 12.74dB with an SNR gain of 2.5dB for BER 10^{-3} and an SNR gain of 0.75dB for BER 10^{-5}; for QPSK modulation, K_G = 16.9dB with SNR gain 1.25dB at BER 10^{-3} and SNR gain – 0.4dB at BER 10^{-5}; for 16QAM modulation, K_G = 25.38dB with SNR gain 0dB at BER 10^{-3} and SNR gain 4.5dB at BER 10^{-5}; for 64QAM modulation, K_G = 29.08dB with SNR gain 0.5dB at BER 10^{-3} and SNR gain - 4dB at BER 10^{-5}. These results are listed in

Table 4.9-2 [27]. The positive SNR correction means that for such a Rician K gain, the described MIMO scheme can still yield a higher SNR gain. A negative value of SNR correction means that instead of yielding an extra SNR gain, this MIMO scheme gives the indicated SNR loss for this Rician K gain. However, we note that the values of the SNR correction are not large. Here, we just list the SNR correction for BER 10^{-3} and BER 10^{-5}. The SNR corrections of other BER values can be obtained in the same way.

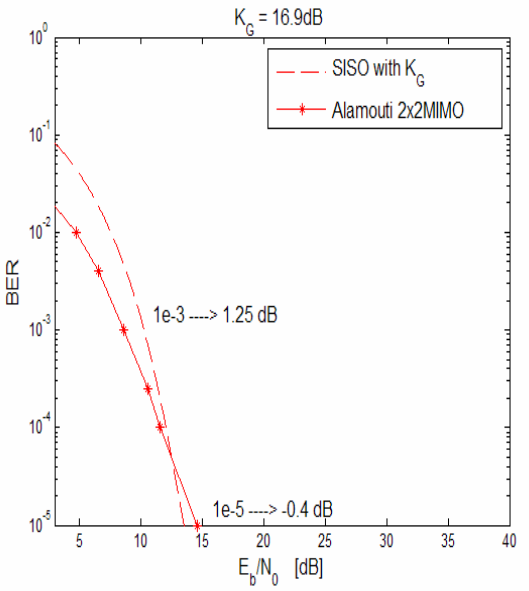
From Table 4.9-2, we learn that the Rician K gain increases with modulation level M. This is because in SISO, the higher the modulation level, the more difficult it is to get a small BER. In other words, MIMO achieves a higher gain in performance at a higher modulation level than at a lower modulation level.

Table 4.9-2. Rician K gain of several 2x2 MIMO schemes with SNR correction

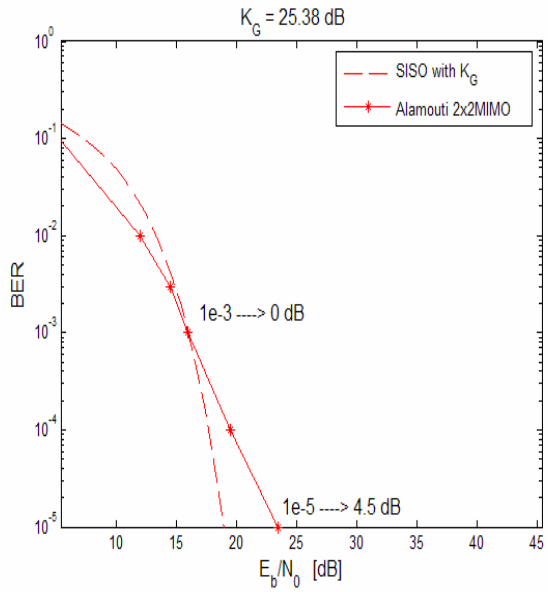
			MIMO-Alamouti	MIMO-tx-sel-rx-MRC	MIMO-OSIC-MMSE
BPSK	K_G [dB]		12.74	12.74	8.12
	SNR correction [dB]	For BER 1e-3	2.5	3.5	-2
		For BER 1e-5	0.75	1.75	0
QPSK	K_G [dB]		16.9	16.9	8.2
	SNR correction [dB]	For BER 1e-3	1.25	2.25	-2.5
		For BER 1e-5	- 0.4	0.6	-0.4
16 QAM	K_G [dB]		25.38	25.38	8.2
	SNR correction [dB]	For BER 1e-3	0	1	-1.8
		For BER 1e-5	4.5	5.5	-0.4
64 QAM	K_G [dB]		29.08	29.08	8.1
	SNR correction [dB]	For BER 1e-3	0.5	1.5	-0.8
		For BER 1e-5	- 4	-3	0.4



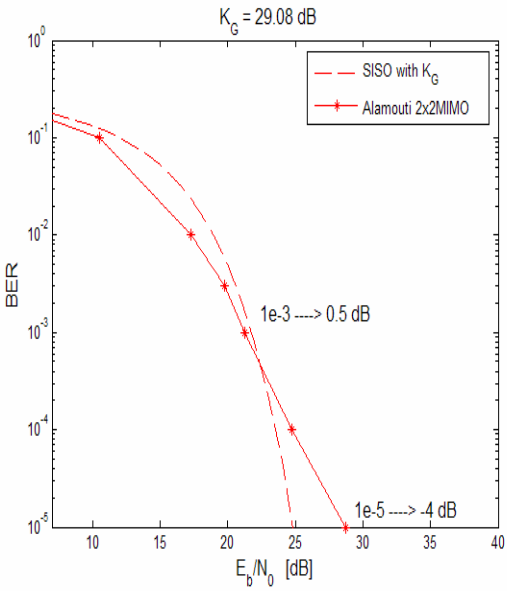
(a) BER of BPSK



(b) BER of QPSK

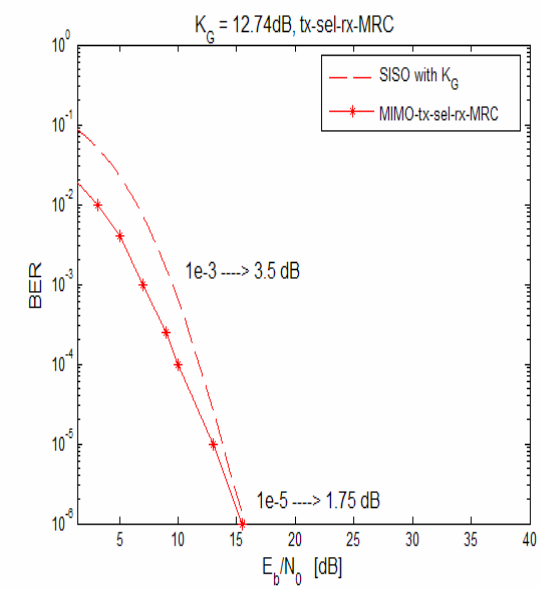


(c) BER of 16QAM

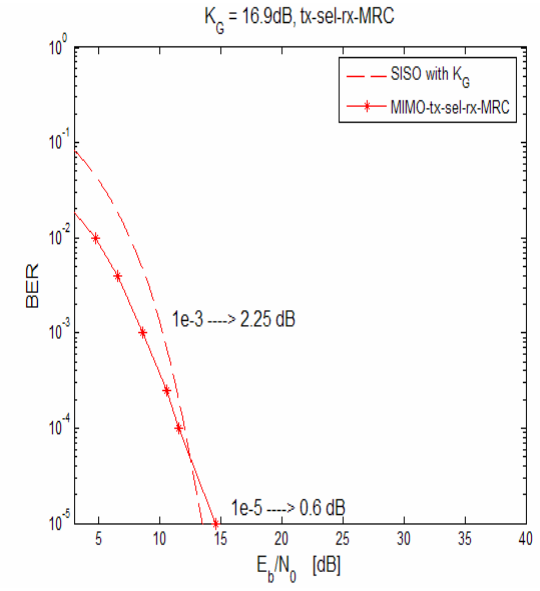


(d) BER of 64QAM

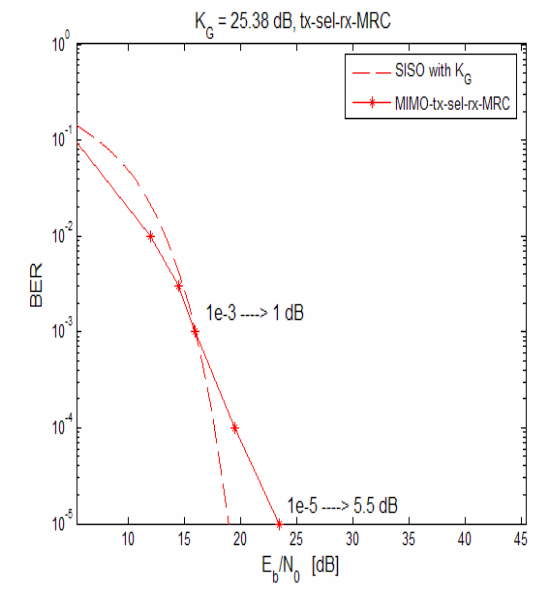
Figure 4.9-4. Rician *K* gain [dB] and SNR correction of MIMO-Alamouti scheme for different modulations [26]



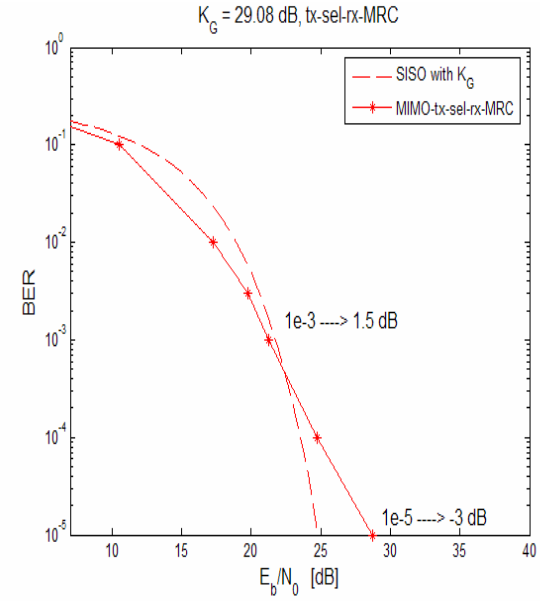
(a) BER of BPSK



(b) BER of QPSK



(c) BER of 16QAM



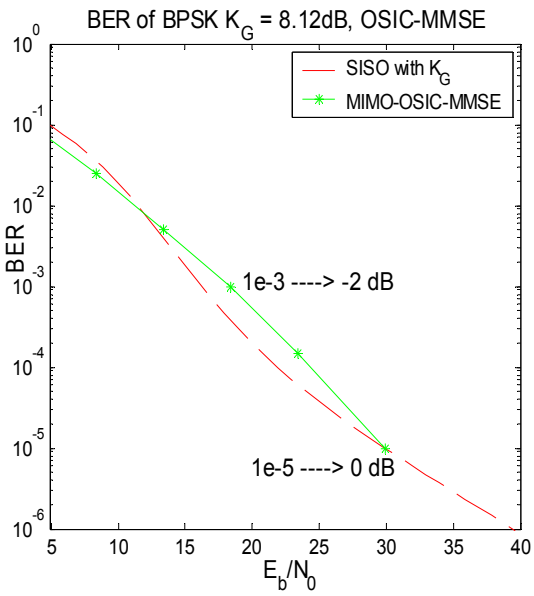
(d) BER of 64QAM

Figure 4.9-5. Rician *K* gain [dB] and SNR correction of MIMO-tx-sel-rx-MRC scheme for different modulations [26]

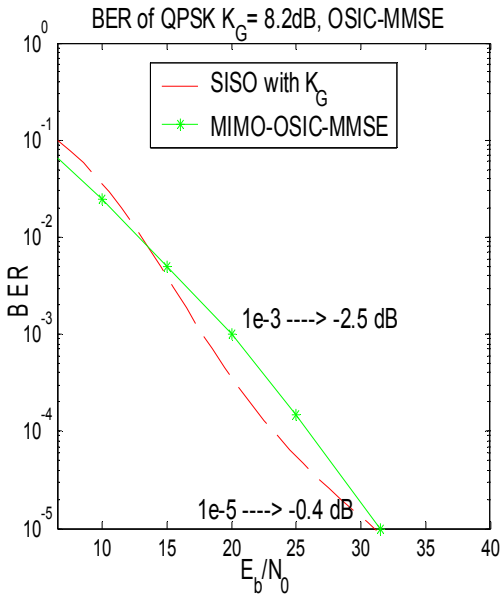
We can get the Rician *K* factor gain of MIMO-tx-sel-rx-MRC in the same way. But from Table 4.7-1, Figure 4.7-1, and Figure 4.7-2, we know that the MIMO-tx-sel-rx-MRC scheme achieves a gain of 1 dB compared to the MIMO-Alamouti scheme. So a simple way is to keep the Rician *K* gain and shift SNR correction about 1 dB. The results are given in Figure 4.9-5. The Rician *K* gain and SNR correction are also listed in Table 4.9-2.

The two technologies just described, MIMO-Alamouti and MIMO-tx-sel-rx-MRC, are diversity schemes. As can be seen from the results above, generally these technologies give a higher SNR gain than the MIMO-OSIC-MMSE one, which is a spatial multiplexing scheme. The question is then raised: "Does this conclusion also hold for the Rician *K* gain?"

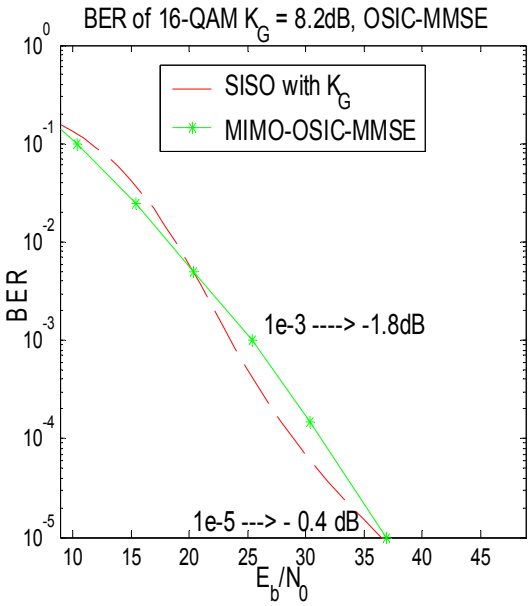
Figure 4.9-6 gives the Rician *K* gain in dB and SNR correction of the MIMO-OSIC-MMSE scheme for different modulations. We can see that for all modulations, the Rician *K* gain is almost constant, around 8.1~8.2 dB. This is different from the Rician *K* gain of the diversity scheme, which varies with modulation, and is higher. The Rician *K* gain and SNR correction of all modulations of the MIMO-OSIC-MMSE scheme are also listed in Table 4.9-2.



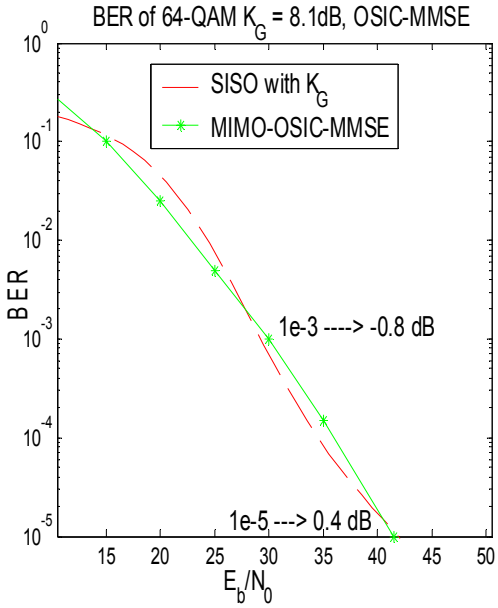
(a) BER of BPSK



(b) BER of QPSK



(c) BER of 16QAM



(d) BER of 64QAM

Figure 4.9-6. Rician *K* gain [dB] and SNR correction of MIMO-OSIC-MMSE scheme for different modulations (E_b/N_0 is in dB) [26]

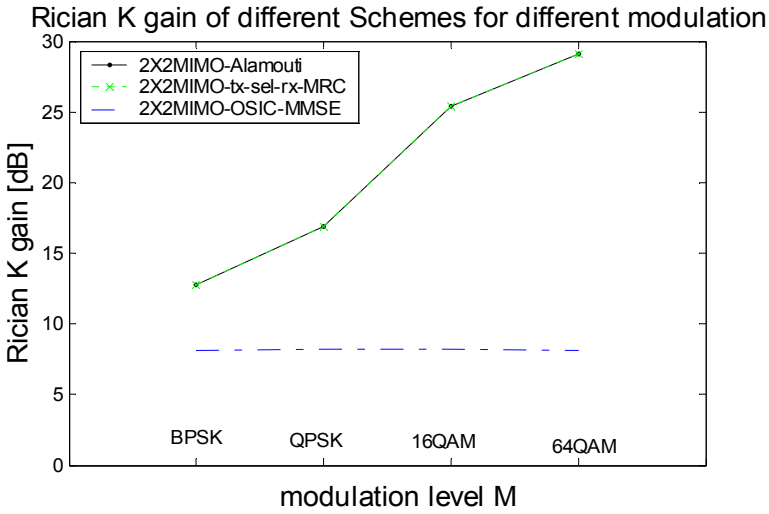


Figure 4.9-7. Rician *K* factor gain of MIMO schemes for different modulations

Figure 4.9-7 gives the Rician *K* factor gain of selected 2x2 MIMO schemes, i.e., the MIMO-Alamouti, MIMO-tx-sel-rx-MRC, and MIMO-OSIC-MMSE, for BPSK, QPSK, 16QAM and 64QAM modulations. From the figure, we can see that the Rician *K* gain versus modulation level curves of MIMO-Alamouti and MIMO-tx-sel-rx-MRC technology overlap here completely. In other words, they have the same Rician *K* gain for all the modulation levels. We can conclude that diversity schemes (i.e., MIMO-Alamouti and MIMO-tx-sel-rx-MRC) achieve a higher Rician *K* factor gain than the SM scheme (MIMO-OSIC-MMSE), and that the Rician *K* gain of the diversity scheme is a function of modulation level, while the Rician *K* factor gain of the SM scheme does not change with modulation.

4.10 Conclusions

In this chapter we analysed the basic definition, structure, and characteristics of MIMO systems; we described different categories of MIMO systems, and carried out simulations to calculate the gains of different MIMO schemes in terms of capacity and SNR and compared these with those of non-MIMO systems. The influence of LOS was considered too. In order to give insight in MIMO gain, we introduced a new parameter, i.e., Rician *K* factor gain. We gave a detailed description of the gains of MIMO systems compared to SISO or SIMO systems. Now we list them briefly in the following tables. "↑" means that the parameter is increased, and "↓" means that it is decreased.

Table 4.10-1 presents the influence of the number of transmit and receive antennas on SNR gain of MIMO compared to SIMO systems. When the number of transmit antennas is increased and/or the number of receive antennas is decreased, the relative SNR gain of MIMO

compared to SIMO will grow for diversity schemes; this relative gain in dB is positive. This is because a larger number of transmit antennas or receive antennas can improve the post-processed SNR for diversity schemes. The number of receive antennas improves the SNR more drastically than the number of transmit antennas. When n increases, $SNR_{n,m}$ increases and $SNR_{1,m}$ does not change, so $R_{n,m}$ increases. For smaller m, the influence of n becomes more visible, so $R_{n,m}$ increases.

The opposite is true for the SM scheme. The relative SNR gain of MIMO with respect to SIMO increases now with the number of receive antennas and decreases with the number of transmit antennas. This relative value in dB is negative, which means that an SNR loss occurs. This loss is partly due to the loss of diversity (compared with SIMO systems) and partly due to the equal division of the total transmit power among n transmit antennas. As a result of the latter, the relative SNR gains decrease with the number of transmit antennas, but grow with the number of receive antennas.

Table 4.10-1 Influence of number of transmit and receive antennas on SNR gain of MIMO vs. SIMO

	SNR Gain
Diversity scheme	$\left.\begin{array}{l} m\downarrow \\ or \\ n\uparrow \end{array}\right\} \Rightarrow \quad R_{n,m}=\dfrac{SNR_{n,m}}{SNR_{1,m}} \quad \uparrow \quad (R_{n,m}[dB]>0)$
SM scheme	$\left.\begin{array}{l} m\uparrow (for \quad high \quad SNR_i) \\ or \\ n\downarrow \end{array}\right\} \Rightarrow R_{n,m}=\dfrac{SNR_{n,m}}{SNR_{1,m}} \quad \uparrow \quad (R_{n,m}[dB]<0)$
n: number of transmit antennas; m: number of receive antennas; $SNR_{n\text{-}m}$: output SNR of n by m MIMO system; $SNR_{1\text{-}m}$: output SNR of 1 by m SIMO system; SNR_i : input SISO SNR;	

Table 4.10-2 lists the factors influencing capacity gain of MIMO versus SIMO. For the selected diversity schemes, the relative capacity gains increase with the number of transmit antennas, but decrease with the number of receive antennas and input SNR. The reason is connected with the relative SNR gain for diversity schemes, since the capacity has a logarithmic relationship with post-processed SNR for diversity schemes.

For SM schemes, the relative capacity gain also increases with the number of transmit antennas. However, in contrast to the diversity scheme, this gain also increases with the number of receive antennas and input SNR. This is because the capacity of SM schemes is a summation of the capacities of the sub-channels.

Table 4.10-2 factors influencing capacity gain of MIMO vs. SIMO

	Capacity Gain
Diversity scheme	$\left.\begin{array}{l} n\uparrow \\ or \\ m\downarrow \\ or \\ SNR_i\downarrow \end{array}\right\} \Rightarrow R_{C_n,m}=\frac{C_{n,m}}{C_{1,m}}\uparrow \quad (R_{C_n,m}>1)$
SM scheme	$\left.\begin{array}{l} n\uparrow \\ or \\ m\uparrow \\ or \\ SNR_i\uparrow \end{array}\right\} \Rightarrow R_{C_n,m}=\frac{C_{n,m}}{C_{1,m}}\uparrow \quad (R_{C_n,m}>1)$
n: number of transmit antennas; m: number of receive antennas; $C_{n\text{-}m}$: mean capacity of n by m MIMO system; $C_{1\text{-}m}$: mean capacity of 1 by m SIMO system; SNR_i : input SISO SNR;	

Table 4.10-3 presents a comparison of SNR gain, Rician *K* factor gain, and SE gain of MIMO systems with respect to SISO systems for SM and diversity schemes. For SM schemes, the SNR gain and Spectral Efficiency (SE) gain of MIMO with respect to SISO are functions of input SNR. The SNR gain decreases, but the capacity gain increases with input SNR. For diversity schemes, the SNR gain and SE gain of MIMO systems to SISO systems are not a function of input SNR. The Rician *K* gain of MIMO compared to SISO is a function of modulation for diversity schemes. This gain increases with modulation level. For the SM scheme, on the other hand, this gain is not a function of modulation level, and constant for all modulation levels.

Table 4.10-3. Comparison of SNR gain, Rician *K* factor gain and SE gain of MIMO with respect to SISO for SM and diversity schemes

	SNR Gain	Spectral Efficiency Gain	Rician *K* gain
SM scheme	$SNR_i \uparrow \Rightarrow G_{SNR} \downarrow$	$SNR_i \uparrow \quad \Rightarrow G_{SE} \uparrow (linearly)$	Constant over M
Diversity scheme	Constant over SNR_i	Constant over SNR_i	$M \uparrow \Rightarrow K_G \uparrow$
SNR_i : input SISO SNR; G_{SNR} : Gain in SNR; K_G: Rician *K* gain; *M*: modulation level;			

References

[1] Lee, Hoo-Jin; Patil, Shailesh; Raj, Raghu G. ; "Fundamental overview and simulation of MIMO systems for Space-Time coding and Spatial Multiplexing" http://www.ece.utexas.edu/~wireless/EE381K11_Spring03/project.htm;

[2] Rappaport, T. S. , " Wireless communications principles and practice", Prentice Hall, Inc., 1996, ISBN 0-13-375536-3;

[3] Foschini, G. J., and Gans, M. J., "On limits of wireless communications in a fading environment when using multiple antennas," Wireless Personal Communications, vol. 6, pp. 311-335, March 1998;

[4] Foschini, G. J., "Layered space-time achitecture for wireless communication in a fading environment when using multielement antennas", Bell Labs tech. J., pp. 41-59, Autumn 1996;

[5] Telatar, E., "Capacity of multi-antenna Gaussian channels", Eur. Trans. Telecomm., vol. 10, pp585-595, Nov./Dec. 1999;

[6] Raleigh, G., and Cioffi, J. M., "Spatial-temporal coding for wireless communications" IEEE Trans. Commun., vol. 46, pp. 357-366, 1998;

[7] Bolcskei, H., Gesbert, D., and Paulraj, A. J., "On the capacity of OFDM-based spatial multiplexing systems", IEEE Trans. Commun., vol. 50, pp. 225-234, Feb. 2002;

[8] Gesbert, D., Member, IEEE, Shafi, Mansoor, Fellow, IEEE, Da-shan Shiu, Member, IEEE, Peter J. Smith, Member, IEEE, and A. Naguib, Senior Member, IEEE, " From Theory to Practice: An Overview of MIMO Space–Time Coded Wireless Systems", http://heim.ifi.uio.no/~gesbert/papers/JSACMIMOtutorial.pdf;

[9] Tarokh, V.; Naguib, A.; Seshadri, N.; and Calderbank, A. R.; "Space-time codes for high data rate wireless communication: performance criteria in the presence of channel estimation errors, mobility, and multiple paths," Communications, IEEE Tranasactions, vol. 47 Issue 2, pp199-207, Feb 1999;

[10] Driessen, P. F., and Foschini, G. J., "on the capacity formula for multiple-input multiple-output wireless channels: A geometric interpretation", IEEE Trans. Commun., vol. 47, pp. 173-176, Feb. 1999;

[11] Farrokhi, F. R.; Foschini, G.J.; Lozano, A.; and Valenzuela, R. A.; "Link-optimal space-time processing with multiple transmit and receive antennas", IEEE Commun. Lett., vol. 5, pp.85-87, 2001;

[12] Catreux, S.; Driessen, P. F.; Greenstein, L. J.; " Data throughputs using Multiple-Input Multiple-Output (MIMO) techniques in a noise –limited cellular environment", http://www.ece.uvic.ca/~peter/papers/MIMOsingle-cellPaper3.doc;

[13] Telatar, E.; "Capacity of multiantenna Gaussian channels", AT&T Bell Laboratories, Tech. Memo., June 1995;

[14] Catreus, S.; Greenstein, L. J.; Erceg, V.; "Some Results and Insights on the Performance Gains of MIMO Systems" IEEE Journal on Selected Areas in Communications, vol. 21, No. 5 June 2003;

[15] Gesbert, D.; and Akhtar, J.; "Breaking the barriers of Shannon's capacity: An overview of MIMO wireless systems", Telenor's J.: Telektronikk. 2001;

[16] Foschini, G. J.; Golden, G. D.; Valenzuela, R. A.; and Wolniansky, P. W.; "Simplified processing for wireless communication at high spectral efficiency wireless communication employing Multi element arrays", IEEE Journal on Selected Areas Communication— Wireless Communication Series, vol. 17, pp. 1841-1852, Nov. 1999;

[17] Gore, D. A.; Heath, R. W. Jr.; and Paulraj, A. J.; "Performance Analysis of Spatial Multiplexing in Correlated Channels", submitted to Communications, IEEE Transactions March 2002;

[18] Bolcskei, H.; and Paulraj, A. ; "Multiple Input Multiple output (MIMO) wireless systems", In J. Gibson, editor, The communications Handbook. CRC Press, 2001;

[19] Zelst, A. van; "Space Division Multiplexing Algorithm", Proc. of IEEE MeleCon 2000.3, pp1218-1221, May 2000;

[20] Guo, Z.; and Nilsson, P.; "On Detection Algorithms and Hardware Implementations for V-BLAST", SsoCC'02, Faukenberg, 2002;

[21] Tarokh, V.; Seshadri, N.; and Calderbank, A. R.; "Space-time codes for high data rate wireless communication: Performance criterion and code construction", IEEE Trans. Inform. Theory, vol. 44, pp. 744-765, Mar. 1998;

[22] Alamouti, S.M.; "A simple transmit diversity technique for wireless communications" IEEE Journal on Selected Areas in Communications, vol. 16, No. 8, pp. 1451-1458, October 1998;

[23] Naguib, A. F., Seshadri, N., and Calderbank, A.R., "Increasing data rate over wireless channels", IEEE Signal Processing Mag., vol. 17, pp. 76-92, May 2000;

[24] Steele, R., *Mobile Radio Communications*, ISBN 0471964190, John Wiley, England, 1996;

[25] Che, H., Nassereddine, A., Nikookar, H., Prasad, R., Ligthart, L. P., "Performance Gain of MIMO System for Adaptive Modulation Algorithm", submitted to IEEE Transactions on Vehicular Technology;

[26] Nassereddine, A., "Analysis of an Adaptive OFDM Algorithm in MIMO Channels" *M.Sc. Graduation Thesis,* IRCTR, EWI, Delft University of Technology, the Netherlands;

[27] Che, H., Nassereddine, A., Nikookar, H., Prasad, R., Ligthart, L. P., "Another Parameter Representing QoS Gain of MIMO System" European Microwave Week-European Conference on Wireless Technology (ECWT) 2004, Amsterdam, the Netherlands; October 2004;

[28] Proakis, John G., *Digital Communications*, ISBN 0-07-051726-6, McGraw-Hill, Inc. 1995;

Chapter 5

Adaptive Modulation Algorithms for SISO and MIMO Channels

5.1 Introduction

In Chapter 3 we investigated the theory, strategy, and work procedures of adaptive modulation. Adaptive OFDM and CDMA algorithms were discussed. In Chapter 4, the theory behind MIMO channels was investigated and their gains with respect to SISO channels. In this chapter we build the complete algorithms for adaptive OFDM and CDMA for SISO and MIMO channels. Simulation results will be presented to evaluate the algorithms.

This chapter is organized as follows: in Sections 5.2 and 5.3 we propose an adaptive OFDM algorithm for SISO channels; in Section 5.4 an adaptive OFDM algorithm for MIMO channels and in Section 5.5 an adaptive CDMA algorithm for MIMO channels; Section 5.6 outlines the simulators and assumptions exploited in our simulations. Sections 5.7 to 5.9 present simulation results and analyses of all these algorithms[1]. Conclusions are given in Section 5.10.

We present a global flow chart of our adaptive OFDM algorithm for SISO channels in Section 5.2.1. Part of the details of this global flow chart, i.e., the guard time setting and the setting of the subcarrier bandwidth, is discussed in Sections 5.2.2 and 5.2.3.

[1] I wish to appreciate the contribution from my student, A. Nassereddine, to implementing the adaptive OFDM algorithm for MIMO channels and simulations. Detailed descriptions of the work can be found in [1].

In Section 5.3 we propose three algorithms for subband settings, i.e., a selective subband setting, a varying subcarrier-subbandsetting, and a constant subcarrier and varying subband setting, in which the flexibility (or adaptivity) decreases. Simulation results for these three algorithms are presented in Section 5.7.

We build an adaptive OFDM algorithm for MIMO channels in Section 5.4. It combines adapting MIMO schemes with adapting OFDM modulation parameters. We describe the simulator and assumptions that we exploit in our simulations. The simulation results are shown to evaluate our algorithm in Section 5.8.

In Section 5.5 we propose an adaptive CDMA algorithm for MIMO channels. We combine adapting MIMO schemes with adapting CDMA parameters in order to get extra gains. Simulation results are used in Section 5.9 to evaluate our algorithm.

In Section 5.10 our conclusions are summarized.

5.2 Adaptive OFDM Algorithms for SISO Channels

5.2.1 A Global Flow Chart of Adaptive OFDM Algorithms for SISO Channels

We have investigated the strategy and work procedures of adaptive OFDM algorithms in Chapter 3. Following those procedures, we obtain the global flow chart of the adaptive OFDM algorithm for SISO channels, shown in Figure 5.2-1.

First, the values of the channel parameters from the channel estimation are required. These channel parameters, i.e., the Rician K factor, SNR, delay spread, and Doppler spread, are the input and the basis of adaptive OFDM algorithms. The OFDM modulation parameters are adapted in accordance with the values of these channel parameters.

Once the channel information has been acquired, the algorithm will detect whether the OFDM modulation parameters have been configured. If not, the algorithm will set the values for these parameters. If they have been set, the algorithm will check whether the channel information has changed compared with the previous moment. If no change in the channel situation has occurred, the OFDM modulation parameters remain the same; if there has been a change, the algorithm will reset the values for the OFDM modulation parameters.

Afterwards, the algorithm will set the OFDM modulation parameters one by one. From the analysis in Chapter 3, we know that the guard time is used to combat ISI and ICI and is determined mainly by the delay spread. Therefore, we can set the guard time first in accordance with the delay spread. The optimal value for the guard time is used to make it equal to the maximum delay spread. In this case the interference is just cancelled and no extra energy is wasted. However, the guard time influences the symbol period, and therefore, it is not practical to set it equal to the maximum delay all the time. In our algorithm, hence, we

choose some values for the guard time and each of them is set for a certain range of the delay spread values. Details of the guard time setting are given in Figure 5.2-2.

After the guard time is set, the algorithm will configure the subband and subcarrier bandwidth in accordance with the current channel situation. This will be explained in detail in Section 5.3.

Finally, the “narrow-sense” modulation parameters (e.g., modulation levels, coding rate.) will be configured for each of the subbands.

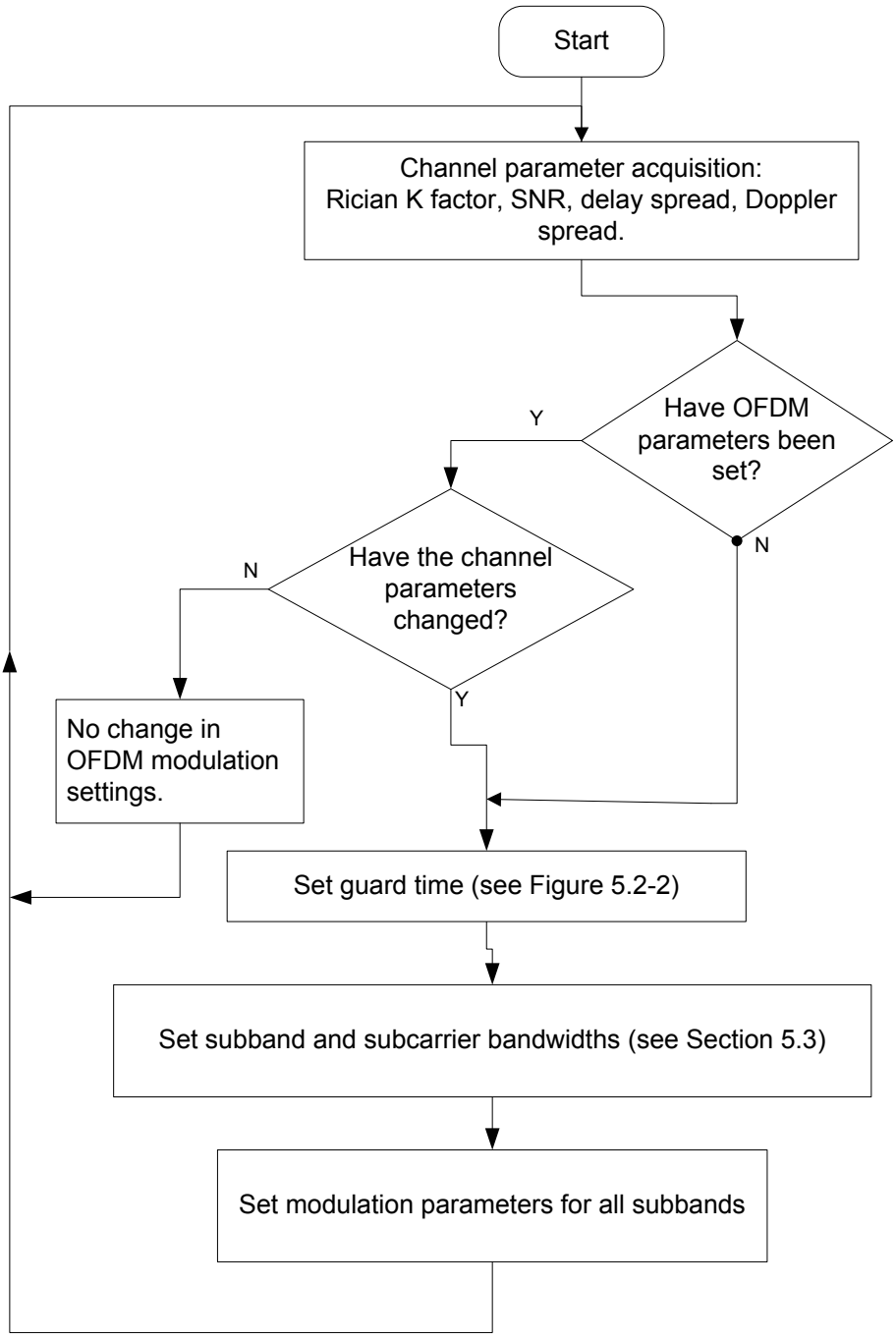


Figure 5.2-1. A global flow chart of adaptive OFDM algorithms for SISO channels

5.2.2 Guard Time Setting

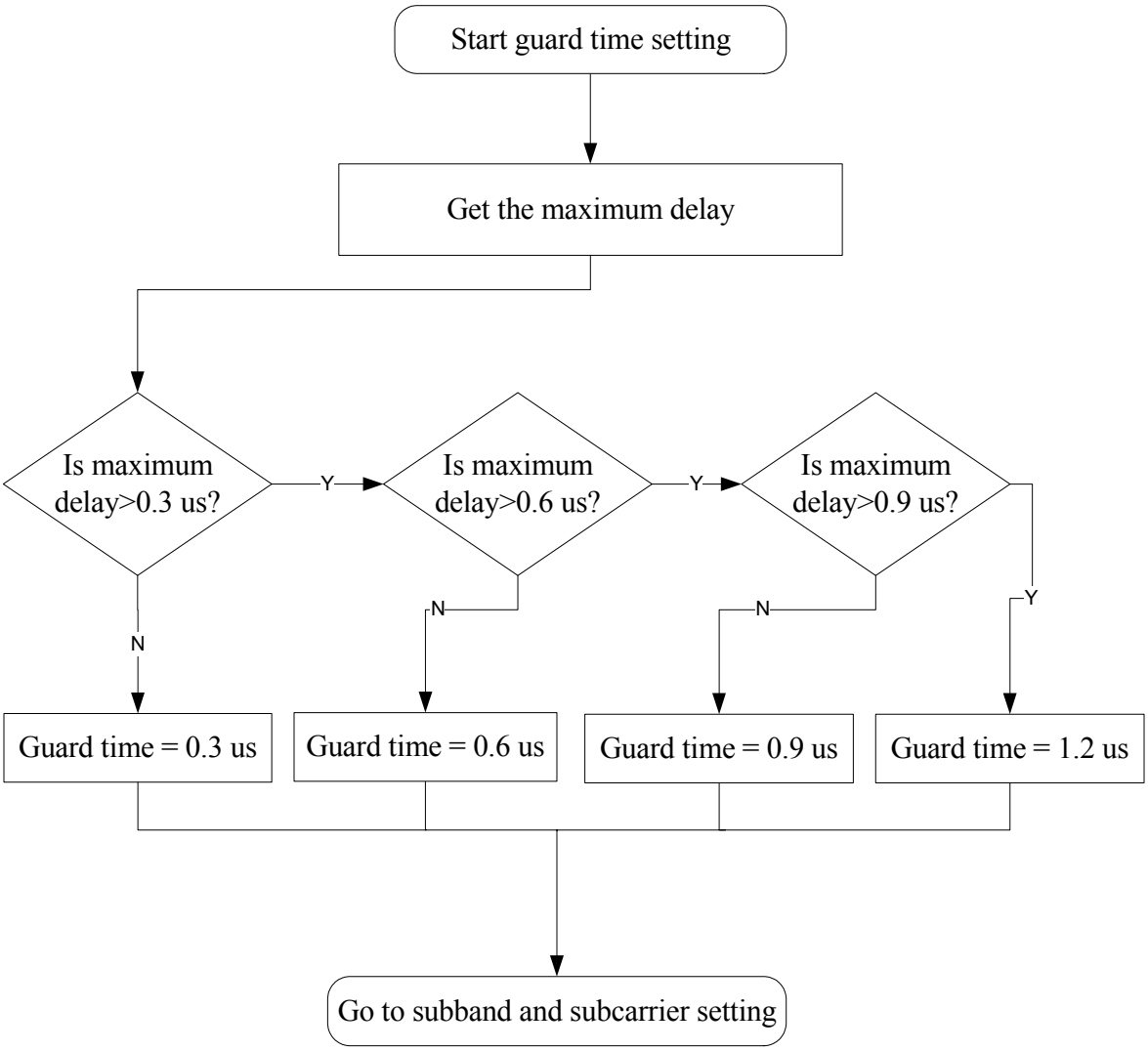


Figure 5.2-2. Guard time setting of adaptive OFDM algorithms

Figure 5.2-2 describes how the guard time is set in our adaptive OFDM algorithms. As said, the guard time of OFDM symbols is determined based on the delay spread; therefore, the algorithms first extract the value of the maximum delay spread from the detected channel parameters. The algorithms can set the guard time to one of these four values: {0.3 0.6 0.9 1.2}. The guard time is set to 0.3μs when the maximum delay of the channel is in the range of [0 0.3] μs, to 0.6μs for a maximum delay of (0.3 0.6) μs, to 0.9μs for a maximum delay of

(0.6 0.9) μs, and to 1.2μs for a maximum delay of (0.9 1.2) μs. This can be seen in Table 5.2-1.

Table 5.2-1. Guard time settings of adaptive OFDM algorithms based on the maximum delay of the channel

Maximum delay of channel [μs]	Guard time setting [μs]
[0 0.3]	0.3
(0.3 0.6]	0.6
(0.6 0.9]	0.9
(0.9 1.2]	1.2

5.2.3 Setting of the Subcarrier Bandwidth

In Chapter 3 we discussed how the subcarrier is set and in what way it influences the transmission quality. We indicated there that the subcarrier bandwidth should satisfy: $\frac{1}{50RDS} \leq \Delta f \leq \frac{1}{\mathrm{RDS}}$. In addition, a parameter related to the subcarrier bandwidth, P_{FR}, will influence transmission quality under certain conditions. What is more, the number of subcarriers has to be a power of two. Following the rules discussed in Chapter 3, we have obtained the parameter setting of adaptive OFDM algorithms, as shown in Table 5.2-2.

Table 5.2-2. Parameter setting of adaptive OFDM algorithms

B [MHz]	N_{sbc}	Subcarrier bandwidth Δf [kHz]	T_s [μs]	Guard time [μs]	$FSR = \frac{T_{FFT}}{T_S}$
20	32	625	1.9	0.3	0.842
	64	312.5	3.5	0.3	0.914
			3.8	0.6	0.842
	128	156.25	7	0.6	0.914
			7.6	0.9	0.876
			7.6	1.2	0.842
	256	78.125	14	1.2	0.914

From Table 5.2-2 we see that there is more than one subcarrier bandwidth value for one guard-time setting. Once guard time has been assigned, we exploit P_{FR} to choose a subcarrier bandwidth that satisfies the requirement of P_{FR} and gives better transmission quality. This has been discussed in Chapter 3.

In Chapter 2 we discussed that Doppler spread, B_D, is one of the parameters representing the channel model. A Doppler spread larger than the signal bandwidth/subcarrier bandwidth will lead to fast fading in the channel. Therefore, we should set the value of the subcarrier bandwidth much larger than the Doppler spread in order to obtain a slow fading channel. Equation (2.2) in Chapter 2 presents the function of the Doppler spread and shows that the Doppler spread is proportional to the carrier frequency and the relative speed between the mobile and base station. If we exploit a carrier frequency of 60GHz and a relative speed of 200km/h (55.56m/s), both of which are pretty high in real systems, we will have a maximum Doppler spread:

$$\max(B_D) = \frac{v \cdot f_c}{c} = \frac{55.56 \times 60 \times 10^9}{3 \times 10^8} = 11.1kHZ .$$

It is straightforward that all the subcarrier bandwidths in Table 5.2-2 are set much larger than this maximum Doppler spread. This proves that our algorithm design can avoid fast fading in the channel.

5.3 Subband Setting of Adaptive OFDM Algorithms

In this section we propose three subband settings. Because it is complicated to set a subband, we devote a separate section to this process. The subband setting can be employed in adaptive OFDM algorithms for both SISO (see Section 5.2) and MIMO (see Section 5.4) channels.

5.3.1 Analysis of Subband Settings

The definition of adaptive modulation indicates that it is mainly used to adapt parameters in time domain. However, it can also be used to adapt parameters in frequency domain. In adaptive OFDM systems, for example, different subcarriers can have different configurations at any moment. In practical OFDM systems, there are hundreds or thousands of subcarriers. Considering the implementation of adaptive OFDM systems, the whole bandwidth containing all subcarriers can be divided into several groups of subbands and each subband can be set to a certain configuration [2].

In [3], the whole bandwidth is divided into several subbands in advance. The channel situation for each subband is estimated, according to which configurations for each subband are set. The advantage of this is that it is easy to implement; the disadvantage is that when subcarrier situations in one subband are quite different, the transmission performance will degrade. For this reason, we propose several more flexible ways to set the subband. We propose to set the subbands in accordance with the fluctuation over the frequency band at the moment concerned.

The subcarrier bandwidth here means the subcarrier spacing. We propose two subband division categories: selective subband setting and consecutive subband setting.

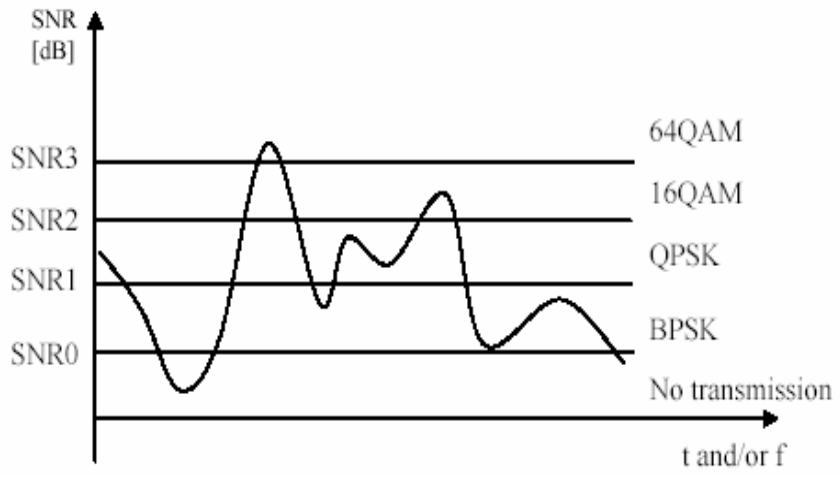


Figure 5.3-1. SNR ranges for different modulation settings for both time and frequency domain

We can divide the SNR values into several ranges (i.e., SNR0, SNR1, SNR2, and SNR3) and each range corresponds to a certain modulation level (i.e., BPSK, QPSK, 16QAM and 64QAM). In Figure 5.3-1, for example, at a certain moment and/or for a certain subband/subcarrier, if SNR is below SNR0, no transmission will be assigned; if SNR is in the range of SNR0 to SNR1, BPSK will be assigned; in the range of SNR1 to SNR2, QPSK will be assigned; in the range of SNR2 to SNR3, 16QAM will be assigned; and if SNR is above SNR3, 64QAM will be assigned.

In Chapter 3 we indicated that to guarantee a BER of 10^{-3}, we need an SNR for each modulation that is a function of Rician *K* factor (shown in Figure 3.6-4). In our simulations, therefore, we determine the SNR boundaries for all modulations (i.e., SNR0, SNR1, SNR2, and SNR3) based on the current value of the Rician *K* factor of the channel. It is easy to see that the SNR boundaries vary with the channel condition.

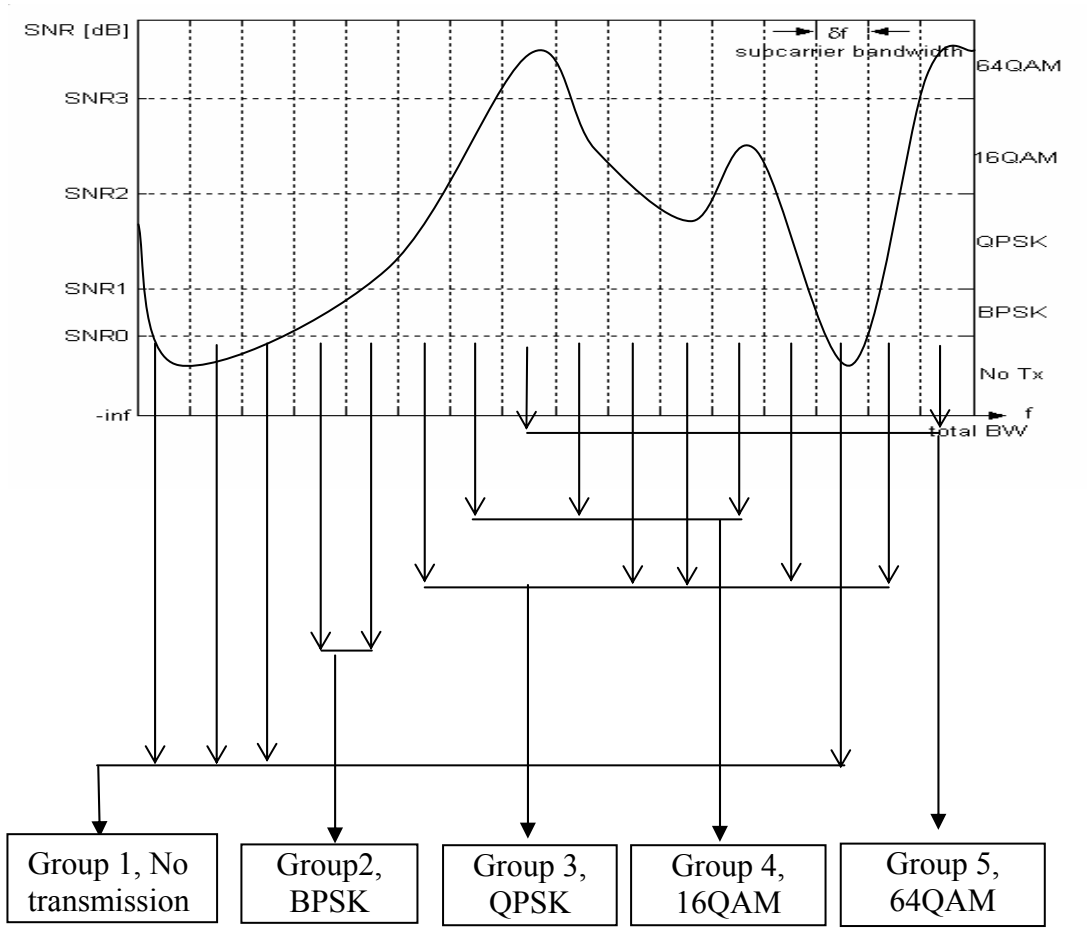


Figure 5.3-2. Selective subband setting.

At a certain moment t_i, different subcarriers may have different SNRs. The selective subband setting is used to select all subcarriers with SNR in the same range and assign them to one group/subband, even if these subcarriers are not consecutive. Figure 5.3-2 shows an example of SNR in frequency domain within the frequency band of interest. All subcarriers with an SNR in the same range for a certain modulation are assigned to one group/subband. Accordingly, we have only five groups, each with a different modulation. Therefore, a channel like the one in figure 5.3-2 can be divided as follows: Group 1 (No transmission), includes subcarriers 1, 2, 3, 14; Group 2 (BPSK), includes subcarriers 4, 5; Group 3 (QPSK), includes subcarriers 6, 10, 11, 13, 15; Group 4 (16QAM), includes subcarriers 7, 9, 12; and Group 5 (64QAM), includes subcarriers 8, 16.

The purpose of consecutive subband setting is to divide the whole frequency bandwidth into several subbands, each of which having consecutive subcarriers (as shown in Figure 5.3-3 and Figure 5.3-4). Based on the channel situation of the whole bandwidth, the bandwidth can be divided into several subbands, where the channel situation for each subband is exploited to configure the modulation parameters. In consecutive subband setting, an approximation has to be made to avoid too many subbands. That is to say, we have to allow the SNR of subcarriers within one subband to differ more and take the average SNR as the SNR of this subband for subband settings. Therefore, performance degradation can be expected if a channel varies fast in frequency domain.

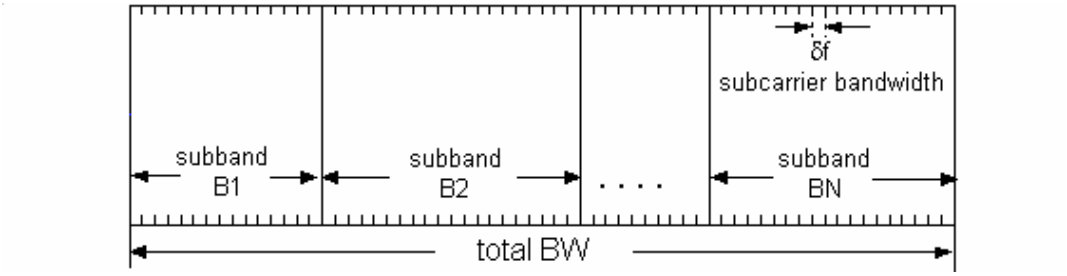


Figure 5.3-3. Divide all the subcarriers into N_{SB} groups of subbands

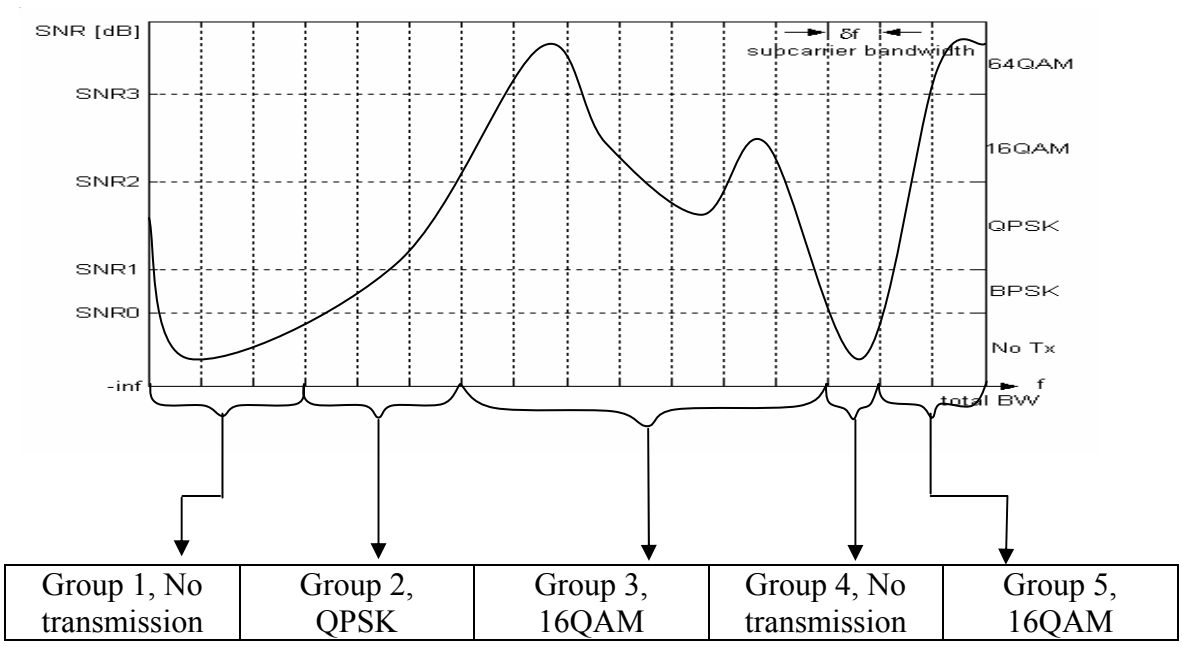


Figure 5.3-4. Consecutive subband setting

Selective subband setting is done more or less on a subcarrier by subcarrier basis, which means that the system has to set configurations for almost every subcarrier. Obviously this is not practical. A solution to this is to modulate the signals as usual, and re-order the subcarriers from different modulators by means of the adaptive algorithm before the parallel signals go to the IFFT, as shown in Figure 5.3-5. At the receiver, the subband and its relative modulation level settings can be obtained from pilot symbols or a pilot channel. The subcarrier order controller recovers the original order of the subcarriers before the parallel signals are converted to serial signals and fed into different demodulators. In this way, the system can set the subbands selectively in a simple way. Consecutive subband setting is done on a group-by-group basis, which means that the system only has to set configurations for several groups. Therefore, at system level, it is easier to implement consecutive subband setting than selective subband setting.

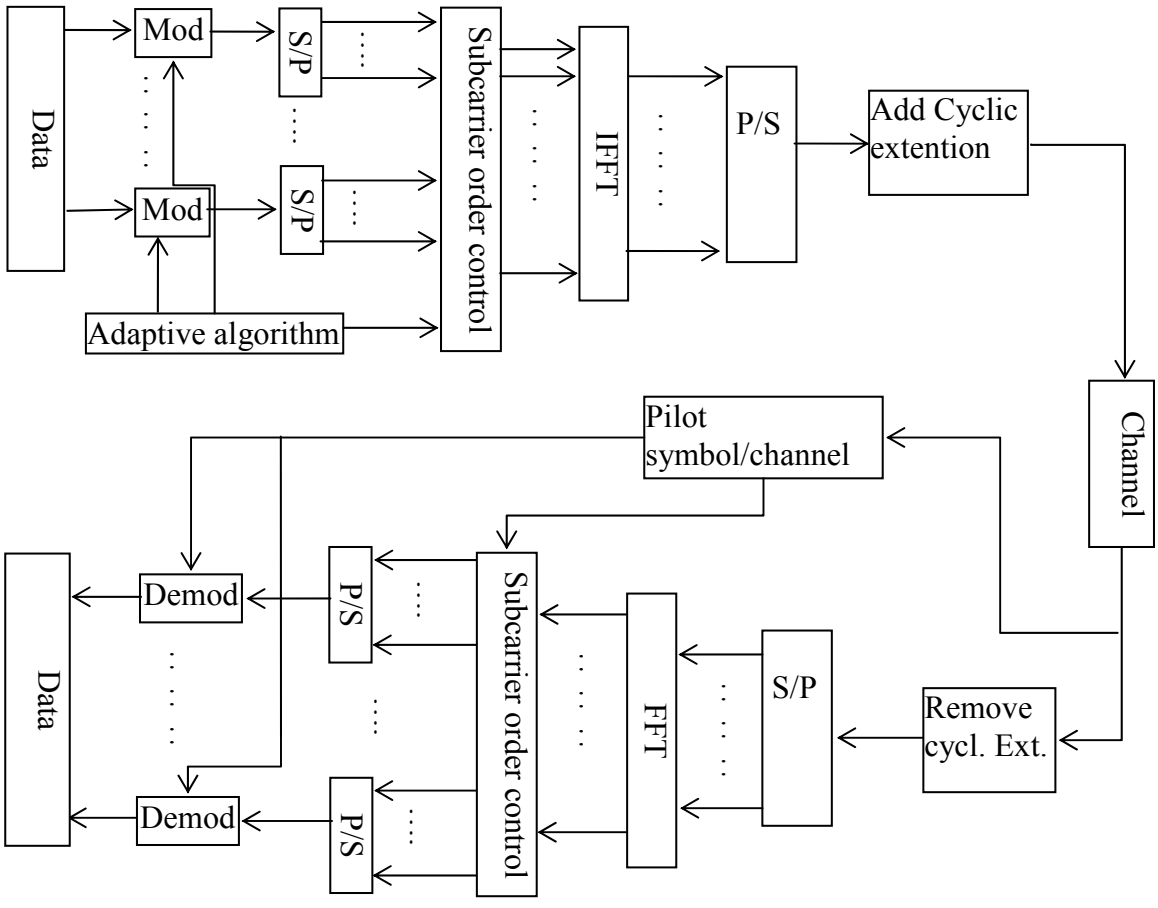


Figure 5.3-5. Structure of Adaptive OFDM systems

5.3.2 Proposals for Consecutive Subband Setting

This section discusses two proposals for consecutive subband setting [4].

1. Constant subcarrier and varying subband

   The subband bandwidths can be different and vary, but all subcarrier bandwidths are the same and constant. We write the total bandwidth B as

   $$B = N_S \cdot \Delta f \ , \tag{5.1}$$

   where N_S stands for the total number of subcarriers and Δf denotes the subcarrier bandwidth. The total number of subcarriers N_S can be represented as the sum of the number of subcarriers N_{sbg} in all subbands, which is written as

   $$N_S = \sum_{g=1}^{N_{SB}} N_{sbg} \ . \tag{5.2}$$

   N_{SB} stands for the number of subbands; N_{sbg} denotes the number of subcarriers in the gth subband; g goes from 1 to N_{SB}. If all subbands have the same number of subcarriers, the above formula becomes

   $$\begin{aligned} &N_S = N_{SB} \cdot N_{sbg} \qquad (g = 1,2,....N_{SB}) \\ &N_{sb1} = N_{sb2} = ... = N_{sbN_{SB}} \end{aligned} \ . \tag{5.3}$$

   In this proposal, B, N_S, and Δf are constant; N_{SB} and N_{sbg} vary as in Table 5.3-1. Thus, subband setting is done by making a flexible combination for certain constant subcarriers.

Table 5.3-1. Parameters for setting constant subcarrier and varying subband

Constant parameters	Adaptive parameters
B	N_{SB}
N_S	N_{sbg}
$\Delta f_g = \Delta f$; (g =1,2,…, N_{SB})	
B: total bandwidth; N_S: number of total subcarriers in the entire bandwidth; Δf: subcarrier bandwidth; Δf_g: subcarrier bandwidth of the gth subband; N_{SB}: number of subbands; N_{sbg}: number of subcarriers in the gth subband.	

This approach also avoids the problem of having to use wavelet or other techniques than FFT in OFDM systems to get different subcarrier bandwidths. That is to say, in this way FFT can still be used in adaptive OFDM systems.

The flow chart of this approach showing how to set the constant subcarrier and varying subband , is given in Figure 5.3-6. First, the algorithm gets the SNR for all the subcarriers. From the analysis in Chapter 3 (Section 3.6) we know that to get a certain BER performance, different SNR is required if there are different Rician K values. Hence, based on the Rician K factor of the current channel situation, the algorithm determines the boundary SNR for different modulation levels: SNR0, SNR1, SNR2, and SNR3. The SNR is then divided into several ranges, each of which relates to a different modulation level, as shown in Figure 5.3-1. I0 (SNR < SNR0) represents no transmission; IB (SNR0 ≤ SNR < SNR1) represents BPSK modulation; IQ (SNR1 ≤ SNR < SNR2) QPSK modulation; I16 (SNR2 ≤ SNR < SNR3) 16QAM modulation; and I64 (SNR3 ≤ SNR), 64QAM modulation. Then the subcarriers are grouped. From the first subcarrier, all adjacent subcarriers with an SNR in the same range have to be assigned to the same group. Quite often, this will result in too many groups. Probably there are groups with only one or two subcarriers due to abrupt fading of the channel at some frequency points. Since we do not want to have too many subbands, we have to combine this kind of group with an adjacent one whose mean SNR and SNR range is close to theirs. The algorithm will repeat this procedure until an appropriate number of subbands has been obtained. We found in Chapter 2 that the larger the delay spread, the more the amplitude of the channel transfer function fluctuates in frequency domain. A large amplitude fluctuation will have as a result that the last step in the algorithm is activated several times to obtain a number of subbands within the maximum value.

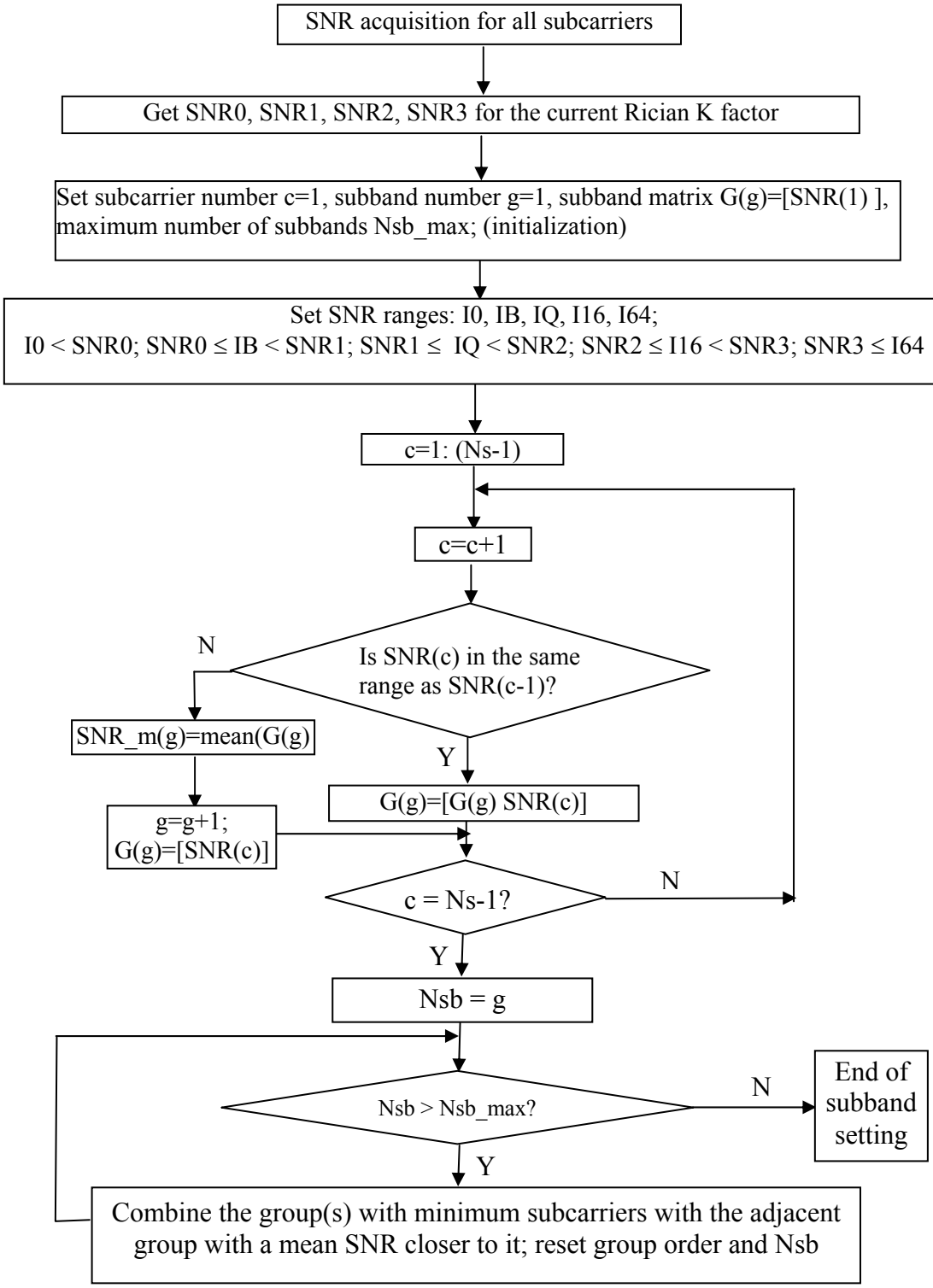


Figure 5.3-6. Flow chart for setting the constant subcarrier and varying subband

2. Varying subcarriers-subbands

In this approach for subband setting, the subcarrier bandwidth can be changed, but all subcarriers in all subbands have the same bandwidth and all are orthogonal. To use FFT, we have to keep the number of subcarriers at 2^n. If 15 subcarriers are got by calculation in an adaptive algorithm, for example, 8 or 16 subcarriers will be set in the system. This approach is more complicated than that for constant subcarrier and varying subband .

Table 5.3-2. Parameters for setting the varying subcarrier-subbandapproach

Constant parameters	Adaptive parameters
B	N_{SB}
	N_{sbg}
	N_S
	$\Delta f_g = \Delta f;\ (g=1,2,\ldots N_{SB})$
B: total bandwidth; N_S: number of total subcarriers in the entire bandwidth; Δf: subcarrier bandwidth; Δf_g: subcarrier bandwidth of the gth subband; N_{SB}: number of subbands; N_{sbg}: number of subcarriers in the gth subband.	

The flow chart for setting varying subcarrier-subband only differs from that for constant ones in that it adds "set subcarrier bandwidth based on delay spread, Doppler spread and Rician K factor" just at the beginning of Figure 5.3-6, see Figure 5.3-7. First, the algorithm requires channel parameters, Rician K factor, Doppler spread and delay spread. As discussed in Chapter 2, when the Rician K is smaller than 10dB, a smaller subcarrier bandwidth should be set in case of larger delay spread; the subcarrier bandwidth should be much larger than the Doppler spread in order to avoid a fast fading channel. In addition, in Chapter 3 we showed that the product of the subcarrier bandwidth and rms delay spread, i.e., P_{FR}, should be in the range of [0.02 1]; the smaller P_{FR}, the better transmission QoS for small K value. Exploiting these results and considering that the number of subcarriers should be a power of 2, we can design the subcarrier bandwidth.

Given the subcarrier bandwidth, we can then calculate the number of subcarriers. Taking the channel SNR in frequency domain from channel estimation, we obtain the SNRs of all subcarriers. Afterwards, assign subbands in the same way as for setting constant subcarrier and varying subband.

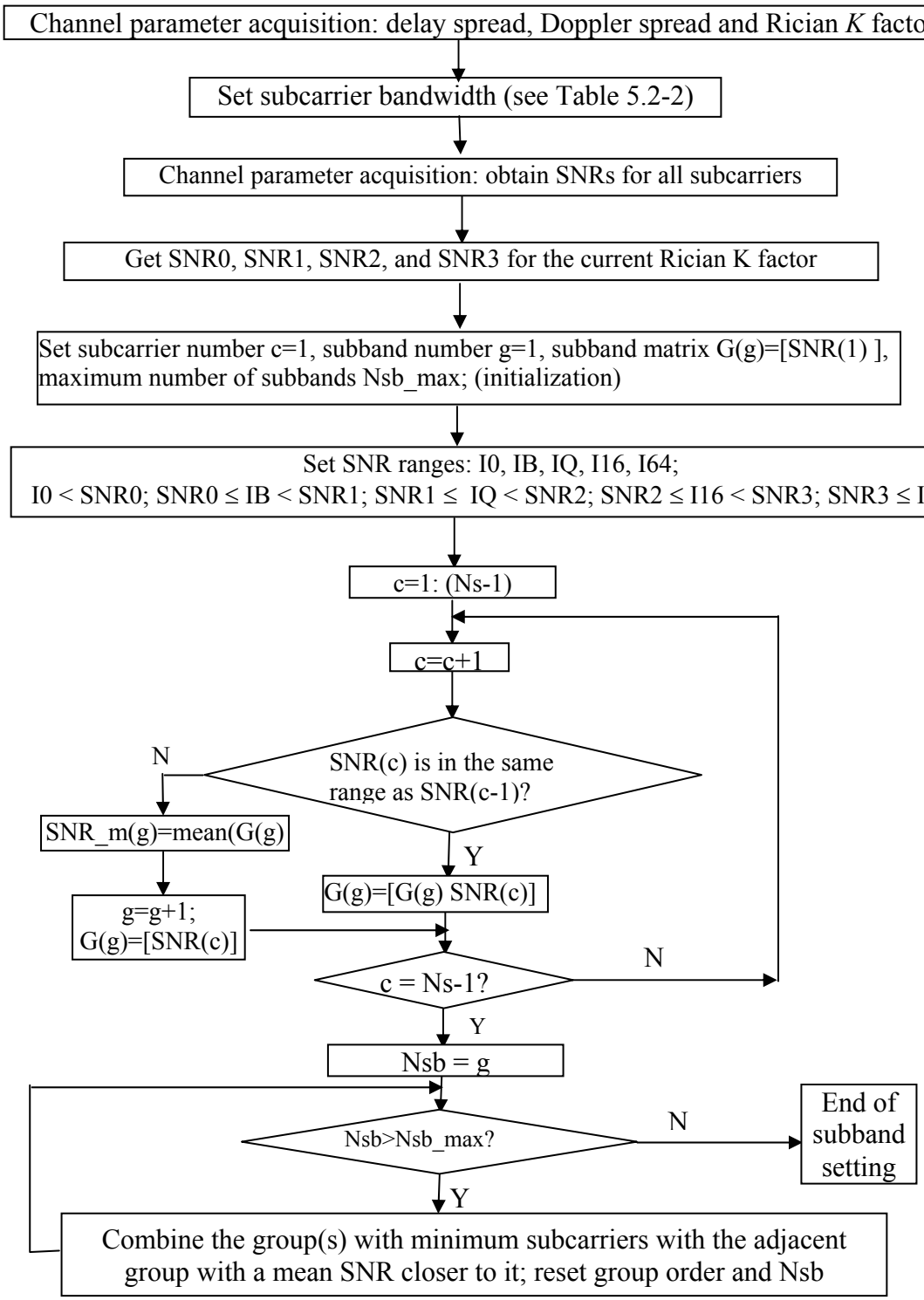


Figure 5.3-7. Flow chart for setting the varying subcarrier-subband

5.4 Adaptive OFDM Algorithms for MIMO Channels

5.4.1 Global Flow Chart of Adaptive OFDM Algorithms for MIMO Channels

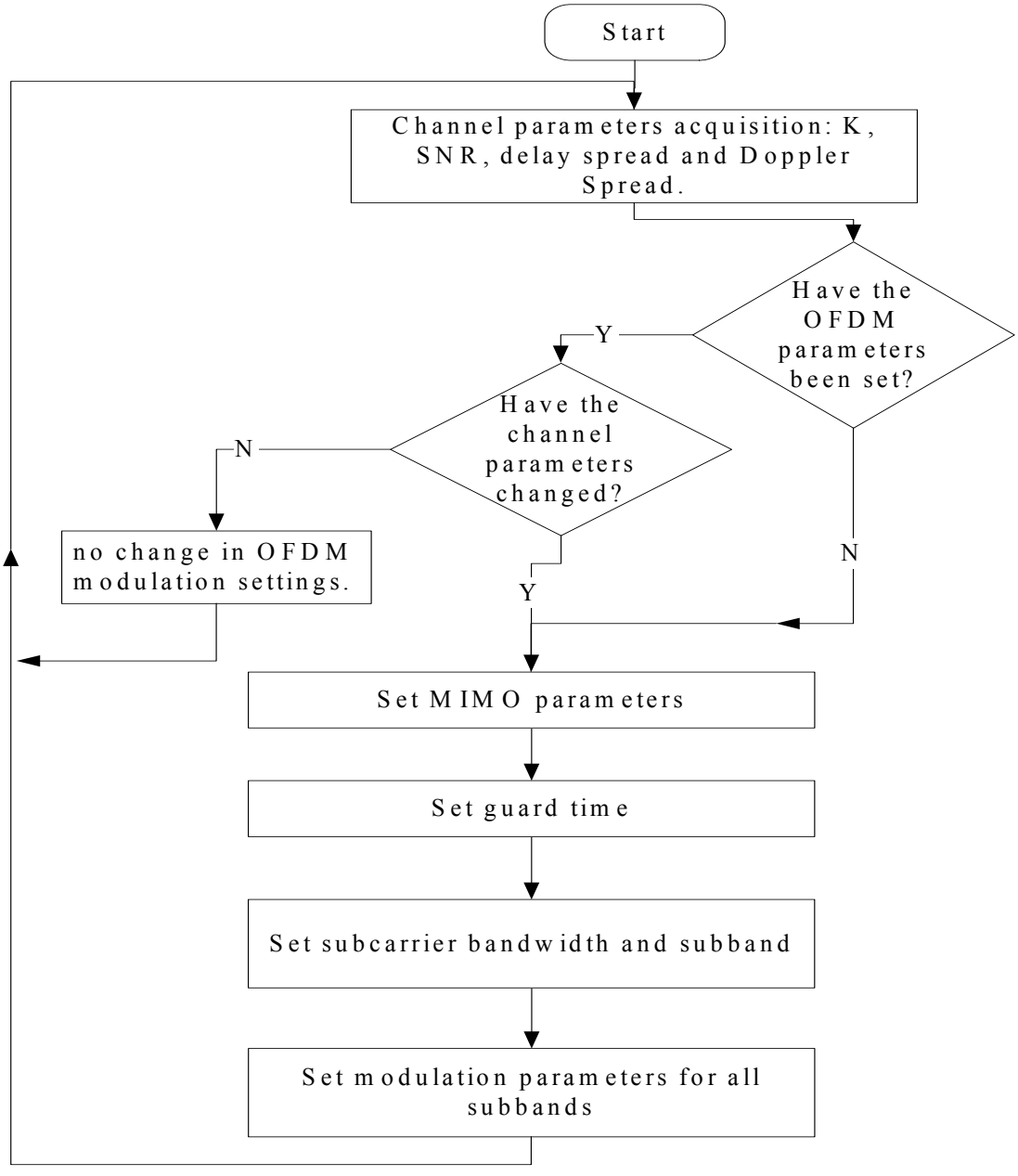


Figure 5.4-1. A global flow chart of an adaptive OFDM algorithm for MIMO channels

Figure 5.4-1 shows the global flow chart of our adaptive OFDM algorithm for MIMO channels. Compared with that for SISO channels in Figure 5.2-1, the flow chart in Figure 5.4-1 has one more procedure: set MIMO parameters. Hence, after detecting the channel parameters, our algorithm for MIMO channels first sets the MIMO parameters. Selective subband setting is employed in our algorithm. The other procedures are the same as our algorithm for SISO channels (as described in Section 5.2.1), so we do not repeat them here.

5.4.2 Setting MIMO Parameters

We employ three MIMO technologies in our adaptive OFDM algorithm for MIMO channels, i.e., MIMO-Alamouti, MIMO-tx-sel-rx-MRC, and MIMO-OSIC-MMSE, all of which were described in Chapter 4. Our algorithm each time chooses one of these technologies based on the current channel parameters K and SNR. The details are given in Figure 5.4-2.

First, the channel parameters, Rician K factor and SNR in the whole bandwidth are detected. If the Rician K factor is not zero, there is a LOS, and it is not necessary to use many transmit antennas, hence, the MIMO-tx-sel-rx-MRC scheme is employed. If the Rician K factor is zero, i.e., if the channel becomes a Rayleigh channel, MIMO-Alamouti or MIMO-OSIC-MMSE is employed for optimum throughput. From Chapter 4, we know that the MIMO-OSIC-MMSE scheme (a SM scheme) outperforms the MIMO-Alamouti scheme in terms of throughput in a channel with high SNR. For SNR around 16 dB the MIMO-Alamouti scheme has a spectral efficiency of 4bps/Hz and that of the MIMO-OSIC-MMSE scheme around 6bps/Hz. If we sample the SNR in the whole frequency bandwidth, if 67% (4/6 *100%) of the received SNR in the whole bandwidth is higher than 16dB, MIMO-OSIC-MMSE can achieve higher throughput than MIMO-Alamouti for the same target BER. Employing this knowledge, our algorithm sets the MIMO scheme for a Rayleigh fading channel.

After assigning a MIMO scheme for the system, our algorithm determines the SNR boundaries of different modulation levels for the selected scheme.

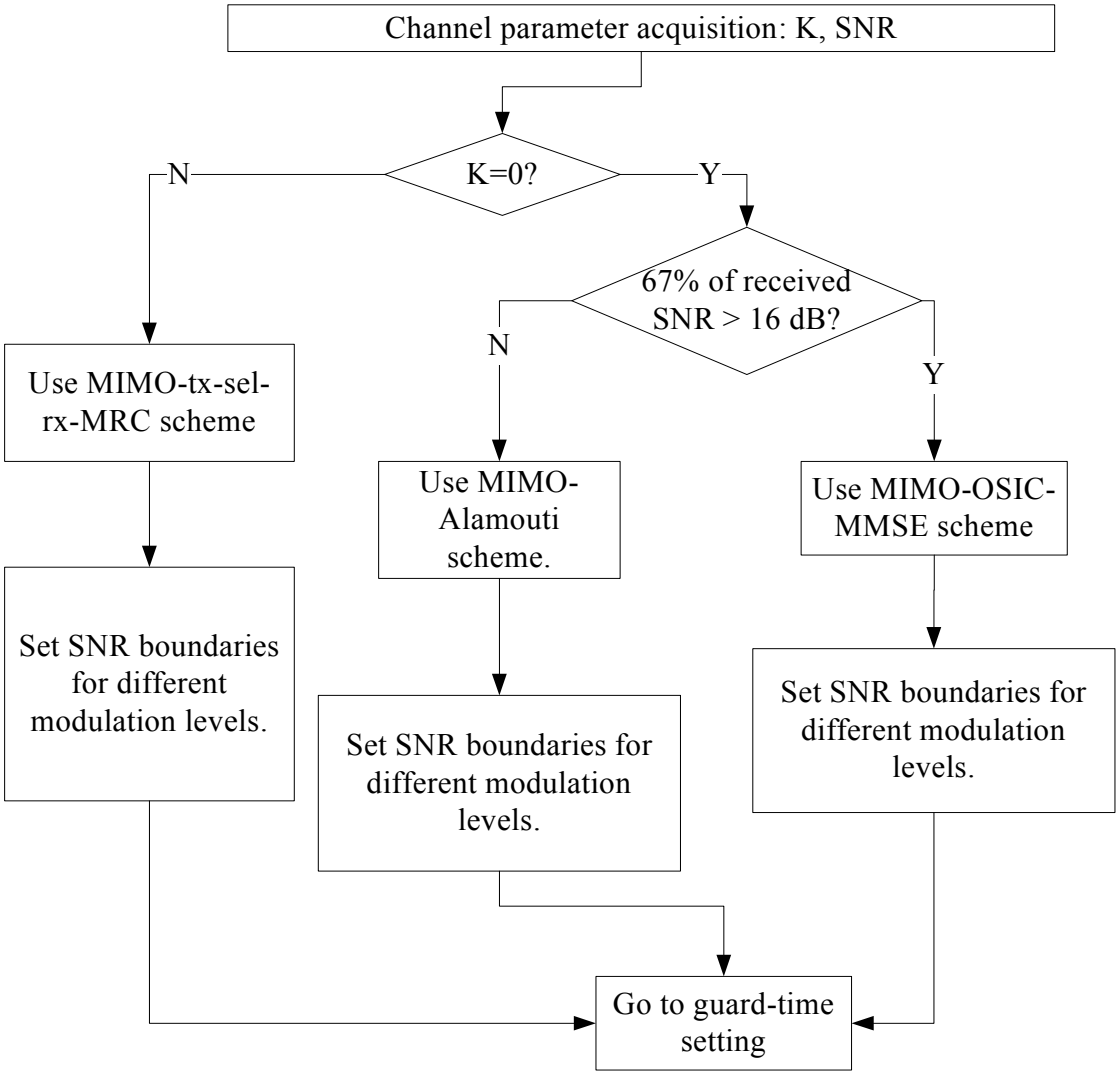


Figure 5.4-2. The flow chart of MIMO-parameter settings

5.5 Adaptive CDMA Algorithms for MIMO Channels

In this section we propose an adaptive CDMA algorithm for MIMO channels. This algorithm combines CDMA modulation adaptation with MIMO parameter adaptation (i.e., it uses different MIMO schemes).

Figure 5.5-1 shows a global flow chart of our adaptive CDMA algorithm for MIMO channels. First, our algorithm requires the values of the current channel and system parameters: the

Rician K factor, SINR, Nu. The Rician K factor is used to set the MIMO parameters. After acquisition of the required parameters, our algorithm asks whether or not the CDMA modulation parameters have been set. If so, our algorithm will compare the current channel parameters with the ones of the previous moment. The algorithm only changes the settings if the channel situation changes. If not, parameter setting begins.

The MIMO parameters are set first. We use the MIMO-tx-sel-rx-MRC scheme for a LOS situation, and the MIMO-Alamouti and MIMO-OSIC-MMSE schemes for a non-LOS channel, as indicated in Section 5.4.2. If the current average SINR is larger than 16dB, MIMO-OSIC-MMSE will be exploited, otherwise MIMO-Alamouti.

Next, CDMA modulation parameters (modulation level M and processing gain Gp) will be assigned. In order to explain our approach, we introduce a SINR-boundary matrix, i.e., SINR_BD, for a BER of 10^{-3}.

$$SINR_BD = D = \begin{matrix} \begin{matrix} BPSK & QPSK & 16QAM & 64QAM \end{matrix} & Gp \\ \begin{bmatrix} (1,1) & \ldots & \ldots & (1,4) \\ . & . & \swarrow & . \\ . & \swarrow & SE\downarrow & . \\ (4,1) & . & . & (4,4) \end{bmatrix} & \begin{matrix} -32 \\ -64 \\ -128 \\ -256 \end{matrix} \end{matrix}. \tag{5.4}$$

This matrix gives the SINR boundaries for BPSK, QPSK, 16QAM, and 64QAM modulations with a processing gain of 32, 64, 128, and 256, in order to obtain a BER of at least 10^{-3}. The first row of this matrix is intended for a processing gain of 32, the second row for Gp=64, the third row for Gp=128, and the fourth row for Gp=256. The first column of this matrix is intended for BPSK modulation, the second for QPSK, the third for 16QAM, and the fourth for 64QAM. SINR_BD(2,3), for example, gives the value of minimum SINR, which is required for 16QAM modulation with a processing gain of 64 in order to get a BER of 10^{-3}. "SE↓" in the matrix means that the spectrum efficiency SE decreases. The diagonal arrow gives the direction that can decrease SE. This is because SE decreases with lower modulation level and higher processing gain, as shown in Chapter 3.

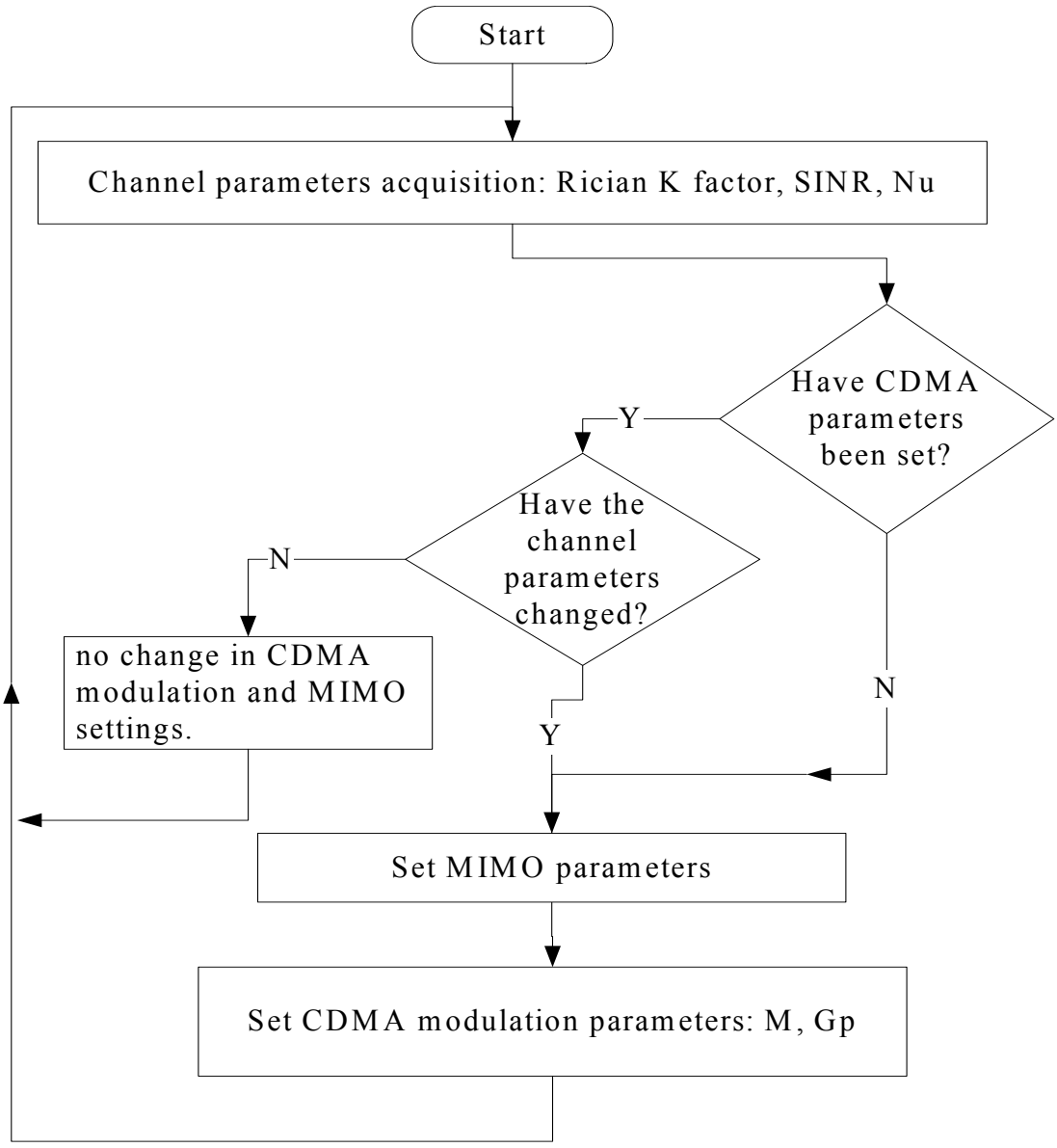


Figure 5.5-1. Global flow chart of our adaptive CDMA algorithm for MIMO channels

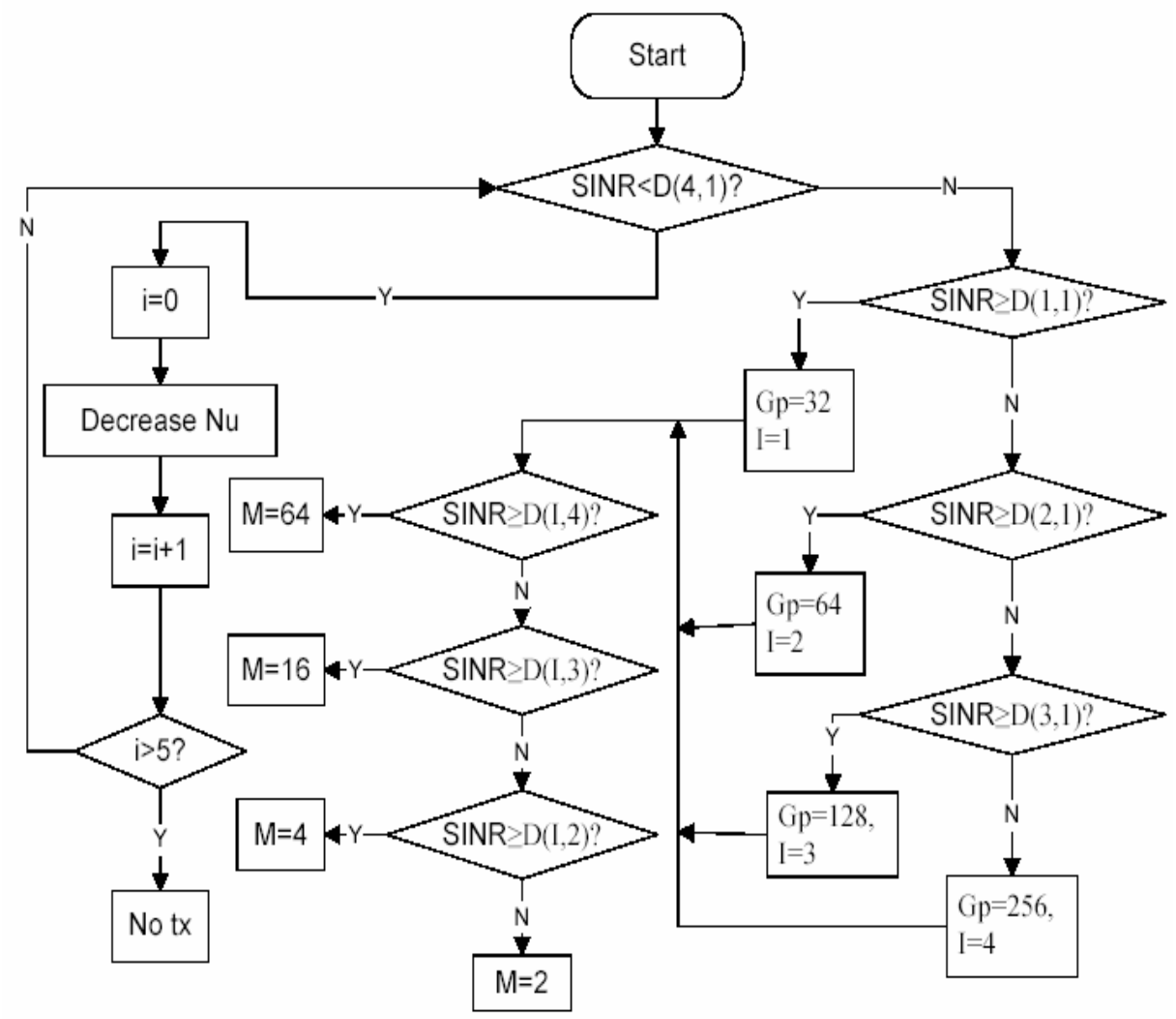


Figure 5.5-2. Settings of modulation level *M* and processing gain *Gp* for downlink

Our adaptive CDMA algorithm for MIMO channels has been designed to get as much throughput as possible while guaranteeing a BER of 10^{-3}. If we translate this into SINR_BD matrix, it means that the closer the SNR is to the top right-hand corner of the matrix, the higher the throughput (SE). Our algorithm sets the modulation level and processing gain based on this rule.

Figure 5.5-2 presents the flow chart of setting modulation levels and processing gains. Our algorithm compares the current channel SINR with D(4,1) first. If it is smaller than D(4,1), it means that the target BER cannot be guaranteed, even if the largest *Gp* and lowest modulation level are assigned. In Chapter 3 we indicated that CDMA systems can also influence the channel situation by changing the number of users, *Nu*. In this case, therefore, the algorithm

decreases the number of users to increase the SINR. This process will be repeated at most five times to make the channel SINR larger than D(4,1). If the channel SINR is still too small for transmission after the number of users has been adjusted for five times, a "no transmission" (no-tx) command will be given by the algorithm.

If the current channel SINR is larger than D(4,1), our algorithm will assign values for the modulation level and processing gain. The current channel SINR will be compared with D(1,1). If the current channel SINR is larger than or equal to D(1,1), *Gp* will be set to 32 and the algorithm will begin to set the modulation level. Otherwise the current SINR will be compared with D(2,1). If it is larger than or equal to D(2,1), *Gp* will be set to 64 and the algorithm will begin to set the modulation level. Otherwise, the current channel SINR will be compared with D(3,1). If it is larger than or equal to D(3,1), *Gp* will be set to 128 and the algorithm begins to set the modulation level. Otherwise, *Gp* will be set to 256 and the algorithm will begin to set the modulation level.

Once the processing gain is set, the row in the matrix of formula (5.4) has been determined. The algorithm will then begin to set the modulation level M, i.e., it will determine the column of formula (5.4). The algorithm compares the current channel SINR with the 4^{th} element in the relevant row. If it is larger than or equal to the 4^{th} element, 64QAM will be assigned. Otherwise, the current SINR will be compared with the 3^{rd} element in the relevant row. If it is larger than or equal to the 3^{rd} element, 16QAM will be assigned. Otherwise, the current SINR will be compared with the 2^{nd} element in the relevant row. If it is larger than or equal to the 2^{nd} element, QPSK will be assigned. Otherwise, BPSK will be assigned for the current transmission.

So far, the modulation level and processing gain have been set. It is obvious that it is difficult for the mobile user to change the number of users in a cell, so this algorithm is actually intended for downlink transmission. However, if we delete the part of adjusting the number of users, our algorithm can be exploited for uplink transmission as well.

5.6 Simulators and Assumptions of the Algorithms

5.6.1 Simulators of Algorithms for SISO/MIMO Channels

In Sections 5.3 and 5.4 we proposed adaptive OFDM algorithms for SISO and MIMO channels. The algorithm for MIMO channels combines OFDM modulation adaptation with MIMO parameter adaptation (i.e., it uses different MIMO schemes). In order to evaluate the algorithms by simulations, we need to build a simulator.

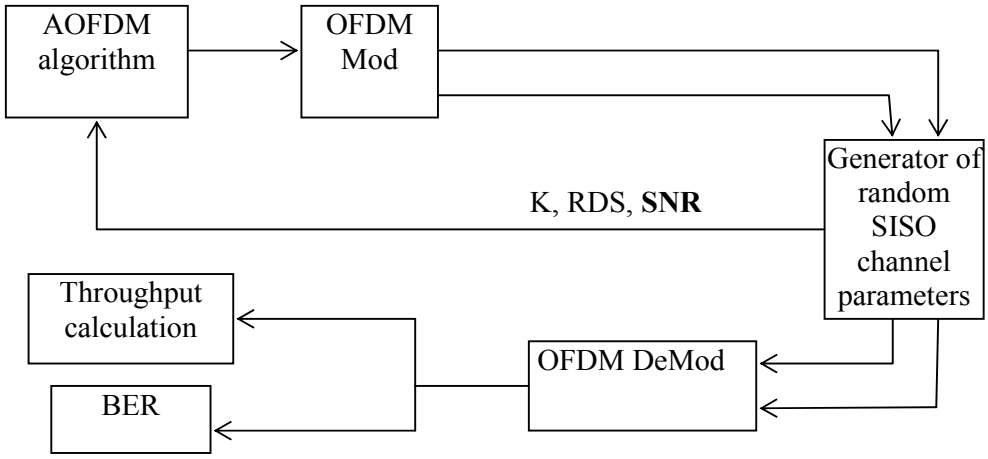


Figure 5.6-1. Simulator of Adaptive OFDM algorithms

Figure 5.6-1 is the simulator we exploit to evaluate our algorithms. First, random channel parameters are generated, i.e., channel SNR matrix, Rician *K* factor, and RDS. The SNR matrix contains many SNR values for different frequency points in frequency domain since the channel is a frequency-selective fading channel. Every moment, i.e., for every transmission, we generate a random Rician *K* value, RDS value, and a random SNR matrix in frequency domain. For each transmission, we also generate channels with frequency-selective fading that are time varying, with an SNR distribution as that in Figures 2.1-2 and 2.1-3. Based on the channel parameters, the adaptive OFDM algorithms (as described in Sections 5.2 and 5.3) assign all OFDM modulation parameters. At the receiver, the signals come to the OFDM demodulator through the channel, and the BER and throughput for each transmission are calculated.

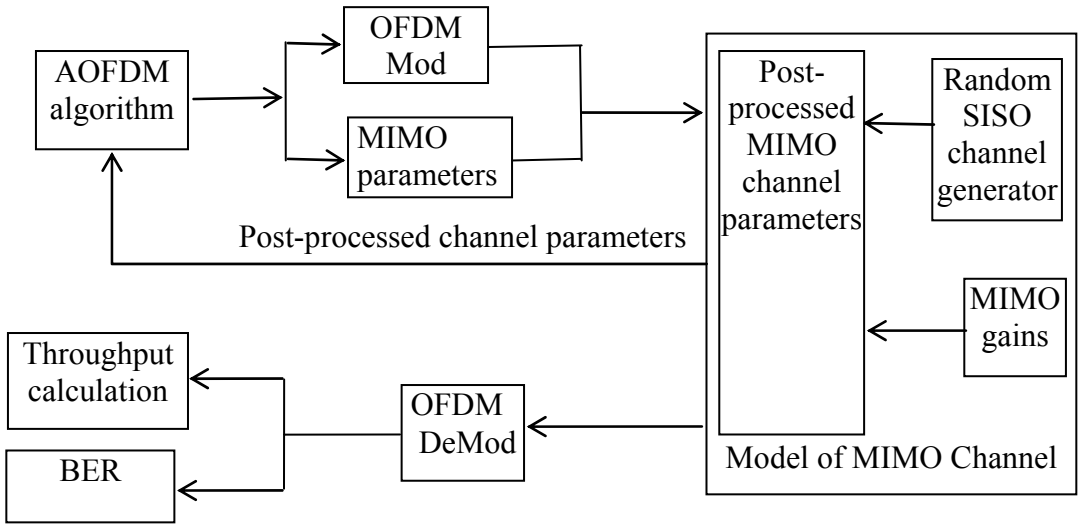


Figure 5.6-2. Simulator of an Adaptive OFDM algorithm for MIMO channels

Figure 5.6-2 shows the simulator that we exploited for our adaptive OFDM algorithm for MIMO channels. In addition to OFDM modulation parameters, the adaptive OFDM algorithm assigns MIMO parameters. First, we generate random SISO channel parameters. For every transmission, we generate a value for Rician K, a value for RDS, and SNR matrix. Exploiting the MIMO gains that we worked out in Chapter 4, we obtain the post-processed channel parameters for MIMO channels. Our adaptive OFDM algorithm assigns all OFDM modulation and MIMO parameters based on the current post-processed parameters of the MIMO channel. At the receiver, the signal is demodulated and the throughput and BER are calculated.

If we replace the block of "Model of MIMO channel" with only the box of "Random SISO channel generator", we obtain the simulator of our adaptive OFDM algorithm for SISO channels.

The simulator we exploited for our adaptive CDMA algorithm for MIMO channels is that shown in Figure 5.6-2, but with CDMA instead of OFDM. Therefore, it is not reproduced here.

5.6.2 Assumptions Used in the Simulations

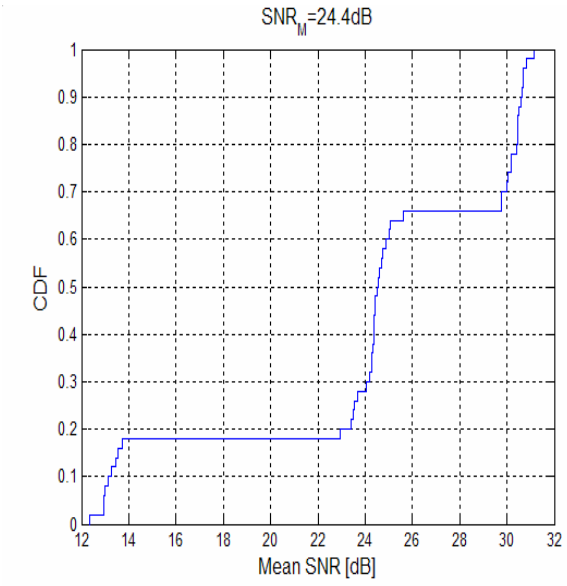
In our simulations for all adaptive modulation algorithms we use the following assumptions:

- The channel has frequency-selective fading, is time varying and follows Rician fading;

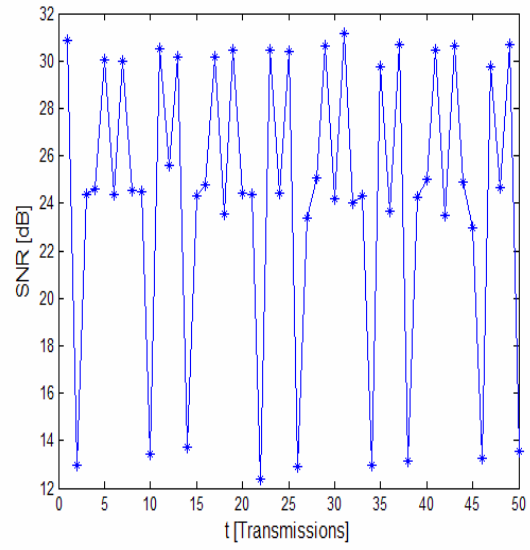
- The total available bandwidth for transmission is constant; we use 20MHz in our simulations;
- Perfect channel estimation is assumed, and the algorithm obtains the channel situation without any delay;
- The time duration between two consecutive transmissions is assumed to be enough for algorithms to finish assigning parameters. In other words, our algorithms can always obtain the current channel situation in time and assign parameters successfully;
- Signals at the transmit antennas are completely uncorrelated, as well as at the receive antennas;
- MIMO SNR gain and Rician *K* gain are constant in the frequency domain.

5.7 Simulation Results of Adaptive OFDM Algorithms for SISO Channels

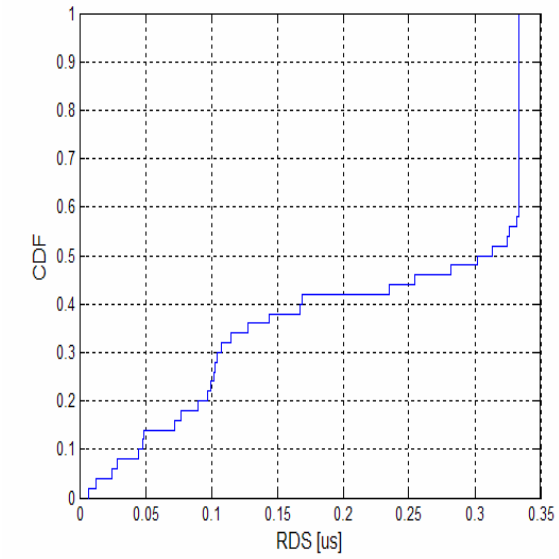
We investigated the adaptive OFDM algorithm for SISO channels in the last sections. This section will evaluate those by using simulations [4]. The algorithms have been designed to guarantee a certain transmission QoS (here we set it as BER of 10^{-3}) and to get as much throughput as possible.



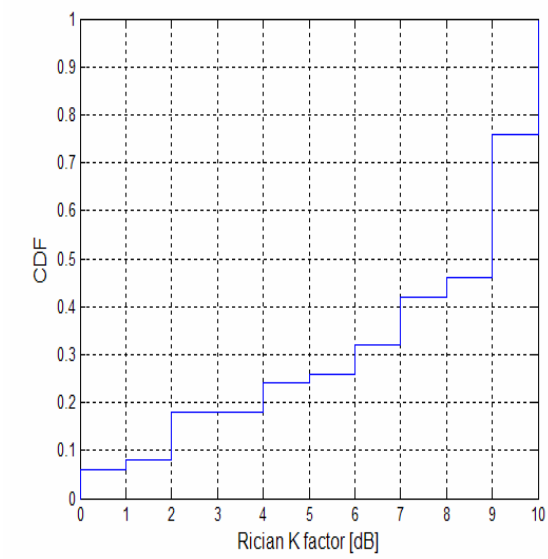
(a) CDF of mean SNR



(b) Mean SNRs in the time domain



(c) CDF of RDS



(d) CDF of Rician *K* factor

Figure 5.7-1. Channel parameters in the simulations (an example)

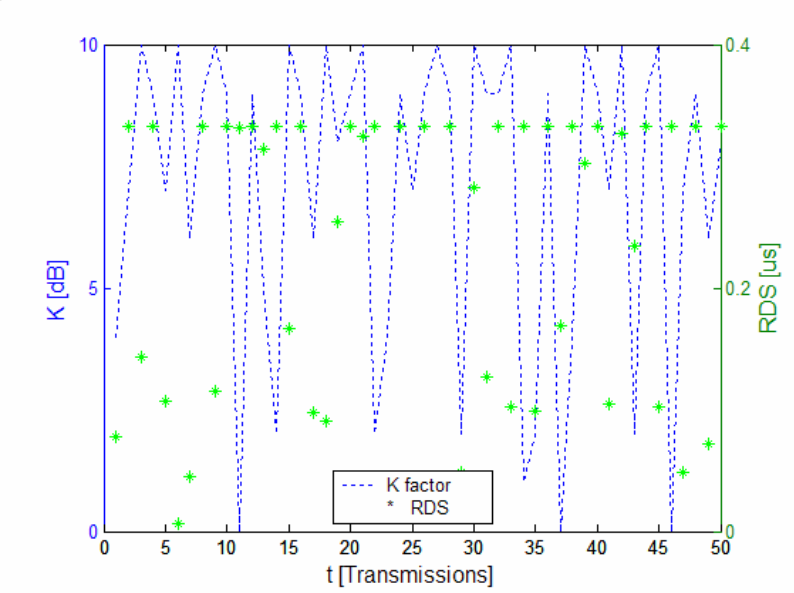
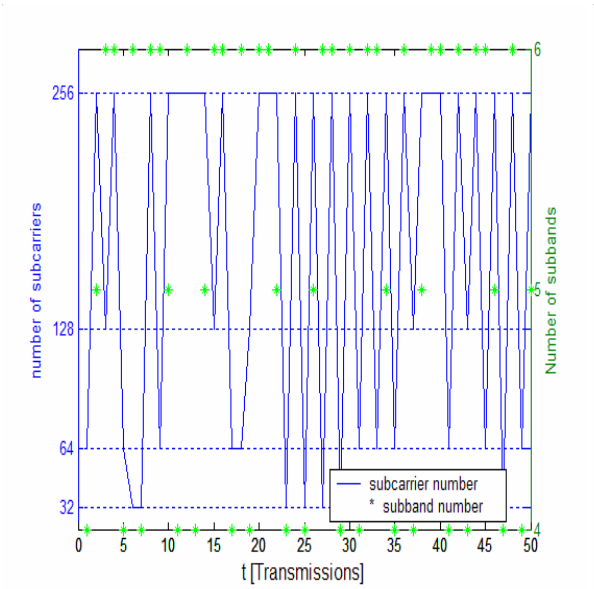
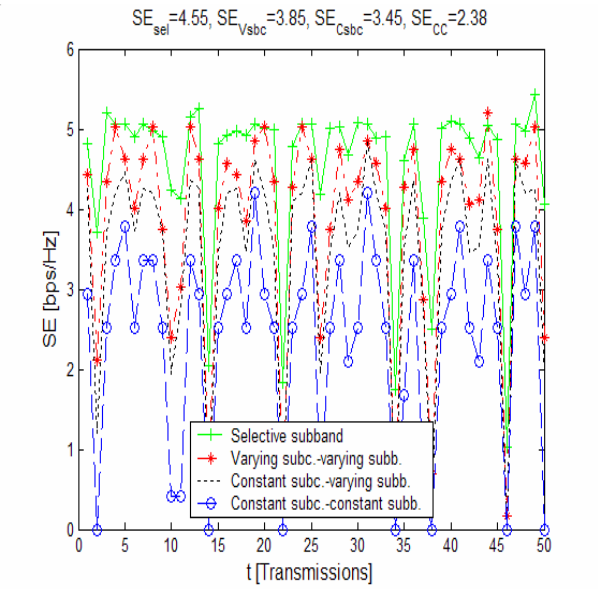


Figure 5.7-2. Rician *K* factor and RDS in the time domain

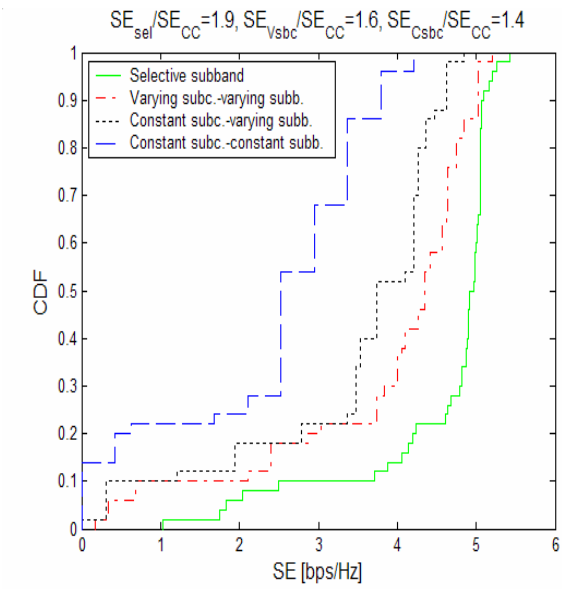
Figure 5.7-1 and 5.7-2 present pseudo-random channel parameters exploited in our simulations. Figure 5.7-1 (a) shows the CDF of the mean SNR over the simulated period. We simulated 50 transmissions, so the CDF consists of 50 samples. From the figure we can see that the mean SNR over the whole frequency band of each transmission ranges from around 12dB to 32dB, and the mean SNR over that bandwidth for the simulated period is 24.4dB. Figure 5.7-1 (b) shows the mean SNR over the whole frequency band for each transmission. We see that the average SNRs are mainly around 13dB, 24dB, and 30dB. This explains why there are some flat parts in Figure (a). Figure 5.7-1 (c) and (d) show the values of RDS and Rician *K* factor exploited in our simulation. From the figures we notice that the maximum RDS is around 0.33 μs, and the Rician *K* factor ranges from 0dB to 10dB. Figure 5.7-2 presents the Rician *K* factor and RDS in time domain for successive transmissions.



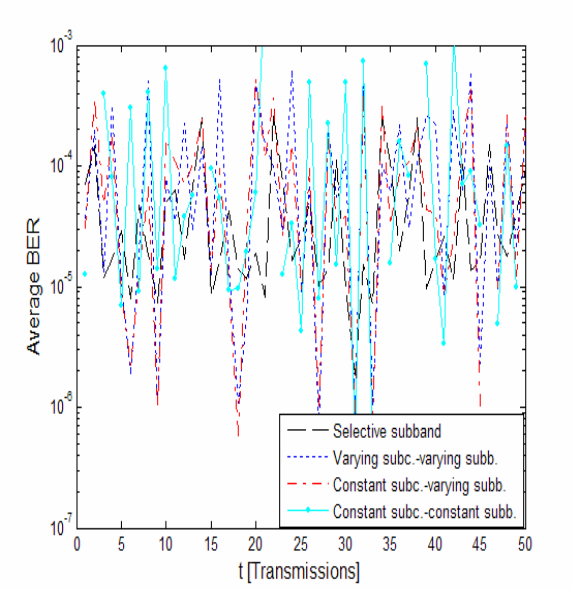
(a) Numbers of subcarriers and subbands in case of varying subcarriers and/or varying subbands



(b) SE of all transmissions for different subband settings



(c) CDF of SE for different subband settings



(d) BER for different subband settings

Figure 5.7-3. Simulation results for adaptive OFDM algorithms with different subband settings under the channel situation in Figure 5.7-1 and 5.7-2

Figure 5.7-3 presents the simulation results for adaptive OFDM algorithms with different subband settings. Figure 5.7-3 (a) presents the number of subcarriers and number of subbands for the algorithms with varying subcarriers and/or varying subbands, i.e., for adaptive OFDM algorithms with selective subband setting, varying subcarrier-subband setting, and constant subcarrier and varying subband setting. From the figure we can see that there are four possible subcarrier numbers, i.e., 32, 64, 128, and 256 subcarriers; and three possible subband numbers, i.e., 4, 5 and 6 subbands. These settings (the number of subcarriers and the number of subbands) are assigned automatically by the adaptive OFDM algorithms based on the current channel situation. We can see the settings for each transmission in Figure 5.7-3 (a).

Figure 5.7-3 (b) presents the Spectrum Efficiency (SE) of the algorithms with the three subband settings we proposed and the constant subcarrier-subband setting. The last setting [3] has a fixed number of subbands and subcarriers. We exploit it here as a reference for the three subband settings we proposed. From the figure we can see that all three subband settings we proposed outperform the constant subcarrier-subband setting in terms of SE. Among our three subband settings, the selective subband setting outperforms the two consecutive subband settings (the varying subcarrier-subband setting and the constant subcarrier and varying subband setting) in terms of SE, with an average SE of 4.55bps/Hz. Of the two consecutive subband settings, the varying subcarrier-subband setting (with an average SE of 3.85bps/Hz) outperforms the constant subcarrier and varying subband setting (with an average SE of 3.45bps/Hz). The average SE of the constant subcarrier-subband setting in this simulation is 2.38bps/Hz.

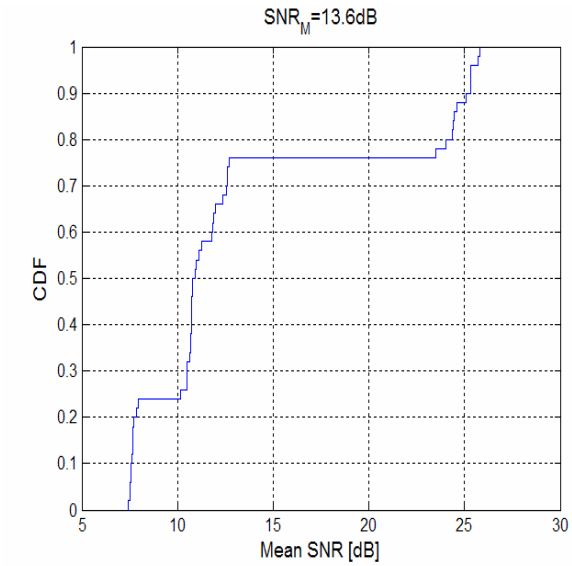
Figure 5.7-3 (c) shows the CDF for the SEs of different subband settings. It shows the same relations of these subband settings as Figure 5.7-3 (b). The SE ratio of the selective subband to the constant subcarrier-subband is 1.9; that of the varying subcarrier-subband to the constant subcarrier-subband is 1.6; and that of the constant subcarrier and varying subband to the constant subcarrier- subband is 1.4.

Figure 5.7-3 (d) presents the BER of the algorithms with all these subband settings. From the figure we conclude that our target BER of 10^{-3} is obtained in our simulations. It is straightforward that if the algorithms set the same OFDM modulation parameters for all these different subband settings, a difference can be expected in BER.

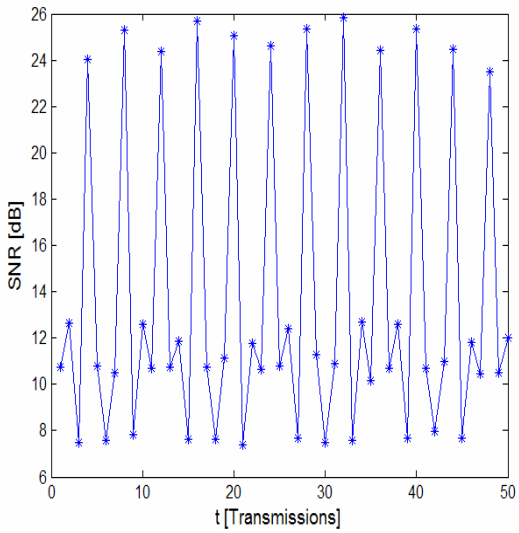
We have to emphasise that the simulation results in Figure 5.7-3 were obtained under the channel situation given in Figure 5.7-1 and 5.7-2. When the channel situation changes, the algorithms will change the settings of the OFDM modulation parameters (including the number of subcarriers and number of subbands for the relevant algorithms), and the throughput (i.e., SE) will change correspondingly. However, the relations hold when the average SNR is in a reasonable range, (12dB to 32dB) according to our simulations. In other words, the selective subband setting always obtains the highest throughput, the varying subcarrier-subband setting has the second highest throughput, the constant subcarrier and varying subband setting leads to the third highest throughput, and the constant subcarrier-subband gives the lowest throughput.

5.8 Simulation Results of Adaptive OFDM Algorithms for MIMO Channels

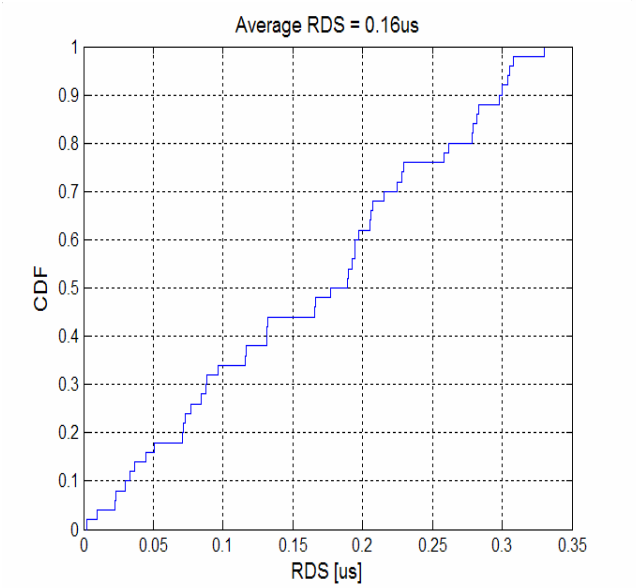
In Section 5.5 we proposed our adaptive OFDM algorithm for MIMO channels. Here, we evaluate its performance by means of simulations. Like the other algorithms, it is designed to guarantee a certain transmission QoS (a BER of 10^{-3}) and to get as much throughput as possible.



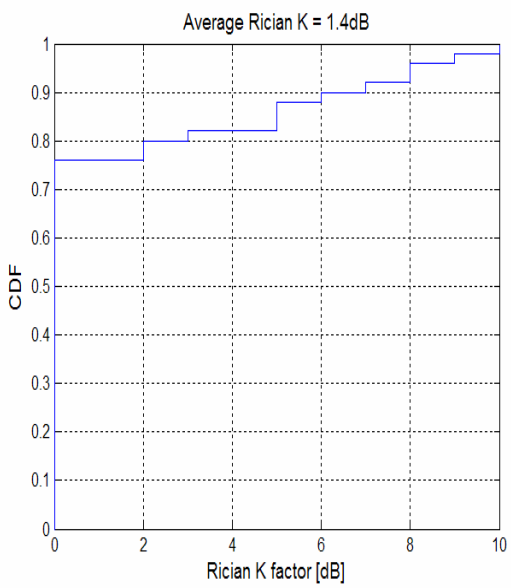
(a) CDF of mean SNR



(b) Mean SNR in the time domain



(c) CDF of RDS



(d) CDF of Rician *K* factor

Figure 5.8-1. Channel parameters in the simulations of our algorithm for MIMO channels

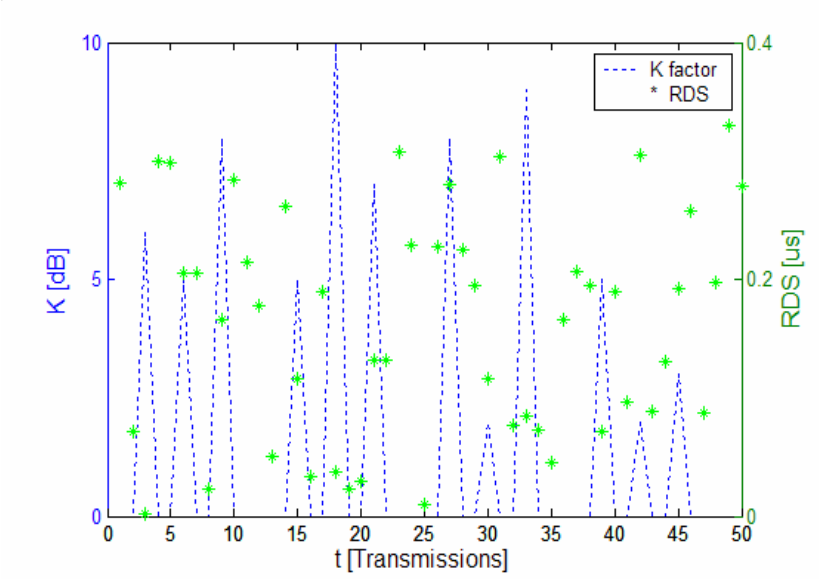
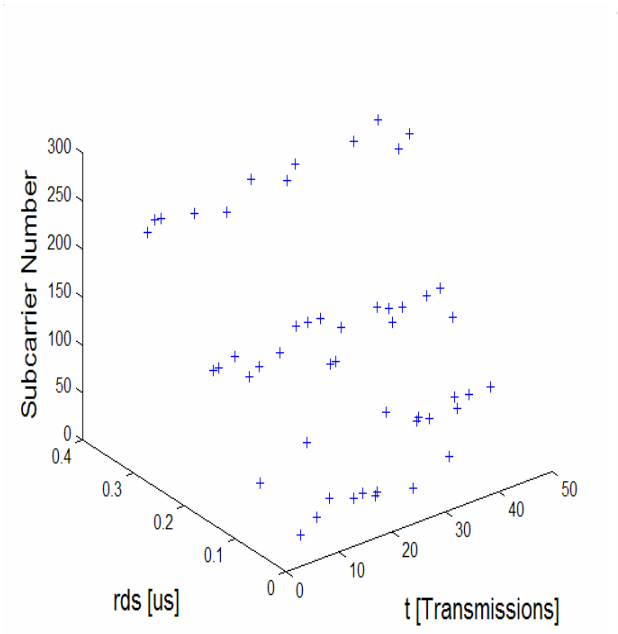
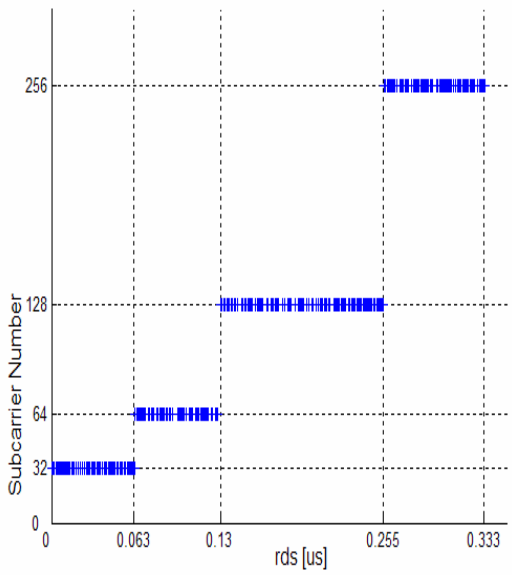


Figure 5.8-2. Rician *K* factor and RDS in the time domain in the simulations of our algorithm for MIMO channels

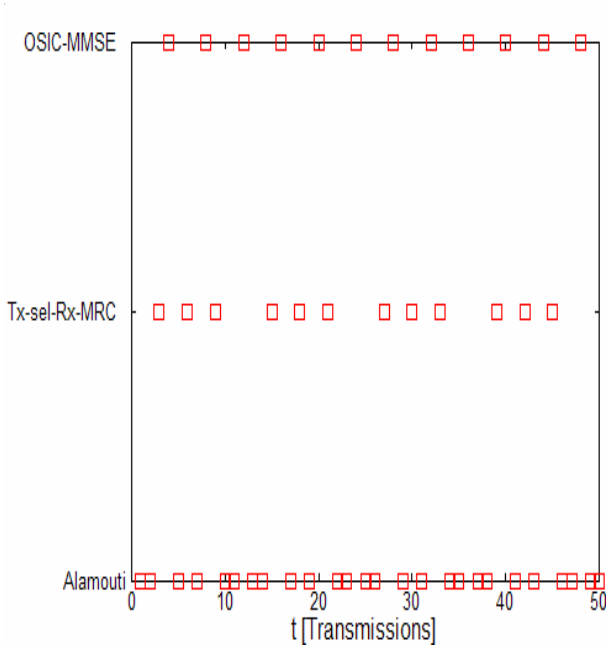
Figure 5.8-1 and 5.8-2 present the pseudo-random channel parameters exploited in our simulations. Figure 5.8-1 (a) shows the CDF of the mean SNR over the whole band of the channel in the simulated period. The mean SNR has been obtained by averaging 256 samples in the frequency band of 20MHz. From the figure we see that for the simulated period the mean SNR over the whole bandwidth of all transmissions ranges from around 7dB to 26dB; and the mean SNR over the band is 13.6dB. Figure 5.8-1 (b) shows the mean SNR over the whole bandwidth for each transmission in time domain. Obviously, they have been generated pseudo-randomly. The distribution of the mean SNR is not uniform, but mainly located in three areas, i.e., around 8dB, 14dB, and 24dB. This explains also the flat part in Figure (a), which is from the non-uniform distribution of the mean SNR. Figure 5.8-1 (c) and (d) shows the CDF of the RDS and Rician *K* factor exploited in our simulations. From the figures we note that the RDS is below around 0.33 μs, and Rician *K* factor ranges from 0dB to 10dB. The average RDS and Rician *K* factor for all transmissions are 0.16μs and 1.4dB, respectively. Figure 5.8-2 presents the Rician *K* factor and RDS in time domain for each transmission.



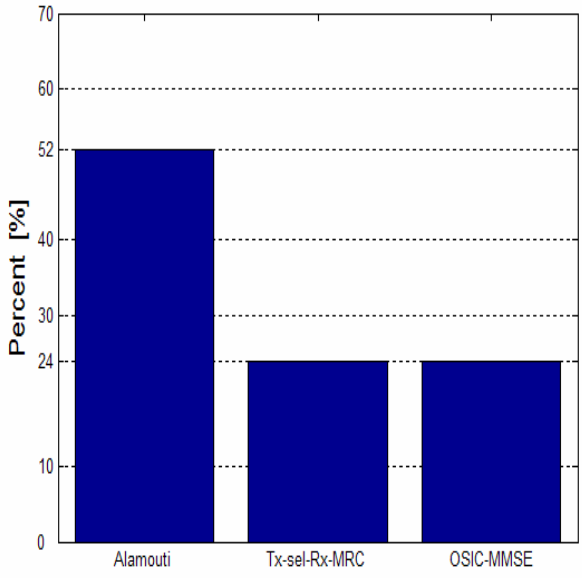
(a) RDS and subcarrier number for every transmission



(b) Side view of subcarrier number assigned to RDS

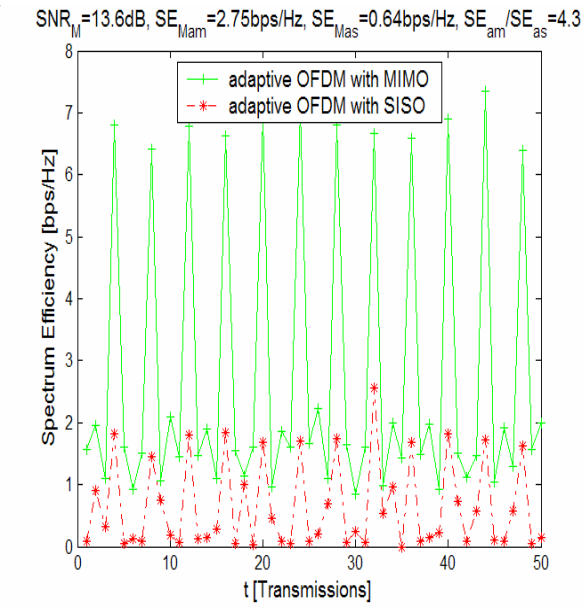


(c) MIMO schemes versus transmission

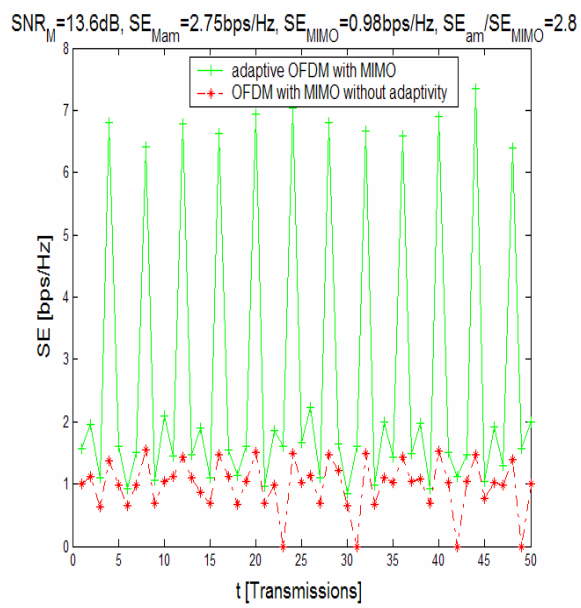


(d) Percentage of the schemes used

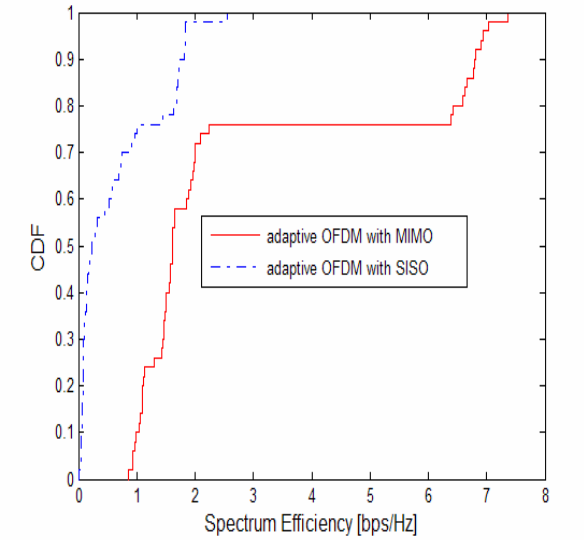
Figure 5.8-3. The settings our algorithm assigned in the simulations



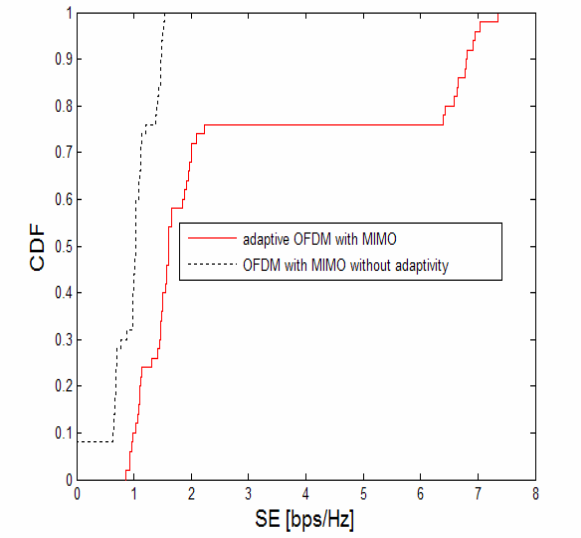
(a) SE of adaptive algorithms for MIMO and SISO channels in the time domain



(b) SE of adaptive and non-adaptive algorithms for MIMO channels



(c) CDF of SE of adaptive algorithms for MIMO and SISO channels



(d) CDF of SE of adaptive and non-adaptive algorithms for MIMO channels

Figure 5.8-4. Spectrum efficiency of the adaptive OFDM algorithm for MIMO channels under channel condition given in Figure 5.8-1 and 5.8-3, compared with non-adaptive OFDM for MIMO channels and adaptive OFDM for SISO channels

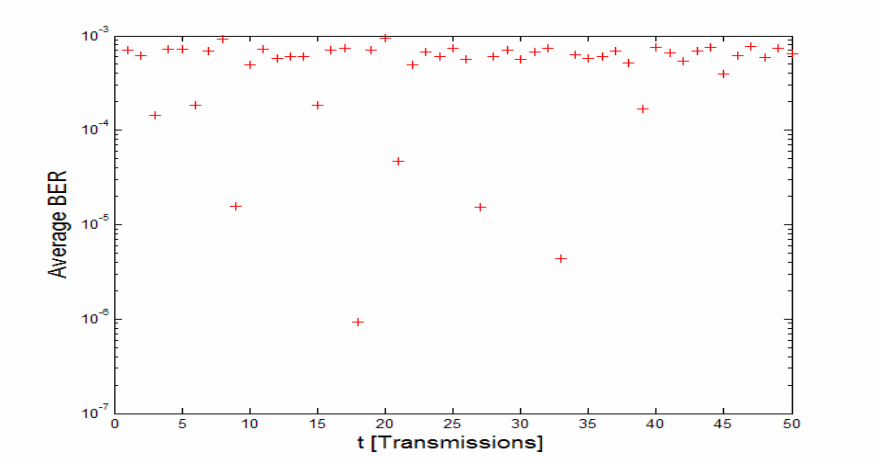


Figure 5.8-5. BER of the adaptive OFDM algorithm for MIMO channels

Our algorithm assigns settings based on the instant channel situation, as shown in Figure 5.8-1 and 5.8-2. Figure 5.8-3 shows the settings assigned by our algorithms during the simulation period. Figure 5.8-3 (a) presents the subcarrier numbers versus RDS for all transmissions. In Section 5.2 we indicated that the delay spread is an important parameter for our algorithm to determine the subcarrier bandwidth/number of subcarriers. Figure 5.8-3 (a) confirms this. The same number of subcarriers is assigned to the transmissions with an RDS in the same range. Figure 5.8-3 (b) is a side view of Figure 5.8-3(a). We can see from Figure 5.8-3 (b) that 32 subcarriers are assigned for an RDS of 0 to 0.063μs, 64 subcarriers for an RDS of 0.063 to 0.13μs, 128 subcarriers for an RDS of 0.13 to 0.255μs, and 256 subcarriers for an RDS of 0.255 to 0.333μs. This is in agreement with Table 5.2-2.

Figure 5.8-3 (c) and (d) present the MIMO schemes that our algorithm assigned during the simulations. Figure 5.8-3 (c) shows the three MIMO schemes versus transmissions in time domain, indicating the MIMO scheme used for each of the transmissions. Figure 5.8-3 (d) presents the percentage of usage of each of the MIMO schemes. We can see that in our simulations, 52% of the transmissions exploited MIMO-Alamouti, 24% MIMO-tx-sel-rx-MRC, and 24% MIMO-OSIC-MMSE. These values can change depending on the actual channel situation.

Under the channel situation given in Figures 5.8-1 and 5.8-2, our algorithm obtained the simulation results shown in Figures 5.8-4 and 5.8-5 by assigning the settings presented in Figure 5.8-3.

Figure 5.8-4 shows the throughput in terms of spectrum efficiency in our simulations. This figure compares the SE of our adaptive OFDM algorithm for MIMO channels with that for SISO channels and with OFDM for MIMO channels without adaptivity. Figure 5.8-4 (a) and

(b) show the SE for all transmissions, i.e., the SE in time domain; Figure 5.8-4 (c) and (d) present the rough CDF of SE based on 50 transmissions. Figure 5.8-4 (a) shows the SE of the adaptive OFDM algorithm for MIMO channels compared with that for SISO channels for each transmission. From the figure we can state that the SE of our algorithm for MIMO channels greatly outperforms that for SISO channels for every transmission. The average SE of the adaptive OFDM algorithm for SISO channels is 0.64bps/Hz, and that of our algorithm for MIMO channels is 2.75bps/Hz, 4.3 times that of the algorithm for SISO channels. Figure (b) compares the SE of our algorithm for MIMO with that of OFDM for MIMO channels without adaptivity for all transmissions. Under the same channel situation, it is obvious that our algorithm for MIMO channels also greatly outperforms that of non-adaptive OFDM for MIMO channels. The SE of non-adaptive OFDM for MIMO channels is 0.98bps/Hz, and that of our algorithm for MIMO channels is 2.8 times as large. We can see that the SE of Figure (a) and (b) are not uniformly distributed but located in mainly two regions: 0~ 2bps/Hz and around 7bps/Hz. This is a result of the non-uniform distribution of the channel SNR, as shown in Figure 5.8-1 (a) and (b).

Figure (c) shows the CDF of our algorithm for MIMO channels compared with that for SISO channels. It confirms in another way that our algorithm for MIMO channels is superior to that for SISO channels with respect to its SE. Besides, we learn from the figure that the SE of the adaptive OFDM algorithm for SISO channels begins with a very small value. This explains why a system with an adaptive OFDM algorithm for SISO channels can hardly transmit under very poor channel conditions. However, adaptive OFDM systems for MIMO channels can still have some throughput. This is because our adaptive algorithm for MIMO channels can "improve" the channel by combining MIMO schemes. When the channel quality is very good, our algorithm for MIMO channels can increase the SE significantly by adapting MIMO schemes (exploiting a favourable scheme for throughput). This explains why the distance between the two curves increases abruptly for a higher SE.

The difference between the two curves in Figure (d) is the presence or absence of adaptivity. It is noted that these two curves are relatively close to each other for small SE, when the channel conditions are poor. When they are good, however, the algorithm with adaptivity obtains a much higher SE by adapting modulation levels and MIMO schemes. This indicates that adaptivity has an advantage for varying channels. There is a flat part in the CDF of the SE of adaptive OFDM for MIMO channels in both Figures (c) and (d). This confirms the non-uniform distribution of the SE, as explained for Figures (a) and (b).

Our algorithm is designed to get as much throughput as possible while guaranteeing transmission QoS. Figure 5.8-5 is the BER of our algorithm in our simulation. We can see that by achieving the high SE shown in Figure 5.8-4, our transmission quality is guaranteed. In other words, the BER of the system with our algorithm is always under the target BER of 10^{-3}.

We emphasize again that simulation results are dependent on the current channel situation. In order to get a statistical value, we ran the simulation several times and averaged the gains. We

kept the average SNR, RDS, and *K* of the channel for all these simulations constant, but the distribution of the SNR in the frequency domain was random and different for each simulation; this also applied to the distribution of RDS and *K* for all transmissions in each simulation. We list the ratio of SE of our adaptive OFDM algorithm for MIMO channels to that for SISO channels and the ratio to that of non-adaptive OFDM systems for MIMO channels in Table 5.8-1. For an average SNR of 13.6dB, average RDS of 0.16μs and average *K* of 1.2dB; we obtained the average ratio of the SE of our adaptive OFDM algorithm for MIMO channels to that for SISO channels (SE_{am}/SE_{as}) of 4.4. The average ratio of our adaptive OFDM algorithm for MIMO channels to non-adaptive OFDM for MIMO channels (SE_{am}/SE_{MIMO}) is 2.8 in this case.

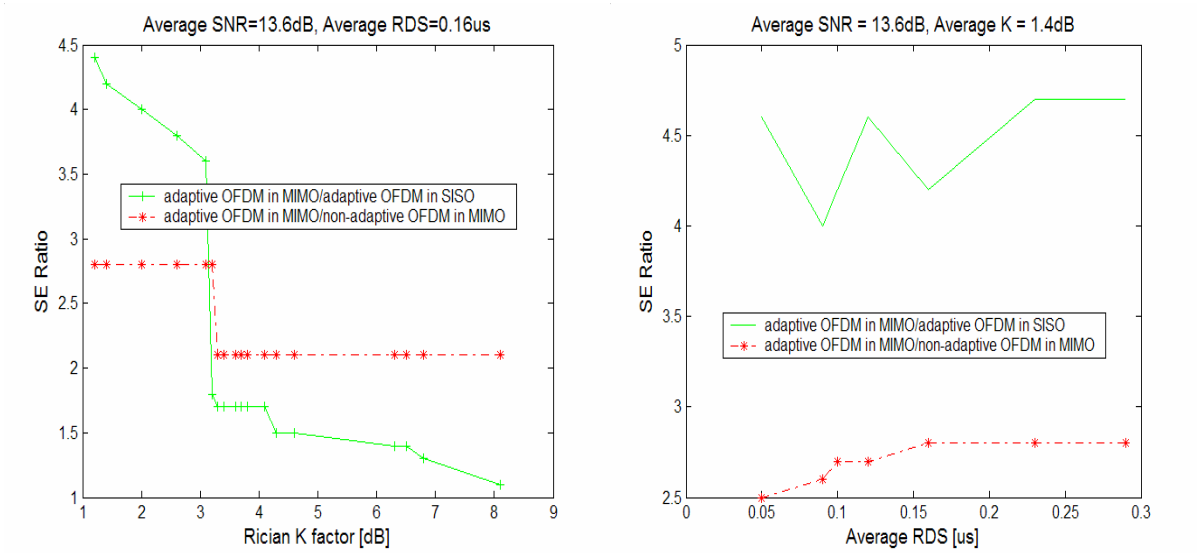
Table 5.8-1. SE gains of adaptive OFDM algorithm for MIMO channels over adaptive OFDM algorithm for SISO channels and the non-adaptive OFDM system for MIMO channels

Average SNR [dB]	Average RDS [μs]	Average K [dB]	Percentage of MIMO schemes %	Ratio of SE	
			Alamouti/tx-sel-rx-MRC/OSIC-MMSE	SE_{am}/SE_{as}	SE_{am}/SE_{MIMO}
13.6	0.16	1.2	52/24/24	4.8	2.8
			52/24/24	4.7	2.9
			52/24/24	4.7	2.8
			52/24/24	4.4	3
			52/24/24	4.2	2.7
			52/24/24	4	3.2
			52/24/24	4	3
			54/22/24	4.6	2.7
			54/22/24	4.5	2.7
			56/20/24	4.3	2.8
Average ratio of SE				4.4	2.8
13.6	0.16	1.4	52/24/24	4.3	2.6
			52/24/24	4.3	2.8
			52/24/24	4.2	2.8
			52/24/24	4.1	3.1
			54/22/24	4.4	2.9
			52/24/24	4.1	2.7
Average ratio of SE				4.2	2.8
Note: SE_{am} means SE of adaptive OFDM algorithm for MIMO channels; SE_{as} means SE of adaptive OFDM algorithm for SISO channels; SE_{MIMO} means SE of OFDM systems for MIMO channels without adaptivity.					

When we change the average *K* to 1.4dB and repeat the simulations, we obtain the average ratio of SE_{am}/SE_{as} of 4.2, which is lower than that with *K* equal to 1.2dB; but the average SE_{am}/SE_{MIMO} is the same, 2.8 (also see Table 5.8-1).

We indicated that the throughput gain depends on the channel situation. How do the channel conditions influence this throughput gain? In order to find this out, we executed the following simulations.

We change the Rician *K* factor while keeping the average SNR and RDS constant, and repeat the simulations to get the SE gains. Figure 5.8-6 (a) shows the result. From the figure we get the information that when the average SNR is 13.6dB and the average RDS is 0.16μs, the SE gain of the adaptive OFDM algorithm for MIMO channels compared to that for SISO channels (SE_{am}/SE_{as}) decreases abruptly with increase of Rician *K* factor. This is because MIMO technology exploits multipath to obtain extra gain; it is more effective for a channel with low *K* factor than for one with a high *K* factor. Under this condition (average SNR = 13.6dB, average RDS = 0.16μs), SE_{am}/SE_{as} drops dramatically for a Rician *K* factor larger than 3 dB. The relative gain of SE_{am}/SE_{MIMO} also drops at a Rician *K* factor of 3dB. This is because the extra gain from adapting MIMO schemes decreases when the MIMO technology is less advantageous. In addition, every Rician *K* factor in Figure 5.8-6 (a) is an average value for 50 transmissions; therefore, an average *K* larger than 3dB means that many of the transmissions among the 50 are with LOS. This explains why the SE ratio drops at 3dB. Nevertheless, the distributions of Rician *K*, SNR and RDS will influence the value of this drop point. When the average *K* is larger than 8dB, the ratio of SE_{am}/SE_{as} decreases to almost one. This means that adaptive OFDM for MIMO channels has almost the same SE as that for SISO channels. In other words, MIMO has lost its advantage completely. However, the ratio of SE_{am}/SE_{MIMO} does not decrease further for *K* larger than 3dB. This is because the adaptivity still gives extra gains compared with a non-adaptive system, even if MIMO no longer has an advantage. We expect that when more simulations are done, the curves in Figure 5.8-6 will be rather smooth.



(a) SE gain versus average Rician *K* factor (b) SE gain versus average RDS

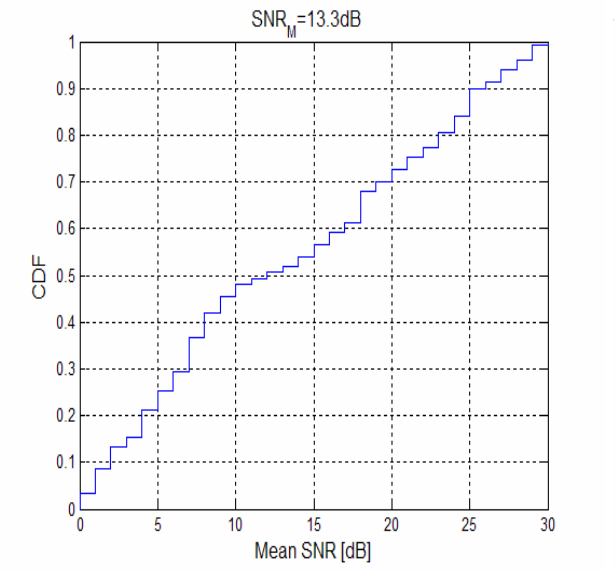
Figure 5.8-6. SE gains versus average Rician *K* factor and RDS

We repeat the process but change the average RDS while keeping the average SNR and *K* constant. Figure 5.8-6 (b) shows the result. We do not see any regular change of SE gain with average RDS. This is because both adaptivity and MIMO can compensate the disadvantage resulted from delay spread.

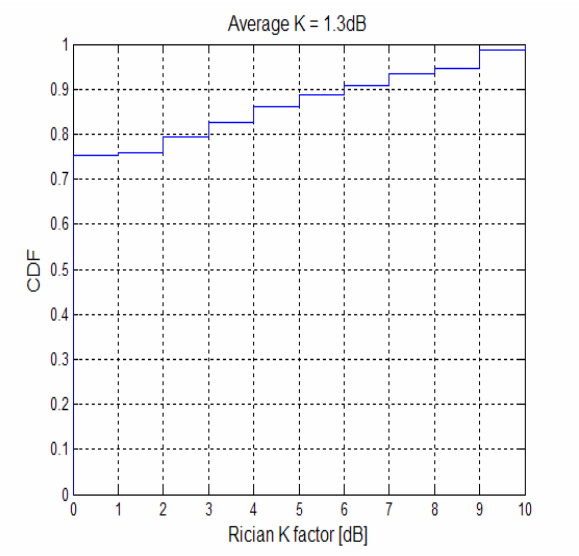
As for the influence of average SNR on relative SE gains, we can compare the SE of Figure 5.8-4 (c) with Figure 5.7-3 (c), for adaptive OFDM algorithm for SISO channels with a selective subband setting. Figure 5.8-4 shows a maximum SE of 2.5bps/Hz for a channel with an average SNR of 13.6dB, while Figure 5.7-3 shows a SE of 5.3bps/Hz for a channel with an average SNR of 24.4dB. It is straightforward that a higher SNR can give a higher throughput. This is because a higher SNR can support a higher modulation level for transmission, which means transmission at a higher data rate.

5.9 Simulation Results of Adaptive CDMA Algorithms for MIMO Channels

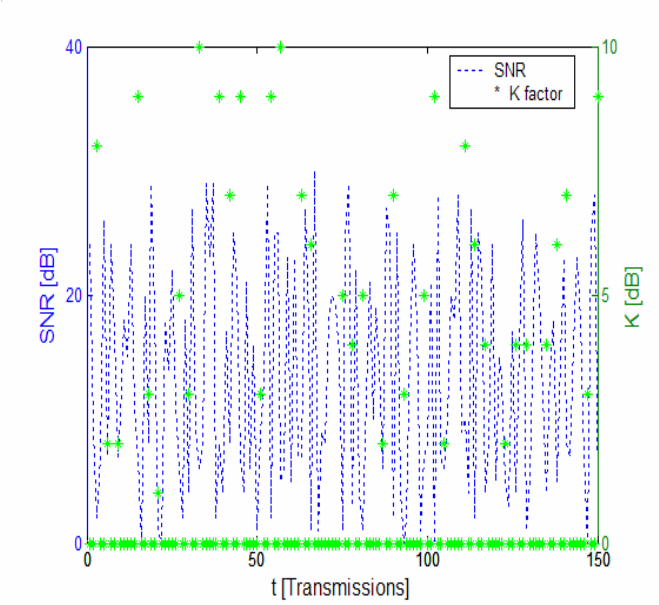
We proposed our adaptive CDMA algorithm for MIMO channels in Section 5.5. In this section we evaluate the algorithm by simulations. The algorithms are designed to guarantee a certain transmission QoS (again a BER of 10^{-3}) and to get as much throughput as possible.



(a) CDF of mean SNR



(b) CDF of Rician *K* factor



(c) SNR and Rician *K* factor for all the transmissions in the time domain

Figure 5.9-1. Channel parameters in the simulations of our adaptive CDMA algorithm for MIMO channels

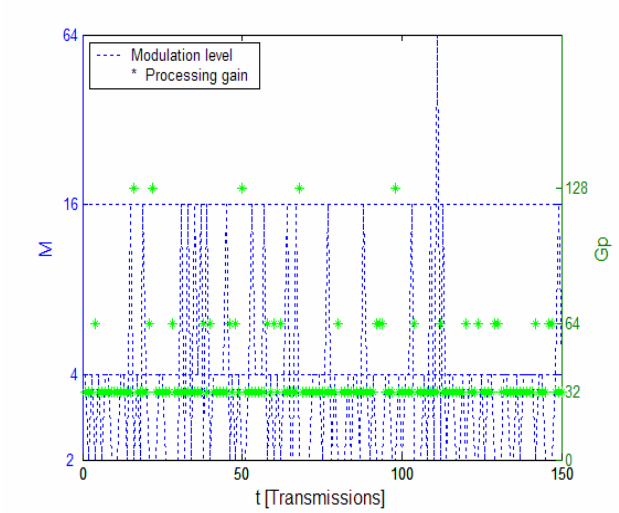
Figure 5.9-1 presents the pseudo-random channel parameters exploited in our simulations. Figure 5.9-1 (a) shows the CDF of the mean SNR of the channel for the simulated period.

From the figure we can see that the mean SNR of all transmissions ranges from around 0dB to 30dB, and the mean SNR for the simulated period is 13.3dB. Figure 5.9-1 (b) shows the CDF of Rician *K* factor exploited in our simulations. The Rician *K* factor ranges from 0dB to 10dB, and the average Rician *K* factor for all transmissions is 1.3dB. Figure 5.9-1 (c) presents the mean SNR and Rician *K* factor in the time domain for each transmission. They were generated pseudo-randomly.

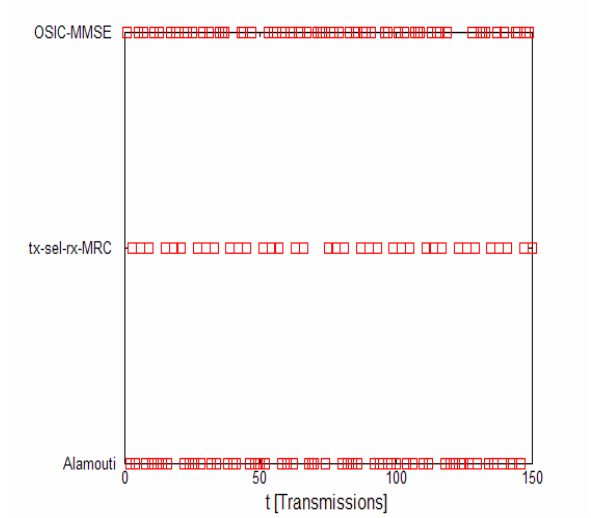
Our algorithm assigns settings based on the instant channel situation shown in Figures 5.9-1. Figure 5.9-2 shows the settings assigned by our algorithms during the simulation period. Figure 5.9-2 (a) presents the modulation levels and processing gains for each transmission. Figure 5.9-2 (b) presents the MIMO schemes that our algorithm assigned for each transmission. Figure 5.9-2 (c) shows the percentage of the usage of each processing gain *Gp* during the simulation. From the figure we learn that our algorithm assigned a processing gain of 32 for 81.33% of the transmissions, a processing gain of 64 for 15.33% of the transmissions, and a processing gain of 128 for 3.34% of the transmissions. No transmission and processing gain of 256 were not employed during the simulation based on the channel situation in Figure 5.9-1.

Figure 5.9-2 (d) shows the percentage of usage of each of the modulation levels during the simulation. BPSK was used for 47.33%, QPSK for 40%, 16QAM for 12%, and 64QAM for 0.67% of the transmissions. Figure 5.9-2 (e) presents the percentage of usage of each of the MIMO schemes. In our simulations, 36.67% of the transmissions exploited MIMO-Alamouti, 24.67% MIMO-tx-sel-rx-MRC, and 38.66% MIMO-OSIC-MMSE. All settings can change with the channel situation.

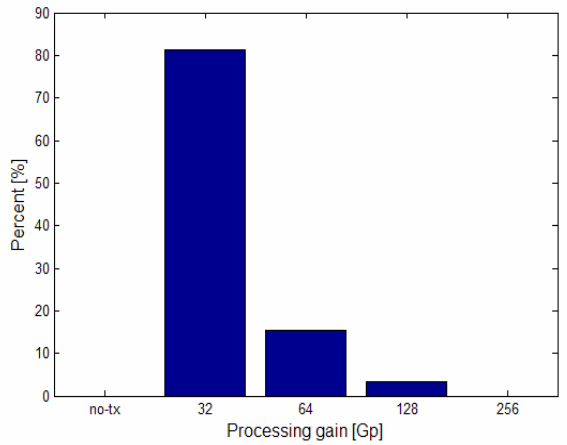
Under the channel situation in Figures 5.9-1, our algorithm obtained simulation results shown in Figure 5.9-3 by assigning the settings presented in Figure 5.9-2.



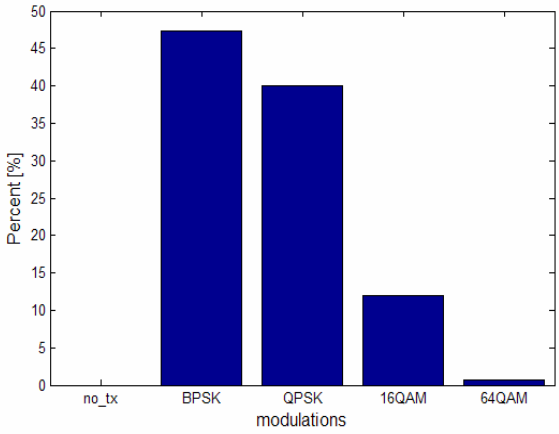
(a) M and Gp for all the transmissions



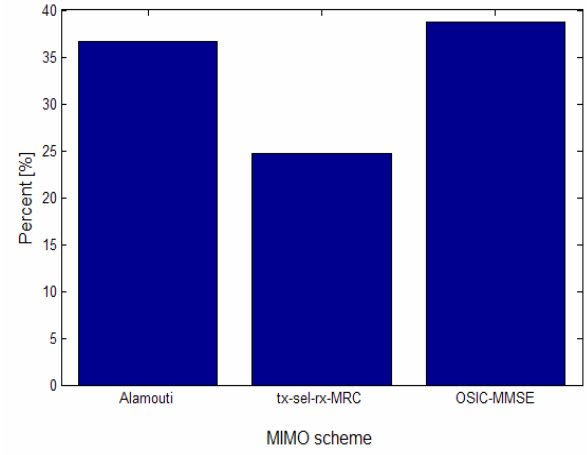
(b) MIMO schemes used in our simulations



(c) Percentage of different Gp

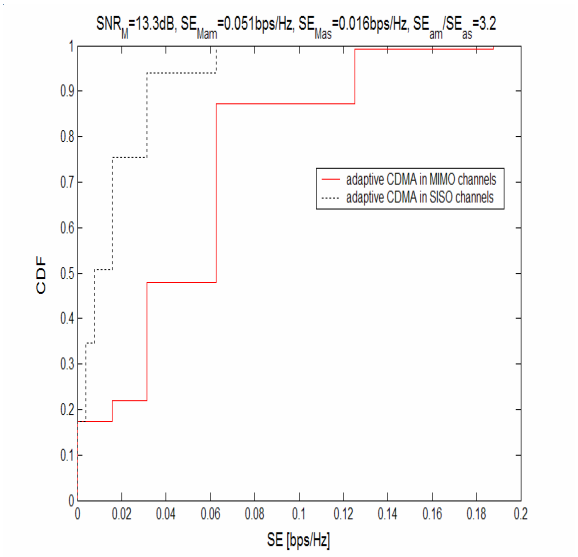


(d) Percentage of different modulations

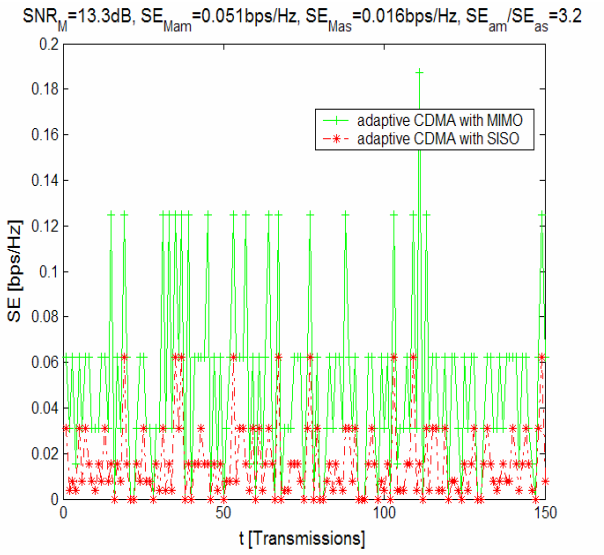


(e) Percentage of different MIMO schemes

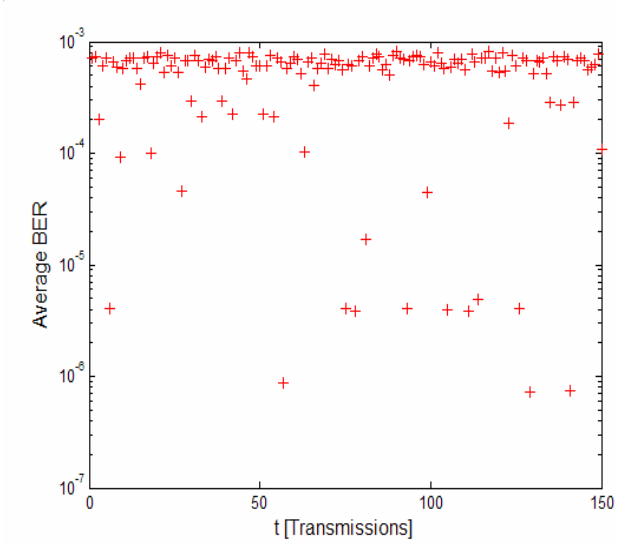
Figure 5.9-2. The settings of M, Gp, and MIMO schemes that our algorithm assigned in the simulations



(a) CDF of SE per user



(b) SE for all the transmissions per user



(c) BER of the adaptive CDMA algorithm in MIMO channels

Figure 5.9-3. Performance of the adaptive CDMA algorithm in MIMO channels

Figure 5.9-3 shows throughput in terms of spectrum efficiency and QoS in terms of BER. This figure compares the SE of our adaptive CDMA algorithm for MIMO with that for SISO channels. Figure 5.9-3 (a) shows the CDF of our adaptive CDMA algorithm for MIMO compared with that for SISO channels. From the figure we can see that the SE of our algorithm for MIMO channels greatly outperforms that for SISO channels. The average SE of the adaptive CDMA algorithm for SISO channels is 0.016bps/Hz per user, and our algorithm

for MIMO channels is 0.051bps/Hz per user, 3.2 times as high. The number of users is dependent on the channel situation, as explained in Section 5.6.1. Here we compare our CDMA-MIMO algorithm with the adaptive CDMA algorithm for SISO channels, so the value of total system throughput is not important. Figure 5.9-3 (b) shows the SE of both adaptive CDMA algorithms. It confirms in another way that our algorithm for MIMO channels is superior to that for SISO channels with respect to its SE.

In addition, we can see from Figure 5.9-3 (a) that the SE of adaptive CDMA algorithm for SISO channels has a very small SE for 50% of the transmissions. This explains why a system with an adaptive CDMA algorithm for SISO channels can hardly transmit under very poor channel conditions. Our adaptive CDMA algorithm for MIMO channels, however, has a higher throughput. This is because our adaptive algorithm for MIMO channels can "improve" the channel quality by combining MIMO schemes. When the channel is very good, our algorithm for MIMO channels can increase the SE significantly by adapting the MIMO schemes (exploiting a favourable scheme for the throughput). This explains why the distance between the two curves increases abruptly with a higher SE.

Our algorithm is designed to get as much throughput as possible while guaranteeing the transmission QoS. Figure 5.9-3 (c) gives the BER results when implementing our algorithm in our simulation. We can see that by achieving the high SE shown in Figure 5.9-3 (a) and (b), our transmission quality is guaranteed. In other words, the BER of the system with our algorithm is under the target BER of 10^{-3}.

5.10 Conclusions

In this chapter we propose three adaptive algorithms, i.e., adaptive OFDM algorithm for SISO channels, one for MIMO channels, and an adaptive CDMA algorithm for MIMO channels. All algorithms assign modulation parameters and/or MIMO parameters in accordance with the instantaneous channel situations. The objective of these algorithms is to get as much throughput as possible under the condition of guaranteeing a certain transmission quality. We explained these algorithms in detail and gave simulation results. Our simulation results indicate that significant gains can be obtained by our algorithms.

In Section 5.2 and 5.3 an adaptive OFDM algorithm for SISO channels is proposed. In Section 5.2.1 we present a global flow chart of this algorithm, with four steps: the channel-parameter acquisition, guard-time setting, setting of the subcarriers and subbands, and setting of the modulation parameters. The guard time setting and the setting of the subcarrier bandwidth are analyzed in Section 5.2.2 and 5.2.3, respectively. We explain that the guard time is assigned based on the current channel delay spread, and the subcarrier bandwidth is set based on guard time, P_{FR}, and Doppler spread.

In Section 5.3 we propose three sub-algorithms for subband setting, i.e., selective subband setting, constant subcarrier and varying subband setting, and varying subcarrier-subband

setting. The constant subcarrier and varying subband setting and varying subcarrier-subband setting are consecutive subband settings. Section 5.7 shows the simulation results of our adaptive OFDM algorithm for SISO channels with three different subband settings. Our simulation results show that under the channel situation shown in Figure 5.7-1 and 5.7-2, the selective subband setting performs best in terms of SE and has an SE 1.9 times that of the constant subcarrier-subband setting; the varying subcarrier-subband setting performs second best: its SE is 1.6 times that of the constant subcarrier-subband setting; the constant subcarrier- varying subband setting performs third: its SE is 1.4 times that of the constant subcarrier-subband setting. The BERs of all these algorithms are under the target BER of 10^{-3}. The settings that our algorithm assigned are shown in Figure 5.7-3.

In Section 5.4, an adaptive OFDM algorithm for MIMO channels is proposed. The algorithm is given by a flow chart in Section 5.4.1. The difference between this algorithm and the adaptive OFDM algorithm for SISO channels is that this algorithm combines adapting MIMO parameters. The selective subband setting is exploited in this algorithm. In Section 5.4.2, we explain how we set MIMO parameters in our algorithm. MIMO-tx-sel-rx-MRC is employed for the Rician channel; MIMO-Alamouti is employed for the Rayleigh fading channel when SNR is not high; and MIMO-OSIC-MMSE for the Rayleigh fading channel when SNR is above a given level.

We show our simulation results for this algorithm in Section 5.8. Under the channel condition shown in Figures 5.8-1 and 5.8-2, our algorithm assigns the modulation and MIMO parameters shown in Figure 5.8-3. The simulation results are given in Figure 5.8-4. The figure indicates that our adaptive OFDM algorithm for MIMO channels can achieve a SE of 4.3 times that of SISO channels, and a SE of 2.8 times that of the non-adaptive OFDM system for MIMO channels. This confirms that combining adaptivity and MIMO is beneficial. Figure 5.8-5 proves that the condition of a target BER of 10^{-3} is satisfied.

We show that the performance of our algorithms depends on the channel situation. In Section 5.8 we study the influence of the channel parameters (i.e., the Rician *K* factor, average SNR and RDS) on the throughput gain. If the Rician *K* factor increases, the SE gain of the adaptive OFDM algorithm for MIMO channels to that for SISO channels (SE_{am}/SE_{as}) decreases abruptly, as shown in Figure 5.8-6. This is because the MIMO technology exploits multipath to obtain extra gains; it gives better results for a channel with a low *K* factor than for a channel with a high one. Under this condition (average SNR = 13.6dB, average RDS = 0.16μs), SE_{am}/SE_{as} drops dramatically for a Rician *K* factor larger than 3 dB. The relative gain of SE_{am}/SE_{MIMO} drops at a Rician *K* factor of 3dB as well. This is because the extra gain from adapting MIMO schemes decreases when the advantage of MIMO technology diminishes. The influence of the RDS has been studied as well. No obvious influence of RDS on the SE gain was found. This is because both adaptivity and MIMO can compensate the disadvantage resulting from the delay spread. The influence of the average SNR on SE of our adaptive OFDM algorithm for SISO channels has been analyzed. The higher the SNR, the higher throughput.

In Section 5.5 we propose an adaptive CDMA algorithm for MIMO channels, which is described in Section 5.5.1. We introduce an SNR boundary matrix for our algorithm to set the processing gains and modulation levels. The channel parameters used in this algorithm are SINR, Rician *K*, and number of users.

In Section 5.9 we present the simulation results of our adaptive CDMA algorithm for MIMO channels. For the channel situation shown in Figure 5.9-1, our adaptive CDMA algorithm for MIMO channels assign settings for the modulation and MIMO parameters, which are shown in Figure 5.9-2. The performance of our algorithm is presented in Figure 5.9-3. Our algorithm achieves a SE gain of 3.2 times that of the adaptive CDMA algorithm for SISO channels. At the same time, the target BER is satisfied, as shown in Figure 5.9-3.

Section 5.6 describes the simulators of our adaptive OFDM/CDMA algorithm for SISO/MIMO channels. We also listed the assumptions that we exploited in our simulations in Section 5.6.

In addition, our simulation results confirm what we assert in Chapter 2. That is, MIMO is a solution to multipath fading of the channel; it can improve performance, especially in a channel with a low Rician *K* factor. Adaptivity is a solution to the time selectivity of the channel: the larger the variation range of the channel, the more adaptive modulation outperforms non-adaptive modulation. The combination of adaptivity with MIMO technology can improve the performance significantly for a time-varying, frequency-selective fading channel.

References

[1] Nassereddine, A., "Analysis of an Adaptive OFDM Algorithm in MIMO Channels" *M.Sc. Graduation Thesis,* IRCTR, EWI, Delft University of Technology, the Netherlands;

[2] Hanzo, L., *Single- and Multi-carrier Quadrature Amplitude Modulation*, ISBN 0-471-49239-6, John Wiley & Sons, Ltd. 2000;

[3] Hanzo, L., Wong, C. H., Yee, M. S., *Adaptive Wireless Transceivers*, John Wiley & Sons, Ltd. 2002;

[4] Che, H., Prasad, R., Ligthart, L.P., "Strategies for Adaptive Modulation Algorithms and Three Subband Settings for Adaptive OFDM Algorithms", submitted to IEEE Communications Magazine;

Chapter 6

Conclusions and Recommendations

In this chapter, the main conclusions and novelties of this thesis are outlined, and recommendations for future work are given.

6.1 Conclusions

In this thesis we have proposed successful algorithms for adaptive modulation for SISO and MIMO channels, i.e., an adaptive OFDM algorithm for SISO channels, one for MIMO channels, and an adaptive CDMA algorithm for MIMO channels. Good results have been obtained in terms of throughput gains given a target BER of 10^{-3}. In order to build these algorithms, we have worked out the MIMO gains, i.e., the Rician K gain and the SNR gain for a large range of SNRs, which have not been described in the literature. Moreover, we have analyzed the parameters influencing the transmission quality and throughput of OFDM and CDMA systems. Effective formulas for the throughput of OFDM and CDMA systems have been derived. A new efficient parameter, P_{FR} (the product of the subcarrier bandwidth and rms delay spread), has been defined to demonstrate the combined effect of the channel and OFDM parameters on the transmission quality. The Normalized Received Power is assumed to be one and the total transmit power is constant for all the transmissions. No power adaptation is considered in our work.

In-depth conclusions of each chapter are given as below.

In Chapter 1 we outline the history of adaptive modulation and the MIMO technique. The Scope of this dissertation and its novelties are outlined.

In Chapter 2 we address the channel properties in terms of the time domain, frequency domain, and space domain, which is efficient for designing adaptive modulation algorithms. Further we indicate solutions for the problems in each of the domains. The MIMO technique provides a solution to space diversity, i.e., the problem in the space domain. MIMO can change the disadvantage of multipath propagation into an advantage. OFDM offers a solution to frequency diversity since it can turn frequency-selective fading into flat fading by using a symbol period that is much longer than the rms delay spread. In addition, adaptivity offers a solution to time-selective fading in the time domain since it is nearly always possible to make the signal bandwidth much wider than the Doppler spread by changing the parameters of the transmission system according to the channel parameters.

Additionally, we list the channel parameters in each of the three domains and analyze the influence of some of them on the channel transfer function in the frequency domain. The delay spread is related to the rate of amplitude variation in the FD channel transfer function. The higher the delay spread, the higher the rate of amplitude variation of the channel. Therefore, we can link the delay spread with the subcarrier bandwidth in OFDM systems. When the delay spread is large, the channel will fluctuate more in the frequency domain. Thus, a smaller subcarrier bandwidth should be assigned correspondingly, and vice versa. The Rician K factor determines the range of variation in the FD channel transfer function. The larger K is, the smaller the variation. We find by simulations that when the Rician K factor is larger than 10dB, the amplitude of the channel transfer function in the frequency domain fades within 2.2dB. Under these conditions it is not necessary to assign a smaller subcarrier bandwidth to combat frequency-selective fading, not even if the channel transfer function fluctuates a lot due to large delay spread. Therefore, only for a Rician K factor smaller than 10dB, a subcarrier bandwidth should be assigned based on the delay spread of the channel: the larger the delay spread, the smaller the subcarrier bandwidth should be set.

In Chapter 3 we propose the strategy and work procedure of adaptive modulation algorithms. We indicate that there are two aspects to the activity of adaptive modulation: the modulation and channel. The channel situation determines the adaptivity of the modulation parameters. We propose in this chapter that investigating adaptive modulation is different from investigating traditional modulation. In traditional modulation, basic modulation technology is studied and combined with new technologies or modified for improvement. In adaptive modulation, it is prerequisite to study the inner relationships within the modulation parameters and the channel parameters themselves as well as the interrelationships between them. Therefore, to build an efficient adaptive modulation algorithm, one first has to carry out a relationship study. Then the criteria should be set up based on which the adaptive modulation algorithm can decide whether and how to change the modulation parameters. The relationships among the OFDM modulation parameters and the CDMA modulation parameters are analyzed as prerequisites for designing adaptive modulation algorithms. We outline the development of adaptive modulation and indicate that the adaptivity is taken to a higher level during this process. We point out that the work in this thesis is to build adaptive modulation algorithms, and we assume perfect channel estimation.

We also derive throughput formulas for OFDM and CDMA systems in this chapter. For the general situation in OFDM systems, i.e., one that is not restricted to identical subcarrier configuration, every subcarrier may have different values for the modulation parameters. In this case, the total bit rate should be the summation of the bit rate of all subcarriers. The throughput formula for CDMA systems in terms of bit rates indicates that the bit rate of CDMA systems is linearly proportional to the coding rate and transmission bandwidth, logarithmically proportional to the modulation level, and inversely proportional to the processing gain.

Following the discussion of parameters influencing throughput, the parameters influencing QoS are investigated. We introduce a new parameter, P_{FR}, as the product of subcarrier bandwidth Δf and RDS. We analyze the range of values of P_{FR}. From the simulations we find that the traditional belief that smaller subcarrier bandwidth gives better BER performance is true only for a constant channel situation. When the product of subcarrier bandwidth and RDS is fixed, changing the values of the subcarrier bandwidth and RDS does not influence BER performance. The product of the subcarrier bandwidth and RDS is therefore an important factor to influence the BER performance. From simulations we learn that when the SNR is above 0 dB, the relationship yields: the smaller the product, the better the BER performance. Nevertheless, for a fixed channel situation, RDS is a constant value, and hence smaller P_{FR} means smaller subcarrier bandwidth. In this case, a smaller subcarrier bandwidth can give better BER performance. The result can be used to improve OFDM system performance for a varying channel situation and is hence important for adaptive OFDM algorithms. Further, we simulate the influence of P_{FR} on the BER performance. We find that only when the SNR is larger than a certain value (which we call the "Start SNR-SSNR"), a change in P_{FR} can influence the BER. When the Rician K factor is very large, the influence of P_{FR} on the BER becomes irregular; we refer to the largest K value that gives a reasonable BER performance for different P_{FR} as *top K*. When K is larger than a certain value (20dB for BPSK, QPSK), the P_{FR} value has no influence on the BER. From the simulations we know that the *top K* and SSNR are functions of the modulation level, M.

In Chapter 4 we analyse the basic definition, structure, and characteristics of the MIMO systems. We describe different categories (Spatial Multiplexing schemes and Diversity schemes) of MIMO systems. What is more, we carry out simulations to calculate the gains of different MIMO schemes in terms of the capacity and SNR and compare these with those of non-MIMO systems. The influence of the LOS is considered as well. In order to give a clear and complete description of the MIMO gain, we introduce a new parameter, i.e., the Rician K factor gain. We give a detailed description of the gains of MIMO systems compared to those of SISO or SIMO systems. We find by simulations that for SM schemes, the SNR gain and Spectral Efficiency (SE) gain of MIMO systems with respect to SISO systems are functions of the input SNR. The SNR gain decreases with the input SNR, but the capacity gain increases with it. For diversity schemes, however, the SNR gain and the SE gain of MIMO systems to SISO systems are not a function of the input SNR. In other words, these two gains are constant over the input SNR. As for the Rician K gain of MIMO compared to SISO

systems, it is a function of the modulation level for diversity schemes. This gain increases with the modulation level. For the SM scheme, on the other hand, this gain is not a function of the modulation level, that is, it is constant for all modulation levels.

In Chapter 5 we propose three adaptive algorithms, i.e., an adaptive OFDM algorithm for SISO channels, one for MIMO channels, and an adaptive CDMA algorithm for MIMO channels. All of these algorithms assign modulation parameters and/or MIMO parameters suitable for the instantaneous channel situation. Perfect channel estimation is assumed in our algorithms. The objective of these algorithms is to get as much throughput as possible under the condition of guaranteeing a certain transmission quality.

We propose three sub-algorithms for subband setting, i.e., selective subband setting, constant subcarrier and varying subband setting, and varying subcarrier-subband setting. The constant subcarrier and varying subband setting and varying subcarrier-subband setting are consecutive subband settings. Our simulation results show that under the channel situation shown in Figure 5.4-2 and 5.4-3, the selective subband setting performs best in terms of SE: it gives 1.9 times the SE of the constant subcarrier-subband setting; the varying subcarrier-subband setting performs second best: its SE is 1.6 times that of the constant subcarrier-subband setting; the constant subcarrier and varying subband setting performs the third: its SE is 1.4 times that of the constant subcarrier-subband setting.

We propose the new idea of employing more than one MIMO scheme in a system and adapting these schemes using our adaptive modulation algorithms. In our systems, MIMO-tx-sel-rx-MRC is employed for the Rician channel; MIMO-Alamouti for the Rayleigh fading channel when SNR is not high; and MIMO-OSIC-MMSE for the Rayleigh fading channel when SNR is high. Our simulation results show that our adaptive OFDM algorithm for MIMO channels can achieve an SE of 4.3 times that of the adaptive OFDM algorithm with SISO channels, and an SE of 2.8 times that of the non-adaptive OFDM system with MIMO channels. This confirms that combining adaptivity with MIMO schemes is beneficial.

We also argue that the performance of our algorithms depends on the channel situation. We study the influence of channel parameters (the Rician K factor and RDS) on the throughput gain. The SE gain of our adaptive OFDM algorithm for MIMO channels to that for SISO channels (SE_{am}/SE_{as}) decreases abruptly with the increase of the Rician K factor. This is because the MIMO technology exploits multipath to obtain extra gains; it is more effective in a channel with a low K factor than in a channel with a high one. Under this condition (average SNR = 13.6dB, average RDS = 0.16μs), SE_{am}/SE_{as} drops dramatically for a Rician K factor larger than 3 dB. The relative gain of SE_{am}/SE_{MIMO} also drops at a Rician K factor of 3dB. This is because the extra gain obtained by adapting MIMO schemes decreases when the MIMO technology is less effective. The influence of RDS is studied as well. No visible influence of RDS on SE gain has been found. This is because both adaptivity and MIMO can compensate the disadvantage resulting from the delay spread.

In the adaptive CDMA algorithm for MIMO channels, we introduce an SNR boundary matrix to set the processing gains and modulation levels. Simulation results show that our algorithm achieves an SE gain of 3.2 times that of the adaptive CDMA for SISO channels.

Our simulation results confirm what we asserted in Chapter 2. That is, MIMO is a solution to the multipath fading of channels; it can improve performance, especially in a channel with a low Rician K factor. Additionally, adaptivity is a solution for time selectivity of channels: the larger the variation range of the channel, the more adaptive modulation outperforms non-adaptive modulation. The combination of adaptivity with MIMO technology can improve the performance of a time-varying, frequency-selective fading channel significantly.

6.2 Novelties

The major contributions of this dissertation are the following:

- We analyze the channel properties in terms of the time domain, frequency domain, and space domain. We indicate three techniques as solutions to the problems in each of these domains, the effectiveness of which has been proved by our work.
- We are the first to state that the development of adaptive modulation technique consists of three stages, in each of which the adaptivity is taken to a higher level.
- We outline the strategy and work procedures of adaptive modulation algorithms.
- We derive throughput formulas for OFDM and CDMA systems, which indicate directly the parameters influencing the throughput of these systems.
- We define a new parameter, P_{FR}, as the product of the subcarrier bandwidth Δf and RDS. We are the first to propose that this is the parameter influencing QoS in OFDM systems instead of the subcarrier bandwidth.
- We find that P_{FR} does not influence QoS all the time; the effect of this parameter depends on other parameters, i.e., the Rician K, SNR, and modulation levels. How P_{FR} works is also studied.
- We introduce a new parameter, i.e., the Rician K factor gain in order to give a clear and complete description of the MIMO gain. We find by simulations that this gain is a function of the modulation level for diversity schemes. This gain increases with the modulation level. For the SM scheme, on the other hand, this gain is not a function of the modulation level, in other words, it is constant for all modulation levels.
- We find by simulations that for SM schemes, the SNR gain and Spectral Efficiency (SE) gain of MIMO systems with respect to SISO systems are functions of the input SNR. The SNR gain decreases with the input SNR, but the capacity gain increases with it. For diversity schemes, the SNR gain and SE gain of MIMO systems to SISO systems are not a function of the input SNR. In other words, these two gains are constant over the input SNR.
- We propose three sub-algorithms for subband setting of adaptive OFDM algorithms, i.e., a selective subband setting, a constant subcarriers and varying subbands setting,

and a varying subcarriers-subbands setting. These subband settings are compared in terms of throughput by simulations.

- We propose three efficient adaptive algorithms, i.e., an adaptive OFDM algorithm for SISO channels, one for MIMO channels, and an adaptive CDMA algorithm for MIMO channels. All of these algorithms have been evaluated by simulations and good results have been obtained.
- We put forward the new idea of employing more than one MIMO scheme in a system and adapting these schemes using our adaptive modulation algorithms. Simulation results show that it is beneficial to combine adapting MIMO schemes into adaptive modulation systems.
- We are the first to point out that some channel parameters can affect the relative throughput gain. Our simulation results prove that the SE gain of the adaptive OFDM algorithm for MIMO channels to that for SISO channels (SE_{am}/SE_{as}) decreases abruptly with an increase in the Rician *K* factor.
- We introduce an SNR boundary matrix to set the processing gains and modulation levels, for the adaptive CDMA algorithm for MIMO channels.

6.3 Recommendations for Future Work

We have proposed three adaptive modulation algorithms in this dissertation successfully. For future work we give recommendations as follows.

- We expect to obtain even higher gains, if adaptive coding rate is combined.
- Further study is recommended on the influence of the Rician *K* and SNR on the relative gains of our adaptive algorithms.
- Correlation among the transmit and receive antennas will be an interesting factor to combine into the adaptive algorithms.
- We employed 2x2 MIMO systems; however, one could increase the number of antennas at both the transmitter and receiver.
- We expect good results from combining adapting the number of transmit- and/or receive-antennas into the adaptive algorithms, since we point out that the number of antennas at the transmitter and receiver does influence the MIMO gains.
- We indicate three techniques as solutions to problems in the time, frequency, and space domain. The degree of dependency of the three techniques in these domains is a subject for further study.
- Implementation of these algorithms in steps, ever improving the technology readiness of systems, is an exciting task.
- It is recommended that the subject of channel estimation should be investigated further.

Appendix A

OFDM Modulation

Orthogonal Frequency Division Multiplexing (OFDM) is a means to deal with the channel-induced linear distortion encountered when transmitting over a dispersive radio channel [1]. The idea of OFDM is to split the total transmit bandwidth into a number of orthogonal subcarriers in order to transmit the signals in these subcarriers in parallel. By doing that, a high rate data stream can be divided into a number of lower-rate streams because the symbol period increases with the number of subcarriers. Therefore, the effect of multipath delay decreases and the frequency selective fading channel is turned into a flat fading channel. Thus, OFDM is a solution to the frequency selectivity of fading channels. It takes advantage of a frequency-selective fading channel and turn the channel into a flat fading channel. It is straightforward that by dividing the total bandwidth into a number of subcarriers, one decreases the subcarrier bandwidth with an increasing number of subcarriers in the frequency domain, and in the time domain, the symbol period increases. The higher the number of subcarriers, the longer the symbol period.

A.1 Schematic of OFDM Transmission Systems

In the OFDM transmission system (as shown in Figure A.1-1), the serial data stream is passed through a serial-to-parallel converter, which splits the data into a number of parallel channels.

The Fast Fourier Transform (FFT) and Inverse Fast Fourier Transform (IFFT) are typically employed in the OFDM modulation/demodulation process. The parallel data symbols S_0 to S_{N-1}, which can be mapped to different subcarriers in the frequency domain, go through IFFT, and the output coefficients s_0 to s_{N-1} in the time domain constitute an OFDM symbol.

The s_0 to s_{N-1} are the time domain samples of the OFDM symbol and are transmitted sequentially over the channel. At the receiver, a spectral decomposition of the received time domain samples r_N is computed employing FFT, and then the recovered data symbols R_N, which can be mapped to different subcarriers in the frequency domain, are restored to serial order and demultiplexed.

From the Figure A.1-1 we can see that the N_S frequency domain samples produce N_S time domain samples. The time domain signal is assumed to repeat periodically for the duration of the channel's memory. Hence, for transmission over time dispersive channels, each time domain OFDM symbol is extended by the "cyclic extension" or a guard interval in order to overcome the inter-OFDM symbol interference due to the channel's memory. The samples of the cyclic extension are copied from the end of the time domain OFDM symbol. The guard time must be chosen larger than the expected delay spread so that multi-path components from one symbol cannot interfere with the next symbol. To ensure that the delayed replicas of the OFDM symbol have an integer number of cycles within the FFT interval, the OFDM symbol is cyclically extended in the guard time. If we translate this fact to the frequency domain, it means that the spacing between the sub-carriers is still preserved. Each sub-carrier has a maximum that corresponds to a zero crossing of all other subcarriers. At the receiver, the cyclic extension is discarded.

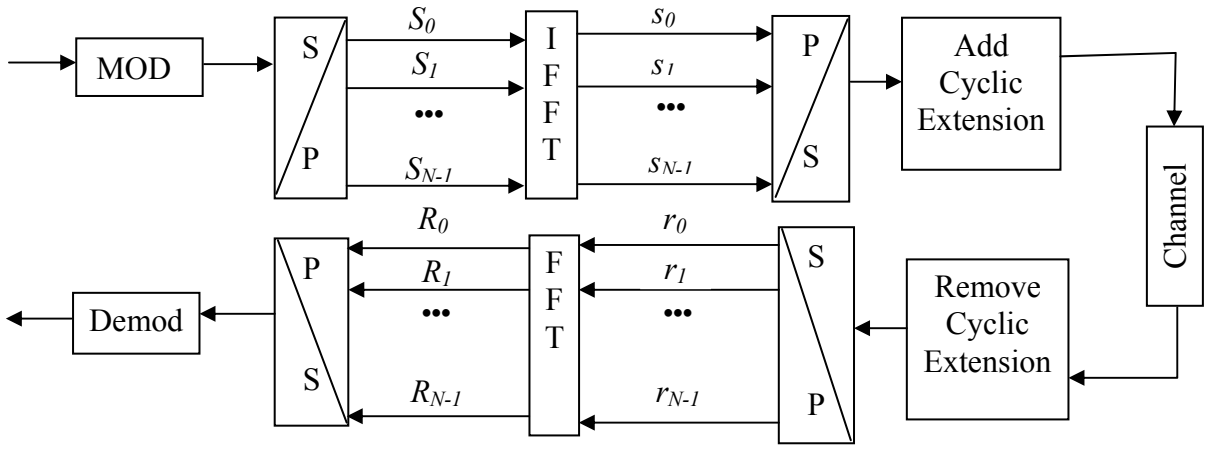


Figure A.1-1. Schematic of N_S - subcarrier OFDM transmission system
(In the figure, $N = N_S$, the number of subcarriers)

An OFDM signal consists of a sum of sub-carriers that are modulated by using PSK (Phase Shift Keying) or QAM (Quadrature Amplitude Modulation). One OFDM symbol can be expressed using the following expression [2]:

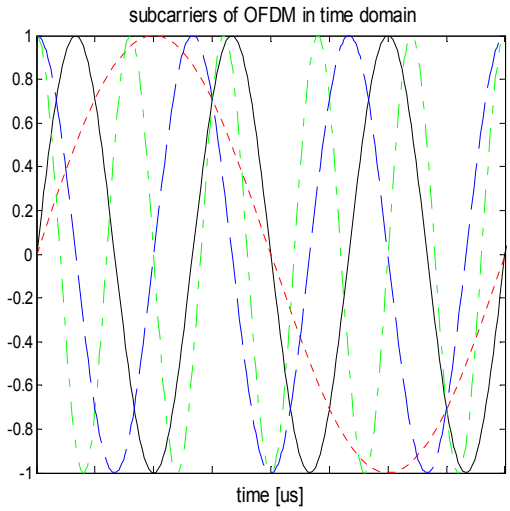
$$s(t) = \mathrm{Re}\left\{ \sum_{i=-\frac{N_S}{2}}^{\frac{N_S}{2}-1} S_{i+\frac{N_S}{2}} \exp\left(j2\pi \left(f_c - \frac{i+0.5}{T_S} \right)(t - t_s) \right) \right\} \quad (t_s \le t \le t_s + T_S)$$
$$s(t) = 0 \quad (t < t_s \wedge t > t_s + T_S) \qquad \text{(A-1)}$$

where S_i is the complex QAM symbol; N_s represents the number of subcarriers; T_S is the symbol duration; f_c the carrier frequency; and t_s the starting time of the symbol.

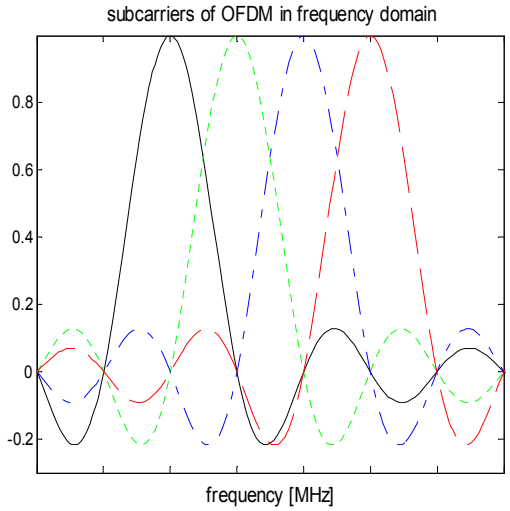
The equivalent complex base-band notation of equation (A-1) is given by

$$s(t) = \sum_{i=-\frac{N_S}{2}}^{\frac{N_S}{2}-1} S_{i+\frac{N_S}{2}} \exp\left(j2\pi \frac{i}{T_S}(t - t_s) \right) \quad (t_s \le t \le t_s + T_S)$$
$$s(t) = 0 \quad (t < t_s \quad \wedge \quad t > t_s + T_S) \qquad \text{(A-2)}$$

Figure A.1-2 (a) shows four subcarriers from one OFDM symbol. The sub-carriers in this example have the same phase and the same amplitude. Each subcarrier has exactly an integer number of cycles in the interval T_S, and the number of cycles between adjacent subcarriers differs only by one. This property accounts for the orthogonality between the sub-carriers.



(a) Example of four subcarriers within one OFDM symbol (Time Domain)



(b) Spectra of individual subcarriers

Figure A.1-2. Subcarriers in time and frequency domain [1]

Figure A.1-2 (b) shows the spectra of individual subcarriers. This pulse shape is present in the frequency domain. By having the maximum of each subcarrier correspond to zero crossings of all others, we can deduce that inter-carrier interference (ICI) is avoided. This result is a direct application of the Nyquist criterion, which is usually applicable for the given pulse shape in the time domain. In the time domain, instead of ICI, it is inter-symbol interference (ISI) that is avoided.

A.2 Structure of OFDM Symbols

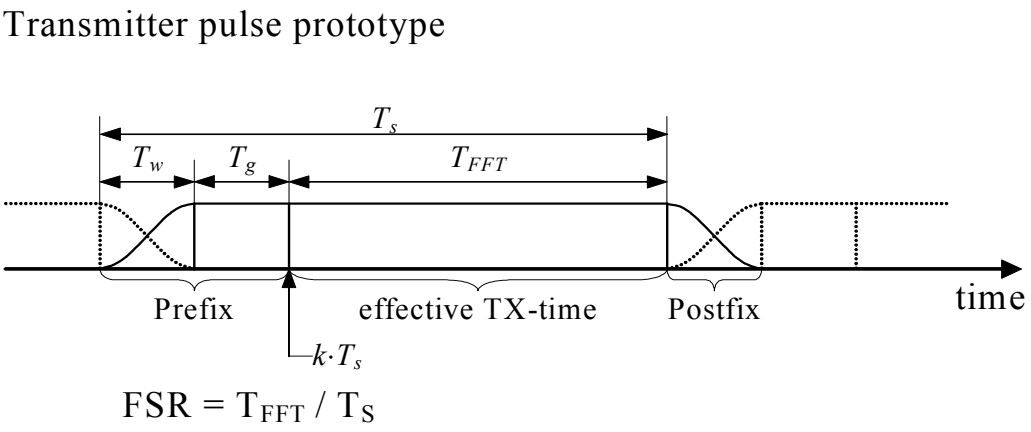


Figure A.2-1. The structure of an OFDM symbol [3]

Figure A.2-1 gives the structure of OFDM symbols in the time domain. The T_{FFT} is the time for effective data transmission, T_g is the guard time. We can see another parameter, T_w, which is the window time. It is easy to see that the relation among the parameters is

$$T_S = T_{FFT} + T_g + T_w . \tag{A-3}$$

Windowing is introduced to make the amplitude go smoothly to zero at the symbol boundaries, and to decrease the sensitivity of the frequency offset. A commonly used window type is the raised cosine window, which is defined as

$$w(t) = \begin{cases} 0.5 + 0.5\cos\left(\pi + \frac{t\pi}{\beta T_S}\right) & (0 \le t \le \beta T_s) \\ 1 & (\beta T_s \le t \le T_s) \\ 0.5 + 0.5\cos\left((t - T_s)\frac{\pi}{\beta T_S}\right) & (\quad T_s \le t \le (1+\beta T_s)\quad) \end{cases} . \tag{A-4}$$

Here β is the roll-off factor of the raised cosine and T_s the symbol interval, which is shorter than the total duration of a symbol because we allow adjacent symbols to partially overlap in the roll-off region.

An OFDM symbol starting at time $t = t_k = kT_s$ (beginning of the *k*th symbol) is defined in equations as

$$s_k(t) = \mathrm{Re}\{w(t-t_k)\sum_{i=-\frac{N_S}{2}}^{\frac{N_S}{2}-1} d_{i+N_S\frac{k+1}{2}} \exp(j2\pi(f_c - \frac{i-0.5}{T_S})(t-t_k-T_{prefix}))\}$$

$$(\quad t_k \le t \le t_k + T_S(1+\beta) \quad) \qquad , \quad \text{(A-5)}$$

$$s_k(t) = 0 \quad (\quad t < t_k \quad \wedge \quad t > t_k + T_S(1+\beta) \quad)$$

where $T_{prefix} = T_w + T_g$, which can be seen in Figure A.2-1.

A.3 OFDM Parameters

- Parameters in the Frequency Domain (FD)

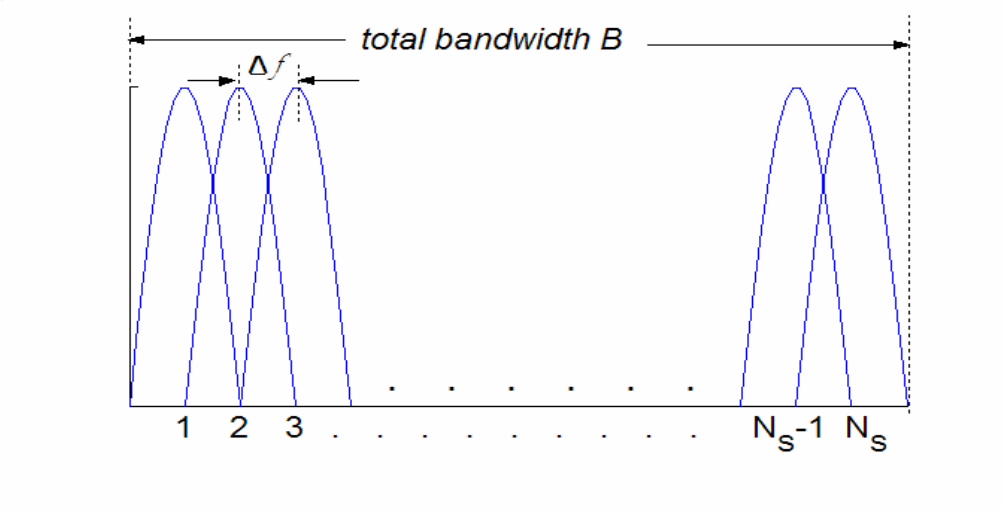


Figure A.3-1. Subcarrier bandwidth Δf and the number of subcarriers *Ns*

Figure A.3-1 presents the OFDM scheme in the frequency domain. There are three parameters (as shown in Table A.3-1): the total bandwidth for all the subcarriers B, the subcarrier bandwidth Δf, and the number of subcarriers N_S. The relationship among them is

$$B = N_S \times \Delta f \ . \tag{A-6}$$

In practice, the total available bandwidth B is given as a limit before the system design. Hence, for system designers, the OFDM parameters in the frequency domain that can be determined are the subcarrier bandwidth Δf and number of subcarriers N_S. Because the subcarrier bandwidth and the number of subcarriers are dependent on each other in terms of equation (A-6), giving value to one of them is enough in the system design. But both of them should be checked using the criteria covering them, respectively. In other words, there are restrictions on the subcarrier bandwidth as well as on the number of subcarrriers. All of them should be checked for the design of the subcarrier bandwidth and for the number of subcarriers.

- Parameters in the Time Domain (TD)

From Figure A.2-1 we can extract the OFDM parameters in the time domain: the symbol period T_S, effective transmit time or FFT time T_{FFT}, guard time T_g, and windowing time T_w. In the research work, we only consider the FFT time and symbol period most of the time (as shown in Table A.3-1). If we do not consider the window time, equation A-3 becomes

$$T_S = T_{FFT} + T_g \, . \tag{A-7}$$

In addition, we define a new parameter, FSR (FFT to Symbol duration Ratio), the ratio of the FFT time and the symbol period,

$$FSR = \frac{T_{FFT}}{T_S} \, . \tag{A-8}$$

This parameter can indicate how efficiently the resource is used in the time domain and it can be used to calculate the throughput.

Table A.3-1. OFDM parameters and their relationship

Domain	Parameters	relations	Parameters to design
FD	B, Δf, N_s	$B = N_S \times \Delta f$	Δf or N_s
TD	T_S, T_{FFT}, FSR, T_g,	$T_S = T_{FFT} + T_g$ FSR=T_{FFT}/T_S $T_{FFT} = \frac{1}{\Delta f}$	T_g

The time domain parameter T_{FFT} and the frequency domain parameter Δf are related to each other, i.e., they are inversely proportional to each other. Therefore, setting the value of one of them is enough in the system assignment. From Table A.3-1 we can see that given a total bandwidth, we need to assign values for the subcarrier bandwidth (or number of subcarriers) and the guard time for an OFDM system. By doing this, we can get other parameters, i.e., the number of subcarriers (or the subcarrier bandwidth), the symbol period, and the FSR.

A.4 Error Probability Analysis

The transmission quality is an essential factor to evaluate a technique or algorithm in wireless communication systems. The error probability is a parameter of the transmission quality. There are two methods to get the error probability of an OFDM system by simulations. One is to build up the OFDM transceiver model by programming and simulating a large number of transmission bits (at least one million bits) to calculate the ratio of the error bits to total transmit bits; the other is to calculate the error probability with a mathematical formula. Here we discuss the latter method.

There are some investigations of the error probability of OFDM and/or multichannel (or multiple subcarriers) systems in the literature, for example, [3], [4], [5], [6]. We exploit [3]. We present the formula here briefly, and the readers may refer to [3] for details.

In [7] the error probability P_e of multichannel signals is given as

$$P_e = \Pr\{D < 0\} = \int_{-\infty}^{0} p(D)dD\,, \tag{A-9}$$

$$D = \sum_{k=1}^{L_D} \left(A_D \mid X_k \mid^2 + B_D \mid Y_k \mid^2 + C_D X_k Y_k^* + C_D{}^* X_k^* Y_k \right), \tag{A-10}$$

where $p(D)$ is the PDF of D; A_D, B_D, C_D are constants; and X_k and Y_k are a pair of correlated complex-valued Gaussian random variables. For the channels considered, the L_D pairs

$\{X_k, Y_k\}$ are mutually statistically independent and identically distributed. L_D is equal to one in our case.

In [3] the error probability of uncoded OFDM systems in Rician fading channels is derived based on the formula above,

$$P_e = Q_1(a,b) - \frac{\upsilon_2 / \upsilon_1}{1+\upsilon_2/\upsilon_1} I_0(ab) e^{-\frac{1}{2}(a^2+b^2)}, \tag{A-11}$$

where $I_n(x)$ is the n-th order modified Bessel function of the first kind and $Q_1(a,b)$ is Marcum's Q function, which can be expressed in terms of Bessel functions as

$$Q_1(a,b) = e^{-\frac{1}{2}(a^2+b^2)} \sum_{n=0}^{\infty} (a/b)^n I_n(ab). \tag{A-12}$$

The parameters a, b, υ_1, and υ_2 must be related to the moments of X_k and Y_k, and to the constants A_D, B_D, and C_D. Like in [7], this is done by

$$\begin{aligned} a &= \left[\frac{2\upsilon_1^2 \upsilon_2 (\alpha_1 \upsilon_2 - \alpha_2)}{(\upsilon_1+\upsilon_2)^2} \right]^{1/2} \\ b &= \left[\frac{2\upsilon_1 \upsilon_2^2 (\alpha_1 \upsilon_1 + \alpha_2)}{(\upsilon_1+\upsilon_2)^2} \right]^{1/2} \end{aligned}, \tag{A-13}$$

$$\begin{aligned} \upsilon_1 &= \sqrt{w^2 + \frac{1}{4(\mu_{xx}\mu_{yy} - |\mu_{xy}|^2)(|C|^2 - A_D B_D)}} - w \\ \upsilon_2 &= \sqrt{w^2 + \frac{1}{4(\mu_{xx}\mu_{yy} - |\mu_{xy}|^2)(|C_D|^2 - A_D B_D)}} + w \\ w &= \frac{A_D \mu_{xx} + B_D \mu_{yy} + C_D \mu_{xy}^* + C_D^* \mu_{xy}}{4(\mu_{xx}\mu_{yy} - |\mu_{xy}|^2)(|C_D|^2 - A_D B_D)} \end{aligned}, \tag{A-14}$$

$$\begin{aligned} \alpha_1 &= 2(|C_D|^2 - A_D B_D)(|\overline{X}_1|^2 \mu_{yy} + |\overline{Y}_1|^2 \mu_{xx} - \overline{X}_1^* \overline{Y}_1 \mu_{xy} - \overline{X}_1 \overline{Y}_1^* \mu_{xy}^*) \\ \alpha_2 &= A_D |\overline{X}_1|^2 + B_D |\overline{Y}_1|^2 + C_D \overline{X}_1^* \overline{Y}_1 + C_D^* \overline{X}_1 \overline{Y}_1^* \end{aligned}. \tag{A-15}$$

Mathematically, the system model in the time domain is

$$y_k = x_k h_k + n_k, \tag{A-16}$$

where x_k and y_k are the transmitted and received signal constellation points (modulated data symbols), respectively, the h_k account for the correlated, complex-valued attenuation factors introduced by the frequency-selective radio channel, and the n_k denote samples of an AWGN process. $\hat{h}_k$ stands for the estimated attenuation factor of channel, i.e., the estimated value of h_k. Further, we get the following expressions

$$\begin{aligned}
&\overline{X}_1 = E\{\hat{h}_k\} \\
&\overline{Y}_1 = E\{y_k\} \\
&\mu_{xx} = \tfrac{1}{2}[E\{|\hat{h}_k|^2\} - |\overline{X}_1|^2], \\
&\mu_{yy} = \tfrac{1}{2}[E\{|y_k|^2\} - |\overline{Y}_1|^2] \\
&\mu_{xy} = \tfrac{1}{2}[E\{\hat{h}_k y_k^*\} - \overline{X}_1 \overline{Y}_1^*]
\end{aligned} \tag{A-17}$$

where $*$ denotes the complex conjugate.

For a more elaborate derivation of this error probability, go to references [3] and [7].

References

[1] Hanzo, L., Webb, W., Keller, T., *Single- and Multi-Carrier Quadrature Amplitude Modulation*, John Wiley & Sons, Ltd, 2000;

[2] Nee, R. v., Prasad, R., *OFDM for Wireless Multimedia Communications*, Artech House, 2000;

[3] Witrisal, Klaus, *OFDM Air-Interface Design for Multimedia Communications,* Ph.D thesis, Delft University of Technology, The Netherlands, 2002;

[4] Rodrigues, M.R.D., Darwazeh, I., O'Reilly, J.J., "Error probability behaviour of nonlinearly distorted OFDM signals" Electronics Letters, v9 , Issue 22, 30 Oct. 2003, p1620 – 1622;

[5] Wang, X, Tjhung, T.T., Ng, C.S., "Error probability performance of OFDM-ADSL systems", Global Telecommunications Conference, 1998. GLOBECOM 98. The Bridge to Global Integration. IEEE , v6 , 8-12 Nov. 1998, p3326 – 3331;

[6] Staley, T.L., Luo, J. X., Ku, W.H., Zeidler, J. R., "Error probability performance prediction for multichannel reception of linearly modulated coherent systems on fading channels", IEEE Transactions on Communications, v50, Issue 9, Sept. 2002, p1423 – 1428;

[7] Proakis, J. G., *"Digital Communications"*, 3rd Edition, McGraw Hill, 1995;

Appendix B

CDMA Modulation

B.1 Schematic of CDMA Systems

CDMA (Code Division Multiple Access) uses a "Spread Spectrum" to transmit signals with a bandwidth much larger than the signal bandwidth. Each user is assigned a code which spreads its signal bandwidth (as shown in Figure B.1-1) in such a way that only the same code can recover it at the receiver end. This method has the property that unwanted signals with different codes spread even more by this process, making them like noise to the receiver. All users exploit the whole frequency bandwidth all the time and they are differentiated by their unique codes.

In Figure B.1-1, the information-bearing signal $d(t)$ with bandwidth B_S multiplies with chip code $c(t)$ with bandwidth B_t and becomes the coded signal with bandwidth B_t. We can see from the figure that the information signal is multiplied with a wide-band signal of the chip code and becomes a wide-band signal. The energy spreads over a wide-band and the amplitude decreases. This figure presents the spreading property in the frequency domain. If $d_k(t)$, $c_k(t)$, $s_k(t)$denote the information-bearing signal before spreading, the chip code and the transmitted signal of the kth user, respectively, this process in the time domain can be expressed as

$$s_k(t) = d_k(t)c_k(t). \tag{B-1}$$

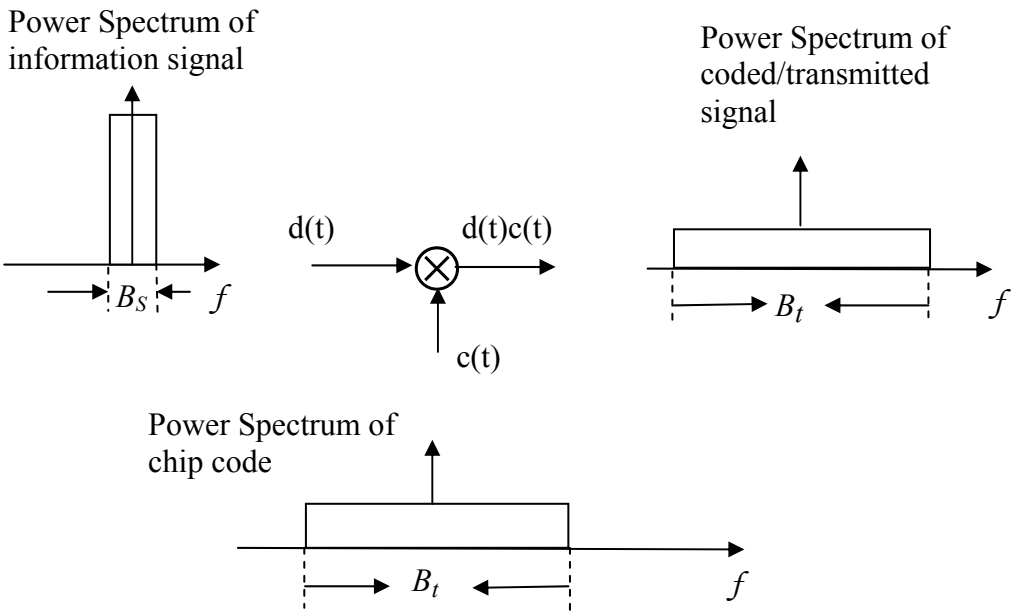


Figure B.1-1. Block diagram of spread spectrum

Figure B.1-1 describes the block diagram of a spread spectrum for one user, but in practice a spread spectrum system has more than one user. Figure B.1-2 shows the theory of how the system manages the multiple access of many users. We can see that the signal from other users is noise like after dispreading. In the figure, B_t is the bandwidth of the transmitted signal; B_S is the bandwidth of the information signal; η is the power spectrum density; and *Gp* is the processing gain, which equals the total transmit bandwidth divided by the signal bandwidth.

We have discussed CDMA in the frequency domain. Now let us take a look at it in the time domain. If $c_k(t)$ is the spreading waveform for the *k*th user, the spreading or code waveform is composed of N_{cd} chips, and if we assume BPSK for the spreading modulation, we have [1]

$$c_k(t) = \sum_{n=0}^{N_{cd}-1} c_{k,n} \prod(t - nT_{cd}), \tag{B-2}$$

where $c_{k,n} \in \{+1, -1\}$ and the chip pulse waveform $\prod(t)$ is a rectangular pulse of duration T_{cd}. If R_{cd} stands for the rate of chip code, we have

$$Bt = R_{cd} = \frac{1}{T_{cd}}, \tag{B-3}$$

where Bt is the bandwidth of the transmitted signal, as mentioned before. This equation relates the time domain parameter, i.e., the chip period, to the frequency domain parameter, i.e., the transmission bandwidth. In other words, the chip period limits the transmission bandwidth. With regard to the information-bearing signal, if R_S is the symbol rate and T_S the symbol period, we have a similar relation, namely,

$$R_S = \frac{1}{T_S}. \tag{B-4}$$

This equation relates the time domain parameter of an information-bearing signal, i.e., its symbol period, to its frequency-domain parameter, i.e., the symbol rate. It is straightforward to extend this relation to the bit rate R_b and bit period T_b for a certain modulation with modulation level M (M=2 for BPSK, 4 for QPSK, 16 for 16QAM, for example). We then get the following equations:

$$B_S = R_S = \frac{1}{T_S} \tag{B-5}$$

$$\begin{aligned} T_S &= T_b \log_2 M \\ R_b &= R_S \log_2 M \end{aligned}, \tag{B-6}$$

where B_S stands for the bandwidth of the information-bearing signal, as mentioned before. It is easy to see that in one symbol the number of bits is $\log_2 M$ for M level modulation.

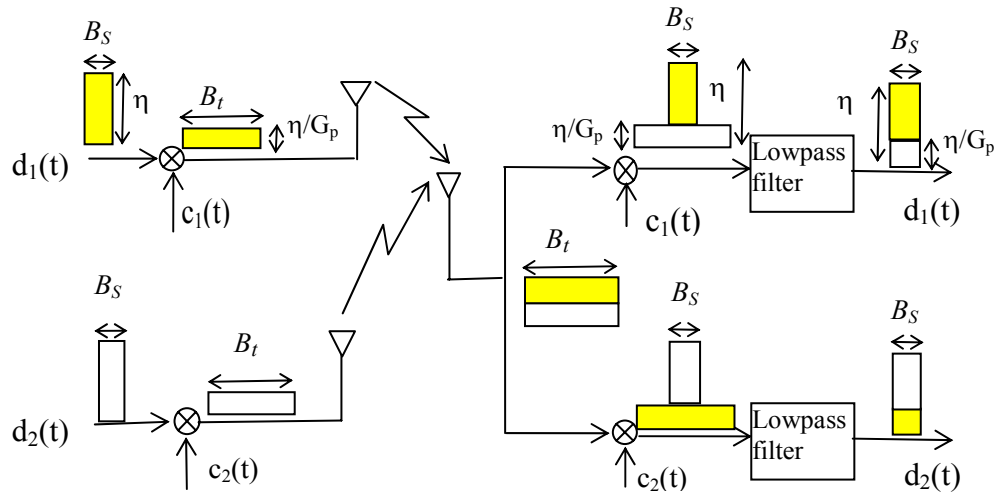


Figure B.1-2. Multiple accesses of two users in a spread spectrum system

Direct Sequence CDMA (DS-CDMA) is the best known Spread Spectrum Technique. Figure B.1-2 describes how DS-CDMA works. Each user is assigned a unique code sequence (spreading code) which the system uses to encode that user's information-bearing signal. The data signal is multiplied by a Pseudo Random Noise Code (PN code). A PN code is a sequence of chips valued -1 and 1 (polar) or 0 and 1 (non-polar) and has noise-like properties. This results in low cross-correlation values among the codes and makes it difficult to jam or detect a data message. The receiver, which has the code sequences of the user, decodes the received signal after reception and recovers the original data.

We use DS-CDMA in our work. Figure B.1-3 shows what happens to the data signal after it has been coded by the chip code in the time domain for BPSK modulation. We can see that the symbol period decreases greatly after the chip coding. Correspondingly the frequency spectrum increases in the frequency domain. Figure B.1-3 gives an example where the length of PN code N_{cd} is 7. The symbol period of the coded signal decreases to 1/7 of the original information-bearing signal. The bandwidth of the data signal is now multiplied by a factor N_{cd}. Hence, in direct-sequence systems, the length of the code is the same as the spreading factor (spreading factor will be introduced in Section B.2), that is [2],

$$Gp \approx N_{cd} . \tag{B-7}$$

The power, however, stays the same, which results in a lower power spectral density, as can be seen in Figure B.1-1. The generation of PN codes is relatively easy: a number of shift registers is all that is required. For this reason it is easy to introduce a large processing-gain in

Direct-Sequence systems. When the length of such a shift-register is L, the length of PN codes N_{cd} can be expressed as [3],

$$N_{cd} = 2^L - 1 . \tag{B-8}$$

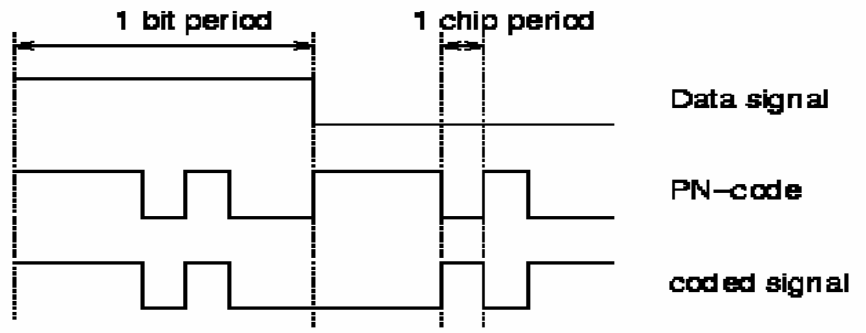


Figure B.1-3. Direct-Sequence (DS) spreading

B.2 CDMA Parameters

- Parameters in the Frequency Domain (FD)

From Figure B.1-1 and B.1-2 we can extract the CDMA parameters in the frequency domain: the bandwidth of the information-bearing signal B_S, the bandwidth of the transmitted signal Bt, the chip rate R_{cd}, and the symbol rate R_S (see Table B.2-1).

The ratio of the transmitted bandwidth to the information bandwidth is called the processing gain or spreading factor Gp of the spread-spectrum system [1], which can be given by

$$Gp = \frac{Bt}{B_S} . \tag{B-9}$$

Therefore, we get another parameter, i.e., the processing gain Gp. The processing gain limits the number of users that can be allowed in a system, it determines how much the multipath effect is reduced, and how difficult it is to jam or detect a signal etc. For spread spectrum systems it is advantageous to have a processing gain as high as possible for better transmission QoS.

By combining equation (B-3), (B-4), (B-7), and (B-9), we can get

$$Gp = \frac{Bt}{B_S} = \frac{R_{cd}}{R_S} = \frac{T_S}{T_{cd}} \approx N_{cd}\,, \tag{B-10}$$

where N_{cd} denotes the length of PN codes; T_{cd} and R_{cd} stand for the period and the rate of chip code respectively; B_S, T_S, and R_S stand for the bandwidth, period and rate of the symbol of the information-bearing signal, respectively; and Bt denotes the bandwidth of the transmitted signal.

Like for OFDM systems, in principle for CDMA systems the total available bandwidth is also limited, i.e., the total available bandwidth can be seen as a constant parameter. If the total available bandwidth is always exploited for transmission, the transmission bandwidth Bt is a constant parameter. Hence, the parameter(s) used to design in the frequency domain should be the bandwidth of the information signal or the processing gain Gp for an adaptive CDMA system based on equation (B-9). These are listed in Table B.2-1.

- Parameters in the time domain

From Figure B.1-3 we obtain the CDMA parameters in the time domain: the chip period T_{cd}, and the symbol period T_S. From equation (B-10) we can see that the symbol period is Gp times the chip period. Equation (B-3) and (B-4) give the relationship between these parameters and the parameters in the frequency domain. The processing gain, hence, restricts the relationship of the parameters in the time domain as well as those in the frequency domain.

- Other parameters

CDMA is a multi-user access system, so the number of users N_u is an important specification in CDMA systems. Like for other modulations, the general modulation parameters, i.e., the modulation level M and coding rate R_c should be considered in the system design.

Table B.2-1. CDMA parameters and their relationship

Domain	Parameters	relations	Parameters to design
FD	B_S, Bt, R_S, R_{cd}, Gp, R_b	$Bt = Gp \times B_S$ $Bt = R_{cd}$ $B_S = R_S = \frac{R_b}{\log_2 M}$	Gp
TD	T_S, T_{cd}, T_b	$T_S = GpT_{cd}$ $T_{cd} = \frac{1}{R_{cd}}$ $T_S = \frac{1}{R_S} = T_b \log_2 M$	none
Other parameters	N_u, M, R_c		N_u, M, R_c

B.3 Signal to Interference plus Noise Ratio (SINR) Analysis for CDMA Systems

In a CDMA system the channel influence includes noise and interference. The system capacity of a traditional CDMA system is interference limited. Traditional CDMA systems are all self-interference systems. Three types of interference are usually considered: Inter Symbol Interference (ISI), which is created by the multi-path replica of the useful signal itself; Mutual (or Multiple) Access Interference (MAI), which is interference created by the signals and their multipath replica from other users in the same cell on the useful signal; and Adjacent Cell Interference (ACI), which is the influence of all the interfering signals from adjacent cells on the useful signal. ISI can be contributed to the signal energy by sequential detection and adding the delayed versions to the signal energy. Since the ACI is small compared to the MAI, many researchers did not consider ACI in their analysis [4]. For the same reason we do not include ISI and ACI in our work either.

A traditional CDMA system has a normalized signal interference ratio (E_S/N_J) of [4]

$$\frac{E_S}{N_J} = \frac{Gp}{N_u - 1}, \tag{B-11}$$

where E_S is the received symbol energy [Joula]; N_J is the received interference power spectrum density (W/Hz); Gp is the processing gain or spreading factor; and N_u is the number of users per sector. Therefore in a CDMA system the number of users per sector limits the channel signal-to-interference ratio according to this formula. In other words, if we regard the

signal-to-interference ratio as a channel parameter instead of as just being influenced by the channel parameters, the CDMA modulation parameter can influence the channel situation, unlike in other modulation systems.

In CDMA systems, the channel situation can be represented by the normalized Signal to Interference plus Noise Ratio (SINR), which is

$$SINR = \frac{E_S}{N_J + N_0}, \tag{B-12}$$

where N_0 is the received noise power spectrum density (W/Hz). If we only consider MAI and ignore other interference, we can use equation (B-11) and (B-12) to obtain

$$N_0 = \frac{E_S}{SINR} - N_J = \frac{E_S}{SINR} - \frac{E_S}{Gp/(Nu-1)} = E_S(SINR^{-1} - \frac{N_u - 1}{Gp}). \tag{B-13}$$

In traditional CDMA systems, the signal power and inference power are much greater than the local noise. Hence, Viterbi, Simon, Omura, Scholtz, and Daben Li [4] etc. all assume that SINR=SIR in their analyses.

B.4 Error Probability Analysis

Here we will analyze the error probability of DS-CDMA systems over Rician fading channels since we exploit Rician fading channel in our work. Rayleigh fading is considered as a special case with Rician *K* factor equal to zero of Rician fading. There are some investigations on the derivation of the error probability for CDMA systems, e.g., [5], [6], [7], [8].

We consider a channel impulse response like that described in equation (2.15) in Chapter 2, which we repeat here,

$$h(\tau;t) = \sum_{i=1}^{N_p} \rho_i(t) e^{j\theta_i(t)} \delta(\tau - \tau_i(t)),$$

where $\rho_i(t), \theta_i(t), \tau_i(t)$ denote the amplitude, phase and excess delay for the *i*th received pulse, respectively; τ represents the excess delay, whereas the *t* dependence represents the changes with time in the very structure of the impulse response; and $\delta(\bullet)$ is the Dirac Delta function. N_p stands for the number of multipath rays and can be given as

$$N_p = [\frac{\sigma_{\max}}{T_{cd}}] + 1, \tag{B-14}$$

where $\sigma_{\max}$ denotes the maximum delay and T_{cd} the chip period. [Q] stands for the largest integer smaller than Q here.

Following the derivation in [8], if the normalized receive power (NRP) is assumed to be one, the error probability of DS-CDMA systems in an AWGN channel with interference can be given as

$$P_e = \frac{1}{2} erfc\left[\frac{\sqrt{2P_r}T_b}{\sqrt{2}\sigma_{tot}}\right], \tag{B-15}$$

where T_b stands for the bit duration of the information signal, and $2P_r$ for the instantaneous received power. If only the interference from the other users in the same cell is considered in the error probability analysis and the interference follows Gaussion distribution, σ_{tot} can be given as

$$\sigma_{tot}^2 = \sigma_n^2 + \sigma_{\text{int}}^2, \tag{B-16}$$

where σ_n^2 denotes the AWGN noise power; σ_{int}^2 denotes the interference power and can be written as [8]

$$\sigma_{\text{int}}^2 = \frac{2P_O T_b^2}{3Gp}\{1 + \frac{1}{K} + N_u(1 + \frac{N_P}{K})\}, \tag{B-17}$$

where K stands for the Rician K factor; $2P_O$ denotes the power of the LOS component; N_u the number of active users in one cell; and Gp the processing gain of the CDMA system; and N_p the number of multipath rays.

The fading of the amplitude of the received signal follows a Rician PDF as in equation (2.13) in Chapter 2 which we repeat here:

$$p(r) = \begin{cases} \frac{r}{\sigma^2} e^{-\frac{(r^2+A^2)}{2\sigma^2}} I_0(\frac{Ar}{\sigma^2}) & (A \geq 0, r \geq 0), \\ 0 \qquad (r < 0) \end{cases}$$

where A is the peak amplitude of the dominant signal and $I_0(\bullet)$ the modified Bessel function of the first kind and zero order. By averaging the error probability of equation (B-15) over this Rician PDF, we can give the error probability of DS-CDMA systems with AWGN noise and inter-cell Multiple Access Interference (MAI) over Rician fading channels as

$$P_e = \frac{1}{2}\int_0^{\infty} erfc\left[\frac{\sqrt{P_r T_b}}{\sigma_{tot}}\right]\frac{K}{P_O}\exp\left[-\frac{K(P_r+P_O)}{P_O}\right]I_0\left[\frac{2K\sqrt{P_r P_O}}{P_O}\right]dP_r . \quad \text{(B-18)}$$

References

[1] Prasad, R., *CDMA For Wireless Personal Communications*, Artech House Publishers, 1996;

[2] Viterbi, A. J., *CDMA Principles of Spread Spectrum Communication*, Addison-Wesley,1995;

[3] Dixon, Robert C., *Spread Spectrum Systems*, 1984;

[4] Li, D., "The Perspectives of Large Area Synchronous CDMA Technology for the Fourth-Generation Mobile Radio" IEEE Communications Magazine. March 2003;

[5] Solaiman, B., Glavieux, A., Hillion, A., "Error probability of fast frequency hopping spread spectrum with BFSK modulation in selective Rayleigh and selective Rician fading channels", IEEE Transactions on Communications, v38, Issue: 2 , Feb. 1990, p233 – 240;

[6] Qu, S., Sheikh, A.U., "An analysis of error probability of a cellular CDMA downlink with M-ary DPSK in a Rician/Rayleigh fading environment", 2nd International Conference on Universal Personal Communications, 1993. 'Personal Communications: Gateway to the 21st Century'., v2, 12-15 Oct. 1993, p965 – 969;

[7] van Nee, D. J. R., Misser, H. S., Prasad, R., "Bit Error Probability For Direct-Sequence Spread-Spectrum In A Shadowed Rician Fading Land Mobile Satellite Channel With Diversity", IEEE International Symposium on Personal, Indoor and Mobile Radio Communications., 23-25 September 1991, p125 – 130;

[8] Misser, H. S., Prasad, R., "Bit Error Probability Evaluation of a Microcellular Spread-Spectrum Multiple Access System in a Shadowed Rician Fading Channel", IEEE 42nd Vehicular Technology Conference, 10-13 May 1992, p439-442, vol.1, Denver, CO, USA;

Appendix C

Results of Capacity and Output SNR of Different MIMO Systems

In this Appendix we give some simulation results of Cumulative Distribution Function (CDF) versus Capacity and CDF versus Output SNR for different MIMO systems for different Input SNR values. All of these simulations are based on the method and formulas provided in the reference.

C.1 Formulas of Output SNR and Capacity of Different MIMO Systems

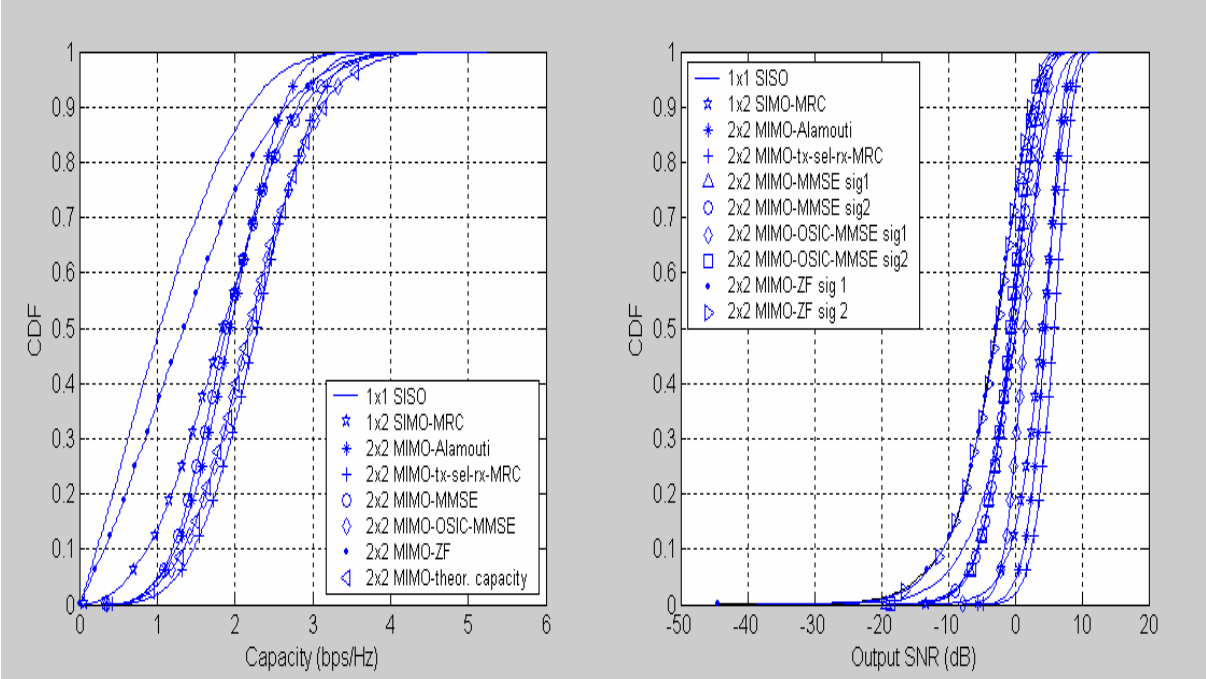
The table below gives the theoretical results of the output SNR for different systems [1].

TABLE I
SUMMARY OF ALL SYSTEMS STUDIED (P = TOTAL TRANSMIT POWER, h_{ij} = INSTANTANEOUS PATH GAIN FROM TRANSMIT ANTENNA j TO RECEIVE ANTENNA i)

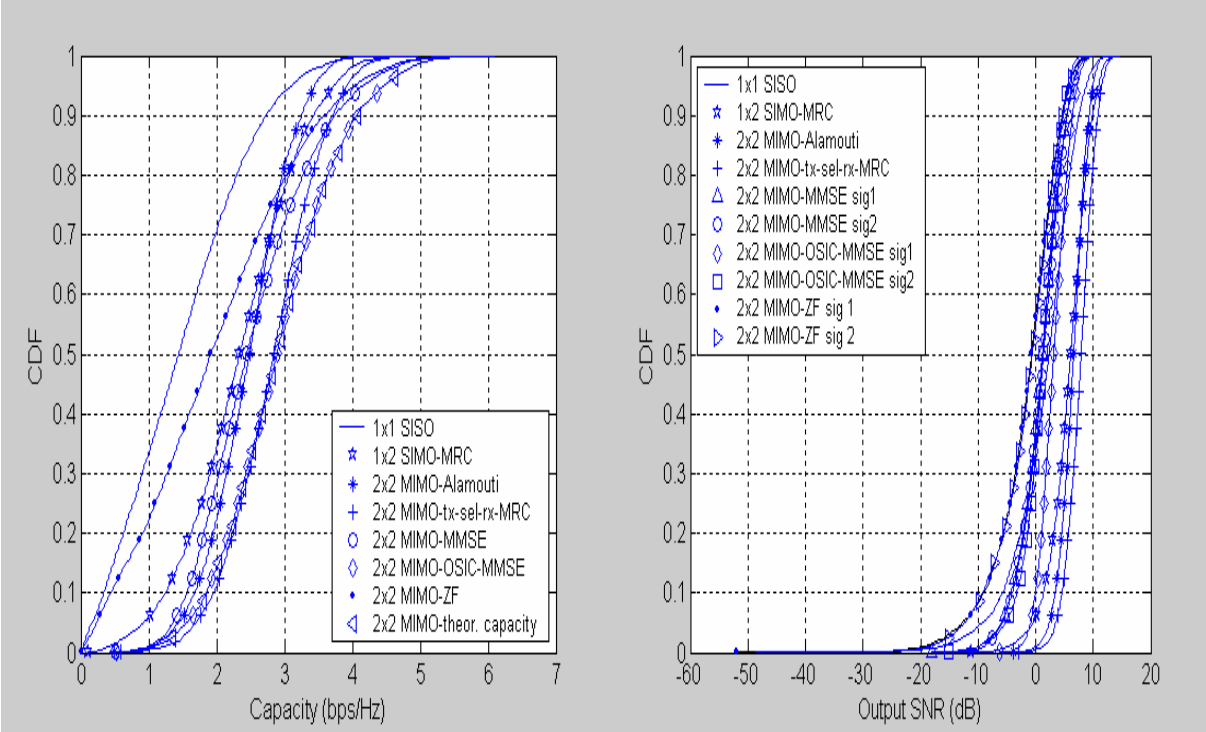
System	Signal Power per tx ant.	Diversity order	Post-proc. SNR	Capacity (ideal coding)
1 x 1	P	1	$\gamma = \lvert h\rvert^2 P/\sigma^2$	$\log_2(1+\gamma)$
1 x 2 MRC $H = [h_1 \quad h_2]^T$	P	2	$\gamma_{1x2mrc} = \gamma_1 + \gamma_2$ where $\gamma_i = \lvert h_i\rvert^2 P/\sigma^2$	$\log_2(1+\gamma_{1x2mrc})$
2 x 2 Alamouti (⇔ 1 x 4 MRC ½ power)	$P/2$	4	$\gamma_{2x2A} = (\gamma_{11}+\gamma_{12}+\gamma_{21}+\gamma_{22})/2$ where $\gamma_{ij} = \lvert h_{ij}\rvert^2 P/\sigma^2$	$\log_2(1+\gamma_{2x2A})$
2 x 2 tx-sel-rx-MRC	P	2<div<4	$\gamma_{2x2sel} = \max\{(\gamma_{11}+\gamma_{21}), (\gamma_{12}+\gamma_{22})\}$	$\log_2(1+\gamma_{2x2sel})$
2 x 2 MIMO MMSE 2 x 2 channel matrix $H = \begin{bmatrix} h_{11} & h_{12} \\ h_{21} & h_{22} \end{bmatrix} = [\underline{h}_1 \quad \underline{h}_2]$	$P/2$	1	$\gamma_{i,mimo_mmse} = \underline{h}_i^H R_i^{-1} \underline{h}_i$ $i = 1, 2$ $R_i = \underline{h}_j \underline{h}_j^H + \frac{2\sigma^2}{P} I_2$ $j \neq i \quad I_2 = \begin{bmatrix} 1 & 0 \\ 0 & 1 \end{bmatrix}$	$\sum_{i=1}^{2} \log_2(1+\gamma_{i,mimo_mmse})$
2 x 2 MIMO OSIC-MMSE	$P/2$	signal 1: 1, signal 2: 2	$\gamma_{1,mimo_osic_mmse} = \max_{i=1,2}\{\gamma_{i,mimo_mmse}\}$ if k index of max $\gamma_{2,mimo_osic_mmse} = \frac{\underline{h}_j^H \underline{h}_j P}{2\sigma^2}$ $\le \frac{\gamma_{1x2mrc}}{2}; \; j \neq k$	$\sum_{i=1}^{2} \log_2(1+\gamma_{i,mimo_osic_mmse})$
2 x 2 MIMO ZF	$P/2$	1	$\gamma_{i,mimo_zf} = P/(2\sigma^2 \lvert \underline{w}_i^H \rvert^2)$ $W^H = H^{-1}; i = 1, 2$	$\sum_{i=1}^{2} \log_2(1+\gamma_{i,mimo_zf})$

C.2 Simulation Results of CDF of Capacity and Output SNR

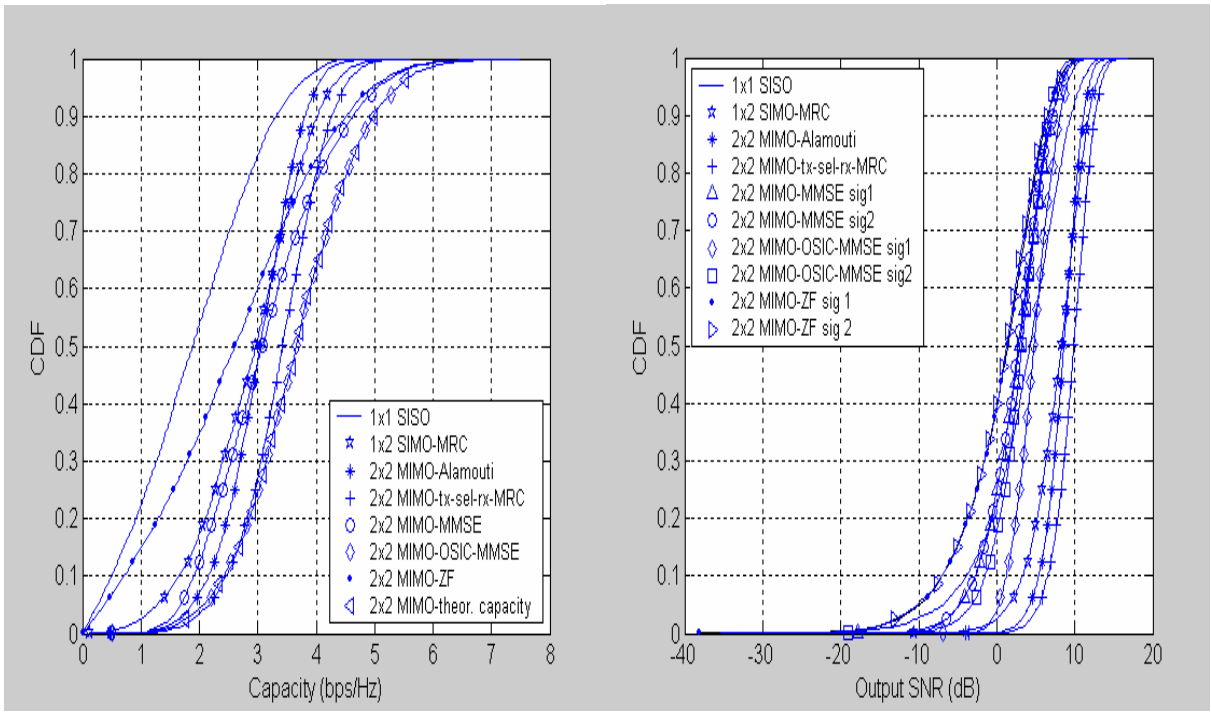
The value of the input SNR is 2 dB



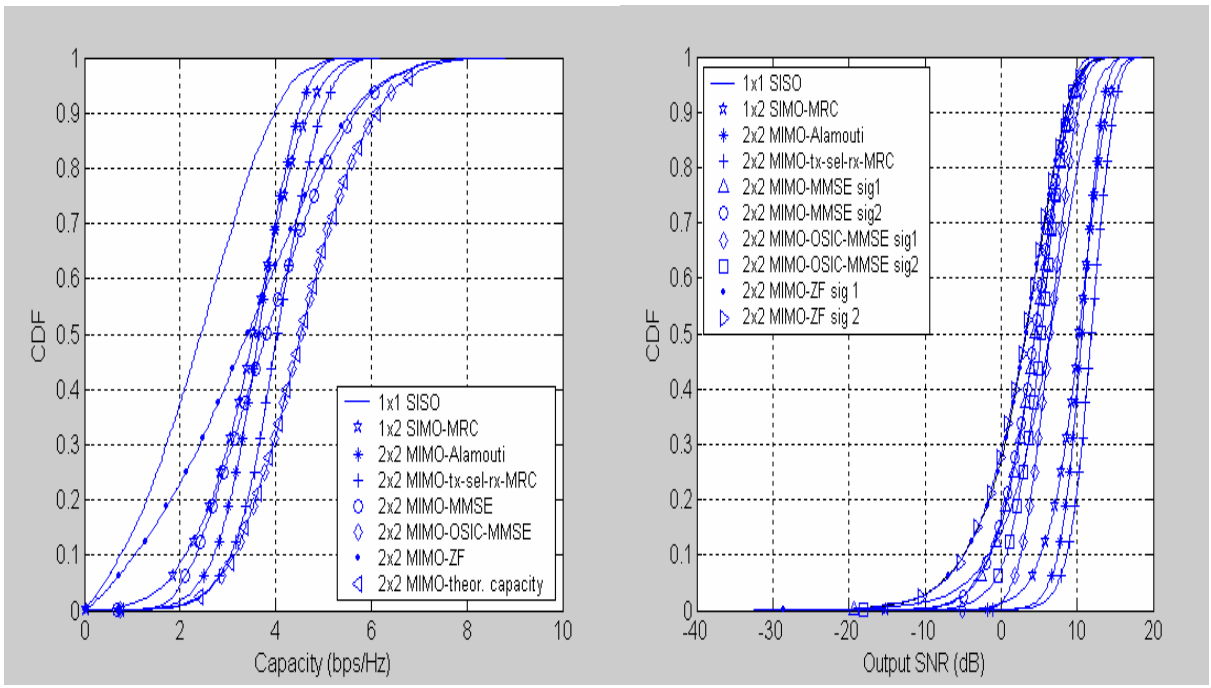
The value of the input SNR is 4 dB



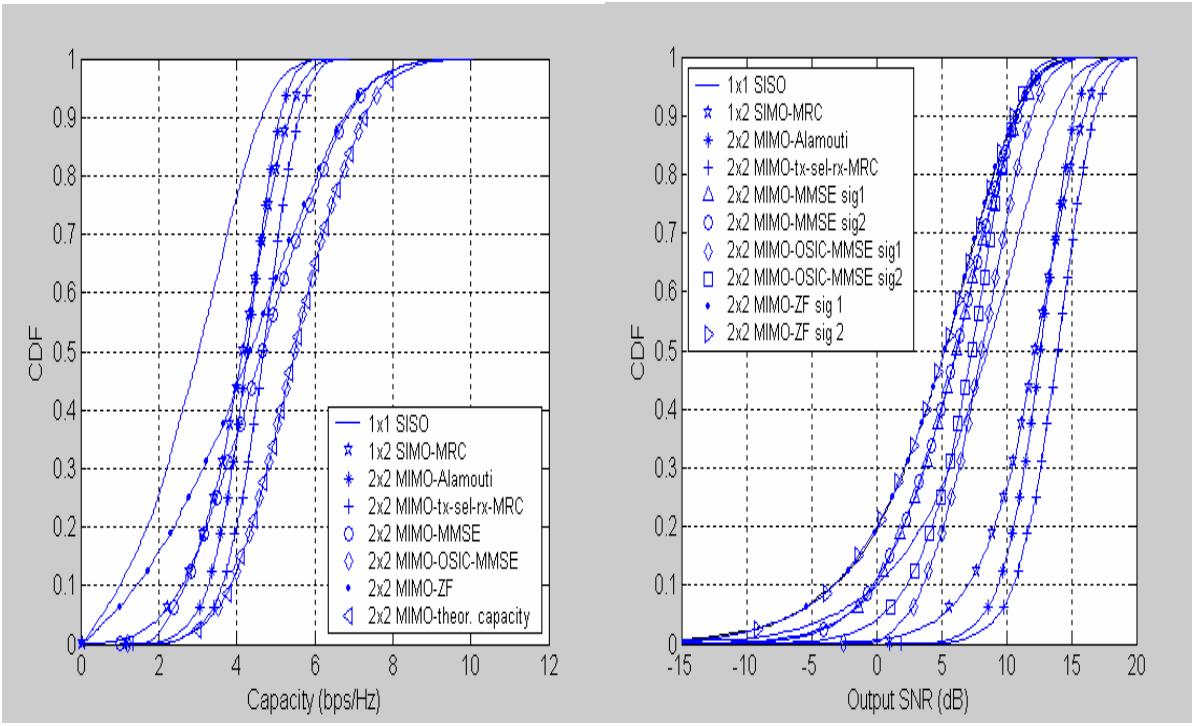
The value of the input SNR is 6dB



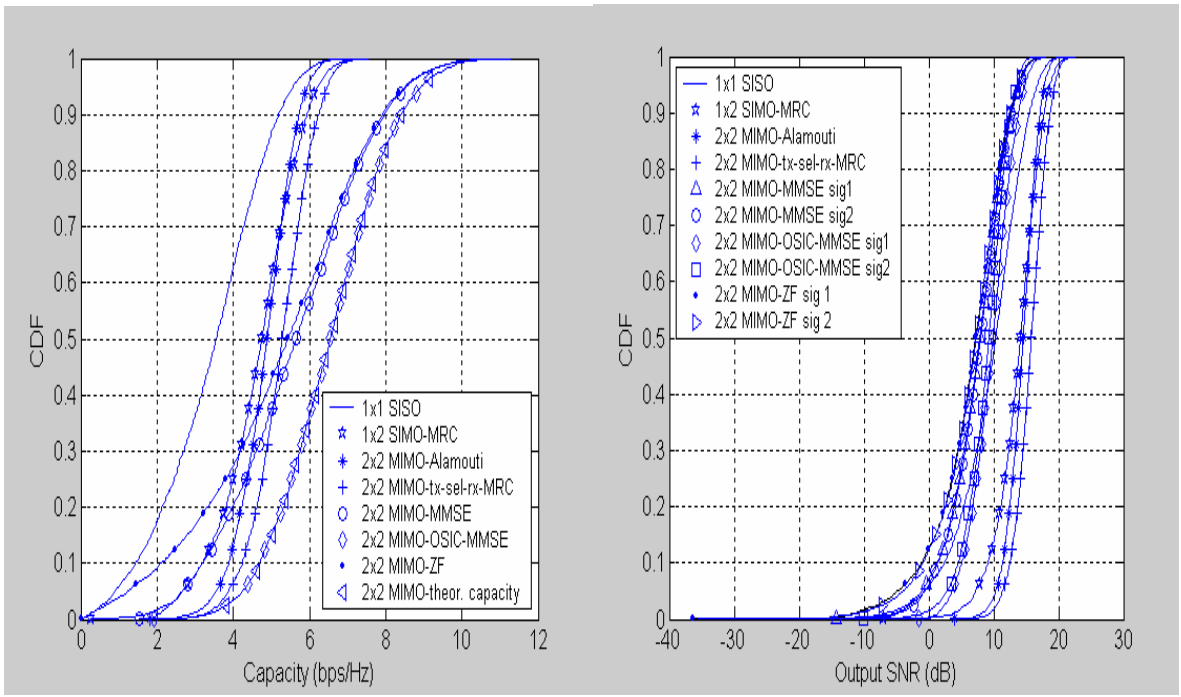
The value of the input SNR is 8dB



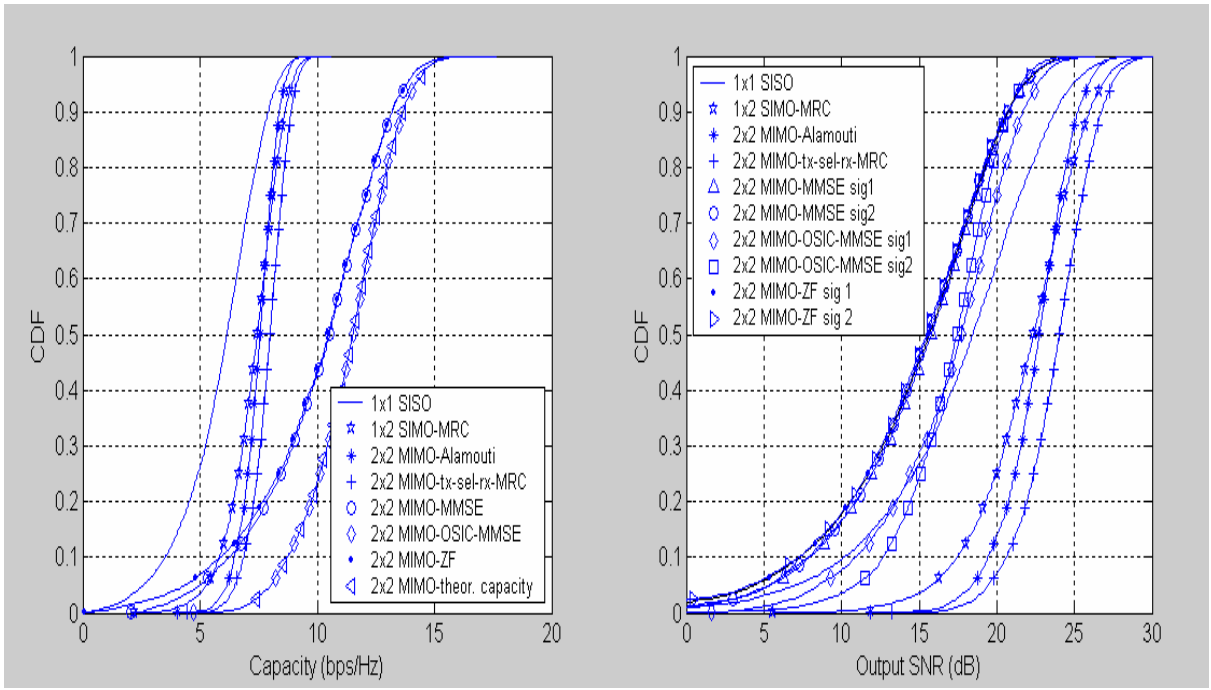
The value of the input SNR is 10dB



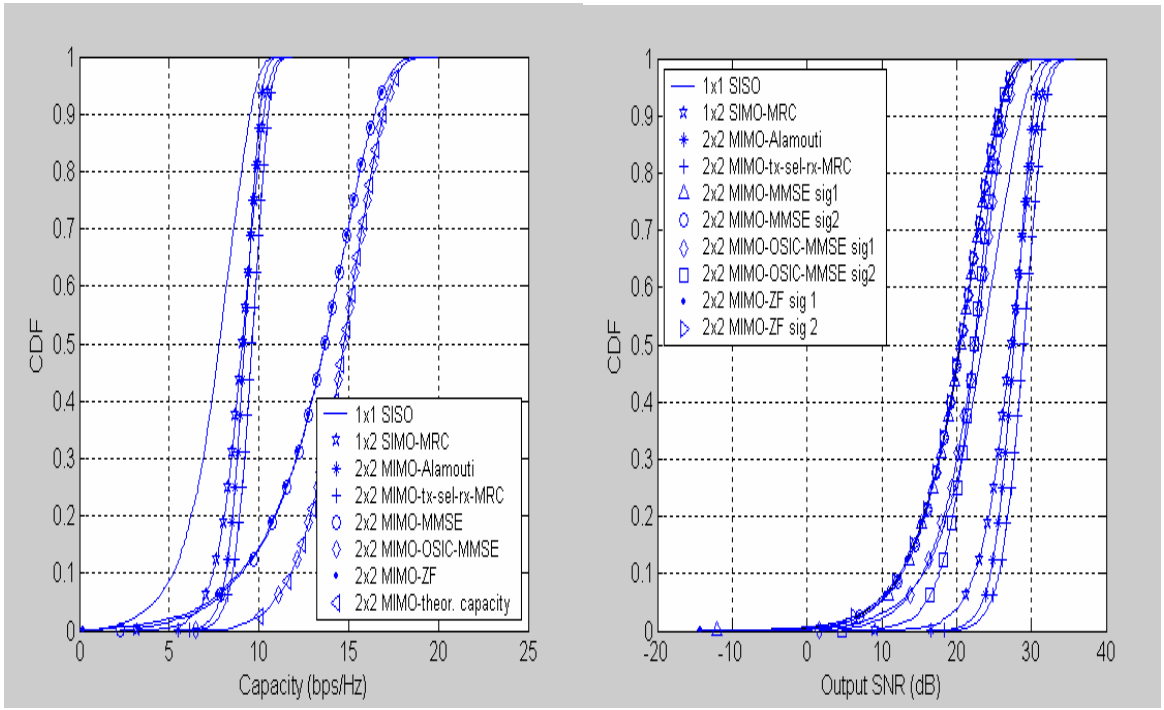
The value of the input SNR is 12dB



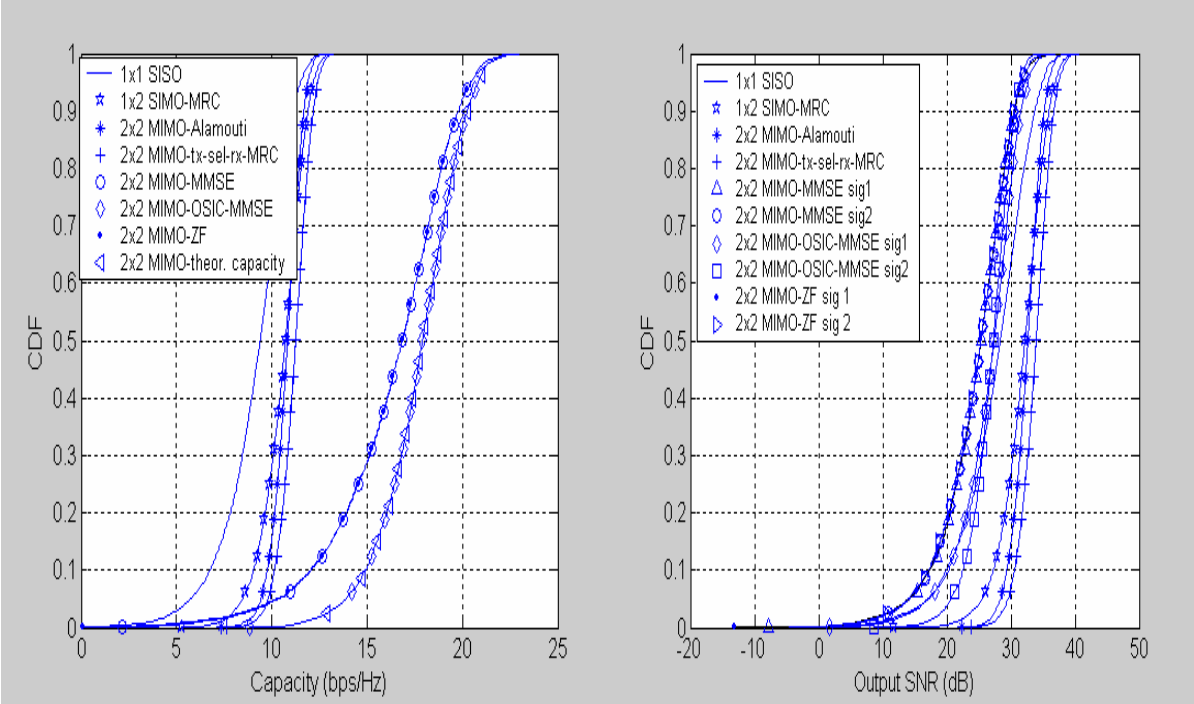
The value of the input SNR is 20dB



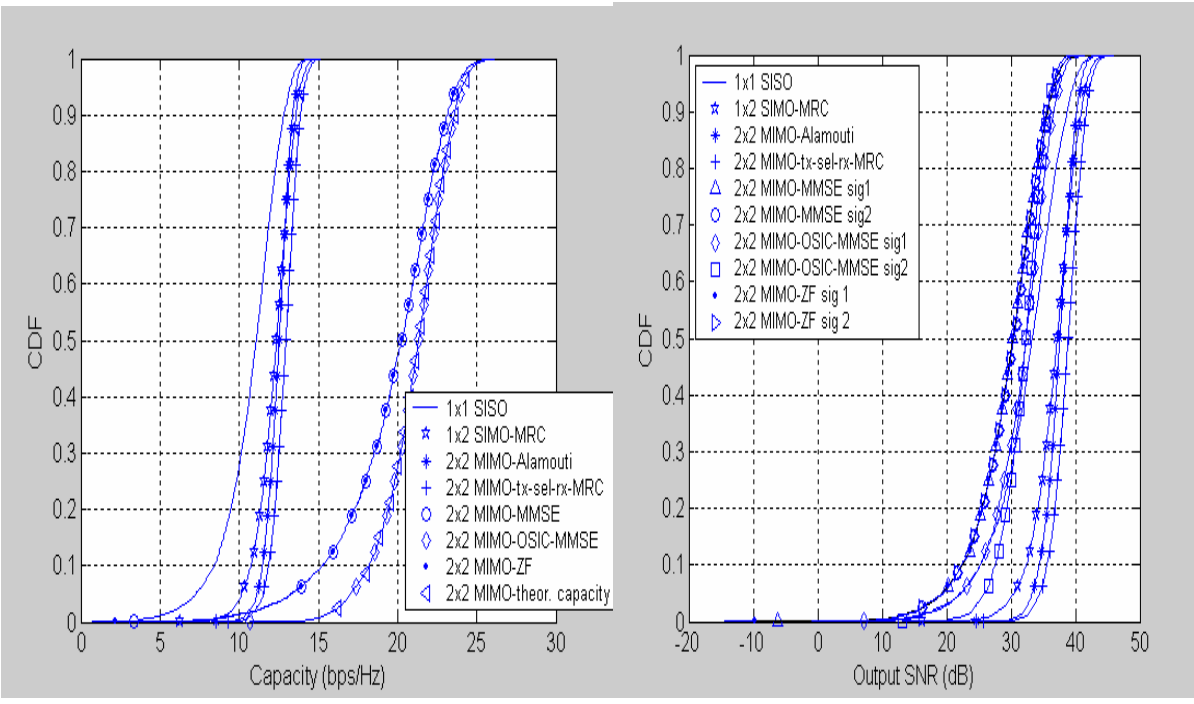
The value of the input SNR is 25dB



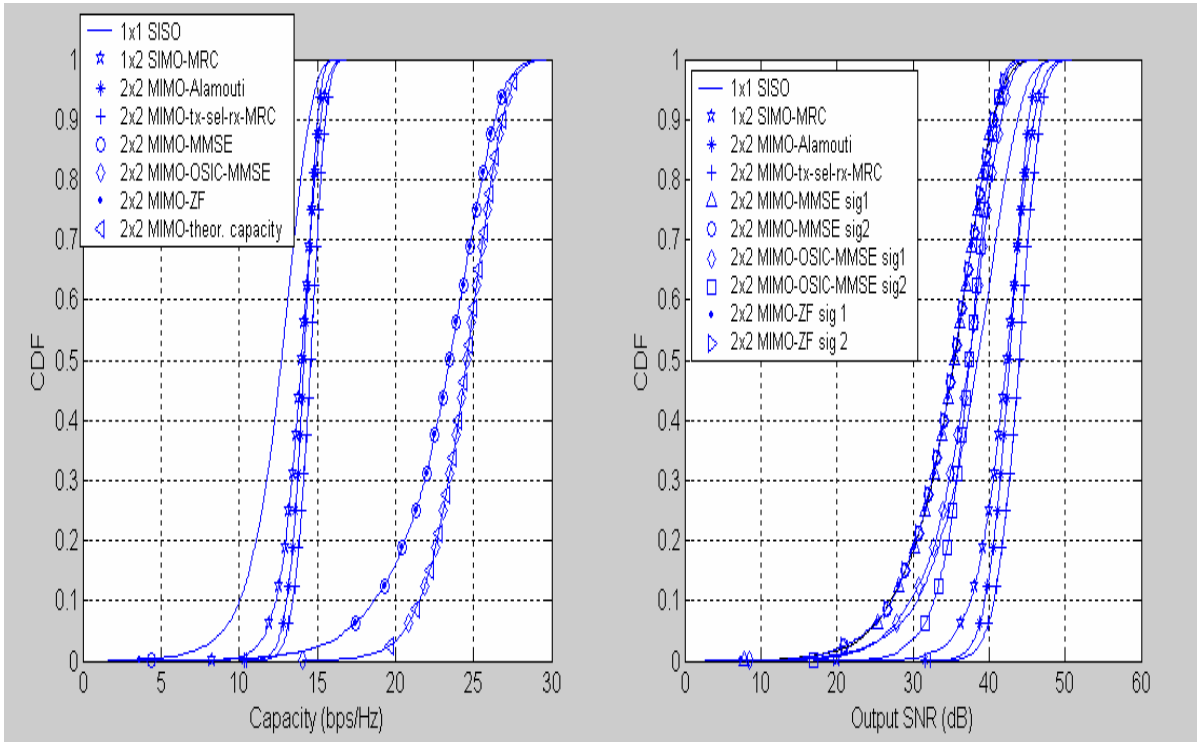
The value of the input SNR is 30dB



The value of the input SNR is 35dB



The value of the input SNR is 40dB



References

[1] David Gesbert, Mansoor Shafi, “From Theory to Practice: An Overview of MIMO Space Time Coded Wireless Systems” IEEE Journal on selected areas in Communications, vol. 21, No. 3, April 2003.

Publications by the Author

Journal Papers

1. H.Che, A.Nassereddine, H. Nikookar, R.Prasad, L.P.Ligthart, "Combining Adaptive MIMO into Adaptive OFDM", submitted to IEEE Transactions on Wireless Communications;

2. H.Che, R.Prasad, L.P.Ligthart, "Strategies for Adaptive Modulation Algorithms and Three Subband Settings for Adaptive OFDM Algorithms", submitted to IEEE Communications Magazine;

3. H.Che, R.Prasad, L.P.Ligthart, "A Strategy for Adaptive Modulation Algorithms Using Rician *K* Gain of MIMO", submitted to IEEE Microwave and Wireless Components Letter;

4. H.Che, A.Nassereddine, H. Nikookar, R.Prasad, L.P.Ligthart, "Performance Gain of MIMO System for Adaptive Modulation Algorithm", submitted to IEEE Transactions on Vehicular Technology;

Conference Papers

5. H.Che, L.P.Ligthart, R.Prasad, "Adaptive CDMA Algorithms for MIMO Channels", submitted to Wireless Personal Multimedia Communications Conference (WPMC) 2005, Aalborg, Denmark; September 2005;

6. H.Che, A.Nassereddine, H.Nikookar, R.Prasad, L.P.Ligthart, "Another Parameter Representing QoS Gain of MIMO System" European Microwave Week-European Conference on Wireless Technology (ECWT) 2004, Amsterdam, the Netherlands; October 2004;

7. H.Che, L.P.Ligthart, R.Prasad, "Working Conditions for an Influencing Factor on the Performance of Adaptive OFDM System under a Varying Channel", The 14th IEEE

International Symposium on Personal, Indoor and Mobile Radio Communications (PIMRC 2003), Beijing, China; September 2003;

8. H.Che, L.P.Ligthart, R.Prasad, “Influencing Factor for OFDM System Performance in a Varying Channel”, 2002 International Conference on Software, Telecommunications and Computer Networks, Split, Croatia; October 2002;

9. H.Che, L.P.Ligthart, R.Prasad, “A Throughput Formula for Adaptive OFDM System”, 5th IEEE Malaysia International Conference on Communications - MICC Conference, P299-303; Kuala Lumpur, Malaysia; October 2001;

10. H.Che, M.Hajian, L.P.Ligthart, R.Prasad, “Software radio is walking into implementation stage”, 12th Tyrrhenian International Workshop on Digital Communications "Software Radio Technologies and Services", Portoferraio, Italy; September 2000, invited paper;

Reports

11. H. Che, “An Adaptive CDMA Algorithm and its Simulation Results”, *Project B3G*, 4th (Final) Progress Report, Deliverable D 1.4.3, Delft University of Technology, Dec. 2004;

12. H. Che, “Strategies of Adaptive CDMA Algorithms”, *Project B3G*, 3th Progress Report, Deliverable D 1.3.3, Delft University of Technology, Oct. 2004;

13. H. Che, “MIMO Technology towards Utilisation of Adaptive CDMA”, *Project B3G*, 2th Progress Report, Deliverable D 1.2.3, Delft University of Technology, Feb. 2004;

14. H. Che, “Adaptive CDMA Investigation and Proposal for B3G Project”, *Project B3G*, 1th Progress Report, Deliverable D 1.1.4, Delft University of Technology, Feb. 2003;

15. H. Che, “Adaptive OFDM in Rician Fading Channels”, Ph.D Progress Report, Delft University of Technology, Jun. 2002;

16. H. Che, “Adaptive Reconfigurable OFDM in AWGN Channels”, Ph.D Progress Report, Delft University of Technology, Mar. 2001;

17. H. Che, “Proposal of Adaptive Modulation using WCDMA for Software Radio Testbed Project”, Progress Report, Delft University of Technology, Apr. 2000;

18. H. Che, “Overview of Adaptive Modulation”, Progress Report, Delft University of Technology, Mar. 2000;

Publication Cross-reference Table

The thesis is based, in part, on the publications listed in the previous sections. The following table indicates the relevance of the publications to the chapters within the thesis.

Publication	Ch. 1	Ch. 2	Ch. 3	Ch. 4	Ch. 5	Ch. 6
1.					◙	
2.			◙		◙	
3.			◙	◙		
4.				◙		
5.					◙	
6.				◙		
7.			◙			
8.			◙			
9.			◙			
10.	◙					
11.					◙	
12.			◙			
13.				◙		
14.	◙		◙			
15.		◙	◙	◙		
16.			◙			
17.	◙		◙			
18.		◙	◙			

Samenvatting

Het doel van dit proefschrift is het bestuderen van zichzelf-aanpassende modulatie-algoritmes voor systemen met één ingang en één uitgang ("Single Input/Single Output" ofwel SISO) en voor systemen met meerdere ingangen en meerdere uitgangen (Multiple Input/Multiple Output ofwel MIMO). De zichzelf-aanpassende modulatie techniek heeft de voordelen van flexibiliteit en het zorgen voor een hoge transmissiekwaliteit en doorvoersnelheid; daarnaast kan door toepassing van genormde algoritimes de radio hardware kleiner van format worden. De strategie voor deze zichzelf aanpassende modulatietechniek en zijn werkprocedures zijn nog niet beschreven in de literatuur. Wij introduceren zo'n strategie en bij behorende werkprocedures in dit proefschrift. Daarnaast wordt er hier voor het eerst voorgesteld dat de ontwikkeling van een zichzelf-aanpassende modulatie uit drie fases bestaat, waarin het aanpassingsvermogen elke keer op een hoger niveau wordt gebracht.

In dit proefschrift tonen wij aan dat zichzelf-aanpassende modulatie-algoritmes twee aspecten met zich meebrengen: het kanaal en type modulatie. We onderzoeken twee soorten kanalen: SISO- en MIMO-kanalen. We bestuderen het SISO kanaal in tijddomein, frequentiedomein, en domein van een 3 dimensionale ruimte, hetgeen practisch blijkt te zijn bij het ontwerpen van zichzelf-aanpassende modulatie-algoritmes. Verder stellen we drie technieken voor die een oplossing vormen voor de problemen in de verschillende domeinen: een techniek die zichzelf-aanpassende modulatie toelaat, een OFDM- en een MIMO-techniek. Deze drie technieken worden diepgaand onderzocht in dit proefschrift. We bestuderen het concept, de structuur en de karakteristieken van MIMO-kanalen. De verbeteringen van drie MIMO-schema's en de parameters die deze verbeteringen beïnvloeden worden gebruikt voor het trekken van algemene conclusies. Bovendien introduceren we een nieuwe factor, de zogenoemde Rician gain factor, om de verbeteringen van het MIMO-schema ten opzichte van SISO te kwantificeren. Daarnaast zoeken we uit wat de SNR (signaal/ruis-verhouding) verbeteringen zijn van deze drie MIMO-schema's vergeleken met die van SISO-kanalen voor een groot bereik in SNR; Dergelijk onderzoek is met eerder beschrijven in de literatuur en is onontbeerlijk voor het ontwerpen van zichzelf aanpassende modulatie-algoritmes voor MIMO-kanalen.

Wat betreft modulatie, worden parameters van OFDM en CDMA modulaties voor de zichzelf aanpassende OFDM en CDMA algoritmes geinventariseerd. Om directe relaties tussen modulatieparameters en datasnelheid per eenheid van bandbreedte te bepalen, leiden we afzonderlijke formules af voor OFDM- en CDMA. We tonen aan dat de algemene veronderstelling dat de bandbreedte van de hulpdraaggolf de transmissiekwaliteit beïnvloedt

juist is voor een kanaal met een constante RDS. Om dit uit te leggen, definiëren we een nieuwe parameter, P_{FR}, als het product van de bandbreedte van de hulpdraaggolf, Δf, en de RDS. In dit proefschrift beschrijven we hoe deze parameter werkt en welke factoren het effect van deze parameter beperken.

Daarna introduceren we drie succesvolle zichzelf-aanpassende modulatie-algoritmen, dat wil zeggen: een zichzelf-aanpassend OFDM-algoritme voor SISO-kanalen, een zichzelf-aanpassend OFDM-algoritme voor MIMO-kanalen, en een zichzelf-aanpassend CDMA-algoritme voor MIMO-kanalen. In dit werk nemen we aan dat het radio kanaal perfect wordt geschat. Voor de zichzelf aanpassende OFDM-algoritmen introduceren we drie instellingen voor subbands. Met deze zichzelf-aanpassende modulatie-algoritmes zijn in simulaties opmerkelijke toenames in de maximum datasnelheid per eenheid van bandbreedte verkregen. We introduceren het idee om meer dan één MIMO-schema te gebruiken in een systeem en deze schema's aan te passen met gebruik van onze nieuwe zichzelf-aanpassende modulatie-algoritmes. Simulatieresultaten laten zien dat met deze methode hogere uitnutting van het radio kanaal kunnen worden behaald. De mate waarin onze algoritmes de prestatie verhogen hangt af van de omstandigheden van het kanaal. De invloed van de kanaalparameters op deze relatieve winsten wordt ook onderzocht in dit werk. Tevens introduceren we een "SNR-grenswaardenmatrix" voor het instellen van "processing gain" en modulatieniveau in het zichzelf-aanpassende CDMA-algoritme voor MIMO-kanalen.

Acknowledgement

The author is indebted to many people who directly or indirectly have contributed to her Ph.D work.

First of all, the author would like to express great gratitude to her promoter, Prof. Leo Ligthart, for his strong and effective support, and for teaching a lot, not only in work, but also in life. The author believes that what she learnt during the period of her Ph.D work will be very important for her future. Working together with such a father-like promoter has been one of the blessings in her life. The author owes gratitude to her co-promoter, Prof. Ramjee Prasad as well, for his guidance to finish the work successfully. Moreover, the author is grateful to Dr. Homayoun Nikookar for reviewing this thesis and for the discussions between him and the author.

The author wishes to acknowledge her room-mate, D.P. Tran, for discussing professional and private matters with her. The author owes gratitude to Cristian Coman, Vsevolod Kovalenko, I.E. Lager, and Andrian Andaya Lestari for discussing efficient programming.

The author is thankful to her students who have made substantial contributions while working on their graduation projects. The author would like to acknowledge the secretaries, Mia van der Voort-Kester, Laura Bauman, Wendy Murtinu-van Schagen, E. Jongeleen, etc. for their efficient organization. Great thanks are due to Michel Wilson, B. Yang and Tim Anten for the computer and network assistance. Further, the author thanks Ms. Mirjam J. Nieman for polishing the English of the dissertation and for translating the propositions and abstract into Dutch.

Additionally, the author thanks Ad de Ridder, Johan Zijderveld, Paul Hakkaart, Frans Bremer, Alex Yarovoy, Ezio Pusone, and all her colleagues and friends for sharing their thoughts and experiences. The author is also grateful to Severine Catreux and P.F.M. Smulders for the remote discussions.

Finally, great thanks are due to the Martens family, Piet Martens, Marie Martens-Gevers, Kees, Marja, Josephine, John, Bernadette, Frens, Caroline, Alex, Isabelle, Martijn, Lieke, Peter, Daniëlle, Bas, Christiaan, Marriele, Fabian, Esmeralda, Kevin, Priscilla, Mark, and Lara for the warm and cozy family feeling and for pleasant time they gave the author. Last but not least, the author is indebted to her parents, sister and Jeff for their permanent assistance.

Curriculum Vitae

Haiyan Che was born in 1972 in Liaoning province, P. R. China. She studied “electronics and telecommunications” at the Electrical Engineering Department of Liaoning University in Shenyang, Liaoning province, P. R. China from 1991 to 1995. In June 1995, she obtained her Bachelor of Science degree in Electrical Engineering. In September of the same year she was admitted to the M.Sc program of the Department of Electrical Engineering, Beijing Institute of Technology in Beijing, P. R. China, waived of the entrance examination. She worked on Digital Multiplexing Systems for her Master’s thesis. In March 1998 she obtained her Master of Science degree in Telecommunications.

In July 1998 she moved to the Netherlands and joined the Delft University of Technology in Delft, the Netherlands. She worked on Microwave Integrated Circuits (MIC) from 1998 to 1999. She joined the International Research Center on Transmission-Telecommunication and Radar (IRCTR) in 1999. From 1999 to 2000 she investigated Software Radio and in September 2000, she began to work on Adaptive Modulation, which has lead to this Ph.D thesis. She was the first person to work on Adaptive Modulation at the Delft University of Technology.